AD_____

Award Number: DAMD17-99-1-9408

TITLE: Measurement of the Electron Density Distribution of Estrogens - A First Step to Advanced Drug Design

PRINCIPAL INVESTIGATOR: Alan A. Pinkerton, Ph.D.

CONTRACTING ORGANIZATION: The University of Toledo
Toledo, Ohio 43606

REPORT DATE: August 2003

TYPE OF REPORT: Final

PREPARED FOR: U.S. Army Medical Research and Materiel Command
Fort Detrick, Maryland 21702-5012

REPORT DOCUMENTATION PAGE

Form Approved
OMB No. 074-0188

1. AGENCY USE ONLY (Leave blank)	2. REPORT DATE	3. REPORT TYPE AND DATES COVERED
	August 2003	Final (15 Jul 1999 - 14 Jul 2003)

4. TITLE AND SUBTITLE
Measurement of the Electron Density Distribution of Estrogen - A First Step to Advanced Drug Design

5. FUNDING NUMBERS
DAMD17-99-1-9408

6. AUTHOR(S)
Alan A. Pinkerton, Ph.D.

7. PERFORMING ORGANIZATION NAME(S) AND ADDRESS(ES)
The University of Toledo
Toledo, Ohio 43606

E-Mail: apinker@uoft02.utoledo.edu

8. PERFORMING ORGANIZATION REPORT NUMBER

9. SPONSORING / MONITORING AGENCY NAME(S) AND ADDRESS(ES)
U.S. Army Medical Research and Materiel Command
Fort Detrick, Maryland 21702-5012

10. SPONSORING / MONITORING AGENCY REPORT NUMBER

11. SUPPLEMENTARY NOTES
Original contains color plates: All DTIC reproductions will be in black and white.

12a. DISTRIBUTION / AVAILABILITY STATEMENT
Approved for Public Release; Distribution Unlimited

12b. DISTRIBUTION CODE

13. ABSTRACT (Maximum 200 Words)

Estrogens bind as ligands to the estrogen receptor initiating biological reactions, which can cause either initiation/progress or inhibition of tumor growth. The principle objective of this proposal was to relate known biological reactions to ligand physical properties such as the electrostatic potential. We have demonstrated the ability to determine the experimental electron potential. We have demonstrated the ability to determine the experimental electron density distribution and electrostatic potential of larger molecular systems such as estrogens. We have developed the methodology of crystallization, the x-ray CCD data treatment and least-squares model refinement procedure for estrogen crystals in order to extract maximum reliable and comparable information from the data. We completed charge density studies of six estrogen derivatives, performed the preliminary analysis and compared the results. We found that the electron density concentration associated with oxygen lone pairs are near sp3 in shape. These configurations as well as the electroscopic potentials are very consistent I the different hydrogen bonding environments. The core estrogen structure is also very consistent between the derivatives. The significant differences are found at the activity-sensitive molecular parts. In order to reliably associate the molecular recognition of a drug molecule to receptor with an electrostatic potential, a bigger data base of charge densities for estrogen molecules has to be built.

14. SUBJECT TERMS
Breast cancer, x-ray crystallography, estrogens, drug design

15. NUMBER OF PAGES
236

16. PRICE CODE

17. SECURITY CLASSIFICATION OF REPORT	18. SECURITY CLASSIFICATION OF THIS PAGE	19. SECURITY CLASSIFICATION OF ABSTRACT	20. LIMITATION OF ABSTRACT
Unclassified	Unclassified	Unclassified	Unlimited

Table of Contents

Introduction

The principal objective of this proposal is to obtain physico-chemical information on estrogen derivatives and correlate this knowledge to their known biological functionality. Slight chemical variation in these molecules can change the carcinostatic potentials from agonistic to inhibitory. Relating these biological reactions to physical properties such as point charges of atoms and the electrostatic potential is a logical first step in the intelligent design of therapeutic drugs [1-4]. We are obtaining information about the electronic properties of estrogen derivatives from experimental determination of their electron density using high quality single crystal X-ray crystallography at low temperatures.

Body

Task 1. Preliminary studies on a series of crystals of estrogen derivatives

- Feasibility study of already available crystals of estrogen derivatives

  Feasibility studies on crystals of 6 commercial estrogen derivatives (17α-estradiol, 17β-estradiol, 4,3,17-estriol, 2,3,17-estriol, 3,16α,17β-estriol and estrone) demonstrated their unsuitability for charge density studies. These studies require high quality crystals of at least 0.015 mm^3. All the crystals under examination proved to be either too small or not of a high enough quality. The 2,3,17-estriol crystals also appeared to be air and light sensitive.

- Development of crystallization methods for the derivatives not yet available as high quality single crystals

  We have developed crystallization methods for obtaining high quality crystals of several different estrogen derivatives. We succeeded in the preparation of high quality crystals of

  - 17α-estradiol•1/2 H_2O (crystallized from methanol)
  - 17α-estradiol (crystallized from methanol)
  - 4,3,17-estriol (crystallized from acetonitrile)
  - 3,16α,17β-estriol (crystallized from acetonitrile)
  - 17β-estradiol•1/2H_2O (crystallized from isopropanol)
  - 17β-estradiol•urea (crystallized from benzene+urea)
  - 17β-estradiol• ⅔ MeOH• ⅓H_2O (crystallized from methanol+water)
  - 17β-estradiol•½ MeOH (crystallized from methanol)
  - estrone (crystallized from ethanol+ethyl acetate)

  For the 17*β*-estradiol or 17*α*-estradiol, the best conditions found involve dissolving the powder in "wet" methanol. Allowing the solvent to evaporate as slowly as possible (~2-4 weeks) will yield charge density quality crystals. This often results in the formation of different crystal systems (such as 17*β*-estradiol • ½ MeOH or 17*β*-estradiol • ⅔ MeOH • ⅓ H_2O). This is probably due to the extremely small difference in packing energy of the different systems. On the contrary, the best estriol crystals were obtained from acetonitrile, and the best estrone crystals - from ethanol: ethyl acetate system.

- Temperature studies on each sample to define the appropriate temperature for the measurement

  Variable temperature studies were performed on the diffractometer on all of the above mentioned crystals. As our criterion for stability we chose the change in mosaicity of the respective crystal as identified by the broadening of the profiles of the diffraction intensities in comparison to a room temperature measurement. In our in-house experiments using Ag- (λ=0.5609 Å) and Mo- (λ=0.71073 Å) radiation, all of the samples proved to be stable under nitrogen cooling to 90 K.

  Further studies with liquid helium cooling (ca. 17 K) were performed with synchrotron radiation at the Argonnne (λ=0.40663 Å) and Brookhaven (λ=0.643 Å) National Laboratories. Surprisingly, these studies showed deviating results: while investigations on estrone at Argonne National Laboratory proved its suitability for He-temperature charge density studies, crystals of 17α-estradiol• ½H_2O, 17β-estradiol•urea, 17β-estradiol•½MeOH, 17β-estradiol•⅔MeOH•⅓H_2O and estrone, studied at Brookhaven National Lab showed a vast increase in their mosaicity after cooling. Modifying the crystal mounting technique and extending the time period during which a crystal was cooled to the final temperature of ca. 17 K proved to be successful for a crystal of 3,16α,17β-estriol.

  Several estrogen crystals were tested in-house with Ag- radiation using helium cooling. Contrary to our previous synchrotron results, we found no significant increase in the crystals' mosaicities after slow cooling using the modified mounts.

  These experiments have shown a vast increase of scattering power of the respective crystals at He-temperature compared to the room temperature diffraction experiment. A typical example is shown in the **Appendix A**; the two pictures compare the scattering ability of the same crystal of 17 α-estradiol•1/2 H_2O at room temperature and at 17 K.

  As a conclusion of these studies, it is preferable to use He temperatures for the charge density experiments, assuring that the crystal quality remains good after cooling. Use of synchrotron radiation is also preferable since it gives a big increase in the scattering power. Finally, a high quality charge density data set has been successfully measured at the Advanced Photon Source at Argonne National Lab at about 18 K on the estrone crystal.

- Routine X-ray crystal structure determination on uncharacterized derivatives

  In the course of our crystallization efforts we crystallized and determined three new crystal modifications of estradiol derivatives:
  - 17β-estradiol•2/3 MeOH•1/3 H_2O (**Appendix B**), reported in Acta Cryst. (2003)
  - 17β-estradiol•1/2MeOH (**Appendix H**), reported in Acta Cryst. (1999)
  - 17α-estradiol•1/2 H_2O (**Appendix D**).

Task2. Electron density studies on the estrogen analogs

- Electron density studies at liquid nitrogen temperatures

  We have collected complete data sets for charge density analyses on crystals of
  - 17α-estradiol•½H_2O
  - 17α-estradiol
  - 3,16α,17β-estriol
  - 17β-estradiol•½H_2O
  - 17β-estradiol•urea
  - 17β-estradiol•½ MeOH
  - estrone

  The first measured data set for the 17β-estradiol•1/2H_2O crystal appeared to be of insufficient quality due to several instrumentation problems. This data set had to be re-measured. Two data sets for the 17β-estradiol•urea crystal were collected due to reflection overlapping problems in the first data set. The other five data sets were of the high quality necessary for electron density analysis.

  To develop a procedure, how to get fast (in several hours) high quality charge density data for estrogens, the estrone and 17β-estradiol•urea crystals have also been measured at the Advanced Photon Source at Argonne National Laboratory. The experiments were unsuccessful due to an instrumentation problem that was discovered after the experiments.

- Electron density studies at helium temperatures

  A complete and high quality charge density measurement has been performed on the estrone crystal at the Argonne National Lab at about 18 K. The data analysis is currently proceeding but incomplete.

- Analysis of the experimental data, comparison of the results, preparation of manuscripts

  After processing several data sets of estrogen derivatives, we faced an unexpected problem: the outcome partially depends on the methodology of the data treatment. Therefore, we had to develop a uniform approach to treat the experimental data, including the CCD data integration and the following model refinement.

  The integration of the raw data involves integrating the intensity of the reflections as measured by a two-dimensional CCD detector. Several parameters must be defined to determine exactly how the software integrates the reflections. It was found that different detector settings, even for the same data set, require different box size parameters and profile fitting limits. The simple sum perimeter limit of 0.02 was found to be the best value for all data sets.

An optimized local atomic coordinate system has been developed (**Appendix C**) in order to better compare the results from studies on different estrogen analogs (the paper is in press in the Journal of Applied Crystallography).

It was also found that the starting values for the multipole model of the electron density greatly influenced the path the refinement would take. It was determined that a specific set of starting values should be applied to each structure to ensure consistency. These optimum values were determined after preliminary refinements of several estrogen derivatives; they are shown in the **Appendix C**. The model parameters in the least-squares process have to be refined in small groups in order to avoid severe correlation problems associated with the relatively large size of the estrogen molecules.

All this work was necessary in order to associate the differences in the electron density and electrostatic potential in estrogens with their chemical behavior, and not with differences in the data treatment.

- 17α-estradiol•½H_2O: As it was discovered during the electron density model refinement, the hydrogen atom in the water molecule was disordered. This complicated the refinement significantly, however it was successfully completed as well as the full topological analysis. The electrostatic potential has also been calculated. The complete results are in **Appendix D**. We are in the process of final data analysis and preparing the manuscript. The results were reported at the DOD Era of Hope Meeting (2002).

- 17α-estradiol: The charge density study has been completed (**Appendix E**). We are in the process of final data analysis. The results were reported at the DOD Era of Hope Meeting (2002).

- 3,16α,17β-estriol: A significant effort was put in the data re-refinement during the methodology development. The new methodology resulted in the significant improvement of the model. The final results are reported in **Appendix F**. We are in the process of final data analysis and preparing the manuscript. The results were reported at the Gordon research conference (2001), Pittsburgh Diffraction conference (2001), Bruker Users Group Meeting (2001) and the DOD Era of Hope Meeting (2002).

- 17β-estradiol•½H_2O: The experimental data have been successfully integrated, and we are currently refining the electron density model.

- 17β-estradiol•urea: The second measured data set appeared to be of sufficient quality. This allowed the multipole refinement to be completed as well as a full topological analysis of the electron density and the electrostatic potential analysis. The manuscript (**Appendix G**) is currently under revision. The results were reported at the DOD Era of Hope Meeting (2002).

- 17β-estradiol•½MeOH: This system was particular challenging, because the crystal has the lowest possible symmetry, resulting in low redundancy of the data. However, the multipole refinement was successfully completed as well as a full

topological analysis of the electron density and the electrostatic potential analysis. The complete results are in **Appendix H**. We are in the process of final data analysis and preparing the manuscript. The results were reported at the DOD Era of Hope Meeting (2002).

- Estrone: Based on our new developed methodology, a significant amount of work has been done in order to extract more information from the data. The experiment has been re-integrated several times in order to get the most precise structure factor list with minimum noise. Then, the model has been re-refined according to the new approach (see above). We are in the process of finishing the manuscript (**Appendix I**). The results were reported at the ACA meeting (2000), IUCR meeting (2000), Pittsburgh Diffraction conference (2001), Bruker Users Group Meeting (2001) and the DOD Era of Hope Meeting (2002).

The comparison of the results from the series of estrogen analogs showed that the core structure of the different estrogen molecules remains relatively unchanged from system to system. As the same time, significant differences are found at the activity-sensitive molecular parts.

Accurate experimental data and the new methodology developed (see above) allowed us to reveal such fine details as oxygen lone pair charge density concentrations. It appeared that each hydroxyl oxygen atom had two lone pairs in approximately sp^3 type geometry. This demonstrates that these lone pairs are surprisingly robust, and they do not significantly change in different hydrogen bonding schemes or/and when the oxygen is bound to the aromatic system.

The critical point analysis of covalent bonds of the estrogen molecules demonstrated the characteristic (3,-1) critical points, with the expected electron density, Laplacian and ellipticity values given the atom hybridization and connectivity. The average electron density values at the critical points are 1.91 $e\text{Å}^{-3}$ for the C – O bond, 2.17 $e\text{Å}^{-3}$ for C_{ar} – C_{ar}, 1.66 $e\text{Å}^{-3}$ for C – C, 1.91 $e\text{Å}^{-3}$ for C – H and 2.07 $e\text{Å}^{-3}$ for the O – H bond based on the 17β-estradiol•urea study. In all compounds, the critical points are well centered in the homonuclear C – C bonds, and proportionally displaced away from the more electronegative atom in the heteronuclear bonds.

Although the influence of the lattice is inherent in the multipole model of the estrogen molecule, the electrostatic potential is believed to provide a reasonable representation of a single molecule isolated from the crystal lattice. In these studies, the electrostatic potentials of the hydroxyl groups on the aromatic rings were qualitatively consistent in both shape and magnitude. Generally covering nearly the entire lone pair region, the maximum magnitudes are ~ -20 $e\text{Å}^{-1}$. The C17 hydroxyl groups are also relatively consistent in their lone pair regions and they exhibit an interesting trend. The potential changes significantly in both shape and magnitude based on the relative position of the hydroxyl hydrogen with respect to H17. 17β-estradiol•urea and 17α-estradiol• ½H_2O displayed a shift in the potential toward the lone pair region opposite H17, as well as increased magnitudes of ~ –35 and ~ –45 $e\text{Å}^{-1}$. H2O and H2O' were virtually opposite H17 in 17β-estradiol• ½MeOH. This resulted in a fairly uniform distribution of the

electrostatic potential with a maximum value of ~ –20 $eÅ^{-1}$. Plots of electrostatic potential isosurfaces are shown in **Appendices J-K**.

Tasks 3-6. Extension of the above mentioned studies to the series of E_2 C-ring analogues and nonsteroidal molecules.

- Feasibility study of already available crystals
  Feasibility studies on commercial diethylstilbestrol crystals demonstrated their unsuitability for charge density studies. These studies require high quality crystals of at least 0.015 mm^3. All the crystals under examination appeared to be too small.

- Development of crystallization methods for the derivatives not yet available as high quality single crystals

  A significant effort was made to obtain crystals of diethylstilbestrol. This is a molecule known to interact strongly with the estrogen receptor. It crystallizes in a centrosymmetric space group with the molecule sitting on a special position, which makes it a good candidate for charge density studies. Unfortunately, slow evaporation studies and solvent diffusion studies using many solvents such as, isooctane, p-chlorophenol, acetonitrile, acetone and several different types of alcohols were not successful. Only a powdery residue was observed, or in the best case, microcrystals.

Task 7. Final analysis

Presumably there is a preferred orientation for the hydrogen of the C17 hydroxyl group in the active site of the estrogen receptor. Unfortunately, the protein crystal structures determined to date do not have enough resolution to determine this. It seems possible that this is one mechanism by which the estrogen ligands could stimulate different responses from the estrogen receptor. Binding of different ligands would most likely result in different orientations of the C17 hydroxyl hydrogen, thereby presenting different electrostatic potentials to the receptor. This could help to account for the changes in binding affinity and activity of the different estrogen derivatives. Continued effort must be made to analyze more systems because a sample of six structures is not enough to confirm the trends that are appearing in the electron density and the electrostatic potential.

Key Research Accomplishments

- ♦ Crystallization of high quality crystals; the best conditions to obtain high quality single crystals

- ♦ Methodology development of the X-ray CCD data treatment and model least-squares refinement:

a) optimized temperature conditions
b) best radiation type determination
c) best data integration options
d) best local atomic coordinate system
e) best first approximation of the model
f) best and uniform refinement procedure

- New crystal structures solved for 17β-estradiol•2/3 MeOH•1/3 H_2O; 17β-estradiol•1/2MeOH; 17α-estradiol•1/2 H_2O
- Charge density and electrostatic potential analysis of the 17α-estradiol•½H_2O; 17α-estradiol; 3,16α,17β-estriol; 17β-estradiol•urea; 17β-estradiol•½ MeOH and estrone
- The core estrogen structure is very consistent among different derivatives
- Parameters describing the activity-sensitive molecular parts are different
- It is possible to locate lone pair densities of oxygen in such large systems
- The deformation electron density distributions of all hydroxyl oxygen atoms are close to sp^3 in shape, even when oxygens are bound to aromatic neighbors
- Hydroxyl oxygen lone pairs appear to be unaffected by completely different hydrogen bonding environments
- The electrostatic potentials around the oxygen atoms are consistent in the different hydrogen bonding environments
- The electrostatic potential around the C17 hydroxyl groups changes significantly in both shape and magnitude based on the relative position of the hydroxyl hydrogen with respect to H17

Reportable Outcomes

1. Parrish, D. & Pinkerton, A.A., *Estradiol Methanol Hemisolvate*, Acta Cryst., 1999, **C55**, IUC9900100.
2. Pre-doctoral Traineeship Award granted by the Department of the Army for Damon Parrish. $66,000 "*Measurement of the Electron Density Distribution of Estrogens - a First Step to Advanced Drug Design*"
3. Parrish, D., Wu, N. & Pinkerton, A.A., *Charge Density Distribution of Estrone*, American Crystallographic Association Meeting, St. Paul, MN, July 22-27, 2000.
4. Parrish, D., Wu, N., Zhurova, E.A. & Pinkerton, A.A., *Preliminary Results for a Charge Density Study of Estrone*, 19th European Crystallographic Meeting, Nancy, France, August 25-31, 2000.

5. Pinkerton, A.A., *Charge Densities from CCD Data – What Can You Believe?*, 59th Pittsburgh Diffraction Conference, Cincinnati, OH, October 25-27, 2001.
6. Kumaradhas, P. & Pinkerton, A.A., *A Charge Density and Electrostatic Potential Study on Estrogen Molecules: Estriol*, Gordon research conference "Electron distribution and chemical bonding", Mount Holyoke College - South Hadley , MA July 8 - 12, 2001.
7. Pinkerton, A.A., *Just How Good IS Your Data?*, Bruker Area Detector Users Group Meeting, Madison, WI, May 21-22, 2001.
8. Parrish, D. & Pinkerton, A.A., *Charge Density Studies of Three Estradiol Systems*, DOD Breast Cancer Research Program Era of Hope Meeting, Orlando, FL, September 25-28, 2002.
9. Pinkerton, A.A., Kirschbaum, K., Kumaradhas, P., Parrish, D., Wu, N. & Zhurova, E.A., *Measurement of the Electron Density Distribution of Estrogens – a First Step to Advanced Drug Design,* DOD Breast Cancer Research Program Era of Hope Meeting, Orlando, FL, September 25-28, 2002.
10. Parrish, D. & Pinkerton, A.A., *A New Estra-1,3,5(10)-triene-3,17β-diol Solvate: Estradiol- Methanol- Water (3/2/1)*, Acta Cryst., 2003, **C59**, o80-o82.
11. Parrish, D., *Comparative Charge Density Studies of 17α-Estradiol and 17β-Estradiol*, A Ph.D. Dissertation, the University of Toledo, 2003.
12. Chen, Yu-Sh., Kirschbaum, K., Kumaradhas, P., Parrish, D., Pinkerton, A.A. & Zhurova, E.A., *A Standard Local Coordinate System for Multipole Refinements of the Estrogen Core Structure*, J. Appl. Cryst., 2003, **36**, in press.
13. Parrish, D. & Pinkerton, A.A., *The Experimental Charge Density Study of Estrogens: 17β-Estradiol•Urea*, manuscript under revision.

Conclusion

The ability to determine the experimental electron density distribution and electrostatic potential of larger molecular systems such as estrogens has been demonstrated. We have developed the methodology of crystallization, the X-ray CCD data treatment and least-squares model refinement procedure for estrogen crystals in order to extract maximum reliable and comparable information from the data. We completed charge density studies of six estrogen derivatives, performed the preliminary analysis and compared the results. We found that the deformation electron density distributions of all hydroxyl oxygen atoms are near sp^3 in shape; their lone pair densities have been reliably located. These configurations as well as the electrostatic potentials around the oxygen atoms are very consistent in different hydrogen bonding environments. The core estrogen structure is also very consistent between the derivatives. As the same time, the significant differences are found at the activity-sensitive molecular parts.

To be able to reliably associate the molecular recognition of a drug molecule to receptor with a electrostatic potential distribution in the molecule, a significant data base of charge density for estrogen molecules has to be built. So far, we have completed six structures, and this small sample is not enough to make any statistical conclusions. More charge density studies of different estrogen analogues are needed to complete this study.

References:

1. Davis, M.D., Butler, W.B. & Brooks, S.C. (1995) J. Steroid Biochem. Molec. Biol., **52**, 421.
2. VanderKuur, J.A., Wiese, T. & Brooks, S.C. (1993) Biochemistry, **32**, 7002.
3. Pilat, M.J., Hafner, M.S., Kral, L.G. & Brooks, S.C. (1993) Biochemistry, **32**, 7009.
4. VanderKuur, J.A., Hafner, M.S., Christman, J.K. & Brooks, S.C. (1993) Biochemistry, **32**, 7016.

List of personnel received pay from the research effort

1. Dr. K. Kirschbaum, senior research associate

2. Dr. P. Kumaradhas, post-doctoral associate

3. Dr. N. Wu, post-doctoral associate

4. Dr. E.A. Zhurova, senior research associate

List of Appendices

A. Scattering of a crystal of 17α-estradiol•1/2 H_2O at room temperature (a) and He (ca.17 K) temperature (b).

B. Parrish, D. & Pinkerton, A.A., *A New Estra-1,3,5(10)-triene-3,17β-diol Solvate: Estradiol-Methanol- Water (3/2/1)*, Acta Cryst., 2003, **C59**, o80-o82.

C. Chen, Yu-Sh., Kirschbaum, K., Kumaradhas, P., Parrish, D., Pinkerton, A.A. & Zhurova, E.A., *A Standard Local Coordinate System for Multipole Refinements of the Estrogen Core Structure*, J. Appl. Cryst., 2003, **36**, in press.

D. Crystal structure and charge density analysis of 17α-estradiol•1/2 H_2O.

E. Crystal structure and charge density analysis of 17α-estradiol.

F. Crystal structure and charge density analysis of 3,16α,17β-estriol.

G. Parrish, D. & Pinkerton, A.A., *The Experimental Charge Density Study of Estrogens: 17β-Estradiol•Urea*, manuscript in revision.

H. Crystal structure and charge density analysis of 17β-estradiol•½ MeOH.

I. Crystal structure and charge density analysis of estrone.

J. *Measurement of the Electron Density Distribution of Estrogens – a First Step to Advanced Drug Design*, DOD Breast Cancer Research Program Era of Hope Meeting (2002).

K. Electrostatic potential isosurfaces for several hydroxyl groups of selected estrogens.

Appendix A.

Scattering of a crystal of 17α-estradiol•1/2 H_2O at room temperature (a) and He (ca.17 K) temperature (b).

?
E:\bnl\aestr\rt1.006
08/12/00 12:20:22
Created 02/23/00
Phi 1.500
Width 0.300
Counts 50,738,413
Time (s) 3.216
Distance 3.500
Size 512
Project aest1
DataDev e:
DataDir ...on\aest\
WorkDev e:
WorkDir ...on\aest\
A 19.0190(9)
B 7.0640(5)
C 13.3480(7)
Alp 89.996(3)
Bet 124.037(2)
Gam 89.998(4)
V 1486.2(2)
Distance 5.140
FloodFld g834h170
Spatial g834h170
Dark None
Siz,Gain 1024 14
771
724
676
629
581
533
UofT - pinkerton - 08/12/00

(a)

?
\bnl\aestr\cool1.006
08/12/00 12:19:07
Created 02/23/00
Phi 1.500
Width 0.300
Counts 36,434,136
Time (s) 3.216
Distance 3.500
Size 512
Project aestl
DataDev e:
DataDir ...on\aestl\
WorkDev e:
WorkDir ...on\aestl\
A 19.0190(9)
B 7.0640(5)
C 13.3480(7)
Alp 89.996(3)
Bet 124.037(2)
Gam 89.998(4)
V 1486.2(2)
Distance 5.140
FloodFld g834h170
Spatial g834h170
Dark None
Siz,Gain 1024 14
771
724
676
629
581
533
UofT - pinkerton - 08/12/00

(b)

Appendix B.

Parrish, D. & Pinkerton, A.A.

A New Estra-1,3,5(10)-triene-3,17β-diol Solvate: Estradiol-Methanol- Water (3/2/1)

Acta Cryst., 2003, **C59**, o80-o82.

Acta Crystallographica Section C
Crystal Structure Communications
ISSN 0108-2701

A new estra-1,3,5(10)-triene-3,17β-diol solvate: estradiol–methanol–water (3/2/1)

Damon A. Parrish and A. Alan Pinkerton*

Department of Chemistry, University of Toledo, Toledo, Ohio 43606, USA
Correspondence e-mail: apinker@uoft02.utoledo.edu

Received 22 October 2002
Accepted 21 November 2002
Online 25 January 2003

The title solvate of the steroid 17β-estradiol (E_2) with methanol and water, $C_{18}H_{24}O_2\cdot0.67CH_4O\cdot0.33H_2O$, is the first E_2 derivative to contain three crystallographically independent molecules in the asymmetric unit. The three steroid molecules, along with two methanol molecules and a water molecule, create a three-dimensional hydrogen-bonded system. Three-sided columns are formed, with the estradiol molecules aligned lengthwise parallel to (101), and joined by solvent molecules at both hydrophilic ends. The three estradiol molecules differ slightly in their ring-bowing angles, *i.e.* the angle between the mean plane of the *A* ring and that of the *BCD* ring; this angle ranges from 7.1 to 12.2°.

Comment

17β-Estradiol, E_2, is a member of the estrogen family of hormones. In recent years, interest in these molecules has focused primarily on understanding their biological role in initiating breast cancer. It is well known that their ability to form hydrogen bonds in the active site of the estrogen receptor (ER) influences biological activity. This ability to form hydrogen bonds has been clearly demonstrated in an array of crystal structures, especially in that of E_2, containing different solvent molecules or other hydrogen-bond acceptors.

When comparing these structures, the flexibility of the hydrophobic region of the molecule, more specifically the *B* ring, becomes very apparent. Several papers have already discussed the ring bowing of this molecule (Cooper *et al.*, 1969; Cody *et al.*, 1971; Busetta *et al.*, 1976; Duax *et al.*, 1979). Weise & Brooks (1994) took it a step further, performing molecular-modeling calculations on observed and novel confirmations. Ivanov and co-workers carried out a related study which included a larger body of compounds and more detailed analysis (Ivanov *et al.*, 1998). They concluded that there are two possible conformations very close in energy, which differ in the *B*-ring arrangement, although the chance of the strained-geometry binding is low, as one quarter of the binding energy (−11.9 kcal mol^{-1}; 1 kcal mol^{-1} = 4.184 kJ mol^{-1}) is predicted to be lost (Anstead *et al.*, 1997). The point initially postulated by Weise & Brooks remains, *i.e.* that the flexibility to allow bending or other conformational changes of the ligand in the receptor appears energetically achievable, and this could be an important property in determining their activity.

Molecular-dynamics studies on the ligand-binding domain (LBD) of the ER demonstrate that the motion of the LBD requires the *A* ring to remain fairly steady while the *CD* ring retains a higher degree of freedom. The range of motion found in that study (Maalouf *et al.*, 1998) agrees very well with the reported crystal structures. It is well known that the hydrogen bonding of the ligand in the LBD causes conformational changes in the recèptor. This seemingly accommodating motion of the LBD and the ligand supports the idea postulated by Weise & Brooks that the flexibility of E_2, or of any other ligand which enters the LBD, could also effect the activity of the ligand. A more rigid or flexible ligand could change the natural motion of the ER complex, resulting in a change in activation factor (AF-2) activity, and therefore possibly effecting co-activator recruitment. This process is not well understood; the flexibility of the ligand is certainly only one of many physical factors associated in the activity of E_2. The structure of the title solvate, (I), continues the trend in observing the flexibility of this molecule from a structural and hydrogen-bonding point of view, while the molecule lies in the lowest energy conformation.

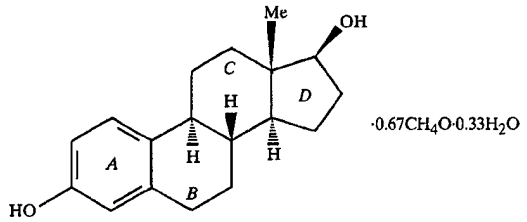

(I)

The crystal of (I) contains three crystallographically unique E_2 molecules (Fig. 1). The *B* rings of the E_2 molecules adopt the typical conformation of a distorted 7α,8β-half-chair, and this is responsible for most of the structural flexibility. Calculation of the ring-bowing angle, as defined by Duax & Norton (1975), reveals a range of 5.1° for the three molecules. Table 1 compares the ring-bowing angles of the currently

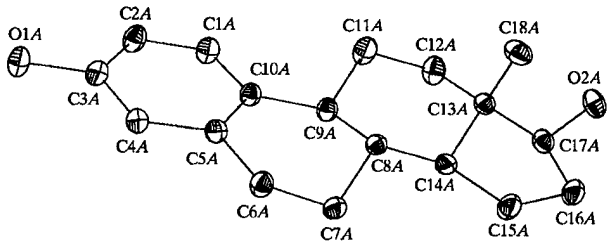

Figure 1
A view of molecule *A* of (I), with the atom-numbering scheme; the other two molecules are similarly labeled, with the corresponding suffix *B* or *C*. Displacement ellipsoids are plotted at the 50% probability level. The solvent molecules have been omitted for clarity.

  DOI: 10.1107/S0108270102021637

known E_2 crystal structures. The spread of over 12°, with angles found distributed over the entire range, indicate the shallowness of the potential associated with the bowing deformation. In a system as dynamic as the human body, the molecule would certainly have a wide range of conformations easily available.

The packing of (I) results in three-sided cylinders of estradiol molecules arranged parallel to (101), with the C18 methyl group pointing towards the center (Fig. 2). This, of course, aligns the large hydrophobic regions of the molecules, as well as the hydrophilic hydroxy groups. These cylinders then stack on top of each other, creating three-sided columns (Fig. 3) held together by hydrogen bonds involving the hydroxy groups and the three solvent molecules. A more detailed picture of the hydrogen bonding between the solvent and E_2 molecules can be seen in Fig. 4 and from the data in Table 3. There is also an intercolumnar hydrogen bond, which occurs between the water molecule and a 3-hydroxy group. This, along with the intercolumnar hydrogen-bonded solvent,

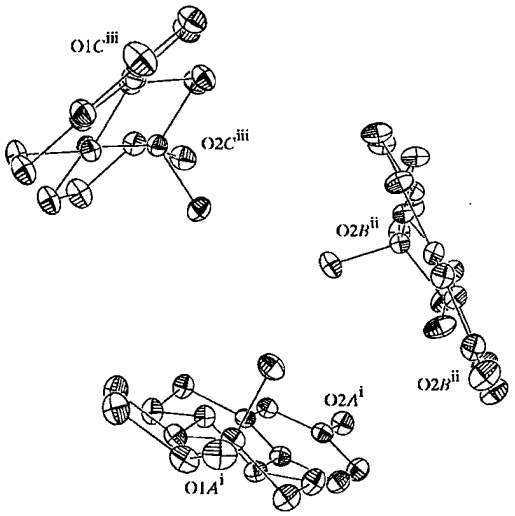

Figure 2
The molecular arrangement of (I), looking down the three-sided column. Displacement ellipsoids are plotted at the 50% probability level [symmetry codes: (i) x, y, z; (ii) $-2-x, y-\frac{1}{2}, -1-z$; (iii) $x-1, y, z$].

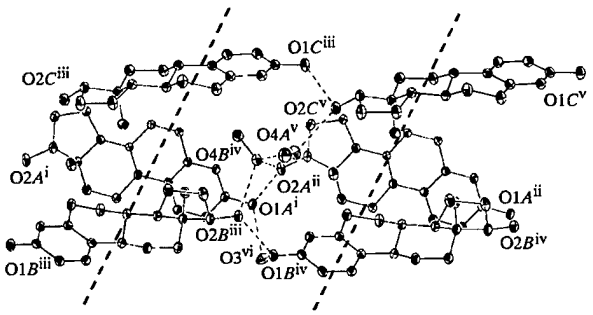

Figure 3
The packing of E_2 groups in (I), with the hydrogen-bonded solvent molecules, viewed perpendicular to the columns. Dotted lines indicate the region detailed in Fig. 4. Displacement ellipsoids are plotted at the 50% probability level [symmetry codes: (i) x, y, z; (ii) $1+x, y, 1+z$; (iii) $-2-x, y-\frac{1}{2}, -1-z$; (iv) $-1-x, y-\frac{1}{2}, -z$; (v) $x, y, 1+z$; (vi) $-x, y-\frac{1}{2}, -z$].

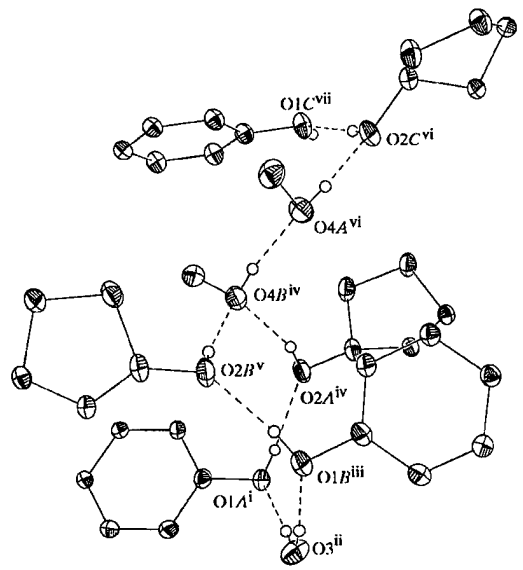

Figure 4
The hydrogen-bonded region of the column shown in Fig. 3, including the solvent molecules and only the A or D rings of E_2. Displacement ellipsoids are plotted at the 50% probability level [symmetry codes: (i) x, y, z; (ii) $-x, y-\frac{1}{2}, -z$; (iii) $-1-x, y-\frac{1}{2}, -z$; (iv) $1+x, y, 1+z$; (v) $-2-x, y-\frac{1}{2}, -1-z$; (vi) $x, y, 1+z$; (vii) $-1-x, y, z$].

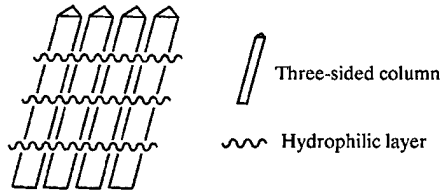

Figure 5
A schematic diagram of the packed columns in (I) and their relation to the hydrophilic layer containing the hydroxy groups and solvent molecules.

creates a hydrophilic layer which is approximately 30° from the perpendicular to the columns (Fig. 5). Structurally, all bond lengths and angles are in expected ranges (Table 2).

Experimental

Crystals were grown by slow evaporation from a methanol solution open to the air. It is presumed that the methanol was either wet prior to use in this experiment or absorbed atmospheric moisture. Crystals of (I) were grown over the course of 3 d and harvested when reaching the appropriate size.

Crystal data

$C_{18}H_{24}O_2 \cdot 0.67CH_4O \cdot 0.33H_2O$
$M_r = 299.74$
Monoclinic, $P2_1$
$a = 11.7152\ (4)$ Å
$b = 19.6270\ (6)$ Å
$c = 12.1310\ (4)$ Å
$\beta = 117.978\ (1)°$
$V = 2463.34\ (14)$ Å^3
$Z = 6$
$D_x = 1.212$ Mg m^{-3}
Ag $K\alpha$ radiation
Cell parameters from 7309 reflections
$\theta = 2.3–27.9°$
$\mu = 0.05$ mm^{-1}
$T = 298\ (1)$ K
Cuboid, colorless
0.4 × 0.3 × 0.3 mm

Data collection

Siemens SMART Platform CCD area-detector diffractometer	44 195 measured reflections 21 122 independent reflections
ω scans	15 597 reflections with $I > 2\sigma(I)$
Absorption correction: empirical *via* multipole expansion (Blessing, 1995) using *SADABS* (Sheldrick, 1996)	$R_{int} = 0.048$ $\theta_{max} = 27.9°$
$T_{min} = 0.840$, $T_{max} = 0.985$	$h = -18 \rightarrow 19$ $k = -32 \rightarrow 29$ $l = -20 \rightarrow 20$

Refinement

Refinement on F^2	H atoms treated by a mixture of independent and constrained refinement
$R[F^2 > 2\sigma(F^2)] = 0.058$	$w = 1/[\sigma^2(F_o^2) + (0.0812P)^2]$ where $P = (F_o^2 + 2F_c^2)/3$
$wR(F^2) = 0.145$	$(\Delta/\sigma)_{max} = 0.001$
$S = 0.99$	$\Delta\rho_{max} = 0.41$ e Å^{-3}
21 122 reflections	$\Delta\rho_{min} = -0.23$ e Å^{-3}
698 parameters	

Table 1
Comparison of ring-bowing angles (°) in reported E_2 crystal structres.

Compound	Molecule 1 angle	Molecule 2 angle	Molecule 3 angle
17β-estradiol-0.5H_2O†	15.6		
17β-estradiol–propanol†	12.9		
17β-estradiol–urea†	5.6		
17β-estradiol-0.5MeOH‡	10.4	3.4	
(I)§	12.2	11.9	7.1

† Wiese & Brooks (1994). ‡ Parrish & Pinkerton (1999). § This work.

Table 2
Selected bond lengths (Å).

O1*A*—C3*A*	1.3716 (18)	O2*A*—C17*A*	1.4354 (19)
O1*B*—C3*B*	1.3792 (17)	O2*B*—C17*B*	1.4305 (19)
O1*C*—C3*C*	1.3691 (18)	O2*C*—C17*C*	1.4400 (19)

Table 3
Hydrogen-bonding geometry (Å, °).

D—H···*A*	*D*—H	H···*A*	*D*···*A*	*D*—H···*A*
O1*A*—H1O*A*···O2*A*^{i}	0.74 (3)	1.89 (3)	2.6226 (17)	171 (3)
O1*B*—H1O*B*···O2*B*^{i}	0.85 (3)	1.83 (3)	2.6654 (18)	171 (3)
O1*C*—H1O*C*···O3	0.76 (3)	1.82 (3)	2.5767 (18)	170 (3)
O2*A*—H2O*A*···O4*B*	0.76 (3)	1.97 (3)	2.7017 (18)	162 (2)
O2*B*—H2O*B*···O4*B*^{ii}	0.73 (2)	2.06 (2)	2.7823 (19)	168 (2)
O2*C*—H2O*C*···O1*C*^{iii}	0.73 (2)	1.99 (3)	2.7169 (17)	175 (3)
O3—H3O*A*···O1*A*^{iv}	0.72 (4)	2.02 (4)	2.743 (2)	178 (4)
O3—H3O*B*···O1*B*^{v}	0.76 (3)	2.04 (3)	2.7926 (19)	173 (3)
O4*A*—H4O*A*···O2*C*	0.83 (3)	1.85 (3)	2.6809 (18)	174 (3)
O4*B*—H4O*B*···O4*A*^{vi}	0.78 (2)	1.88 (2)	2.6462 (17)	166 (2)

Symmetry codes: (i) $1+x, y, 1+z$; (ii) $-3-x, \frac{1}{2}+y, -2-z$; (iii) $x-1, y, z-1$; (iv) $-x, \frac{1}{2}+y, -z$; (v) $1+x, y, z$; (vi) $x-1, y, z$.

The absolute configuration of the E_2 molecules in (I) was known from the natural product starting material. The intensity data were corrected for decay and absorption using *SADABS* (Sheldrick, 1996). All H atoms of the solvent molecules and the hydroxy groups of the E_2 molecules were located in a difference map and refined with isotropic displacement parameters. The remaining H atoms were included with idealized geometries (C—H = 0.96–0.98 Å), and their isotropic displacement parameters were refined.

Data collection: *SMART* (Bruker, 1998); cell refinement: *SAINT* (Bruker, 1999); data reduction: *SAINT*; program(s) used to solve structure: *SHELXS*97 (Sheldrick, 1990); program(s) used to refine structure: *SHELXL*97 (Sheldrick, 1997); molecular graphics: *SHELXTL* (Siemens, 1994); software used to prepare material for publication: *SHELXTL*.

We thank the College of Arts and Sciences of the University of Toledo for generous financial support of the X-ray diffraction facility.

Supplementary data for this paper are available from the IUCr electronic archives (Reference: SQ1003). Services for accessing these data are described at the back of the journal.

References

Anstead, G. M., Carlson, K. E. & Katzenellenbogen, J. A. (1997). *Steroids*, **62**, 268–303.
Blessing, R. H. (1995). *Acta Cryst.* A**51**, 33–58.
Bruker (1998). *SMART*. Version 5.622. Bruker AXS Inc., Madison, Wisconsin, USA.
Bruker (1999). *SAINT*. Version 6.20. Bruker AXS Inc., Madison, Wisconsin, USA.
Busetta, B., Barrans, Y., Precigoux, G. & Hospital, M. (1976). *Acta Cryst.* B**32**, 1290–1292.
Cody, V., DeJarnette, F., Duax, W. & Norton, D. A. (1971). *Acta Cryst.* B**27**, 2458–2468.
Cooper, A., Norton, D. A. & Hauptman, H. (1969). *Acta Cryst.* B**25**, 814–828.
Duax, W. L. & Norton, D. A. (1975). In *Atlas of Steroid Structures*. New York: Plenum.
Duax, W. L., Rohrer, D. C., Blessing, R. H., Strong, P. D. & Segaloff, A. (1979). *Acta Cryst.* B**35**, 2656–2664.
Ivanov, J., Mekenyan, O., Bradbury, S. P. & Schuurmann, G. (1998). *Quant. Struct. Activity Rel.* **17**, 437–449.
Maalouf, G. J., Xu, W. R., Smith, T. F. & Mohr, S. C. (1998). *J. Biomol. Struct. Dyn.* **15**, 841–852.
Parrish, D. A. & Pinkerton, A. A. (1999). *Acta Cryst.* C**55**, IUC9900100.
Sheldrick, G. M. (1990). *Acta Cryst.* A**46**, 467–473.
Sheldrick, G. M. (1996). *SADABS*. University of Göttingen, Germany.
Sheldrick, G. M. (1997). *SHELXL*97. University of Göttingen, Germany.
Siemens (1994). *SHELXTL*. Release 5.03. Siemens Analytical X-ray Instruments Inc., Madison, Wisconsin, USA.
Wiese, T. E. & Brooks, S. C. (1994). *J. Steroid Biochem. Mol. Biol.* **50**, 61–73.

Appendix C.

Chen, Yu-Sh., Kirschbaum, K., Kumaradhas, P., Parrish, D., Pinkerton, A.A. & Zhurova, E.A.

A Standard Local Coordinate System for Multipole Refinements of the Estrogen Core Structure

J. Appl. Cryst., 2003, **36**, in press.

A Standard Local Coordinate System for Multipole Refinements of the Estrogen Core Structure

Yu-Sheng Chen, Kristin Kirschbaum, Poomani Kumaradhas, Damon A. Parrish, A. Alan Pinkerton,* and Elizabeth A. Zhurova

Department of Chemistry, University of Toledo, 2801 W. Bancroft Street, Toledo, OH 43606, USA. E-mail: apinker@uoft02.utoledo.edu

Synopsis The initiation of a comparative charge density study on a series of estrogen derivatives revealed the need for a standardized local coordinate system for each atom in order to facilitate comparison of the multipole refinements. Herein we propose such a system for the core structure of a generic estrogen molecule and suggest starting parameters for the population of the most prominent multipoles.

Abstract A comparative charge density study on a series of estrogen derivatives has been initiated. The study utilizes the Hansen-Coppens atom centered multipole model to describe the valence electron density distribution. Direct comparison of the population parameters for each estrogen after the respective multipole refinements requires standardization of the atom centered local coordinate systems. Such a standard coordinate system for the common estrogen core is reported, taking advantage of the shape of those multipoles which have the spatial characteristics of sp^2 and sp^3 hybrid orbitals. Additionally, populating these principal multipoles at the beginning stage of the refinements improves the stability of these large, highly correlated calculations.

Keywords: Estrogen; charge density; coordinate system

1. Introduction

Recent advances in computers, software, and X-ray data collection technology have made charge density studies on a series of larger "small molecules" in a reasonable amount of time feasible. A comparative charge density analysis has been initiated to study a series of estrogen derivatives.

Electron density refinements from experimental X-ray diffraction data have been performed using the XD suite of programs (Koritsanszky et al., 1995), which utilizes the Hansen-Coppens model to describe the valence electron density (Coppens 1997, Hansen & Coppens 1978). This model is based on multipole expansions centred on the atoms and concomitantly requires a user defined local Cartesian coordinate system for each atom in the structure .

In a comparative study, consistency in this model setup is essential to enable direct comparison of the parameters of the multipole refinements for different molecules in a related series. This article proposes a standard local coordinate system for the atoms of the core structure of a generic estrogen molecule.

As well as being responsible for the development of secondary sexual characteristics, it has been determined that some estrogens are responsible for the initiation and progression of certain types of breast cancer. This study attempts characterization of the physical and electronic features of these molecules and the relationship of such submolecular properties to biological activity.

Most biologically active estrogens are A-ring or D-ring isomers of the naturally occurring estradiol or derivatives thereof, containing the same hydrocarbon ring core structure. With careful choice of directions, the local coordinate system can take advantage of the spatial characteristics of certain multipoles that, if populated, would mimic the shape of the bonding electron density derived from sp^2 and sp^3 hybrid orbitals.[1] (Pichon-Pesme et al., 1995; Coppens, 1997) This allows a majority of the valence electron density to be modelled by the linear combination of only a few multipoles. Given the number of parameters for such large, non-centrosymmetric systems, typically greater than 40 atoms, this approach can considerably stabilize the initial multipole refinements. By using a standard coordinate system, upon completion of the multipole refinement, a rational comparison can then be made among various related charge density studies.

The 17β-estradiol molecule, along with the labelling scheme of the core structure, is shown in scheme 1. For all methylene groups, hydrogen atoms on the same side of the core as the methyl group at position 18 are labelled b, those on the other side are labelled a. The C and D rings projected down the C18-C13 bond are provided as an insert to define the orientation of the methyl group hydrogen atoms.

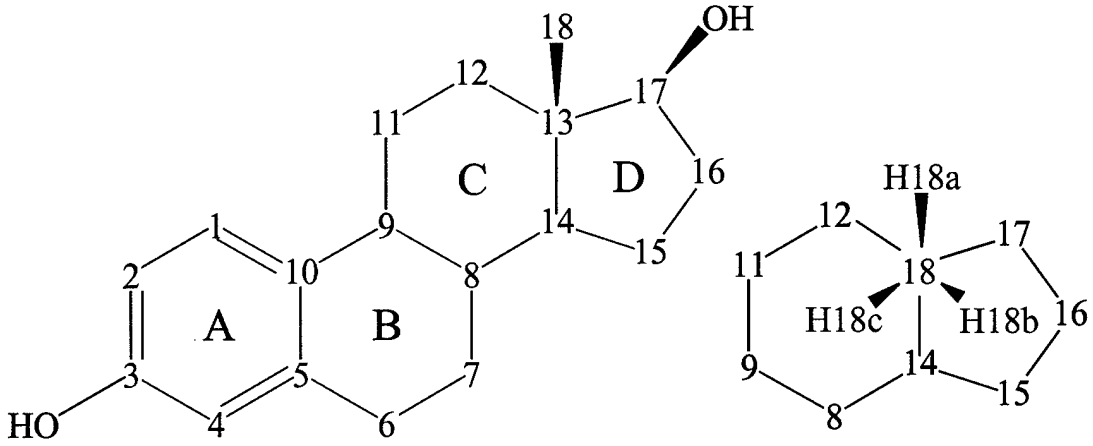

Scheme 1

[1] It is important to distinguish between the multipoles, which are density functions, and orbitals, which are derived from wavefunctions.

2. Method

The Cartesian axes *x,y,z* of the above mentioned atom centered coordinate systems are calculated in the program XD (Koritsanszky et al., 1995) based on two user defined vectors. In general, the first vector ($\mathbf{v}_1$) for a given atom (1) originates at its nucleus, is directed towards another atom (2) in the system - or, if necessary, a "dummy" atom - and defines axis(1). A second vector ($\mathbf{v}_2$) with the same origin points towards another atom (3), or dummy atom, describing the axis(1) - axis(2) plane. A third vector ($\mathbf{v}_3$) is taken perpendicular to this plane,

$$\mathbf{v}_1 = (\mathbf{r}_2 - \mathbf{r}_1) \qquad \mathbf{v}_2 = (\mathbf{r}_3 - \mathbf{r}_1) \qquad \mathbf{v}_3 = \mathbf{v}_1 \times \mathbf{v}_2$$

where $\mathbf{r}_1$, $\mathbf{r}_2$, and $\mathbf{r}_3$ are the position vectors of atom(1), atom(2), and atom(3), respectively.
An orthonormal vector triplet ($\mathbf{e}_{ax1}$, $\mathbf{e}_{ax2}$, $\mathbf{e}_{ax3}$) is then formed which we have chosen to be right handed.

$$\mathbf{e}_{ax1} = \mathbf{v}_1/|\mathbf{v}_1| \qquad \mathbf{e}_{ax2} = (\mathbf{v}_3 \times \mathbf{v}_1)/|(\mathbf{v}_3 \times \mathbf{v}_1)| \qquad \mathbf{e}_{ax3} = \mathbf{v}_3/|\mathbf{v}_3|$$

Although axes 1, 2 and 3 can be assigned labels *x,y,z* arbitrarily, for the current molecules we define axis(1) as *x*, axis(2) as *y*, and axis(3) as *z* for non-hydrogen atoms, and axis(1) as *z*, axis(2) as *y* and axis(3) as *x* for hydrogen atoms.

Given these assignments, the valence electron density of the aromatic sp^2 type carbons atoms in the A-ring (scheme 1), can be initially approximated by populating two multipoles, the 33+ and 20. Pictorial representations of the angular function for these multipoles can be seen in Figure 1. Defining the *xy* plane of the coordinate system to lie in the plane of the bound atoms, i.e. the aromatic plane, will allow the positive lobe of the 33+ octupole to align with the three covalent bond regions. The 20 quadrupole will then be positioned perpendicular to this plane, a negative populations adding to the in plane σ bonding and depopulating the p orbital as required for π bond formation.

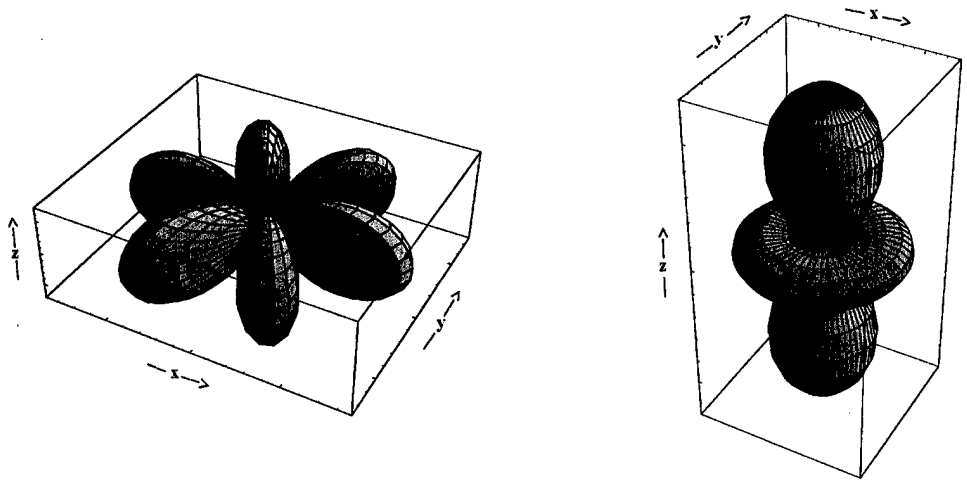

Figure 1 Coordinate system and angular functions of the 33+ and 20 multipoles with blue representing positive regions and red, negative. Functions visualized using MATLAB (2000).

The covalent bonding regions of the sp^3 type carbon atoms in the B, C, and D-rings of the generic estrogen can effectively be modelled by a single multipole, the 32- octupole. The axes associated with the 32-

octupole do not correspond to the populated regions, hence two "dummy" atoms must be used to define the local coordinate system in this case. Their positions are calculated on the bisectors of the bond angles (the two-folds axes of the tetrahedron) at the atom of interest. An example of an sp^3 coordinate system and the 32- octupole is shown in Figure 2.

Approximation of the bond density of the hydrogen atoms can be achieved by initially populating a single dipole along *z*. A complete list of vector definitions for carbon and hydrogen atoms for the estrogen core are given in Tables 1 and 2. Using this standardized set of coordinates systems for future theoretical and experimental electron density studies on estrogen derivatives (and possibly expanding it for other steroids like progesterone) it will be possible to compare individual multipole populations for different molecules in this series.

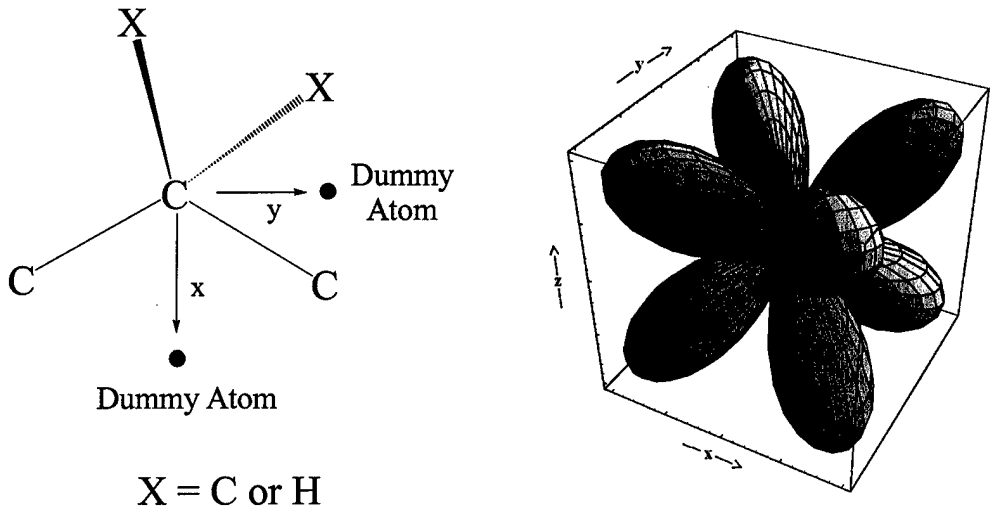

Figure 2 Model coordinate system for a sp^3 type atom and 32- multipole, with blue representing positive density and red, negative. (MATLAB, 2000).

Populating these principal multipoles at the beginning stage of the refinements may improve the stability of these large, highly correlated calculations. We have thus listed suitable values for the core structure based on our own refinements (Chen et al., 2003) of six different estrogen molecules (Table 3). We note that the sum of the monopole populations do not sum to zero for the estrogen core. To maintain electroneutrality, it is essential that appropriate starting values be assigned to other substituents, e.g. for estradiol, values of –0.47 and 0.29 would be appropriate monopole populations for the O and H atoms of the hydroxy groups.

3. Conclusion

Examples of typical input for the XD program and pictorial representation of the coordinate schemes for the hydrocarbon core of estrogens as recommended in this paper are available as supplementary material.

Table 1 Atoms used to define vectors $\mathbf{v}_1$ and $\mathbf{v}_2$ for carbon atoms[a]

Atom(1)	Atom (2)	Atom(3)
C1	C2	C10
C2	C3	C1
C3	C4	C2
C4	C5	C3
C5	C10	C4
C6	Dum1 (C5 - C7)	Dum2 (C5 - H6a)
C7	Dum3 (C6 - C8)	Dum4 (C6 - H7a)
C8	Dum5 (C7 - C9)	Dum6 (C7 - C14)
C9	Dum7 (C8 - C11)	Dum8 (C8 - C10)
C10	C1	C5
C11	Dum9 (C9 - C12)	Dum10 (C12 - H11a)
C12	Dum11 (C11 - C13)	Dum12 (C13 - H12a)
C13	Dum13 (C12 - C14)	Dum14 (C14 - C17)
C14	Dum15 (C8 - C15)	Dum16 (C8 - C13)
C15	Dum17 (C14 - C16)	Dum18 (C14 - H15a)
C16	Dum19 (C15 - C17)	Dum20 (C15 - H16a)
C17	Dum21 (C13 - C16)	Dum22 (C16 - O2)
C18	Dum23 (H18a - H18b)	Dum24 (H18b - H18c)

[a] Bond lengths of atoms used to calculate dummy atom positions (in parentheses) are adjusted to be equidistant from the atom of interest to ensure a true bisection.

Table 2. Atoms used to define vectors $\mathbf{v}_1$ and $\mathbf{v}_2$ for hydrogen atoms

Atom(1)	Atom(2)	Atom(3)
H1	C1	C9
H2	C2	H1
H4	C4	O1
H6a	C6	H6b
H6b	C6	H6a
H7a	C7	H7b
H7b	C7	H7a
H8	C8	C13
H9	C9	H14
H11a	C11	H11b
H11b	C11	H11a
H12a	C12	H12b

H12b	C12	H12a
H14	C14	H9
H15a	C15	H15b
H15b	C15	H15a
H16a	C16	H16b
H16b	C16	H16a
H17	C17	O2
H18a	C18	H18b
H18b	C18	H18c
H18c	C18	H18a

Table 3: Initial set of population parameters for the most important multipoles.

		sp^2		sp^3			
Atom	00	20	33+	32-	Atom	00	10
C1	-0.22(3)	-0.22(5)	0.32(5)		H1	0.24(4)	0.14(4)
C2	-0.28(7)	-0.21(5)	0.34(5)		H2	0.24(4)	0.15(4)
C3	0.15(4)	-0.18(5)	0.34(7)		H4	0.23(4)	0.16(2)
C4	-0.26(5)	-0.20(4)	0.33(4)		H6x	0.18(4)	0.15(2)
C5	-0.13(3)	-0.22(4)	0.36(7)		H7x	0.18(4)	0.14(2)
C6	-0.27(4)			0.31(7)	H8	0.19(4)	0.13(5)
C7	-0.28(6)			0.31(6)	H9	0.18(2)	0.12(4)
C8	-0.18(6)			0.38(5)	H11x	0.18(4)	0.12(2)
C9	-0.16(6)			0.33(9)	H12x	0.18(4)	0.14(4)
C10	-0.13(3)	-0.20(3)	0.36(4)		H14	0.18(3)	0.14(3)
C11	-0.28(6)			0.33(4)	H15x	0.19(5)	0.12(4)
C12	-0.28(5)			0.32(6)	H16x	0.17(5)	0.15(3)
C13	-0.21(6)			0.38(7)	H17	0.10(2)	0.18(2)
C14	-0.15(4)			0.34(3)	H18x	0.14(3)	0.13(4)
C15	-0.32(7)			0.30(7)			
C16	-0.35(5)			0.32(7)			
C17	0.16(4)			0.30(5)			
C18	-0.39(6)			0.22(6)			

Hydrogen labels such as H6x, represent both H6A and H6B. Populations are average values from 6 studies on - 17β-estradiol.½MeOH, 17β-estradiol.urea, 17α-estradiol, 17α-estradiol.½H_2O, 16α,17β -estriol, estrone. κ's for H atoms were fixed at 1.4. Other values for κ would be expected to introduce small changes to the refined monopole populations, but to have minimal effect on the higher poles.

Acknowledgements We thank to the Department of Defense, USAMRMC for financial support (Grants DAMD17-00-1-0468 and DAMD17-99-1-9408)

References

Chen Yu-S., Kirschbaum K., Kumaradhas P., Parrish D.A., Pinkerton A.A., Wu N., Zhurova, E.A. (2003) to be published.

Coppens P. (1997) *X-Ray Charge Density Analysis and Chemical Bonding* (Oxford University Press, Oxford)

Hansen, N.K. and Coppens P. (1978) *Acta Cryst.* A34, 909-921.

Koritsanszky T., Howard S., Mallison P.R., Su Z., Richter T., and Hansen N.K. (1995) XD. A Computer Program Package for Multipole Refinement and Analysis of Electron Densities from Diffraction Data. Free University of Berlin, Berlin.

MATLAB Version 6. (2000) The Mathworks Inc., Natick, MA USA.

Pichon-Pesme V, Lecomte C., and Lachekar H. (1995) *J. Phys. Chem.* 99, 6242-6250.

Appendix D.

Crystal structure and charge density analysis of 17α-estradiol•1/2 H_2O

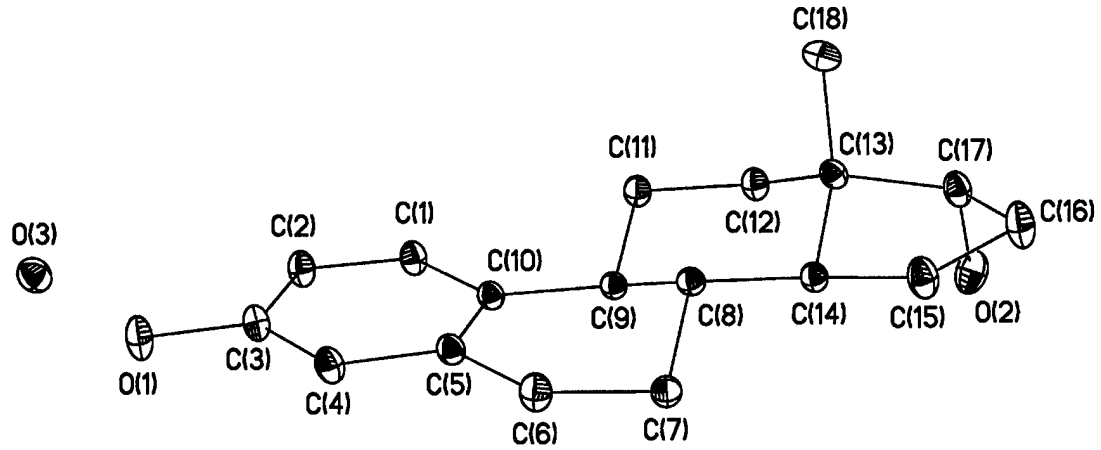

Figure 1. Thermal ellipsoid plot of 17*a*-estradiol•½H_2O where ellipsoids represent 50% probability electron density of the atom. Hydrogen atoms are omitted for clarity.

Run	2θ	ω	ϕ	Scan Width (°)	# of Frames	Frame Times (sec)
1	0	10	0	-0.30	660	96
2	0	10	90	-0.30	660	96
3	0	10	180	-0.30	660	96
4	0	10	270	-0.30	660	96
5	0	10	0	-0.30	100	96
6	-60	-50	45	-0.30	660	180
7	-60	-50	135	-0.30	660	180
8	-60	-50	225	-0.30	660	180
9	-60	-50	315	-0.30	660	180
10	-60	-50	45	-0.30	100	180

Table 1. Data collection parameters for 17*a*-estradiol•½H_2O.

Crystal Data			
Chemical Formula	$C_{18}H_{25}O_{2.5}$		
Temperature	100.0(1) K		
Crystal Dimensions	0.24 x 0.33 x 0.33 mm		
Space Group	C2		
A	19.0235(5) Å		
B	7.0653(2) Å		
C	13.3496(3) Å		
β	124.0544(10)		
Volume	1486.56(10) $Å^3$		
Z (Crystallographic)	4		
Integration Parameters			
	Box Size (°)	Profile Fitting (I/σ)	Simple Sum Perimeter Limit
Low Angle	1.2 x 1.2 x 0.8	40 10	0.02
High Angle	1.0 x 1.0 x 0.6	30 10	0.02
Reflection Statistics (from SORTAV)			
Total Reflections	85540		
Rejected Outliers	69		
Unique Reflections	14593		
Average Redundancy	5.9		
Resolution	1.319 $Å^{-1}$		
Completeness	98.2 %		
R_1	3.76 %		
R_2	4.13 %		
R_w	13.52 %		
Z (Refinement)	1.949		

Table 2. Selected crystal, integration, and reflection data for 17*a*-estradiol•½H_2O.

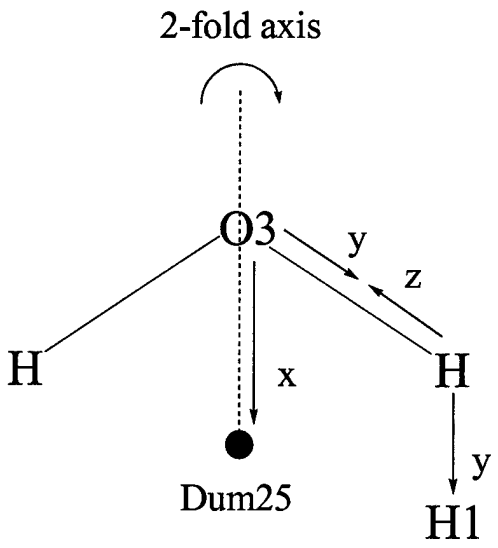

Figure 2. Coordinate system for the water molecule.

	n	m	$\langle n \rangle$	R_1	R_2	R_w	Z	V
Q < -4	0	0	0.0	0.0000	0.0000	0.0000	0.000	0.000
-4 < Q < -3	0	0	0.0	0.0000	0.0000	0.0000	0.000	0.000
-3 < Q < -2	2	1	2.0	0.3784	0.3657	0.3695	1.086	0.381
-2 < Q < -1	43	14	3.1	0.3661	0.4037	0.4846	0.886	0.368
-1 < Q < 0	1161	326	3.6	1.0974	1.1150	1.0573	1.801	3.167
0 < Q < 1	6088	1550	3.9	0.9922	0.9414	0.9133	2.031	1.676
1 < Q < 2	6618	1657	4.0	0.5715	0.5985	0.5448	2.092	0.650
2 < Q < 3	5241	1299	4.0	0.3530	0.4112	0.3720	2.237	0.386
3 < Q < 4	4586	1054	4.4	0.2565	0.3076	0.2699	2.257	0.277
4 < Q < 6	7017	1516	4.6	0.1805	0.2214	0.1905	2.353	0.195
6 < Q < 8	5775	1128	5.1	0.1290	0.1586	0.1406	2.153	0.141
8 < Q < 10	5187	896	5.8	0.0995	0.1227	0.1095	1.999	0.109
10 < Q < 20	17218	2529	6.8	0.0575	0.0728	0.0725	1.645	0.067
20 < Q < 30	16066	1596	10.1	0.0340	0.0467	0.0399	1.227	0.038
30 < Q < 50	10194	745	13.7	0.0244	0.0340	0.0283	1.235	0.027
50 < Q < 100	144	17	8.5	0.0148	0.0164	0.0170	1.048	0.016
100 < Q	0	0	0.0	0.0000	0.0000	0.0000	0.000	0.000

Table 3. Intensity-Significance Intervals where n is the number of reflections, m is the number of unique reflections, $\langle n \rangle$ is the average measurement multiplicity, and Q=I/Max ($\sigma_{int}/\sigma_{ext}$) respectively for 17$a$-estradiol•½$H_2O$.

	n	m	$\langle n \rangle$	R_1	R_2	R_w	Z	V
D > 1.029	13550	791	17.1	0.0273	0.0387	0.1137	1.986	0.030
1.029 > D > 0.817	13830	774	17.9	0.0329	0.0362	0.1057	1.817	0.039
0.817 > D > 0.713	6005	743	8.1	0.0362	0.0381	0.1209	2.082	0.041
0.713 > D > 0.648	4332	750	5.8	0.0384	0.0368	0.1320	2.145	0.044
0.648 > D > 0.602	4119	748	5.5	0.0480	0.0463	0.1379	2.182	0.053
0.602 > D > 0.566	3914	749	5.2	0.0565	0.0537	0.1396	2.137	0.064
0.566 > D > 0.538	3668	735	5.0	0.0706	0.0660	0.1467	2.076	0.079
0.538 > D > 0.514	3508	729	4.8	0.0891	0.0866	0.1593	2.163	0.100
0.514 > D > 0.495	3483	752	4.6	0.1057	0.1058	0.1609	2.089	0.116
0.495 > D > 0.478	3201	721	4.4	0.1066	0.1015	0.1629	2.055	0.117
0.478 > D > 0.463	3092	720	4.3	0.1054	0.0935	0.1688	2.063	0.114
0.463 > D > 0.449	3023	728	4.2	0.1491	0.1327	0.1945	2.020	0.163
0.449 > D > 0.438	2820	697	4.0	0.1950	0.1897	0.2191	1.970	0.212
0.438 > D > 0.427	2819	720	3.9	0.2140	0.2053	0.2331	1.947	0.236
0.427 > D > 0.417	2608	686	3.8	0.2517	0.2218	0.2650	2.007	0.280
0.417 > D > 0.408	2594	700	3.7	0.2849	0.2656	0.2784	1.927	0.320
0.408 > D > 0.400	2537	712	3.6	0.3111	0.2877	0.3036	1.932	0.351
0.400 > D > 0.393	2331	678	3.4	0.3549	0.3364	0.3461	1.926	0.405
0.393 > D > 0.386	2277	682	3.3	0.3852	0.3783	0.3658	1.941	0.431
0.386 > D > 0.379	1629	513	3.2	0.4653	0.4655	0.4370	1.769	0.540

Table 4. Equal-Volume Resolution Shells where n is the number of reflections, m is the number of unique reflections, $\langle n \rangle$ is the average measurement multiplicity, and D=sinθ/λ (Å^{-1}) respectively for 17a-estradiol•½H_2O.

	Monopole	sp^2		sp^3
		20	33+	32-
O1	-0.50			
O2	-0.49			
C1	-0.30	-0.22	0.34	
C2	-0.38	-0.19	0.37	
C3	0.27	-0.21	0.38	
C4	-0.33	-0.17	0.36	
C5	-0.18	-0.22	0.33	
C6	-0.26			0.31
C7	-0.31			0.34
C8	-0.21			0.39
C9	-0.17			0.31
C10	-0.25	-0.18	0.37	
C11	-0.31			0.35
C12	-0.28			0.31
C13	-0.16			0.38
C14	-0.20			0.38
C15	-0.26			0.33
C16	-0.35			0.42
C17	0.20			0.38
C18	-0.32			0.27

	Monopole
H1O	0.40
H2O	0.38
H1	0.23
H2	0.22
H4	0.26
H6x	0.20
H7x	0.17
H8	0.20
H9	0.16
H11x	0.17
H12x	0.16
H14	0.19
H15x	0.16
H16x	0.18
H17	0.13
H18x	0.18

Atoms	Kappa	κ	κ'
O1, O2	1	0.97	1.16
C3	2	1.01	0.92
C17	3	1.02	0.95
C1, C2, C4	4	0.97	0.92
C5, C10	5	0.98	0.87
C6, C7, C8, C9, C11, C12, C13, C14, C15, C16, C17, C18	6	0.98	0.95
all C-H hydrogen atoms	7	1.20	1.29
H1O, H2O	8	1.20	1.29
O3	9		
H3O	10		

Table 5. Starting values entered into the model for the multipole refinement for 17*a*-estradiol•½H_2O. Units for multipole populations are e^-.

Atom	X	Y	Z
O1	0.11679(1)	0.53051(6)	-0.40619(2)
O2	0.59212(2)	0.40154(6)	0.50812(2)
C1	0.25908(2)	0.32552(6)	-0.10524(2)
C2	0.19311(2)	0.34213(6)	-0.22673(3)
C3	0.18285(2)	0.51139(6)	-0.28726(2)
C4	0.24011(2)	0.65930(6)	-0.22661(2)
C5	0.30786(2)	0.64004(6)	-0.10514(2)
C6	0.37135 (2)	0.80070(6)	-0.04731(3)
C7	0.43341(2)	0.78376(6)	0.08978(2)
C8	0.46397(2)	0.58022(6)	0.12773(2)
C9	0.38729(2)	0.45262(6)	0.09205(2)
C10	0.31740(2)	0.47201(6)	-0.04185(2)
C11	0.41421(2)	0.24647(6)	0.13289(2)
C12	0.48474(2)	0.23044(6)	0.26845(2)
C13	0.56071(2)	0.35552(6)	0.30229(2)
C14	0.52936(2)	0.56082(6)	0.26359(2)
C15	0.61131(2)	0.67896(6)	0.32646(3)
C16	0.67369(2)	0.56827(7)	0.44502(3)
C17	0.62831(2)	0.38263(7)	0.43874(3)
C18	0.60695(2)	0.27766(7)	0.24600(3)
O3	0.00000	0.23142(6)	-0.50000

Atom	X	Y	Z
H1O	0.0858(5)	0.4125(12)	-0.4373(7)
H2O	0.5776(5)	0.2772(12)	0.5221(7)
H1	0.2662(4)	0.1964(10)	-0.0571(6)
H2	0.1501(4)	0.2251(10)	-0.2723(5)
H4	0.2325(4)	0.7893(9)	-0.2743(5)
H6A	0.3381(4)	0.9357(10)	-0.0691(6)
H6B	0.4076(3)	0.7980(8)	-0.0879(5)
H7A	0.4029(3)	0.8300(8)	0.1345(5)
H7B	0.4877(4)	0.8759(9)	0.1198(5)
H8	0.4908(3)	0.5308(8)	0.0777(5)
H9	0.3621(3)	0.5067(8)	0.1432(5)
H11A	0.3595(3)	0.1651(8)	0.1144(4)
H11B	0.4347(3)	0.1816(9)	0.0792(5)
H12A	0.4574(3)	0.2717(8)	0.3184(5)
H12B	0.5030(3)	0.0821(8)	0.2897(5)
H14	0.4967(3)	0.5946(8)	0.3080(5)
H15A	0.6023(4)	0.8213(9)	0.3488(5)
H15B	0.6368(4)	0.6833(10)	0.2710(6)
H16A	0.6891(4)	0.6405(10)	0.5271(6)
H16B	0.7310(4)	0.5301(10)	0.4497(6)
H17	0.6733(3)	0.2639(8)	0.4791(4)
H18A	0.6315(4)	0.1412(9)	0.2813(6)
H18B	0.6599(4)	0.3615(11)	0.2676(6)
H18C	0.5672(4)	0.2631(10)	0.1507(5)
H3O	-0.0329(6)	0.1294(14)	-0.4989(8)

Table 6. Fractional atomic coordinates for 17*a*-estradiol•½H_2O.

Atom	U^{11}	U^{22}	U^{33}	U^{12}	U^{13}	U^{23}
O1	0.01474(8)	0.01787(9)	0.01159(8)	-0.00278(7)	0.00232(7)	0.00226(7)
O2	0.02309(10)	0.02411(11)	0.01353(9)	-0.00461(9)	0.00994(8)	-0.00101(8)
C1	0.01204(9)	0.01148(9)	0.01149(9)	-0.00201(7)	0.00414(8)	0.00130(7)
C2	0.01229(9)	0.01414(10)	0.01165(9)	-0.00233(8)	0.00411(8)	0.00150(8)
C3	0.01088(9)	0.01535(10)	0.01028(9)	-0.00064(7)	0.00421(7)	0.00195(8)
C4	0.01196(9)	0.01291(9)	0.01167(9)	0.00007(7)	0.00481(8)	0.00282(7)
C5	0.01117(8)	0.00945(8)	0.01079(8)	0.00050(7)	0.00505(7)	0.00167(7)
C6	0.01588(10)	0.00952(8)	0.01253(9)	-0.00106(7)	0.00521(8)	0.00213(7)
C7	0.01282(9)	0.00788(8)	0.01220(9)	-0.00003(7)	0.00565(8)	0.00038(7)
C8	0.01065(8)	0.00806(7)	0.01068(8)	0.00034(6)	0.00579(7)	0.00082(6)
C9	0.01013(8)	0.00851(8)	0.01017(8)	0.00023(6)	0.00513(7)	0.00084(6)
C10	0.01026(8)	0.00922(8)	0.01016(8)	0.00013(6)	0.00499(7)	0.00115(6)
C11	0.01317(9)	0.00837(8)	0.01196(9)	-0.00036(7)	0.00511(8)	0.00119(7)
C12	0.01257(9)	0.01020(8)	0.01198(9)	-0.00066(7)	0.00537(8)	0.00224(7)
C13	0.01036(8)	0.01021(8)	0.01170(9)	0.00115(7)	0.00540(7)	0.00168(7)
C14	0.01012(8)	0.00939(8)	0.01077(8)	-0.00013(6)	0.00488(7)	0.00063(7)
C15	0.01293(9)	0.01331(10)	0.01594(10)	-0.00301(8)	0.00472(8)	0.00240(8)
C16	0.01292(10)	0.01801(11)	0.01616(11)	-0.00385(9)	0.00231(9)	0.00290(9)
C17	0.01204(9)	0.01325(9)	0.01289(9)	0.00060(7)	0.00418(8)	0.00286(8)
C18	0.01651(11)	0.01638(11)	0.02061(12)	0.00425(9)	0.01234(10)	0.00207(9)
O3	0.01581(12)	0.01773(13)	0.02136(14)	0.00000	0.00928(11)	0.00000

Table 7. Anisotropic thermal parameters of non-H atoms for 17*a*-estradiol•½H_2O.

Atom	U_{iso}
H1O	0.0386(18)
H2O	0.0471(20)
H1	0.0519(16)
H2	0.0460(14)
H4	0.0447(14)
H6A	0.0564(15)
H6B	0.0449(13)
H7A	0.0413(13)
H7B	0.0434(12)
H8	0.0380(12)
H9	0.0392(12)
H11A	0.0436(13)
H11B	0.0464(13)
H12A	0.0410(12)
H12B	0.0445(13)

Atom	U_{iso}
H14	0.0407(12)
H15A	0.0470(13)
H15B	0.0550(15)
H16A	0.0586(16)
H16B	0.0598(16)
H17	0.0426(12)
H18A	0.0577(15)
H18B	0.0644(17)
H18C	0.0538(14)
H3O	0.1065(51)

Table 8. Isotropic thermal parameters of H atoms for 17*a*-estradiol•½H_2O.

Atoms	Bond Length (Å)
O1 – C3	1.3724(3)
O2 – C17	1.4365(4)
C1 – C2	1.3927(4)
C1 – C10	1.4024(4)
C2 – C3	1.3945(4)
C3 – C4	1.3951(4)
C4 – C5	1.4030(3)
C5 – C6	1.5162(4)
C5 – C10	1.4087(3)
C6 – C7	1.5289(4)
C7 – C8	1.5274(3)
C8 – C9	1.5457(3)
C8 – C14	1.5261(3)

Atoms	Bond Length (Å)
C9 – C10	1.5232(3)
C9 – C11	1.5390(3)
C11 – C12	1.5390(4)
C12 – C13	1.5305(4)
C13 – C14	1.5432(3)
C13 – C17	1.5444(4)
C13 – C18	1.5431(4)
C14 – C15	1.5382(4)
C15 – C16	1.5560(4)
C16 – C17	1.5465(4)

Table 9. Bond distances of non-H atoms of 17*a*-estradiol•½H_2O.

Atoms	Bond Angle (°)
C3 – O1 – H1O	110.8(5)
C17 – O2 – H2O	109.3(5)
C2 – C1 – C10	122.2(1)
C2 – C1 – H1	119.7(4)
C10 – C1 – H1	118.1(4)
C1 – C2 – C3	119.3(1)
C1 – C2 – H2	119.7(4)
C3 – C2 – H2	120.9(4)
O1 – C3 – C2	119.7(1)
O1 – C3 – C4	120.6(1)
C2 – C3 – C4	119.7(1)
C3 – C4 – C5	120.8(1)
C3 – C4 – H4	119.5(4)
C5 – C4 – H4	119.8(4)
C4 – C5 – C6	118.0(1)
C4 – C5 – C10	120.1(1)
C6 – C5 – C10	121.8(1)
C5 – C6 - C7	114.3(1)
C5 – C6 – H6A	110.0(4)
C5 – C6 – H6B	106.2(3)
C7 – C6 – H6A	109.3(4)
C7 – C6 – H6B	108.3(3)
H6A – C6 – H6B	108.5(5)
C6 – C7 – C8	111.5(1)
C6 – C7 – H7A	109.9(3)
C6 – C7 – H7B	109.3(3)
C8 – C7 – H7A	108.7(3)
C8 – C7 – H7B	109.5(4)
H7A – C7 – H7B	107.8(4)
C7 – C8 – C9	109.2(1)
C7 – C8 – C14	112.6(1)

Atoms	Bond Angle (°)
C9 – C8 – C14	108.3(1)
C7 – C8 – H8	108.5(4)
C9 – C8 – H8	107.8(3)
C14 – C8 – H8	110.3(3)
C8 – C9 – C10	111.2(1)
C8 – C9 – C11	111.9(1)
C10 – C9 – C11	113.5(1)
C8 – C9 – H9	105.7(3)
C10 – C9 – H9	107.5(3)
C11 – C9 – H9	106.4(4)
C1 – C10 – C5	117.9(1)
C1 – C10 – C9	121.2(1)
C5 – C10 – C9	120.9(1)
C9 – C11 – C12	112.6(1)
C9 – C11 – H11A	109.4(3)
C9 – C11 – H11B	109.6(4)
C12 – C11 – H11A	108.7(3)
C12 – C11 – H11B	110.2(3)
H11A – C11 – H11B	106.1(5)
C11 – C12 – C13	111.2(1)
C11 – C12 – H12A	107.4(3)
C11 – C12 – H12B	108.5(3)
C13 – C12 – H12A	111.1(3)
C13 – C12 – H12B	111.6(3)
H12A – C12 – H12B	106.8(5)
C12 – C13 – C14	108.7(1)
C12 – C13 – C17	116.4(1)
C12 – C13 – C18	110.6(1)
C14 – C13 – C17	100.9(1)
C14 – C13 – C18	113.0(1)
C17 – C13 – C18	107.1(1)

Atoms	Bond Angle (°)
C8 – C14 – C13	112.8(1)
C8 – C14 – C15	120.2(1)
C13 – C14 – C15	104.1(1)
C8 – C14 – H14	106.9(3)
C13 – C14 – H14	104.6(3)
C15 – C14 – H14	107.1(3)
C14 – C15 – C16	104.2(1)
C14 – C15 – H15A	112.5(3)
C14 – C15 – H15B	110.2(4)
C16 – C15 – H15A	109.4(3)
C16 – C15 – H15B	109.2(4)
H15A – C15 – H15B	111.0(5)
C15 – C16 – C17	106.7(1)
C15 – C16 – H16A	114.2(4)
C15 – C16 – H16B	110.6(4)
C17 – C16 – H16A	106.2(4)
C17 – C16 – H16B	107.6(4)
H16A – C16 – H16B	111.1(5)
O2 – C17 – C13	112.9(1)
O2 – C17 – C16	109.9(1)
C13 – C17 – C16	103.9(1)
O2 – C17 – H17	106.1(3)
C13 – C17 – H17	112.9(3)
C16 – C17 – H17	111.3(3)
C13 – C18 – H18A	109.8(4)
C13 – C18 – H18B	112.5(4)
C13 – C18 – H18C	113.7(4)
H18A – C18 – H18B	105.8(6)
H18A – C18 – H18C	106.6(6)
H18B – C18 – H18C	108.1(5)
H3O – O3 – H3O'	82.7(10)

Table 10. Bond angles of 17*a*-estradiol•½H_2O.

Atom	Monopole Population ($P_{0,0}$)
O1	6.519(12)
O2	6.526(12)
C1	4.222(23)
C2	4.254(22)
C3	3.855(20)
C4	4.247(22)
C5	4.127(21)
C6	4.217(22)
C7	4.217(21)
C8	4.127(21)
C9	4.122(21)
C10	4.101(21)
C11	4.226(20)
C12	4.236(20)
C13	4.189(22)
C14	4.121(22)
C15	4.308(21)
C16	4.302(21)
C17	3.849(19)
C18	4.379(22)
O3	3.274(8)

Atom	Monopole Population ($P_{0,0}$)
H1O	0.621(11)
H2O	0.611(11)
H1	0.780(11)
H2	0.788(10)
H4	0.783(11)
H6A	0.853(9)
H6B	0.853(9)
H7A	0.854(7)
H7B	0.854(7)
H8	0.818(10)
H9	0.821(10)
H11A	0.858(8)
H11B	0.858(8)
H12A	0.852(8)
H12B	0.852(8)
H14	0.844(11)
H15A	0.853(8)
H15B	0.853(8)
H16A	0.851(9)
H16B	0.851(9)
H17	0.908(10)
H18A	0.879(7)
H18B	0.879(7)
H18C	0.879(7)
H3O	0.726(8)

Table 11. Monopole populations (e^-) of 17*a*-estradiol•½H_2O.

Multipoles	O1	O2	O3
$P_{1,+1}$	-0.011(7)	-0.036(7)	0.0
$P_{1,-1}$	0.020(11)	0.030(11)	0.048(10)
$P_{1,0}$	0.029(8)	0.014(6)	0.0
$P_{2,0}$	0.096(7)	0.083(7)	0.0
$P_{2,+1}$	-0.037(6)	-0.016(6)	0.0
$P_{2,-1}$	-0.035(7)	-0.046(7)	0.0
$P_{2,+2}$	-0.064(7)	-0.021(7)	0.0
$P_{2,-2}$	0.022(7)	0.065(7)	0.0
$P_{3,0}$	0.014(12)	-0.040(9)	0.0
$P_{3,+1}$	-0.015(9)	-0.081(8)	0.0
$P_{3,-1}$	0.029(12)	-0.017(13)	0.0
$P_{3,+2}$	0.026(10)	-0.016(9)	0.0
$P_{3,-2}$	0.022(11)	0.089(13)	0.0
$P_{3,+3}$	0.124(8)	0.077(9)	-0.100(7)
$P_{3,-3}$	0.020(11)	-0.042(14)	0.0
$P_{4,0}$	0.0	-0.080(11)	0.0
$P_{4,+1}$	0.0	0.034(10)	0.0
$P_{4,-1}$	0.0	0.0	0.0
$P_{4,+2}$	0.0	0.011(10)	0.0
$P_{4,-2}$	-0.018(10)	0.021(11)	0.0
$P_{4,+3}$	-0.062(10)	0.032(10)	0.0
$P_{4,-3}$	0.0	0.047(11)	0.0
$P_{4,+4}$	0.018(9)	-0.023(10)	-0.059(6)
$P_{4,-4}$	-0.090(10)	-0.071(11)	0.0

Table 12. Multipole populations (e^-) of Oxygen and Nitrogen atoms of 17*a*-estradiol•½H_2O.

Multipoles	C1	C2	C3	C4	C5	C6	C7	C8	C9
$P_{1,+1}$	-0.048(11)	-0.153(16)	-0.089(14)	0.047(12)	0.186(16)	0.114(15)	0.108(14)	-0.019(11)	-0.021(11)
$P_{1,-1}$	-0.074(16)	-0.041(13)	0.155(13)	0.172(17)	0.104(13)	0.0	-0.027(11)	-0.131(13)	0.122(14)
$P_{1,0}$	0.073(11)	0.075(11)	0.091(12)	0.064(11)	0.0	0.023(11)	-0.119(12)	-0.103(13)	0.0
$P_{2,0}$	-0.242(9)	-0.175(10)	-0.226(9)	-0.171(10)	-0.250(10)	-0.021(9)	-0.028(9)	0.039(9)	0.0
$P_{2,+1}$	0.035(9)	0.066(10)	-0.017(10)	0.0	0.0	-0.010(9)	0.023(9)	-0.018(9)	0.0
$P_{2,-1}$	0.0	0.0	-0.039(9)	-0.011(10)	0.012(9)	0.038(9)	0.0	0.0	0.018(8)
$P_{2,+2}$	0.011(10)	0.035(10)	0.067(11)	0.0	0.031(11)	0.0	0.036(8)	-0.027(8)	0.017(8)
$P_{2,-2}$	-0.063(10)	-0.055(10)	-0.013(10)	-0.055(11)	-0.018(11)	-0.069(9)	0.010(9)	0.029(9)	0.0
$P_{3,0}$	-0.050(17)	-0.026(16)	-0.070(17)	-0.064(16)	0.0	-0.018(16)	0.0	0.103(14)	0.223(15)
$P_{3,+1}$	0.0	0.0	0.060(13)	0.0	0.023(14)	-0.085(12)	-0.085(12)	0.054(15)	0.105(14)
$P_{3,-1}$	0.022(14)	-0.019(13)	0.044(13)	-0.027(13)	0.015(14)	-0.046(13)	0.096(13)	0.124(15)	0.128(12)
$P_{3,+2}$	0.029(15)	0.0	-0.050(16)	0.019(14)	0.0	0.048(15)	-0.029(14)	-0.187(15)	0.025(15)
$P_{3,-2}$	0.018(14)	-0.020(15)	0.028(15)	0.0	-0.049(17)	0.170(14)	0.313(15)	0.301(11)	0.145(12)
$P_{3,+3}$	0.310(12)	0.293(12)	0.301(13)	0.288(13)	0.334(14)	-0.222(14)	-0.082(13)	0.081(12)	0.122(13)
$P_{3,-3}$	0.0	0.0	-0.124(18)	0.039(16)	-0.045(18)	0.059(13)	-0.048(14)	-0.027(13)	-0.111(14)

Multipoles	C10	C11	C12	C13	C14	C15	C16	C17	C18
$P_{1,+1}$	0.085(16)	-0.108(13)	-0.069(12)	0.0	0.128(13)	0.097(16)	0.109(12)	-0.028(10)	0.138(11)
$P_{1,-1}$	-0.142(14)	0.109(13)	-0.056(13)	-0.084(13)	-0.069(11)	0.0	-0.171(13)	0.0	0.0
$P_{1,0}$	0.026(12)	0.044(11)	0.129(12)	-0.123(12)	-0.123(12)	0.090(11)	-0.101(11)	-0.148(13)	-0.150(12)
$P_{2,0}$	-0.168(10)	0.0	-0.019(10)	-0.031(10)	-0.012(9)	-0.086(10)	0.0	0.046(9)	-0.024(10)
$P_{2,+1}$	0.0	-0.023(8)	0.0	0.046(9)	0.032(9)	-0.019(9)	-0.027(9)	0.018(9)	0.027(9)
$P_{2,-1}$	0.073(10)	-0.035(9)	0.010(8)	-0.018(9)	-0.010(9)	-0.031(9)	0.026(10)	0.055(9)	0.045(9)
$P_{2,+2}$	-0.042(11)	-0.027(9)	0.025(9)	-0.018(9)	-0.064(9)	0.086(8)	0.039(10)	-0.024(8)	-0.047(8)
$P_{2,-2}$	-0.050(10)	-0.041(8)	0.035(8)	-0.014(9)	0.034(9)	-0.016(9)	0.019(9)	-0.021(8)	0.041(9)
$P_{3,0}$	-0.058(18)	0.046(15)	0.055(15)	0.062(15)	0.021(15)	0.0	0.023(13)	-0.038(15)	0.029(14)
$P_{3,+1}$	-0.028(13)	-0.110(13)	-0.171(14)	0.0	-0.018(11)	-0.143(12)	-0.071(13)	0.067(13)	0.058(15)
$P_{3,-1}$	-0.019(14)	0.024(14)	-0.037(14)	0.119(13)	0.103(13)	-0.032(13)	0.042(15)	0.054(15)	0.160(14)
$P_{3,+2}$	-0.098(16)	0.104(14)	-0.051(12)	-0.130(15)	-0.058(13)	0.0	-0.106(16)	0.050(14)	-0.086(14)
$P_{3,-2}$	-0.024(16)	0.280(13)	0.201(13)	0.335(12)	0.327(14)	0.273(14)	0.288(13)	0.283(13)	0.134(12)
$P_{3,+3}$	0.361(14)	-0.110(14)	-0.134(13)	0.051(13)	-0.034(13)	-0.206(15)	-0.082(15)	0.048(11)	0.215(12)
$P_{3,-3}$	0.045(18)	0.099(12)	0.015(13)	-0.117(14)	-0.027(13)	0.036(14)	-0.081(11)	-0.018(12)	-0.117(13)

Table 13. Multipole populations (e^-) of Carbon atoms of 17*a*-estradiol•½H_2O.

Atoms	$P_{1,0}$	$P_{2,0}$
H1O	0.155(14)	0.021(18)
H2O	0.290(15)	0.033(19)
H1	0.128(15)	0.023(19)
H2	0.186(14)	0.038(18)
H4	0.161(14)	0.041(17)
H6A	0.192(9)	0.026(11)
H6B	0.192(9)	0.026(11)
H7A	0.140(8)	0.041(10)
H7B	0.140(8)	0.041(10)
H8	0.139(11)	0.0
H9	0.107(11)	0.015(15)
H11A	0.135(8)	0.057(12)
H11B	0.135(8)	0.057(12)
H12A	0.159(8)	0.043(10)
H12B	0.159(8)	0.043(10)
H14	0.107(13)	0.038(17)
H15A	0.165(9)	0.0
H15B	0.165(9)	0.0
H16A	0.183(9)	0.031(11)
H16B	0.183(9)	0.031(11)
H17	0.193(13)	0.0
H18A	0.134(7)	-0.018(9)
H18B	0.134(7)	-0.018(9)
H18C	0.134(7)	-0.018(9)
H3O	0.141(16)	0.035(23)

Table 14. Multipole populations (e^-) of Hydrogen atoms of 17*a*-estradiol•½H_2O.

Bond	$\rho(r_c)$	$\nabla^2\rho(r_c)$	R_{ij}	d_1	d_2	λ_1	λ_2	λ_3	ε
O1 – C3	2.120	-15.427	1.3757	0.8070	0.5687	-17.48	-15.51	17.57	0.13
O1 – H1O	2.170	-24.028	0.9703	0.7454	0.2249	-33.19	-32.56	41.72	0.02
O2 – C17	1.727	-5.757	1.4367	0.8340	0.6027	-11.99	-11.06	17.30	0.08
O2 – H2O	2.370	-37.913	0.9701	0.7433	0.2267	-37.48	-36.47	36.04	0.03
C1 – C2	2.237	-21.462	1.3953	0.6846	0.7107	-16.78	-14.23	9.54	0.18
C1 – C10	2.179	-20.448	1.4025	0.7211	0.6814	-16.21	-13.30	9.06	0.22
C1 – H1	1.993	-17.855	1.0801	0.6682	0.4119	-18.44	-17.63	18.22	0.05
C2 – C3	2.127	-19.668	1.3965	0.6541	0.7424	-16.14	-13.30	9.77	0.21
C2 – H2	2.059	-19.553	1.0801	0.6492	0.4309	-18.84	-17.27	16.56	0.09
C3 – C4	2.195	-20.099	1.3957	0.6645	0.7313	-17.10	-13.55	10.55	0.26
C4 – C5	2.158	-19.740	1.4048	0.7200	0.6848	-15.80	-13.25	9.31	0.19
C4 – H4	1.797	-16.893	1.0805	0.6243	0.4562	-16.36	-14.58	14.04	0.12
C5 – C6	1.679	-11.363	1.5163	0.7319	0.7844	-11.53	-10.13	10.30	0.14
C5 – C10	2.165	-21.077	1.4113	0.7604	0.6510	-16.47	-13.10	8.49	0.26
C6 – C7	1.728	-10.606	1.5301	0.7886	0.7415	-11.40	-10.59	11.38	0.08
C6 – H6A	1.791	-13.393	1.0901	0.6155	0.4747	-15.37	-12.82	14.79	0.20
C6 – H6B	1.812	-13.339	1.0906	0.6185	0.4721	-15.23	-13.08	14.97	0.16
C7 – C8	1.692	-11.578	1.5280	0.8049	0.7231	-11.55	-10.52	10.49	0.10
C7 – H7A	1.949	-17.580	1.0902	0.6472	0.4431	-17.72	-16.49	16.63	0.07
C7 – H7B	1.778	-14.845	1.0901	0.6271	0.4631	-14.99	-14.84	14.99	0.01
C8 – C9	1.630	-9.845	1.5468	0.8050	0.7419	-10.55	-10.01	10.72	0.05
C8 – C14	1.667	-11.245	1.5278	0.7631	0.7647	-11.17	-10.58	10.50	0.06
C8 – H8	1.880	-14.232	1.1000	0.6681	0.4319	-16.32	-15.97	18.06	0.02
C9 – C10	1.700	-10.657	1.5255	0.7407	0.7848	-11.32	-9.98	10.65	0.13
C9 – C11	1.645	-10.410	1.5394	0.7939	0.7456	-10.79	-10.30	10.68	0.05
C9 – H9	1.825	-14.327	1.1002	0.6682	0.4320	-16.31	-15.61	17.60	0.04

Table 15. Topological properties of bond critical points in 17*a*-estradiol•½H_2O.

Bond	$\rho(r_c)$	$\nabla^2\rho(r_c)$	R_{ij}	d_1	d_2	λ_1	λ_2	λ_3	ε
C11 – C12	1.550	-8.036	1.5406	0.7751	0.7655	-9.84	-9.04	10.84	0.09
C11 – H11A	2.023	-18.370	1.0906	0.6579	0.4326	-18.66	-17.46	17.74	0.07
C11 – H11B	1.965	-16.884	1.0901	0.6517	0.4383	-17.38	-16.77	17.27	0.04
C12 – C13	1.717	-10.751	1.5339	0.7449	0.7889	-10.95	-10.88	11.08	0.01
C12 – H12A	1.890	-16.414	1.0902	0.6346	0.4556	-16.38	-15.72	15.69	0.04
C12 – H12B	2.031	-17.189	1.0903	0.6553	0.4350	-17.75	-17.29	17.85	0.03
C13 – C14	1.632	-9.730	1.5434	0.7366	0.8068	-10.29	-10.06	10.61	0.02
C13 – C17	1.647	-8.917	1.5507	0.7879	0.7628	-11.22	-9.62	11.93	0.17
C13 – C18	1.688	-10.826	1.5436	0.7674	0.7762	-11.27	-10.57	11.02	0.07
C14 – C15	1.647	-9.329	1.5399	0.7335	0.8064	-10.51	-9.95	11.14	0.06
C14 – H14	1.825	-14.820	1.1001	0.6597	0.4403	-16.15	-15.66	16.99	0.03
C15 – C16	1.592	-9.009	1.5578	0.8083	0.7495	-10.37	-9.69	11.05	0.07
C15 – H15A	1.830	-15.696	1.0910	0.6296	0.4613	-16.67	-14.53	15.51	0.15
C15 – H15B	1.918	-15.537	1.0908	0.6429	0.4478	-17.05	-15.35	16.86	0.11
C16 – C17	1.695	-10.605	1.5467	0.8271	0.7196	-11.51	-10.72	11.63	0.07
C16 – H16A	1.889	-16.413()	1.0901	0.6256	0.4644	-16.48	-14.99	15.05	0.10
C16 – H16B	1.918	-15.979()	1.0906	0.6336	0.4570	-16.06	-15.91	15.98	0.01
C17 – H17	1.975	-15.631	1.1004	0.6469	0.4535	-17.73	-16.64	18.74	0.07
C18 – H18A	2.060	-16.196	1.0601	0.6334	0.4267	-18.22	-16.43	18.45	0.11
C18 – H18B	1.851	-13.606	1.0638	0.6195	0.4443	-16.56	-14.36	17.31	0.15
C18 – H18C	1.910	-13.904	1.0605	0.6196	0.4408	-17.12	-14.02	17.24	0.22
O3 – H3O	2.413	-67.609	0.9607	0.7967	0.1640	-51.40	-48.06	31.85	0.07

Table 16. Topological properties of bond critical points in 17*a*-estradiol•½H_2O continued.

Bond	$\rho(r_c)$	$\nabla^2\rho(r_c)$	R_{ij}	d_1	d_2	λ_1	λ_2	λ_3	ε
O1—H1O··O3	0.124	3.237	1.8746	1.2378	0.6367	-0.75	-0.68	4.67	0.11
O2—H2O··O1	0.094	2.431	2.0909	0.7521	1.3388	-0.70	-0.47	3.60	0.49
O3—H3O··O2	0.165	2.371	1.9303	0.6247	1.3056	-0.99	-0.92	4.28	0.08

Table 17. Topological properties of bond critical points in the hydrogen bonds of 17*a*-estradiol•½H_2O.

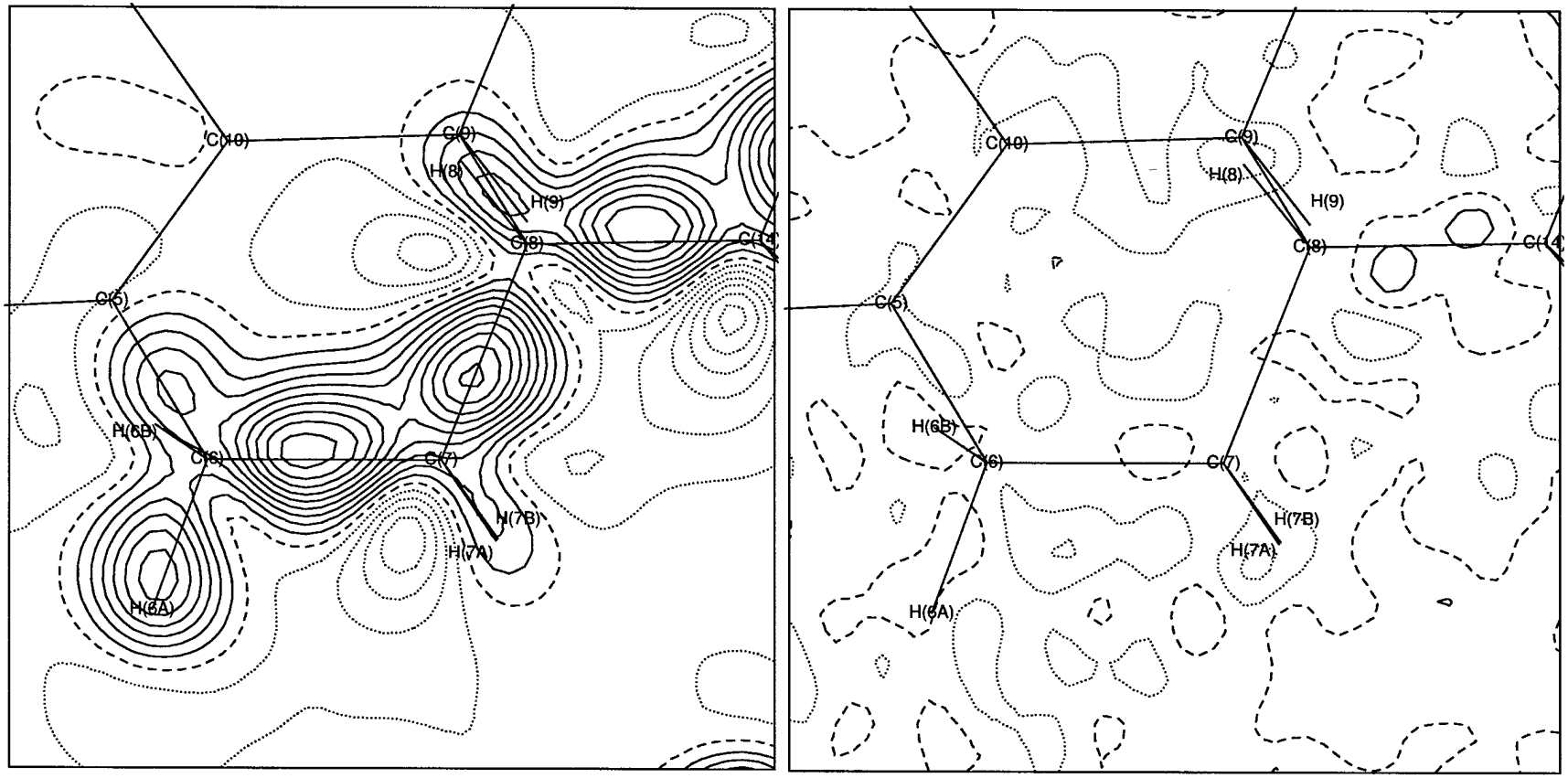

Figure 3. Dynamic model map and residual map in the C6 – C7 – C8 plane of 17*a*-estradiol•½H_2O. Contour intervals are 0.05 $eÅ^{-3}$ with solid lines positive, dashed lines zero, and dotted lines negative.

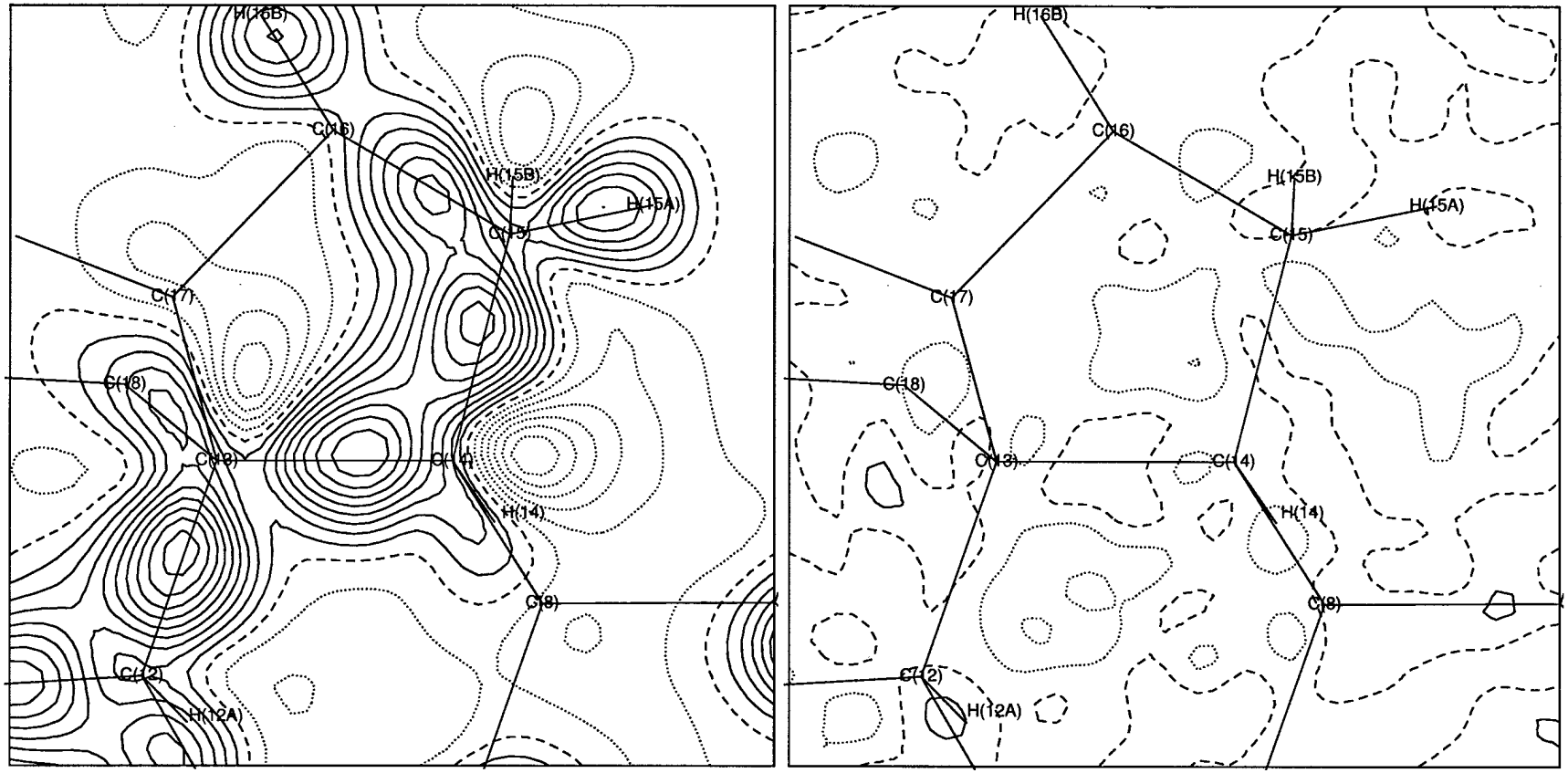

Figure 4. Dynamic model map and residual map in the C13 – C14 – C15 plane of 17*a*-estradiol•½H_2O. Contour intervals are 0.05 e$Å^{-3}$ with solid lines positive, dashed lines zero, and dotted lines negative.

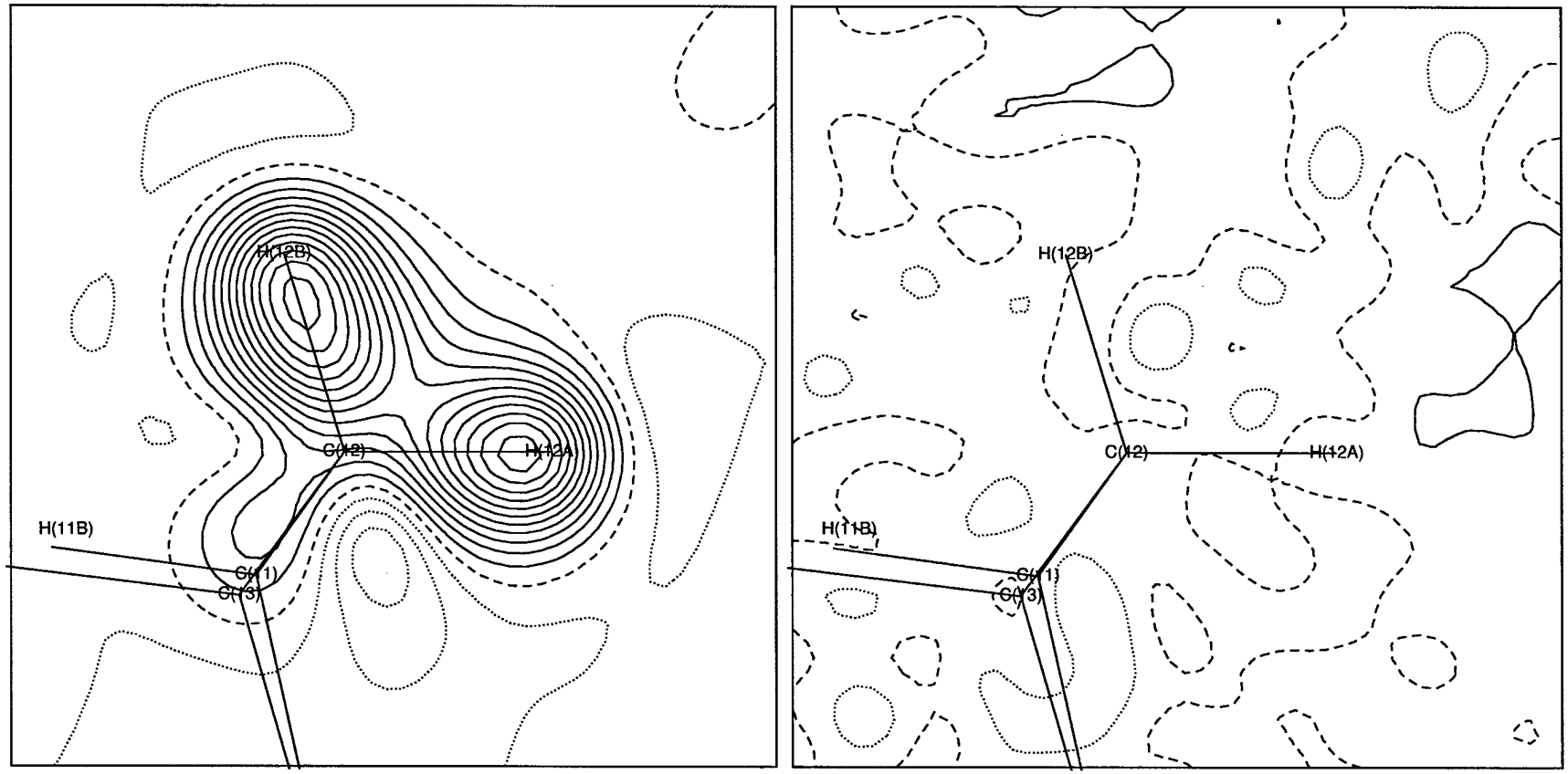

Figure 5. Dynamic model map and residual map in the C12 – H12A – H12B plane of 17*a*-estradiol•½H_2O. Contour intervals are 0.05 eÅ^{-3} with solid lines positive, dashed lines zero, and dotted lines negative.

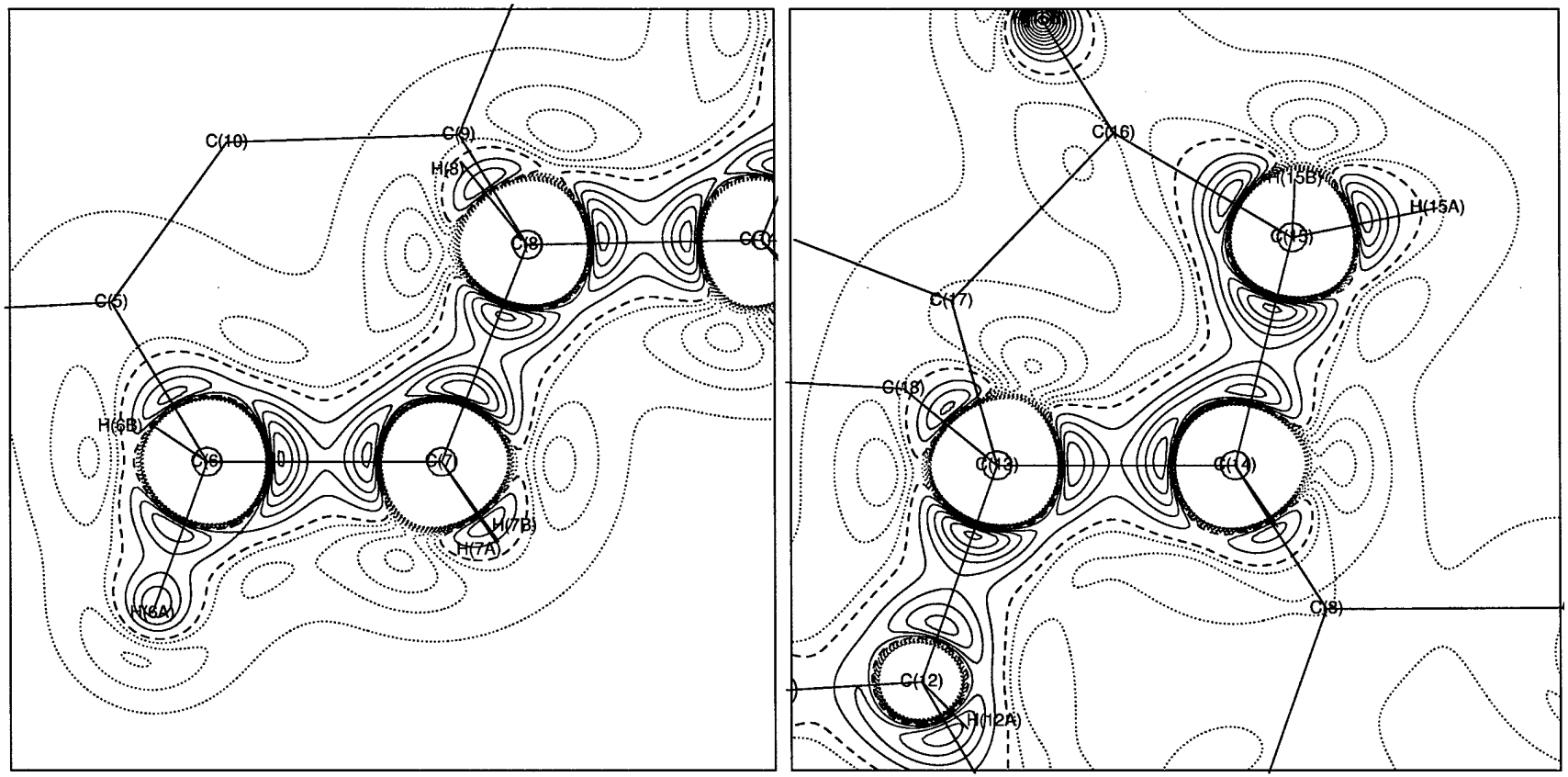

Figure 6. The Laplacian of the total electron density of atoms at rest in the C6 – C7 – C8 and C13 – C14 – C15 planes of 17*a*-estradiol•½H_2O. Contour intervals are 5 eÅ^{-5} starting at 5 eÅ^{-5} (solid blue lines), -2 eÅ^{-5} starting at -2 eÅ^{-5} (dotted red lines), and the dashed line equals 0 eÅ^{-5}.

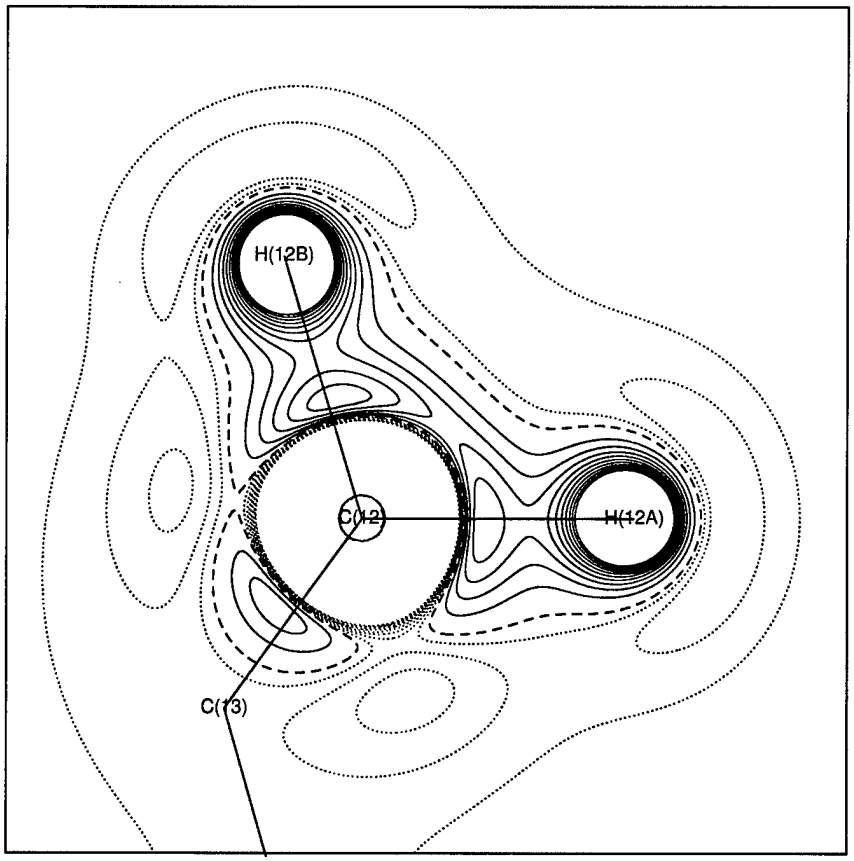

Figure 7. The Laplacian of the total electron density of atoms at rest in the H12A – C12 – H12B plane of 17*a*-estradiol•½H_2O. Contour intervals are 5 e$Å^{-5}$ starting at 5 e$Å^{-5}$ (solid blue lines), -2 e$Å^{-5}$ starting at -2 e$Å^{-5}$ (dotted red lines), and the dashed line plots 0 e$Å^{-5}$.

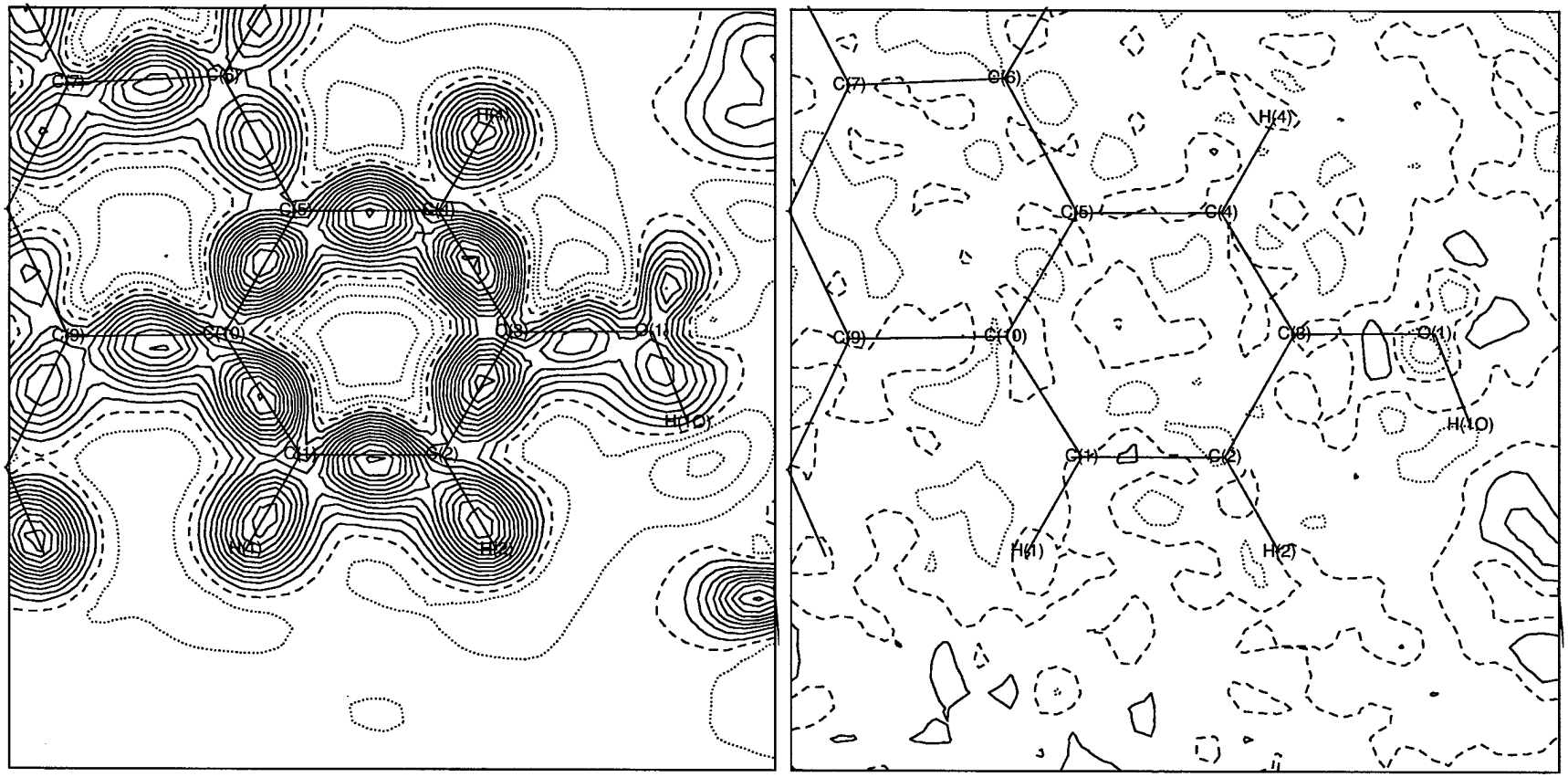

Figure 8. Dynamic model map and residual map in the plane of the aromatic ring of 17*a*-estradiol•½H_2O. Contour intervals are 0.05 e$Å^{-3}$ with solid lines positive, dashed lines zero, and dotted lines negative.

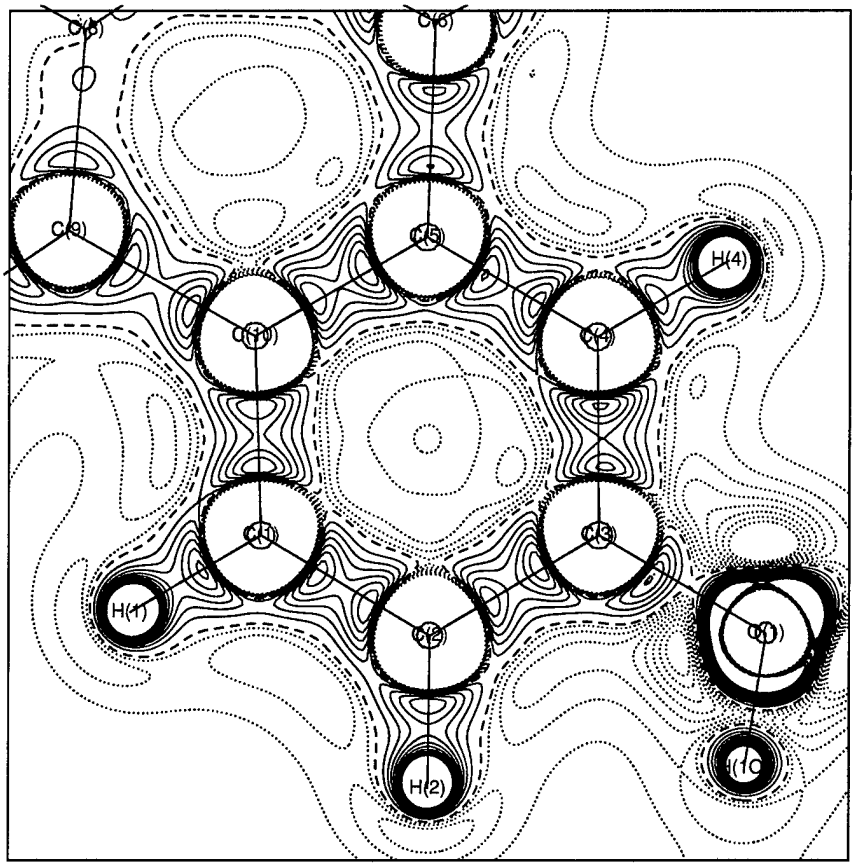

Figure 9. The Laplacian of the total electron density of atoms at rest in the plane of the aromatic ring of 17*a*-estradiol•½H_2O. Contour intervals are 5 eÅ^{-5} starting at 5 eÅ^{-5} (solid blue lines), -2 eÅ^{-5} starting at -2 eÅ^{-5} (dotted red lines), and the dashed line plots 0 eÅ^{-5}.

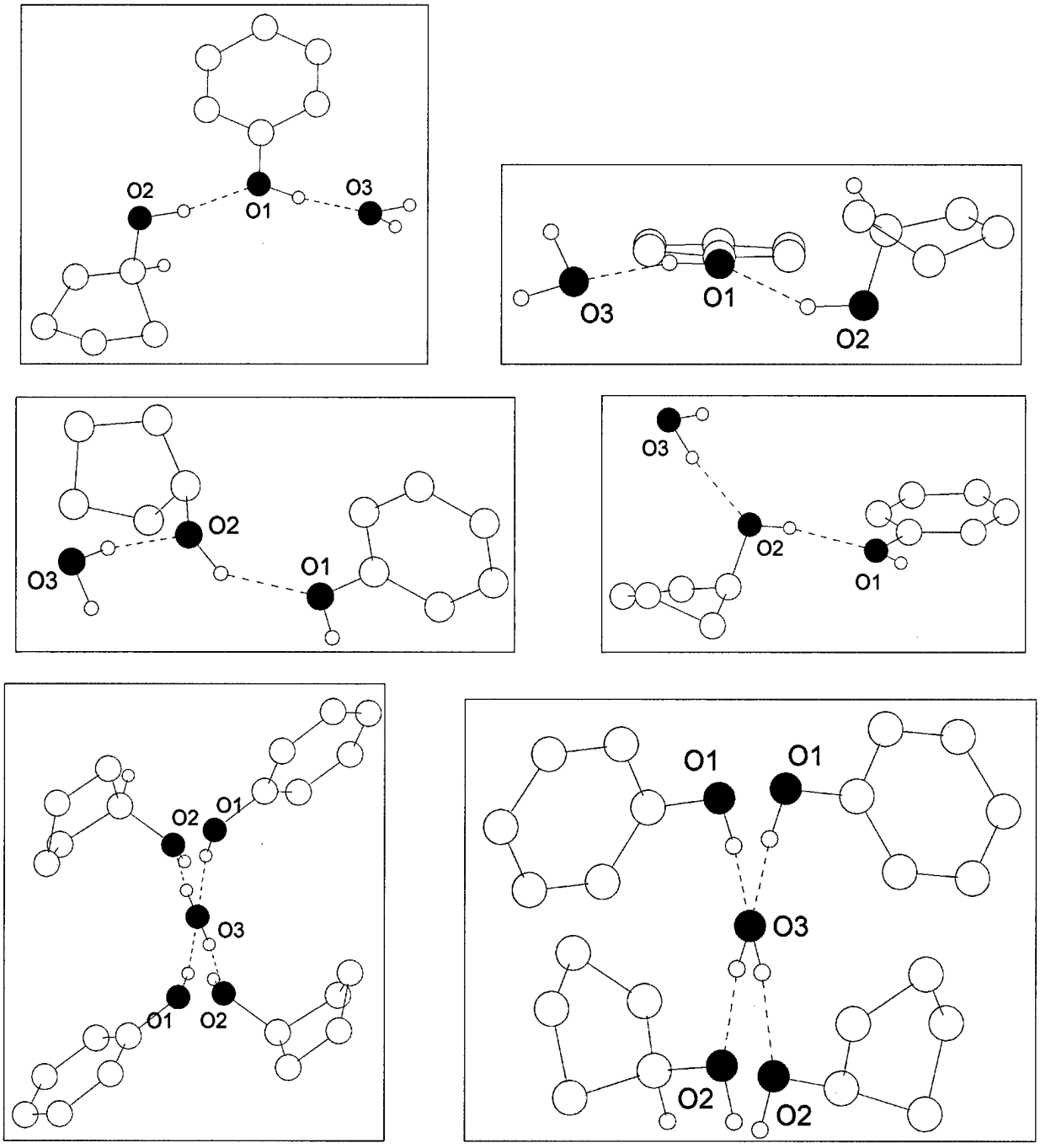

Figure 10. Geometry of hydrogen bonding interactions of 17*a*-estradiol•½H_2O.

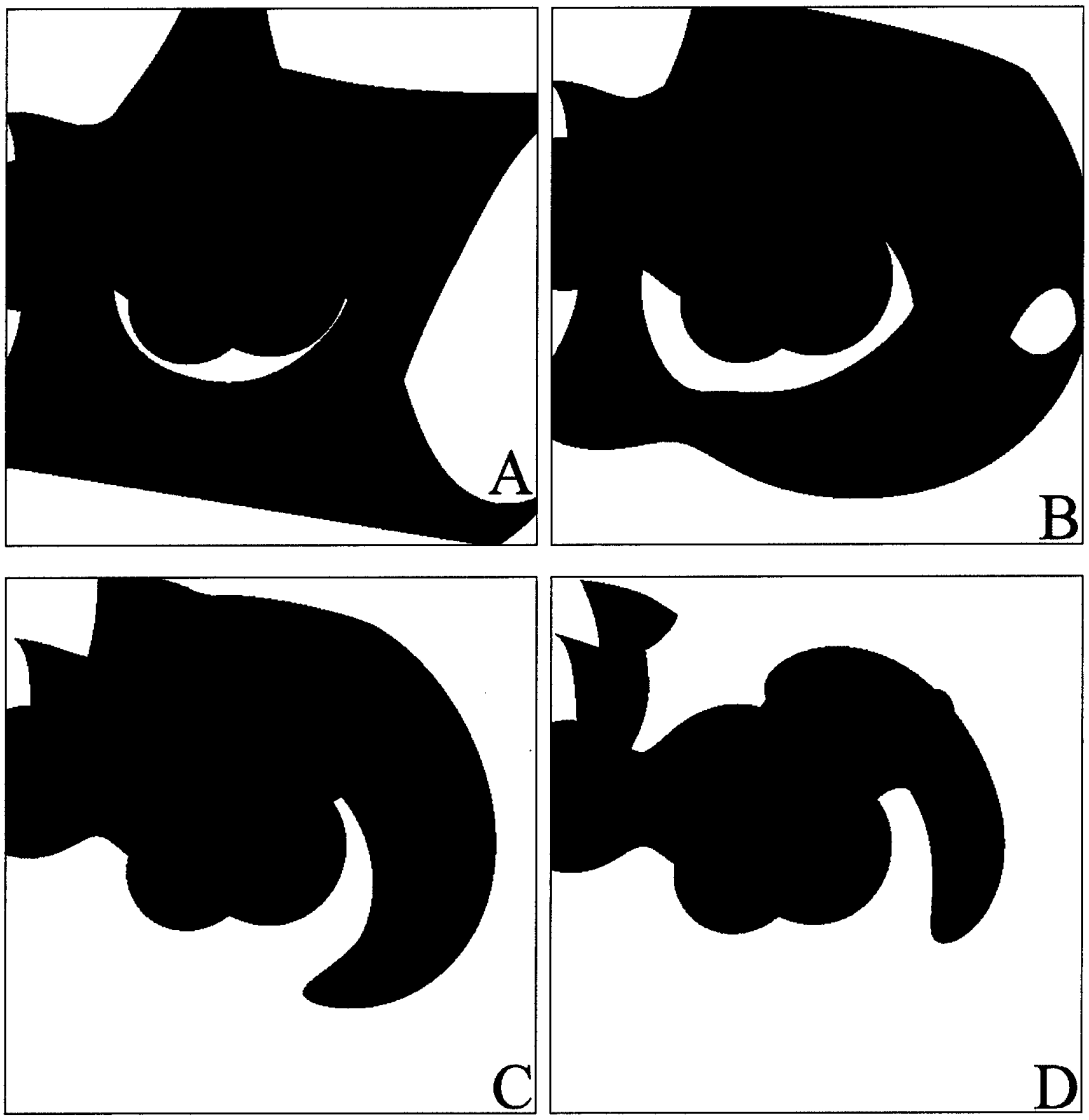

Figure 11. Electrostatic potential isosurfaces of the O1 hydroxy group of $\alpha E_2 \cdot \frac{1}{2}$water. The blue surface in each picture represents +1.0 eÅ^{-1}. The red surfaces represent the following potentials: A –0.05 eÅ^{-1}, B –0.10 eÅ^{-1}, C –0.15 eÅ^{-1}, D –0.20 eÅ^{-1}.

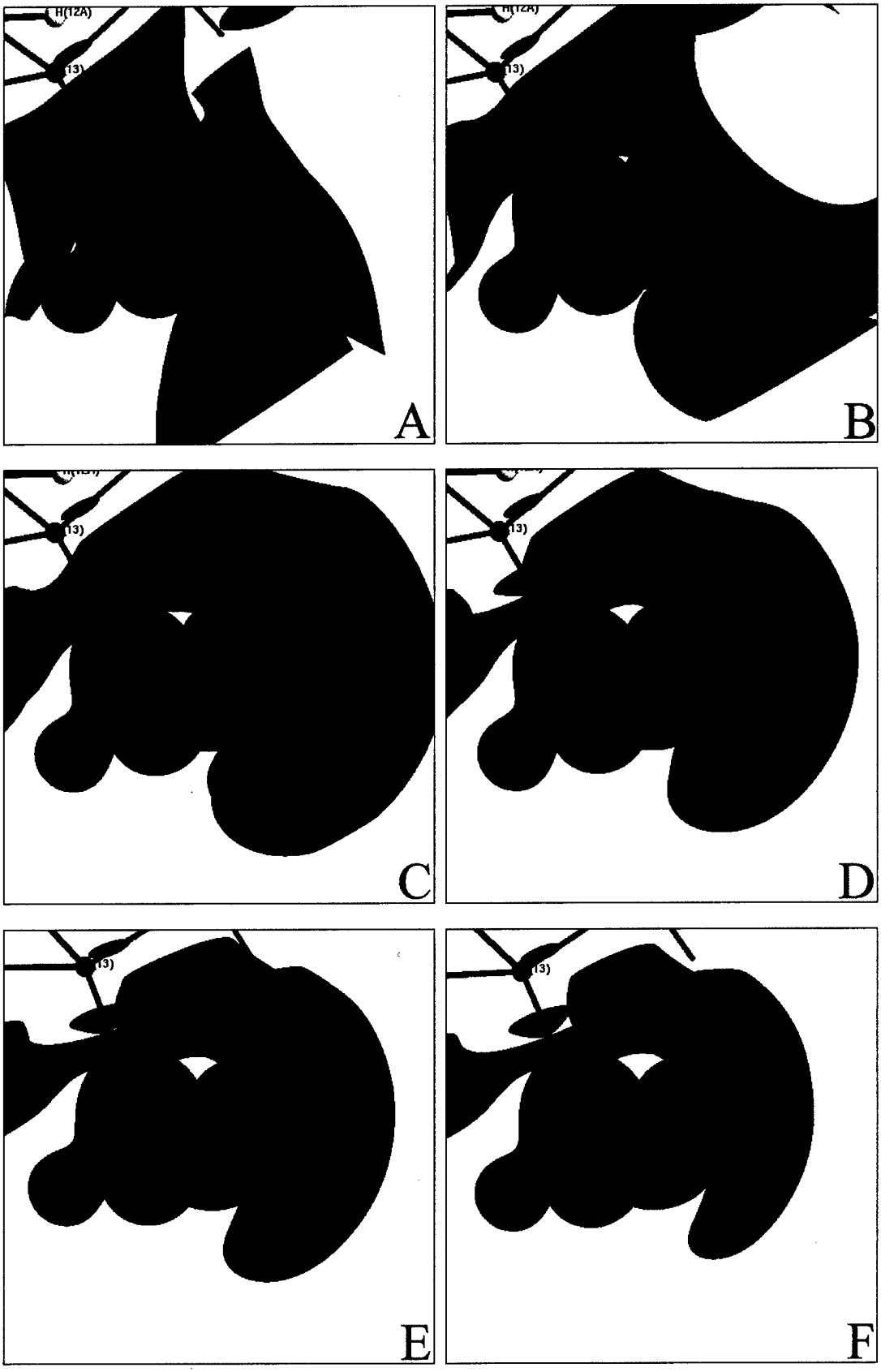
A
B
C
D
E
F

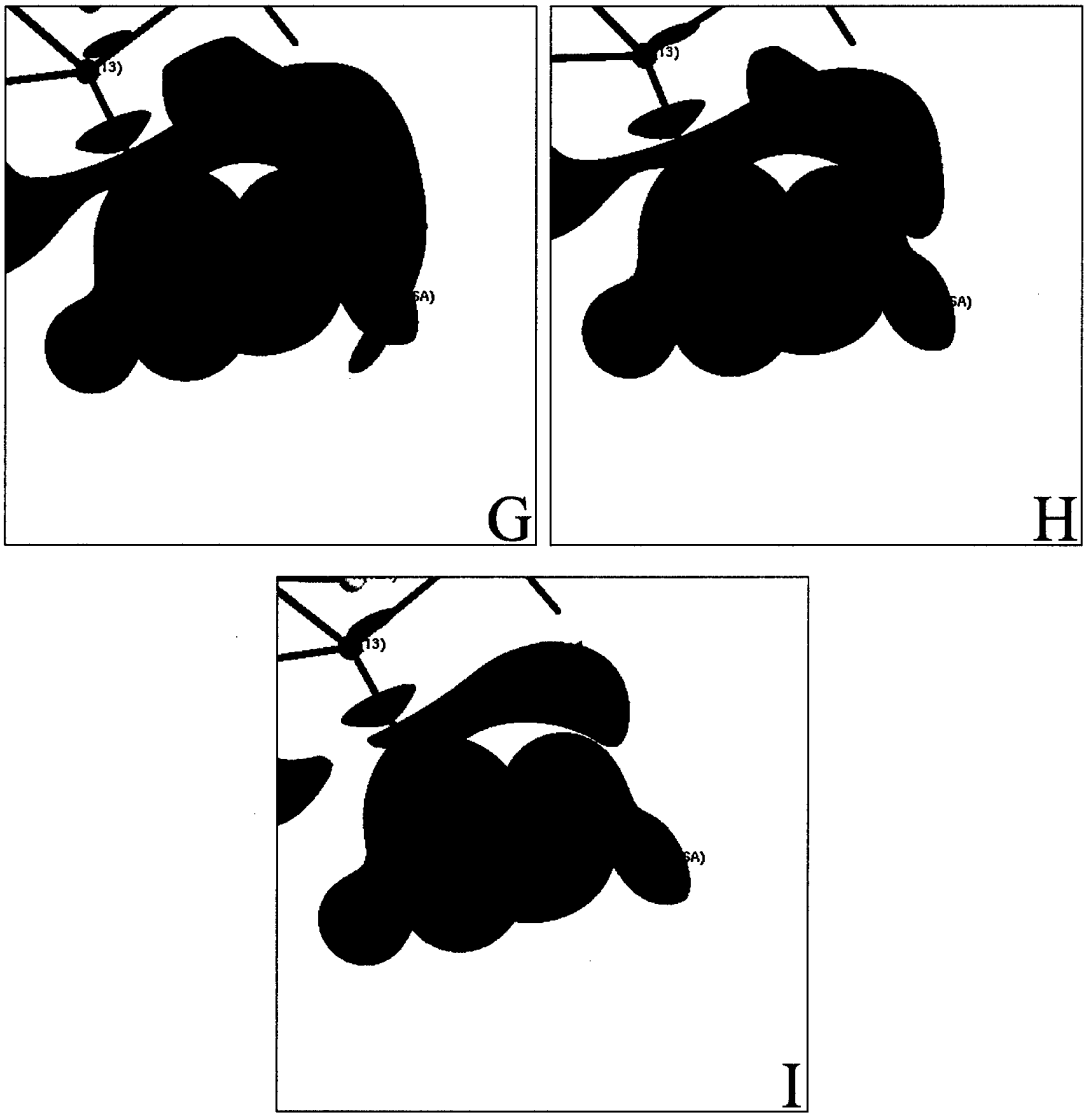

Figure 12. Electrostatic potential isosurfaces of the O2 hydroxy group of $\alpha E_2 \cdot \frac{1}{2}$water. The blue surface in each picture represents +1.0 eÅ^{-1}. The red surfaces represent the following potentials: A –0.05 eÅ^{-1}, B –0.10 eÅ^{-1}, C –0.15 eÅ^{-1}, D –0.20 eÅ^{-1}, E –0.25 eÅ^{-1}, F –0.30 eÅ^{-1}, G –0.35 eÅ^{-1}, H –0.40 eÅ^{-1}, I –0.45 eÅ^{-1}.

Appendix E.

Crystal structure and charge density analysis of 17α-estradiol

17α-ESTRADIOL

Data collection, Processing, conventional and multipole refinement Details.

Unit Cell parameters

a=7.1176(9)Å b=23.2881(29)Å c=9.0614(11)Å β=98.985(3)°

$P2_1$ Z=4

Radiation used: Mo

Data processing

Saint integration

Sadabs 2.03 Ver.

Sortav scaling and averaging

Scaling

I	SCALEK(I)	SIGMAK(I)	R(I)	Z(I)	NDATA(I)
1	1.00000	0.00000	0.0389	1.018	4701
2	1.00994	0.00086	0.0389	1.034	4720
3	1.02345	0.00088	0.0386	1.026	4673
4	1.03665	0.00087	0.0387	1.028	4717
5	1.03349	0.00086	0.0384	1.032	4706
6	1.02760	0.00089	0.0386	1.027	4733
7	1.01383	0.00089	0.0376	1.021	4716
8	1.00551	0.00086	0.0379	1.015	4731
9	1.01740	0.00093	0.0452	0.899	7780
10	1.02698	0.00097	0.0423	0.856	7541
11	1.03336	0.00096	0.0468	0.947	7198
12	1.01940	0.00097	0.0359	0.927	4915
13	1.01988	0.00093	0.0421	0.900	7764
14	1.03243	0.00091	0.0395	0.852	7635
15	1.01698	0.00138	0.0598	0.939	4088

99238 TOTAL MEASUREMENTS

2 MEASUREMENTS REJECTED AS ABNORMAL OULIERS

99236 MEASUREMENTS ACCEPTED

3164 UNIQUE DATA MEASURED ONLY ONCE

3626 UNIQUE DATA MEASURED TWICE

14692 UNIQUE DATA MEASURED THREE OR MORE TIMES

21482 UNIQUE DATA

	NTERMS	NMEANS	<N>	R1	R2	RW	Z
ALL DATA	96072	18318	5.2	0.0288	0.0233	0.0863	1.083
Q > 0	96008	18294	5.2	0.0288	0.0233	0.0862	1.083
Q > 1	94579	17943	5.3	0.0285	0.0233	0.0835	1.070
Q > 2	91107	17017	5.4	0.0280	0.0233	0.0775	1.041
Q > 3	86715	15890	5.5	0.0274	0.0232	0.0712	1.015
Q > 4	82101	14781	5.6	0.0268	0.0232	0.0653	0.993
Q > 6	73564	12735	5.8	0.0257	0.0232	0.0559	0.955

BIVARIATE ANALYSIS OF VARIANCE

<Q>, Q = RMSD(Y)/ESD(Y)
<E>, E = ESD(Y)
<Y>, Y = F OR F^2
<S>, S = SIN(THETA)/LAMBDA
N, N = NUMBER OF UNIQUE DATA

0.93	0.90	0.90	0.92	0.81	0.83	0.88	0.92	0.98	1.03
0.317E+01	0.162E+01	0.133E+01	0.130E+01	0.109E+01	0.986E+00	0.972E+00	0.871E+00	0.809E+00	0.796E+00
0.163E+03	0.408E+02	0.220E+02	0.206E+02	0.167E+02	0.119E+02	0.108E+02	0.754E+01	0.572E+01	0.514E+01
0.332	0.504	0.599	0.671	0.732	0.785	0.833	0.877	0.918	0.941
2147	2149	2147	2105	1983	1931	1893	1843	1815	305

SHELX-refinement

R1 = 0.0496 for 19870 Fo > 4sig(Fo) and 0.0550 for all 21482 data
wR2 = 0.1092, GooF =1.167,

17-α ESTRADIOL

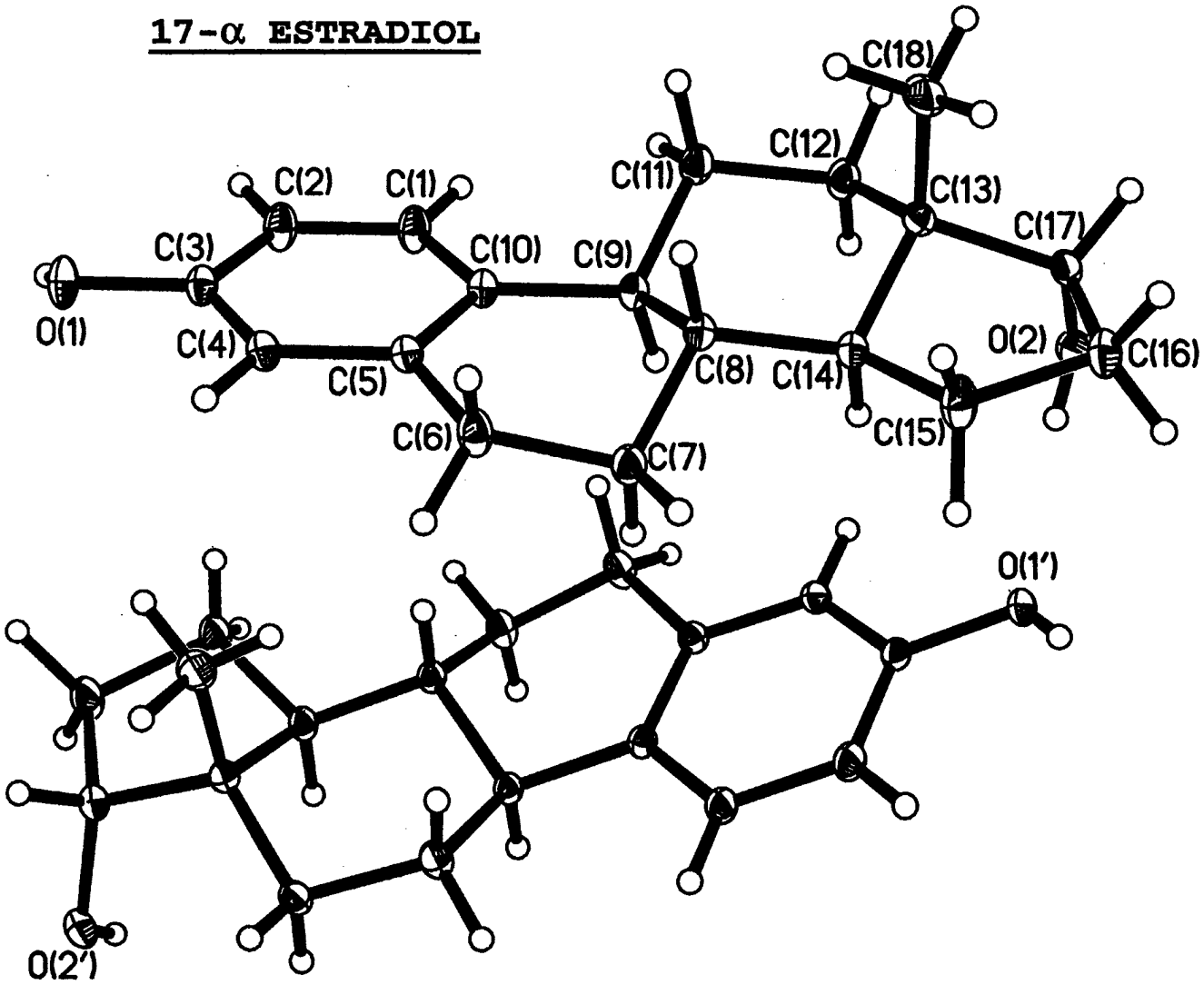

MODEL 1

(Kappa values K_{CH} & K_{OH}= 1.2)

XD-refinement

Resolution Used $(\sin\theta/\lambda)_{max}$=1.059Å^{-1}

R(F) = 0.0347	Rall(F) = 0.0460	Rw(F) = 0.0336
$R(F^2)$ = 0.0384	$Rall(F^2)$ = 0.0414	$Rw(F^2)$= 0.0601
GOFw = 1.1113	GOF = 1.1113	Nref/Nv=18.5587

Refined First Kappa values

	κ	κ' (fixed)
O1, O2	0.983	1.16
C3	1.002	0.92
C16,C17	1.004	0.95
C1,C2,C4	0.980	0.92
C5,C10	0.974	0.87
C6,C7,C8,C9,C11, C12,C13,C14,C15	0.986	0.95
H-atoms	OH: 1.2	0.29
	CH: 1.2	0.29

Differences of Mean-Squares Displacement Amplitudes (DMSDA) (1.E4 A2) along interatomic vectors (*bonds)**

ATOM-->	ATOM	/	DIST	DMSDA	ATOM	/	DIST	DMSDA	ATOM	/	DIST	DMSDA
Molecule 1												
O(1)	C(3)	*	1.3729	1								
O(2)	C(17)	*	1.4361	10								
C(1)	C(2)	*	1.3948	2	C(10)	*	1.4021	-1				
C(2)	C(3)	*	1.3966	1								
C(3)	C(4)	*	1.3883	-3								
C(4)	C(5)	*	1.3991	-5								
C(5)	C(6)	*	1.5107	10	C(10)	*	1.4066	0				
C(6)	C(7)	*	1.5258	7								
C(7)	C(8)	*	1.5270	-5								
C(8)	C(9)	*	1.5426	-4	C(14)	*	1.5263	-1				
C(9)	C(10)	*	1.5261	-6	C(11)	*	1.5416	3				
C(11)	C(12)	*	1.5392	-3								
C(12)	C(13)	*	1.5260	1								
C(13)	C(14)	*	1.5416	0	C(17)	*	1.5447	-3	C(18)	*	1.5381	19
C(14)	C(15)	*	1.5347	1								
C(15)	C(16)	*	1.5570	1								
C(16)	C(17)	*	1.5514	11								
Molecule 2												
O(1')	C(3')	*	1.3654	-12								
O(2')	C(17')	*	1.4332	9								
C(1')	C(2')	*	1.3926	9	C(10')	*	1.4010	-9				
C(2')	C(3')	*	1.3943	3								
C(3')	C(4')	*	1.3906	-11								
C(4')	C(5')	*	1.3960	2								
C(5')	C(6')	*	1.5130	7	C(10')	*	1.4074	-4				
C(6')	C(7')	*	1.5252	2								
C(7')	C(8')	*	1.5239	-1								
C(8')	C(9')	*	1.5436	2	C(14')	*	1.5232	-3				
C(9')	C(10')	*	1.5265	-1	C(11')	*	1.5378	6				
C(11')	C(12')	*	1.5384	-3								

```
C(8')    C(9')    * 1.5440     3 C(14')   * 1.5234    -2
C(9')    C(10')   * 1.5267     0 C(11')   * 1.5378     6
C(11')   C(12')   * 1.5384    -2
C(12')   C(13')   * 1.5265    -4
C(13')   C(14')   * 1.5405    -2 C(17')   * 1.5448     7 C(18')   * 1.5395     2
C(14')   C(15')   * 1.5297     1
C(15')   C(16')   * 1.5490     1
C(16')   C(17')   * 1.5517     6
-------------------------------------------------------------------------------
```

Monopole populations from the multipole refinement

Atom	Mol 1	Mol 2		Atom	Mol1	Mol2
O1	-0.33	-0.43		H1A	0.18	0.20
O2	-0.46	-0.42		H2A	0.16	0.22
C1	-0.19	-0.23		H1	0.29	0.29
C2	-0.28	-0.33		H2	0.21	0.20
C3	0.15	0.10		H4	0.21	0.19
C4	-0.25	-0.27		H6A=H6B	0.20	0.23
C5	-0.13	-0.13		H7A=H7B	0.22	0.23
C6	-0.29	-0.25		H8	0.19	0.23
C7	-0.32	-0.26		H9	0.20	0.18
C8	-0.19	-0.17		H11A=H11B	0.20	0.20
C9	-0.16	-0.14		H12A=H12B	0.22	0.23
C10	-0.09	-0.17		H14	0.21	0.19
C11	-0.30	-0.32		H15A=H15B	0.20	0.18
C12	-0.34	-0.31		H16A=H16B	0.19	0.14
C13	-0.21	-0.28		H17	0.12	0.13
C14	-0.24	-0.16		H18A=H18B=H18C	0.13	0.19
C15	-0.33	-0.35				
C16	-0.35	-0.39				
C17	0.17	0.16				
C18	-0.48	-0.43				

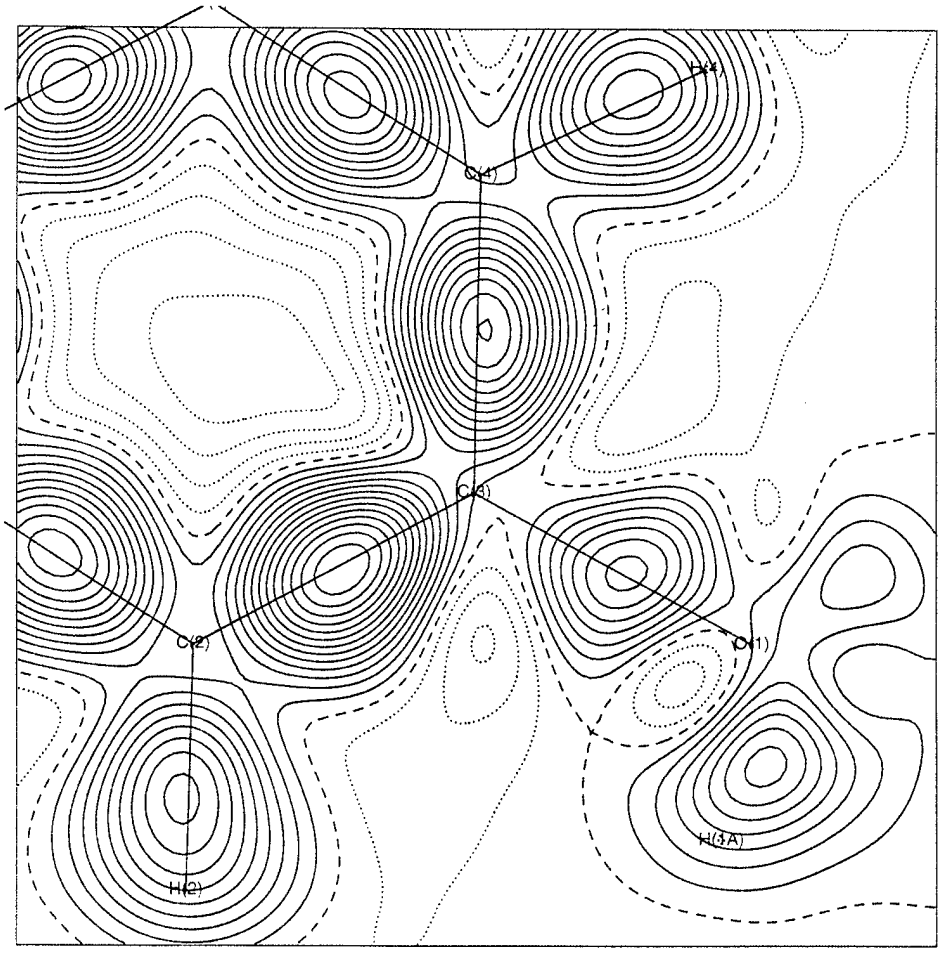

Figure 1. Model multipole deformation electron density in the aromatic ring plane. Contour interval is 0.05 eA^{-3}.

Bond critical points in α- estradiol

Bond	ρ	$\nabla^2\rho$	ε		ρ	$\nabla^2\rho$	ε
C3-O1	2.10	-21.9	0.12	------	2.32	-23.3	0.10
C17-O2	1.85	-12.6	0.11		1.97	-11.7	0.06
A-ring							
C1-C2	2.23	-22.4	0.32		2.30	-23.4	0.19
C2-C3	2.32	-25.6	0.29		2.28	-23.4	0.31
C3-C4	2.24	-24.2	0.35		2.34	-26.2	0.22
C5-C10	2.20	-22.6	0.34		2.23	-23.7	0.32
C1-C10	2.21	-23.3	0.33		2.24	-23.5	0.20
B-ring							
C5-C6	1.82	-14.2	0.07		1.75	-12.8	0.22
C6-C7	1.69	-11.2	0.12		1.73	-13.2	0.03
C7-C8	1.65	-11.6	0.10		1.73	-13.6	0.04
C8-C9	1.62	-12.4	0.06		1.63	-11.1	0.04
C9-C10	1.76	-14.9	0.14		1.69	-12.5	0.16
C & D-ring							
C9-C11	1.64	-11.0	0.13		1.67	-11.8	0.12
C11-C12	1.67	-11.5	0.03		1.67	-10.8	0.08
C12-C13	1.70	-12.1	0.09		1.80	-12.2	0.03
C13-C14	1.63	-11.2	0.03		1.70	-11.4	0.06
C14-C15	1.66	-10.7	0.05		1.65	-10.5	0.07
C15-C16	1.52	-9.6	0.13		1.64	-10.4	0.09
C16-C17	1.57	-9.1	0.06		1.66	-11.1	0.01
C17-C13	1.69	-11.9	0.15		1.60	-10.4	0.02
C13-C18	1.75	-10.4	0.09		1.81	13.1	0.06
	ρ	$\nabla^2\rho$	ε		ρ	$\nabla^2\rho$	ε
O1-H1A	2.45	-32.8	0.01	------	2.41	-34.3	0.03
O2-H2A	2.65	-37.5	0.04		2.76	-47.6	0.04
C1-H1	1.86	-21.0	0.10		1.84	-18.8	0.08
C2-H2	1.87	-18.0	0.09		1.88	-18.6	0.09
C4-H4	1.88	-19.6	0.12		1.90	-19.6	0.11
C6-H6A	1.80	-16.2	0.06		1.84	-17.6	0.08
C6-H6B	1.74	-13.8	0.07		1.77	-16.2	0.06
C7-H7A	1.82	-16.9	0.02		1.89	-18.0	0.06
C7-H7B	1.74	-14.9	0.11		1.76	-16.3	0.07
C8-H8	1.78	-13.2	0.04		1.77	-17.0	0.01
C9-H9	1.81	-15.6	0.01		1.83	-16.0	0.02
C11-H11A	1.73	-14.3	0.05		1.80	-15.0	0.02
C11-H11B	1.78	-14.7	0.08		1.89	-17.7	0.06
C12-H12A	1.74	-14.9	0.04		1.87	-18.0	0.02
C12-H12B	1.81	-12.2	0.06		1.82	-17.3	0.03
C14-H14	1,87	-18.2	0.06		1.83	-16.4	0.03
C15-H15A	1.70	-14.3	0.05		1.82	-15.9	0.10
C15-H15B	1.76	-15.2	0.08		1.74	-14.7	0.08
C16-H16A	1.88	-18.2	0.06		1.79	-14.8	0.19
C16-H16B	1.85	-17.6	0.03		1.83	-16.3	0.14
C17-H17	1.91	-18.5	0.04		1.80	-16.7	0.03
C18-H18A	1.82	-12.3	0.14		1.95	-19.3	0.03
C18-H18B	1.63	-8.8	0.15		1.85	-16.5	0.15
C18-H18C	1.81	-13.7	0.14		1.93	-18.5	0.10

MODEL 2

(Kappa values K_{CH} =1.4, K_{OH}=1.3)

Xd-refinement

Resolution Used $(\sin\theta/\lambda)_{max}$=1.059Å^{-1}

R{ F } = 0.0350	Rall{ F } = 0.0464	Rw{ F } =	0.0337
R{ F^2} = 0.0397	Rall{F^2} = 0.0426	Rw{ F^2} =	0.0604
GOFw = 1.1160	GOF = 1.1160	Nref/Nv =	18.5587

Refined first Kappa values

		κ	κ' (fixed)
O1, O2		0.984	1.16
C3		1.001	0.92
C16,C17		1.008	0.95
C1,C2,C4		0.974	0.92
C5,C10		0.975	0.87
C6,C7,C8,C9,C11, C12,C13,C14,C15		0.984	0.95
H-atoms	OH:	1.3	0.29
	CH:	1.4	0.29

Differences of Mean-Squares Displacement Amplitudes (DMSDA)
(1.E4 A**2) along interatomic vectors (*bonds)

ATOM-->	ATOM	/	DIST	DMSDA	ATOM	/	DIST	DMSDA	ATOM	/	DIST	DMSDA
Molecule 1												
O(1)	C(3)	*	1.3728	4								
O(2)	C(17)	*	1.4361	12								
C(1)	C(2)	*	1.3948	2	C(10)	*	1.4023	-1				
C(2)	C(3)	*	1.3966	2								
C(3)	C(4)	*	1.3883	-3								
C(4)	C(5)	*	1.3990	-5								
C(5)	C(6)	*	1.5108	8	C(10)	*	1.4068	0				
C(6)	C(7)	*	1.5259	7								
C(7)	C(8)	*	1.5272	-5								
C(8)	C(9)	*	1.5428	-4	C(14)	*	1.5264	-1				
C(9)	C(10)	*	1.5261	-6	C(11)		1.5420	3				
C(11)	C(12)	*	1.5393	-3								
C(12)	C(13)	*	1.5260	1								
C(13)	C(14)	*	1.5417	0	C(17)	*	1.5447	-3	C(18)	*	1.5382	19
C(14)	C(15)	*	1.5347	1								
C(15)	C(16)	*	1.5570	1								
C(16)	C(17)	*	1.5512	12								
Molecule 2												
O(1')	C(3')	*	1.3655	-10								
O(2')	C(17')	*	1.4332	10								
C(1')	C(2')	*	1.3927	8	C(10')	*	1.4011	-8				
C(2')	C(3')	*	1.3943	3								
C(3')	C(4')	*	1.3906	-9								
C(4')	C(5')	*	1.3960	2								
C(5')	C(6')	*	1.5131	6	C(10')	*	1.4076	-3				
C(6')	C(7')	*	1.5254	3								
C(7')	C(8')	*	1.5242	-1								

```
C(12')   C(13')  * 1.5266    -4
C(13')   C(14')  * 1.5401    -3 C(17')  * 1.5447     8 C(18')  * 1.5396     3
C(14')   C(15')  * 1.5295     2
C(15')   C(16')  * 1.5490     2
C(16')   C(17')  * 1.5514     4
-------------------------------------------------------------------------------
```

Monopole populations from the multipole refinement

Atom	Mol 1	Mol 2		Atom	Mol1	Mol2
O1	-0.29	-0.41		H1A	0.18	0.19
O2	-0.44	-0.38		H2A	0.11	0.15
C1	-0.13	-0.18		H1	0.27	0.27
C2	-0.19	-0.24		H2	0.16	0.17
C3	0.19	0.12		H4	0.19	0.16
C4	-0.13	-0.20		H6A=H6B	0.15	0.19
C5	-0.12	-0.12		H7A=H7B	0.18	0.18
C6	-0.23	-0.19		H8	0.16	0.21
C7	-0.27	-0.21		H9	0.16	0.15
C8	-0.15	-0.11		H11A=H11B	0.14	0.14
C9	-0.12	-0.10		H12A=H12B	0.17	0.18
C10	-0.09	-0.16		H14	0.19	0.17
C11	-0.24	-0.29		H15A=H15B	0.17	0.15
C12	-0.28	-0.28		H16A=H16B	0.16	0.10
C13	-0.16	-0.24		H17	0.10	0.12
C14	-0.20	-0.11		H18A=H18B=H18C	0.07	0.14
C15	-0.26	-0.26				
C16	-0.28	-0.30				
C17	0.17	0.18				
C18	-0.44	-0.41				

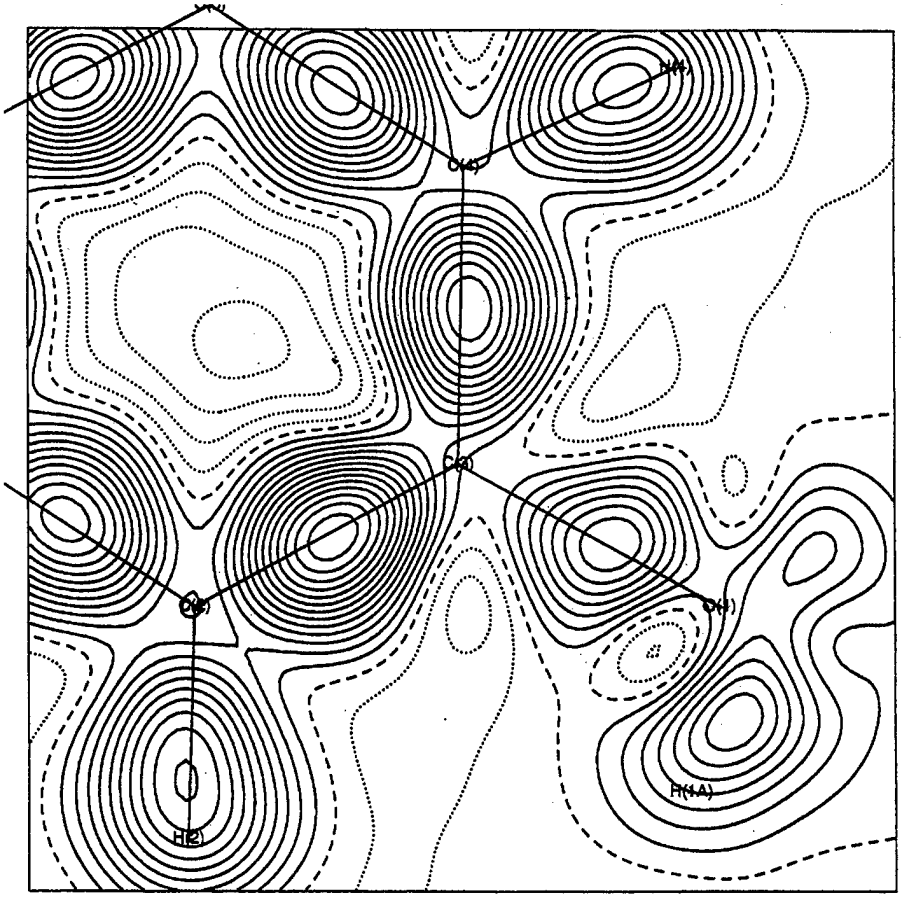

Figure 2. Model multipole deformation electron density in the aromatic ring plane. Contour interval is 0.05 eA^{-3}.

U_{iso} for the hydrogen atoms

Atom	Mol1	Mol2
H1A	0.048	0.048
H2A	0.050	0.047
H1	0.042	0.043
H2	0.050	0.050
H4	0.047	0.048
H6A	0.052	0.054
H6B	0.049	0.045
H7A	0.042	0.047
H7B	0.053	0.045
H8	0.038	0.041
H9	0.041	0.045
H11A	0.057	0.044
H11B	0.045	0.035
H12A	0.041	0.037
H12B	0.051	0.044
H14	0.046	0.043
H15A	0.051	0.060
H15B	0.055	0.049
H16A	0.047	0.055
H16B	0.050	0.067
H17	0.043	0.046
H18A	0.064	0.046
H18B	0.061	0.051
H18C	0.050	0.053

Multipole populations

Atom	Mol 1			Mol 2			Atom	Mol1	Mol2
	20	33+	32-	20	33+	32-		D10	D10
C1	-0.19	0.33		-0.29	0.32		H1A	0.18	0.14
C2	-0.22	0.33		-0.23	0.31		H2A	0.17	0.24
C3	-0.15	0.38		-0.19	0.36		H1	0.21	0.13
C4	-0.19	0.33		-0.25	0.33		H2	0.09	0.15
C5	-0.25	0.36		-0.19	0.39		H4	0.15	0.18
C6			0.33			0.35	H6A=H6B	0.12	0.16
C7			0.34			0.35	H7A=H7B	0.12	0.13
C8			0.39			0.41	H8	0.02	0.12
C9			0.43			0.35	H9	0.06	0.14
C10	-0.24	0.43		-0.24	0.40		H11A=H11B	0.11	0.11
C11			0.29			0.36	H12A=H12B	0.07	0.18
C12			0.34			0.32	H14	0.16	0.15
C13			0.41			0.26	H15A=H15B	0.08	0.13
C14			0.36			0.32	H16A-H16B	0.14	0.18
C15			0.31			0.18	H17	0.17	0.16
C16			0.36			0.30	H18A=B=C	0.07	0.17
C17			0.31			0.29			
C18			0.13			0.24			

Bond critical points in α- estradiol

Bond	ρ	$\nabla^2\rho$	ε		ρ	$\nabla^2\rho$	ε
C3-O1	2.10	-20.3	0.12	-----	2.27	-22.6	0.10
C17-O2	1.82	-11.7	0.12		1.94	-10.4	0.10
A-ring							
C1-C2	2.22	-22.1	0.29		2.28	-23.0	0.19
C2-C3	2.32	-24.7	0.27		2.26	-22.5	0.29
C3-C4	2.23	-23.3	0.32		2.33	-24.8	0.20
C5-C10	2.20	-22.0	0.32		2.19	-22.0	0.31
C1-C10	2.20	-22.6	0.30		2.22	-22.5	0.20
B-ring							
C5-C6	1.81	-13.9	0.09		1.75	-13.1	0.21
C6-C7	1.70	-11.4	0.09		1.71	-12.4	0.05
C7-C8	1.64	-10.7	0.08		1.72	-12.7	0.02
C8-C9	1.62	-11.8	0.04		1.63	-10.5	0.04
C9-C10	1.77	-14.2	0.14		1.69	-12.1	0.14
C & D-ring							
C9-C11	1.63	-10.4	0.12		1.66	-11.2	0.11
C11-C12	1.66	-11.1	0.03		1.64	-10.2	0.08
C12-C13	1.68	-11.5	0.10		1.76	-11.4	0.03
C13-C14	1.62	-10.6	0.03		1.69	-10.6	0.07
C14-C15	1.65	-10.0	0.04		1.67	-10.3	0.07
C15-C16	1.49	-8.7	0.16		1.64	-9.9	0.06
C16-C17	1.55	-8.2	0.05		1.64	-10.0	0.01
C17-C13	1.67	-10.9	0.17		1.62	-9.8	0.01
C13-C18	1.73	-10.1	0.06		1.78	12.4	0.06
	ρ	$\nabla^2\rho$	ε		ρ	$\nabla^2\rho$	ε
O1-H1A	2.61	-23.7	0.02	-----	2.59	-27.3	0.03
O2-H2A	2.74	-28.9	0.04		2.78	-38.5	0.04
C1-H1	1.93	-20.1	0.11		1.97	-17.9	0.08
C2-H2	1.92	-16.0	0.10		1.93	-17.1	0.10
C4-H4	1.94	-17.7	0.13		1.97	-18.9	0.10
C6-H6A	1.86	-14.6	0.07		1.91	-16.2	0.11
C6-H6B	1.79	-12.4	0.10		1.84	-14.7	0.06
C7-H7A	1.87	-15.1	0.01		1.92	-15.4	0.08
C7-H7B	1.81	-13.2	0.12		1.80	-14.2	0.09
C8-H8	1.86	-11.4	0.05		1.87	-16.3	0.02
C9-H9	1.87	-14.3	0.01		1.92	-15.4	0.01
C11-H11A	1.78	-12.5	0.05		1.82	-13.2	0.03
C11-H11B	1.82	-12.5	0.10		1.93	-15.8	0.08
C12-H12A	1.80	-12.4	0.05		1.93	-16.7	0.02
C12-H12B	1.79	-12.3	0.07		1.90	-16.5	0.04
C14-H14	1.97	-17.3	0.07		1.93	-15.5	0.05
C15-H15A	1.74	-11.6	0.08		1.87	-13.6	0.11
C15-H15B	1.80	-12.5	0.11		1.80	-13.1	0.08
C16-H16A	1.90	-15.5	0.09		1.84	-13.1	0.20
C16-H16B	1.89	-15.5	0.06		1.88	-14.6	0.15
C17-H17	1.94	-16.2	0.06		1.85	-14.4	0.03
C18-H18A	1.83	-8.9	0.19		1.95	-16.5	0.03
C18-H18B	1.68	-7.5	0.16		1.90	-14.8	0.19
C18-H18C	1.81	-10.9	0.15		1.95	-16.4	0.05

Appendix F.

Crystal structure and charge density analysis of 3,16α,17β-estriol

Charge density and electrostatic potential study on estrogen molecules: 16α, 17β - Estriol

Abstract

The measurements of the electron density distribution of the principal members of the estrogen family, the derivatives estriol, estradiol and estrone are now in progress. As a part of our study, the electron density distribution of 16α,17β-estriol ($C_{18}H_{24}O_3$) was determined from the high-resolution single crystal X-ray diffraction measurements at 100 K. Estriol crystallizes with two molecules in the asymmetric unit. Intensity data were collected using SMART 2K CCD area detector with Ag Kα radiation up to resolution $(\sin\theta/\lambda)_{max} = 1.29$ Å^{-1}. The structure was solved, and a conventional spherical atom refinement was carried out. A multipole pseudo atom refinement was then performed using the program XD. The electron density at the critical point of aromatic C–C bonds are larger than the other ring systems in the molecule. The electrostatic potential has been calculated for both molecules removed from the crystal lattice. Strong electro negative regions were found in the vicinity of the oxygen atoms of the 16α, 17β regions of both molecules. A small net negative electrostatic potential around 3-hydroxyl regions in both molecules may be related to low binding affinity of estriol. Net atomic charges were calculated from the kappa refinement. A group charge calculation indicates that the central region is close to neutral, but the head and tail regions form charged units. The topological analysis of the hydrogen bonds indicates the strength of the intermolecular interactions.

Introduction

In the recent years much attention has been paid on estrogen research[1]. The major role of estrogen molecules in the body influences the growth, development, and behavior, and affect many other body parts such as tissues, skin, bone, liver. Importantly, this family of steroid hormones regulates and sustains female sexual development and reproductive function[2a]. In other words, it stimulates tissue growth by promoting cell proliferation (DNA synthesis and cell division) in the female sex organs (breast, uterus)[2b]. Subtle changes in the structure of the estrogen molecules affect their chemical/biological behavior and can result in the development of growth inhibitors for tumors. For example, moving the hydroxy group from C(3) (estradiol)[3] to one of the adjacent C-atoms can change the carcinostatic potentials from agonistic (estradiol) to inhibitory (2-and 4-hydroxy estratrien -17β-ol)[4,5]. In this way, more than 60% of all breast cancers are known to be hormone dependent, i.e.,

initiation and progress can be influenced by estrogens and related compounds. These molecules bind as ligands to the estrogen receptor and hereby initiate a series of events resulting in the activation or repression of selective genes. While most changes modify the affinity of the ligand for the estrogen receptor, this does not necessarily correlate with the stimulation ability of the transcription of estrogen responsive genes. Several articles focused on identification and characterization of receptor ligand binding affinities. A recent comparative QSAR analysis of estrogen receptor ligands generalizes the effect of different substituents in estrogen molecules; more importantly, the substituents which increase the electron density in the A-ring appear to increase the binding affinity, and the steric character of substituent and polar character reduce the ligand receptor binding affinity[6]. An extensive crystallographic structural study reports the conformational features of these molecules and proposing the possibilities of ligand binding[7,8]. The knowledge of receptor or receptor complex model is essentially important to understand the binding mechanism. In this context the structural analysis of ligand binding domain (LBD) of two estrogen receptors (α and β) complexed with various ligands [9-11] has been reported. These studies emphasize the agonist and antagonist effect of certain hormones and drugs with the receptor. Furthermore, molecular modeling of a series of estrogen molecules has been conducted suggesting that conformational flexibility is the important property of specific ligands for the estrogen receptor[12]. However, still the mechanism by which the ligands regulate the gene expression is currently unknown, but it has been suggested[13] that the differences in electrostatic potential (ESP) can contribute to the variation in the regulation of hormone dependent genes. This information can be obtained from studies of the electronic properties in estrogen derivatives.

An experimental multipole representation of the charge distribution has been becoming very successful method to determine the electrostatic properties and to investigate the intermolecular interactions. An interesting study on the determination of ESP from multipole moments shows the importance of multipole moments in the intermolecular interactions[14,15]. Currently, various quantum mechanical models are available to explore the charge distribution, molecular ESP and its topological characteristics using multipole model[16-19]. However, it is highly desirable for the model to include the effect of intermolecular interactions to understand the molecular recognition processes. The multipole model experimental electron density analysis of molecules by the X-ray diffraction methods includes this aspect. In the recent years, experimental multipole model results have been extensively analyzed to elucidate the electronic properties of atoms in molecules. A widely accepted Bader's theory[20] of "Atoms in Molecules" is a useful tool to obtain electronic properties such as electron density at the critical point, Laplacian of charge density (charge concentration or depletion), bond ellipticity, charges of atoms and the electrostatic potential, which, in turn, aid in the prediction of how this molecule might react with a given environment. Moreover, the hydrogen bond topology studies characterize the strength of

intermolecular interactions.

We have begun a systematic study of estrogen compounds by investigating crystals of the derivatives of the principal estrogens, estriol, estradiol and estrone. The first study in this series, on estra-1,3,5(10)-triene-3,16α,17β-triol, (see Figure 1) is reported here. Estriol is the one of the active estrogens found in the body. The main source of estriol is the placenta, which produces a large amount of estriol during pregnancy[21], while the other two estrogens are produced in comparatively small amounts. Estriol does not associated with the cancer activity in the female body but it protects this disease. Estriol has much less stimulating effect on the breast and utrine lining than estradiol and estrone. Receptor binding studies have indicated that estriol has low binding affinity to estrogen receptors and, in general, it has the shortest receptor occupancy. From the distinct biological characteristics of estriol over the other two estrogens (estrone and estradiol), it implies that these molecules must differ in some way in their electronic properties and/or physical properties. The knowledge of the properties of these estrogens may help to understand the detailed mechanism of estrogenic activity of these molecules. The commercially available estriol has been crystallized from acetonitrile. We have carried out the crystallographic structure and electron density analysis from the high resolution X-ray diffraction measurement.

Experimental Section

1. Data collection

Estriol has been crystallized from acetonitrile by slow evaporation at room temperature. The crystals were found to be colorless and prismatic. In order to find a sample with good reflection profiles, several crystals were examined on the diffractometer for the low and high angle scattering. A well shaped 0.48 x 0.26 x 0.24 mm size crystal was selected and mounted on a Bruker SMART 2K CCD diffractometer using graphite monochromatized Ag Kα (λ = 0.56089Å) radiation (50V, 35mA). As a preliminary check, a room temperature data set was collected for a hemisphere. Refinement of the structure from this data gave results comparable to the reported crystal structure[22]. Then, the crystal was cooled to 100 K using an Oxford Cryostream N_2 open flow cryostat. After cooling, no significant unit cell modification was observed and the unit cell was very stable over the period of the entire data collection.

Initially the orientation matrix and the unit cell parameters were obtained from least-squares refinement using 88 well centered reflections measured in three sets of matrix runs of each 20 frames. The low temperature cell obtained in this way was ~2 % smaller than that at room temperature. A full sphere of low and high angle reflection intensities were measured using two detector settings at 2θ = 0° and 2θ = -50°, using the ω scan method for different φ angles (0, 45, 90, 135, 180, 225, 270 and 315°).

The CCD detector was placed at 5.1 cm from the crystal to minimize the reflection overlap. A total of 600 frames were collected for each φ angle with a scan width of 0.3°. The frame times for low (40 sec) and high angles (160 sec) were picked after the careful observation of the most intense reflection, avoiding detector overflow, but utilizing the full dynamic range. The crystal decay was monitored by re-measuring the initial 50 frames at the end of each data collection, and it was found to be negligible. The data collection strategy was checked with the program ASTRO[24] incorporated into the software package SMART[25]. We obtained 100% coverage for a resolution of $(\sin\theta/\lambda)_{max} = 1.2$ Å^{-1} with good redundancy. A total of 9600 frames were collected over the period of two weeks.

2. Data reduction and averaging

The best unit cell and the orientation matrix were determined by thresholding [$I/\sigma(I) > 20$] of reflections from each run of the data set. This orientation matrix fits well with the entire reciprocal space observed. The data has been integrated and corrected for the background, Lorentz and polarization effects using the software's advanced integrating procedures SAINT[26]. The method of integration of the collected frames was as described by Kabch[26] for area detectors. During the integration the orientation matrix and unit cell were not allowed to vary. Appropriate three dimensional box sizes were used in low and high angle integrations to account for the $K\alpha_1$ and $K\alpha_2$ splitting in high order reflections. No absorption correction was applied because of the low value of the absorption coefficient (0.055 mm^{-1}). All the corrected reflection intensities were scaled and averaged based on the point group symmetry using the program SORTAV[27]. A total of 277952 reflections were measured up to $\sin\theta/\lambda = 1.29$ Å^{-1}. 43918 are unique reflections with an average redundancy of 6.2. Of these, 989 unique data were measured only once, 3028 twice and 39882 three or more times. We note that, in the complete set of unique reflections, 29528 reflections were found to be greater than $3\sigma(I)$. The internal agreement factors[27] based on the averaging of symmetry equivalent reflections are R1 = 0.044, R2 = 0.031, wR = 0.11 and S = 1.4. The unit cell parameters, data collection, averaging and other crystallographic parameters are summarized in Table 1.

3. Conventional refinement

The room temperature crystal structure[22] of 16α, 17β-estriol has been previously reported. We solved the 100 K low temperature structure by direct methods and the spherical atom least squares refinement was carried out using the program SHELXTL[28]. All the hydrogen atoms, except one, were located from a difference Fourier synthesis. In the least squares refinement, all non-hydrogen atoms were treated anisotropically, and the hydrogen atoms were isotropic. The refinement converged with all data to R = 0.058, wR = 0.151 GOF = 1.01. Comparison of F_o and F_c values of the largest

structure factors gave no indication of the effect of extinction in the data. A thermal ellipsoid diagram (Figure 2) shows the two molecules in the asymmetric unit and the standard atom numbering scheme.

4. Multipole refinement

In order to model the deformation electron density and explore the bond topological characteristics like $\rho(\mathbf{r})$, $\nabla^2\rho(\mathbf{r})$, bond ellipticity (ε), molecular electrostatic potential etc., a multipole aspherical atom refinement was carried out using the Hansen-Coppens[29] multipole formalism implemented in the program XD[30]. According to this formalism, the total electron density of an aspherical atom is parameterized using an atom-centered multipole expansion

$$\rho_{atom}(\mathbf{r}) = P_c\,\rho_c(\mathbf{r}) + P_v\,\kappa^3\,\rho_v(\kappa\mathbf{r}) + \sum_{l=0}^{l_{max}} \kappa'^3_l\, R_l(\kappa'\mathbf{r}) \sum_{m=0}^{l} P_{lm\pm}\, d_{lm\pm}(\theta,\varphi)$$

The first two terms $\rho_c(\mathbf{r})$ and $\rho_v(\kappa\mathbf{r})$ are the spherically averaged Hartree-Fock atomic core and valence densities normalized for one electron; the third term describes the aspherical part of the pseudo atom; $R_l(\mathbf{r}) = [\alpha_l{}^{n_l+3}/(n_l+2)!]r^{nl}\,e^{-\alpha_l r}$ are the normalized radial distribution functions; α_l are the Hartree Fock optimized single zeta values; κ and κ' are radial expansion/contraction parameters which are optimized in the least-square refinement along with P_v and P_{lm}; P_{lm} are the multipole population coefficients; $d_{lm\pm}$ are density normalized real spherical harmonic angular functions and r, θ and φ are user defined local atom centered coordinates expressed in a polar coordinate system. In the multipole refinement, all carbon and oxygen atoms were allowed to expand up to the hexadecapole and the hydrogen atoms up to the dipole level. The κ and κ' parameters of all non-H atoms were refined, but hydrogen atoms κ' was fixed at 1.2.

In order to obtain accurate positional and thermal parameters for the non-hydrogen atoms, a high-angle refinement was carried out using the data with $\sin\theta/\lambda > 0.7$ Å^{-1}. All C-H distances were then reset to the neutron bond lengths [C_{sp2}–H = 1.083, C_{sp3}–H = 1.099(CH), 1.092(CH_2), 1.059(CH_3) and O–H = 0.967 Å] as reported in the International Tables[31]. This high-angle refinement converged without any significant change of scale factor, thus indicating the quality of the high angle data. The multipole refinement was carried out on the 25520 reflections [$I > 3\sigma(I)$] with the resolution $(\sin\theta/\lambda)_{max} = 1.1$ Å^{-1}. The refinement strategy was as follows:

In the first step, Pv, κ and scale factor were refined; second step P_{lm}, κ'; third step xyz, U_{ij}, scale factor. Finally, xyz, U_{ij} and all electronic parameters were refined together. Since there are two molecules in the asymmetric unit, their multipole parameters were constrained to be equal at the beginning of the refinement, except the O–H group atoms as these are involved in the strong hydrogen bonding. In addition, to avoid the phase problem[32], all chemically equivalent atoms were initially constrained to be equal, but no site symmetry was imposed on any atoms in the molecules. At the later

stages of the refinement, the chemical atom constraints within the molecules were released, but not between the molecules. The residual index from the final refinement is given in Table 1. An attempt was made to refine the two molecules independently after the final refinement. This refinement did not give a meaningful result so we did not proceed further. The net atomic charges were calculated from a κ-refinement[33] (P_v, κ, and scale). During the refinements, the unit cell was constrained to be neutral and no charge transfer was allowed between the molecules. The featureless residual density maps of the two molecules (Figure 4) from the Fourier summation (F_o–F_{mul}) indicates the adequacy of the model refinement.

It is essential to test the physical significance and the correctness of the thermal parameters obtained from the model refinement. To accomplish this, Hirshfeld's[34] "rigid bond" test was performed for both the molecules leading to a satisfactory result. The maximum difference $\Delta_{A,B}$ between the atomic mean square displacement amplitudes along the interatomic vectors was 0.0013 Å.

Result and Discussion

1. Structural aspects

The report of the room temperature crystal structure[22] indicated significant conformational differences between the two molecules in the asymmetric unit. We observe some notable differences between the reported room temperature and current low temperature structure, so it is worth revisiting the structural analysis. Figure 2 shows the thermal ellipsoid representation of estriol with two independent molecules in the asymmetric unit obtained from the low temperature (100 K) measurement. The geometrical comparison of the two molecules explicitly indicates how the two molecules are conformationally different. On comparing the bond distances between the two molecules, no significant difference were observed, in contrast to the previous report[22]. The maximum deviation in the bond lengths of the ring (A-D) systems between the two molecules is 0.01 Å (Table 2). There is no evidence for C(2)–C(3) bond shortening in the A-ring systems as the room temperature structure reports[22]. The average C_{ar}–C_{ar} bond distances of A-ring atoms of molecule 1 and 2 are 1.3995 and 1.3990 Å respectively. The CH_3 group of the second molecule lies above the aromatic ring of the first producing distortion in the aromatic ring. This effect is reproduced here giving a folding in the A-ring of molecule 1 with a dihedral angle of 2.99°. There is no such effect in the second molecule where the A-ring system is planar (0.52°). There are differences in bond angles between the molecules 1 and 2 around the atoms C(9), C(13) and C(14) [Table 2]. However, we observe a maximum deviation of 2.5° compared to 3.9° as previously reported. The torsion angles in the Table 2 indicate the distortion of the B and C ring systems. The steric hindrance between the C-ring equatorial hydrogen atom at C(11) and the hydrogen

atom at C(1) produce different conformations of the B and C ring systems in the two molecules. Comparison of torsion angles between the molecules shows the major distortion appears at the head and tail part of the molecules (see Table 2). This is attributed to the different environment of intermolecular interactions of the molecules (1 and 2) with their neighbors. The relative strengths of the hydrogen bonds to O(3) in the two molecules was previously discussed on the basis of 0.04 Å difference in the C(16)–O(3) bond length. We observe less than 0.01 Å difference in this distance between molecules 1 and 2. Hydrogen bonding does, however, have an effect on the geometry of the hydroxyl groups. In the second molecule the 16α and 17β-hydroxyl C–O–H bond angles are systematically less compared with the first, the maximum difference being 8.8°. There is less of a differentiation in the 3-hydroxyl bonds, the deviation being 2.1°. The structure is characterized by strong hydrogen bonding. Figure 3 depicts the hydrogen-bonding environment of the two molecules in the asymmetric unit. Each hydroxyl group is involved in, at least, two hydrogen bonds. The hydrogen bonds O–H···O and O···H–O type of interactions in the molecules indicates the O-atoms behave as donor as well as acceptor. Moreover, O(1') has one additional hydrogen bond resulting in a tetrahedral coordination of the O-atom. The head to tail hydrogen bonds link the molecules into chains. The hydrogen bond geometrical parameters are given in Table 3.

2. Charge density distribution

The model static deformation density map in Figure 5 shows the bonding features of the different atoms in the estriol molecule. All chemical bonds show an increase in the electron density with respect to neutral spherical atoms as well as density associated with the lone pair regions of the oxygen atoms. The featureless residual electron density map was computed using the program XDFOUR[35] after the multipole refinement. The featureless residual maps (Figures 4a and b) of the two molecules in the asymmetric unit confirm the validity and the adequacy of the model refinement and the quality of the data set. The minimum and maximum residual density calculated for the molecules are 0.21, -0.29 (molecule1) and 0.22, -0.27eÅ^{-3} (molecule 2) respectively. As specified earlier, in the multipole refinement, the respective chemically equivalent ring atoms of the two molecules were constrained pair wise. No constraint was imposed on the hydroxyl groups, since they involved in strong hydrogen bonding. All further discussions are based on this constrained model.

In order to further characterize the interaction of atoms in a molecule, a topological analysis was performed based on Bader's theory[20] of "Atoms in Molecules" implemented in XDPROP[35]. This analysis includes the determination of electron density, $\rho(\mathbf{r}_c)$, at the bond critical point (CP), where $\nabla\rho(\mathbf{r}_c) = 0$, between the bonded atoms, its Laplacian, $\nabla^2\rho(\mathbf{r}_c)$, and bond ellipticity [$\varepsilon = (\lambda_1/\lambda_2)-1$]. Also, the eigenvalues of the second derivatives of $\rho(\mathbf{r}_c)$ was calculated to characterize the nature of the

bond critical point. The bond path analysis[36,37] gives information about the amount of deviation of the bond critical point from the internuclear axis, thus obtaining an additional measure of a strain. All these results, including the length of bond paths and internuclear distances, are listed in Table 4.

A-ring system: The topological analysis results reported in Table 4, such as $\lambda_1, \lambda_2, \lambda_3$, $\rho(\mathbf{r}_c)$, $\nabla^2\rho(\mathbf{r}_c)$, ε reveals the electronic insight into the estriol molecules. The magnitude of $\rho(\mathbf{r}_c)$ at the bond critical point is a clear indicator of the chemical bond strength. The electron density, $\rho(\mathbf{r}_c)$, at the critical points of the aromatic ring (C_{sp2}–C_{sp2}) bonds range from 2.04 to 2.19 eÅ^{-3}. The average value (2.1 eÅ^{-3}) is a typical value for aromatic bonds, but these values are 0.1 eÅ^{-3} smaller than in the reported p-nitrophenol[38]. The Laplacian, $\nabla^2\rho(\mathbf{r}_c)$, is a very sensitive parameter which identifies the areas where charge is concentrated (negative value) or depleted (positive value) in the bonding region. In this respect, we observe the maximum negative Laplacian in the A-ring bonds being –22.1(1) eÅ^{-5}, and this value appears less in the bonds linked to B ring atoms. However, the average value is –18.52 eÅ^{-5}, which is very close to an earlier observation for the benzene molecule[39]. The dispersion of bond ellipticity is attributed to the preferential charge accumulation in the bond. Bader's theory on ellipticity[20,40] emphasis the concept of the σ-π character of the bond. Explicitly, it is the measure of deviation of charge density from spherical symmetry (at the critical point). In this aspect the average value (0.18) of ellipticity of C_{sp2}–C_{sp2} bonds indicates the significant π (aromatic) character. This value is smaller than reported for the benzene ring bonds but completely agree with those in tris-annealed benzene[41]. The $\rho(\mathbf{r}_c)$'s in the C_{sp2}–H bonds range from 1.78(4) to 1.90(1) eÅ^{-3}, and this density is consistent with one would expect for the single C–H bonds. The Laplacian of the C(1)–H(1) bond is small compared with the other two C–H bonds, perhaps indicating weakening of the bond due to steric interactions with hydrogen atoms at C(11). The small ellipticity of C_{sp2}–H bonds is consistent with only a σ contribution in the single bonds.

B and C ring systems: The density of chemically equivalent C_{sp2}–C_{sp3} bonds in the B-ring are equal and their Laplacian's are very close (see Table 4). In both ring systems, the average values (1.70 and 1.67 eÅ^{-3}) of $\rho(\mathbf{r}_c)$'s in the C_{sp3}–C_{sp3} bonds are not very different and a similar trend appears for the Laplacian. The $\rho(\mathbf{r}_c)$'s and Laplacian for these bonds are significantly less than the aromatic ring system in agreement with their single bond character. In the C-ring the ellipticity of the bonds C(11)–C(12) and C(12)–C(13) are unexpectedly larger compared to the similar bonds having small values (see Table 4), indeed the values approach those of the aromatic ring. In all C_{sp3}–H (CH_2) bonds the density ranges from 1.64 to 1.86 eÅ^{-3} and C_{sp3}–H (CH) bonds 1.75 to 1.81 eÅ^{-3}. The average effect is same in both types of bonds. The Laplacian of these bonds is consistently smaller than for the C_{sp2}–H bonds. The maximum and minimum values are –8.9(2) and -18.6(1) eÅ^{-5}.

D-ring system: Having 5 members in the ring and due to the different hydrogen bonding

environments, this ring is highly strained in both molecules (1 and 2). Nevertheless, no significant difference was observed in the $\rho(\mathbf{r}_c)$'s at the bond critical points, except for C(14)–C(15) = 1.57 eÅ^{-3} implying a weakening of this bond. The average value of the Laplacian is -12.88 eÅ^{-5}. We observe the ellipticity of this five-member system being close to the B-ring bonds, and it is relatively small, consistent with the single bonds. The electron density (1.94 eÅ^{-3}) and the Laplacian of the C(16)–H(16) bond is surprisingly higher than the similar C(17)–H(17) bond in this ring (see Table 4).

C–O and O–H groups: In general, these groups play a significant role in the whole geometry of estrogen molecules. Especially the OH group perturbs the electron density of aromatic system and its electron density distribution is important in the ligand binding domain[13]. The $\rho_c(\mathbf{r})$'s of C_{sp2}–O [A-rings] bonds of both molecules (1 and 2) are larger than $\rho_c(\mathbf{r})$'s of the C_{sp3}–O bonds of D-ring, in agreement with conjugation of O(1) to the aromatic ring. The average values are 2.11 and 1.89 eÅ^{-3}. The Laplacians of the C_{sp2}–O bonds are not equal to C_{sp3}–O bonds, which indicates a strengthening of the bond to the aromatic ring. Whereas the ellipticity of the C(3)–O(1) bond in molecule 1 is a strong indicator of a π component of the bond, that in molecule 2 is closer to the value observed for the D ring. We attribute this to the difference in the hydrogen bonding in these two molecules. The small values of the ellipticity (0.05 - 0.1) in the C_{sp3}–O for both molecules indicate an unperturbed pure σ bond.

Bond path: In Table 4, Δd describes the deviation of bond critical point (CP) from an internuclear axis of a pair of bonded atoms in molecule. Essentially, the bond path[40,41] is a line which links two atoms by a maximum charge density. The bond path length significantly differs from internuclear distance and the amount of deviation indicates the extent at which the bond is strained. The distances d_1 and d_2 (see Table 4) are the bond path lengths between CP and the respective bonded atoms. Their inequality implies the degree of polarization of atom in the bond[38,42]. On inspecting all homonuclear atoms of the ring systems A through C, the minimum and maximum deviations are 0.004 and 0.03 Å. These deviations are smaller compared with the D-ring homonuclear bonds showing maximum deviation 0.044 Å. It confirms that the D-ring bonds are strained. However, this deviation is smaller than the highly strained C–C bonds of cyclopropane[43], bullvalence[44] (0.12 Å) and cubane[45] (0.17 Å) structures. The hetronuclear C–O bonds show marked differences in both molecules. The CP of C_{sp2}–O bond in the first molecule deviates by 0.03 Å from the internuclear axis, while in molecule 2 it lies very close (0.01 Å). In molecule 1, the deviation of BCP in the bonds C(17)–O(2) and C(16)–O(3) are 0.03 and 0.01 Å respectively. But these deviations are exactly opposite in the bonds C(17')–O(2') [0.01 Å] and C(16')–O(3') [0.04 Å] of molecule 2.

Topological properties of hydrogen bonds: Table 5 reports the hydrogen bond (O–H···O) topological properties of molecules 1 and 2. A (3,-1) hydrogen bond critical point's (HCP) which are located in

between H and O atoms of neighboring molecules. As we mentioned earlier, there are three hydrogen bonds exist in each molecule. Of the three hydrogen bonds from molecule 1, the two bonds [O(1)–H(1A)···O(3) and O(3)–H(3A)···O(1')] display approximately linear hydrogen bonding, 171.7, 170.5° respectively. The corresponding electron densities of these bonds at the HCP are similar with values of 0.23 and 0.20 eÅ^{-3}, respectively. Both of these bonds have a positive Laplacian $\nabla^2\rho(\mathbf{r}_c)$ at the HCP. This is characteristic of closed shell interactions[20] which are governed by the contraction of the electron density towards each of the interacting atoms. In molecule 2, we observe the similar electron densities and Laplacians for the bonds O(1')–H(1'A)··· O(3') and O(2')–H(2'A)···O(2'). The hydrogen bond O(2)–H(2A)···O(1) in molecule 1 shows a moderate electron density at the HCP (0.11 eÅ^{-3}) with a positive Laplacian. Although the hydrogen bond O(2')–H(2'A)···O(1') is approximately linear (169.2°), the electron density is very small at the CP (0.05 eÅ^{-3}). This may be attributed to the longer H(2'A)···O(1'A) distance and the fact that O(1'A) accepts one additional hydrogen bond. Further more, we have calculated bond path of H···O bonds. In H(1A)···O(3) bond the CP is not much deviated (0.056 Å) from internuclear axis and it is close (0.045 Å) to similar bond H(1'A)···O(3') in molecule 2. But in the 16α, 17β region of molecule 1, the H(2A)···O(1) deviates significantly (0.26 Å) compared with H(3A)···O(1') showing 0.05 Å. Similarly in molecule 2, the HCP's both for the bonds H(2'A)···O(1') and H(3'A)···O(2) are deviated by 0.36 and 0.1 Å respectively. This strange deviation in 17β regions of both molecules indicates that these are highly strained hydrogen bonds. Wide-angle deviations are larger than the reported value (0.12 Å) which was obtained from extensive electron density study on O–H···O hydrogen bonds[46].

3. Electrostatic potential

An additional important application of the multipole model is that it provides an opportunity to understand the chemical reactivity of molecules. That is to identify the places where nucleophilic or electrophilic attack may take place. The regions of the positive potential will attract nucleophilic reagents and the electronegative regions of the molecule will determine the approach of the electrophilic reagents. The electrostatic potential not only plays an important role in directing chemical attack, but also in the molecular recognition[47,48] (hormone receptor, drug receptor, enzyme-substrate interaction). This is because electrostatic forces are long-range interactions which determine the most stable geometrical orientation of two molecules. To investigate the aspect of the estrogen hormone receptor interaction, we have calculated the electrostatic potential around the molecules by the method of Su and Coppens[49] based on the populations obtained from the multipole refinement. The advantage of this method is that it allows to compute the ESP at points inside and outside the Van der Waals surface of the

charge distribution[30] and explore the topology of V(r)[50,51]. Generally, intermolecular potential involves the effect of electrostatic, induction, short range and dispersion interactions[52]. Although all these kinds of interactions alter the intermolecular interaction, the first one contributes significantly[53]. Thus, the molecules extracted from crystal lattice account for this many body effect. We have mapped the ESP of the isolated estriol single molecule and the fragments of the molecules which are involved in hydrogen bonding.

Figures 6a and 6b show contour plots (in the molecular mean plane) of the electrostatic potential of molecules 1 and 2 isolated from the crystal lattice. The view of positive contours around the aromatic rings are more diffuse than those of the saturated rings. In molecule 1, the positive contours are very compact around the atoms of the rings B, C, D compared with molecule 2. In Figure 6a, an empty (no ESP contours inside the ring) view of A-ring of molecule 1 indicates that the net electrostatic effect is zero, in comparison with the other ring systems showing the moderate potential values. The negative contours around the 16α, 17β oxygen atoms are much more pronounced than for the A-ring. The potential around molecule 1 is more symmetric than for molecule 2.

We have computed a 3D isosurface electrostatic potential of the pseudomolecule extracted from the crystal. In Figure 7, the anti-parallel view of two molecules reveals the difference of their ESP in the asymmetric unit. The positive equipotential (+0.5 $eÅ^{-1}$) surface shows the extension of ESP bound to the molecules 1 and 2. Especially, the bulk surface bound by aromatic ring of molecule 1 confirms the previous 2D observation. The negative equipotential surface indicates the amount of extended region for the value -0.15 $eÅ^{-1}$. More importantly, both the molecules have strong extended electronegative regions at the 16α, 17β-hydroxy groups, in contrast to the less electronegative regions observed at the 3-hydroxy groups. The negative region of molecule 1 exhibit spherically bounded ESP surface than in molecule 2. These distinct features can be attributed, at least to some extent, to the difference in polarization of such as weak and strong hydrogen bonded atoms. This kind of isosurface ESP analysis is becoming common in the biological and medicinal important molecules[54-56]. Finally, the view of the rich electronegative 16α, 17β hydroxyl region of two molecules together implies the diagonal orientation of ESP field vector[57-59] in the molecular geometry.

Furthermore, we have added the fragments of both molecules involved in strong hydrogen bonding to visualize the polarization. Figures 8a and b show the hydrogen bond environment of the O-atoms in molecules 1 and 2. Since ESP is attributed to the long-range electrostatic interaction, the hydrogen bonded atoms affect the existing potential around the molecule. The amount of variation of the ESP of the unperturbed molecules depends upon the direction and charge distribution of the two or more interacting molecules or fragments. The hydrogen bonded fragments of the neighboring molecules show the visual representation of polarization of hydrogen bonded atoms and the net effect of ESP in the inter

molecular region. Similar effects were observed in phosphorylethanolamine[56] crystal structure. Figure 8 emphasizes the net effect of ESP around each O–H groups of both molecules, after adding the hydrogen bonding fragments.

4. Net atomic charges

The net atomic charges (Table 6a) have been calculated from a κ-refinement (κ, P_v, scale). In this refinement the chemically equivalent atoms were constrained as described in the multipole refinement, and no charge transfer has been allowed between the molecule 1 and 2. Both molecules were kept neutral. All oxygen atoms carry significant negative charges in the range –0.63 to –0.87e. Similarly all hydroxyl hydrogen atoms carry high positive charges, approximately double the amount of charge of the other hydrogen atoms in the molecules. The charges of chemically equivalent aromatic atoms C(2) and C(3) are equal and they are much smaller than C(1), as expected. The equivalent C_{sp3} atoms C(6), C(7), C(11), and C(12) are carrying moderate charges and they are almost equal. A similar C_{sp3} (CH) kind of atoms C(8), C(9) and C(14) carrying small amount of charge except C(9). These charges are effectively larger than for the similar D-ring atoms C(16) and C(17) (see Table 6), this anomaly may be due to the different environment. The overall charge distribution of C- atoms in the ring systems A through D indicates that the aromatic A-ring and D-ring are holding lesser amount of charge compared to B and C ring systems. A group charge calculation (Table 6b) on both molecules indicates that the central regions are close to neutral, whereas the head and tails form charged units. Surprisingly, the 3-hydroxy (molecule 1) and 16α (molecule 2) regions are holding less negative charges (see Table 6b).

Conclusion

The present study on estriol gives an information on both the structural and electronic properties of the molecule. The differences in hydrogen bonding, molecular packing environment, and interamolecular steric effects are responsible for the small differences in the two molecules in the asymmetric unit. The significant differences reported for the room temperature structure were not confirmed here. The comparison of torsion angles between the two molecules shows that the major difference at the head and tail portions of the molecules may be attributed to the different hydrogen bonding environment, both molecules being involved in the strong hydrogen bonding.

The electronic information of A-ring system of the estrogen molecules is very important for the ligand receptor binding[13,6]. The electron densities at the CP of the aromatic C–C bonds are larger than for the C_{sp3}–C_{sp3} bonds of the B, C and D ring systems. The additional electron density accumulation in the aromatic bonds along with the ellipticity indicates a π contribution. The unconstrained refinement of

the hydroxyl groups between the two molecules shows differences in both C–O and O–H bond electron densities at the CP. The average C_{sp3}–O bond density is significantly less than C_{sp2}–O density. The charge accumulation in the O–H (16α,17β position) bond is slightly larger than in the 3-hydroxy O–H bond. Strong electronegative regions were found in the electrostatic potential maps at the vicinity of the oxygen atoms of the 16α,17β groups of both molecules. The extension of positive and negative contours explicitly indicates the electrostatic interaction with the neighboring molecules.

The hydrogen bonding O–H···O and O···H–O interaction at the head and tail portion of the molecule shows the possibility of having the positive and negative regions of the ligand binding domain of the receptor. The favored direction of alignment of the non-identical molecules together in the crystal lattice is along the direction of maximum negative ESP. The large electron density at the hydrogen bond CP's encourages the very strong nature of the hydrogen bonding in the estriol crystal.

Net atomic charges computed from the κ-refinement gave a reasonable distribution of charges. In the 16α,17β position, the oxygen atoms O(2), O(3) (molecule 1) and O(2'), O(3') (molecule 2) carry more negative charges than 3-hydroxy atoms O(1) and O(1').

To relate the results obtained from the electron density analysis and ESP with biological characteristics of estriol, the small negative ESP at the 3-hydroxy positions and the broad shape of negative ESP at the 16α,17β around O-atoms overlapping with the neighboring groups, and the conformational flexibility (i.e., two molecules arises in the asymmetric unit with different conformations) reduces the effective binding of molecules with the receptor. The first two of these results support the conclusion derived in isopotential study[13] in which the strong extended ESP at the 3-hydroxyl region is expected.

Thus, the way of representing and analyzing the experimental ESP brings out the approximate electrostatic characteristics of a molecule in the nonbonding environment. And the ESP extracted from the crystal lattice is suitable for the simulation of hormone-receptor interactions at different physiological situations.

References

1. Jaouen, G. Chemistry in Britain 2001, 37, 36-37.

2. (a) Hertz, R. 1985. The estrogen problem: retrospect and prospect. In: Estrogen in the Environment II: Influences on Deveoplment. Ed. J. A. McLachlan. New York: Elsevier., pp 1-11.
(b) Miller, W. R. Estrogen and Breast Cancer. 1996; Springer-Verlag GmbH & Co. KG, Tiergartenstrasse 17, D-69121 Heidelberg, Germany, pp 1-2.

3. Busetta, P. B.; Hospital, M. Acta Crystallogr. Sect. B. 1972, 28, 560-567.

4. Swenson, D. C.; Daux, W. L.; Strong, P. D.; Weisz, J.; Hershey, M. S. Acta Crystallogr. Sect. A. 1981, 'C56'.

5. Wawrzak, Z.; Duax, W. L.; Strong, P. D.; Weisz, J. J. Steroid Biochem. 1998, 29, 387-392.

6. Gao, H.; Katzenellenbogen, J. A.; Garg, R.; Hansch, C. Chem. Rev. 1999, 99, 723-744.

7. Daux, W. L; Norton, D. A. Atlas of steroid structure. 1975. Plenum Press, New York.Vol.1.

8. Griffin, J. F.; Daux, W. L.; Weeks, C. M. Atlas of steroid structure. 1984. Plenum Press, New York.Vol.2.

9. Brzozowski, A. M.; Pike, A. C. W.; Dauter, Z.; Hubbard, R. E.; Bonn, T.; Engström, O.; Öhman, L.; Greene, G. L; Gustafsson, J.; Carlquist, M. Nature, 1997, 389, 753-758.

10. Pike, A. C. W; Brzozowski, A. M.; Hubbard, R. E.; Bonn, T.; Thorsell, A.; Engström, O.; Ljunggren, J.; Gustafsson, J.; Carlquist, M. Embo. J, 1999, 18, 4608-4618.

11. Shiau, A. K; Barstad, D.; Loria, P. M.; Cheng, L.; Kushner, P. J.; Agard, D. A.; Greens, G. L. Cell, 1998, 95, 927-937.

12. Wiese, T. E.; Brooks, S. C. J. Steroid Biochem. Molec. Biol. 1994, 50, 61-73.

13. VanderKuur, J. A.; Wiese, T.; Brooks, S. C. Biochemistry, 1993, 32, 7002-7008.

14. Buckingham, A. D. Quat. Rev. Chem. Soc. 1959, 13, 183-214.

15. Kihara, T. Adv. Chem. Phys. 1963, 5, 147-188.

16. Pathak, R. K.; Gadre, S. R. J. Chem. Phy. 1990, 93,1770-1773.

17. Kosov, D. S.; Popelier, L. A. J. Phys. Chem. Sect A. 2000, 104, 7339-7345.

18. Stone, A. J. Chem. Phys. Lett. 1981, 83, 233-239.

19. Jug, K.; Gerwens, H. J. Phys. Chem. Sect. B. 1998, 102, 5217-5227.

20. Bader, R. F. W. Atoms in molecules. A quatum theory; Oxford University Press: Oxford, 1990.

21. Follingstad, A. H. JAMA, 1978, 239, 29-30.

22. Cooper, A.; Norton, D. A.; Hauptman, H. Acta Crystallogr., Sect. B. 1969, 25, 814-828.

23. Bruker (1997). ASTRO Ver. 5.007 Data simulation software for the SMART system. Bruker Analytical X-ray Instruments Inc.: Madison, Wisconsin, USA.

24. Bruker (2001). SMART Ver. 5.622. Brukers Analytical X-ray Instruments Inc.: Madison, Wisconsin, USA.

25. Bruker (2000). SAINT-Plus Ver.6.02a. Brukers Analytical X-ray Instruments Inc.: Madison, Wisconsin, USA.

26. Kabsch, W. J. Appl. Crystallogr. 1993, 26, 795-800.

27. Blessing, R. H. Crystallogr. Rev. 1987, 1, 3-58.

28. Sheldrick, G. M. (1997). SHELXTL, Version 5.1. A computer program for the structure determination. University of Göttingen, Germany.

29. Hansen, N. K.; Coppens, P. Acta Crystallogr. Sect. A 1978, 34, 909-921.

30. Koritsanszky, T.; Howard, S. T; Mallinson, P. R.; Su, Z.; Richter, T.; Hansen, N. K. XD, a computer program package for multipole refinement and analysis of charge densities from diffraction data, 1995; Institute of Crystallography, Freie Universität, Berlin Germany.

31. Macgillavery, C. H.; Rieck, G. D. International tables for crystallography, 1968,Vol. III, p275-276, The Kynoch Press, Birmingham, England.

32. El Haouzi, A; Hansen, N. K.; Le Hénaff. C.; Protas, J. Acta Crystallogra. Sect A. 1996, 52, 291-301.

33. Coppens, P.; Guru, T. N.; Leung, P.; Stevens, E. D.; Becker, P.; Yang, Y. W. Acta. Crystallogr. Sect. A. 1979, 35, 63-72.

34. Hirshfeld, F. L. Acta Crystallogr., Sect. A. 1976, 32, 239-244.

35. XDFOUR, XDPROP are incorporated to XD program.

36. Runtz, G. R.; Bader, R. F. W.; Messer, R. R. Can. J. Chem. 1977, 55, 3040-3045.

37. Bader, R. F. W. J. Phys. Chem. A. 1998, 102, 7314-7323.

38. Kulkarni, G. U.; Kumaradhas, P.; Rao, C. N. R. Chem. Mater. 1998, 10, 3498-3505.

39. Stewart, R. F. In The application of Charge Density Research to Chemistry and Drug Design; NATO-ASI Ser. B; Jeffrey, G. A., Piniella, J. F., Eds.; Plenum Press: New York, 1991; Vol. 250, pp 63-101.

40. Bader, R. F. Chem. Rev. 1991, 91, 893-928.

41. Rathore, R.; Lindeman, V.; Kumar, A. S.; Kochi, J. K. J. Am. Chem. Soc. 1998, 120, 6012-6018.

42. Macchi, P.; Proserpio, D. M.; Sironi, A. J. Am. Chem. Soc. 1998, 120, 1447-1455.

43. Boese, R.; Miebach, T.; Meijere, A. J. Am. Chem. Soc. 1991, 113, 1743-1748.

44. Koritsanszky, T.; Buschmann, J, Luger, P. J. Phys. Chem. 1996, 100, 10547-10553.

45. Irngartinger, H.; Strack, S. J. Am. Chem. Soc. 1998, 120, 5818-5819.

46. Espinosa, E.; Souhassou, M.; Lachekar, H.; Lecomte, C. Acta Crystallogr. Sect. B. 1999, 55, 563-572.

47. Koritsanszky, T.; Coppens, P. Chem. Rev. 2001, 101, 1583-1628.

48. Coppens, P. X-ray Charge Densities and Chemical Bonding, Oxford Science Publications, 1997.

49. Su, Z.; Coppens, P. Acta crystallogr., Sect. A. 1992, 48, 188-197.

50. $V(r)= \Sigma_j Z_j / |r-R_j| - \int \rho(r)/ |r-r'| dr'$ Where R_j and Z_j are the position and charge of the j-th nucleus, respectively.

51. Pathak, R. K; Gadre, S. R. J. Chem. Phys. 1990, 93, 1770-1773.

52. Buckingham, A. D.; Fowler, P. W.; Hutson, J. M. Chem. Rev. 1988, 88, 963-988.

53. Wheatleg, R.; Mitchell, J. B. O. J. Comput. Chem. 1994, 15, 1187-1198.

54. Koritsanszky, T,; Flaig, R.; Zobel, D,; Krane, H. –G,; Morgenroth, W.; Luger, P. Science, 1998, 279, 356-358.

55. Flaig, R.; Koritsanszky, T.; Janxzak,; Krane, H. –G,; Morgenroth, W.; Luger, P. Angew. Chem. Int. Ed. 1999, 38, 1397-1400.

56. Flaig, R.; Korisanszky, T.; Zobel, D,; Luger, P. J. Am. Chem. Soc. 1998, 120, 2227-2238.

57. Swaminathan, S.; Craven. Acta crystallogr. Sect. B. 1984,40, 511-518.

58. Weinstein, H.; Chou, D.; Kang, S.; Johnson, C. L.; Green, J. P. Int. J. Quatum Chem., Quantum Biol. Symp. 1976, 3, 134- 150.

59. Politzer, P.; Truhlar, D. G. Chemical Applications of Atomic and Molecular Electrostatic Potentials, New York Plenum Press; (1981), pp 309-334.

Table 1. Crystal data and Experimental conditions[a]

Crystal Data	
Empirical formula	$C_{18}H_{24}O_3$
Formula weight	288.37
Crystal system	Monoclinic
Space group	$P2_1$
a (Å)	7.5077(4)
b (Å)	23.0809(12)
c (Å)	9.1632(5)
β (deg)	110.957(2)
V ($Å^3$)	1482.8
Z	4
F(000)	624
Dx (Mg/m^3)	1.292
μ (mm^{-1})	0.055
Data collection	
Diffractometer	Brukers SMART 2K CCD
Radiation, λ (Å)	Ag Kα, 0.56087
Scan method, width (deg)	ω-scan, 0.3
No. of reflections measured	278184
$\sin(\theta/\lambda)_{max}$ ($Å^{-1}$)	1.29
R_{int}	0.042
No. of unique data	43918
Multipole refinement	
No. of relections ($F \geq 3\sigma$, $\sin(\theta/\lambda)_{max} = 1.1$ $Å^{-1}$)	25520
R(F), wR(F)	0.032, 0.035
GOF	0.98
N_{obs}/N_{par}	26.6

[a] $R_{int} = \Sigma|I-I_{mean}|/\Sigma I$; $R(F)=\Sigma(||F_o|-|F_c||/\Sigma|F_o|)$; $wR(F)=(\Sigma(F_o-F_c)^2/\Sigma wF_o^2)^{1/2}$; $w=1/\sigma^2(F_o)$

Table 2. Selected geometrical parameters of molecule 1 and 2[a]

Bond lengths (Å)

bond	*m1*	*m2*
C(1)–C(2)	1.3938(8)	1.3962(7)
C(2)–C(3)	1.3952(8)	1.3936(7)
C(3)–C(4)	1.3939(7)	1.3921(7)
C(4)–C(5)	1.3991(7)	1.3978(6)
C(5)–C(10)	1.4084(7)	1.4111(7)
C(1)–C(10)	1.4064(7)	1.4034(7)
O(1)–C(3)	1.3693(8)	1.3785(7)
C(5)–C(6)	1.5146(7)	1.5154(7)
C(6)–C(7)	1.5255(7)	1.5250(7)
C(7)–C(8)	1.5293(7)	1.5264(7)
C(8)–C(9)	1.5444(7)	1.5424(6)
C(9)–C(10)	1.5278(7)	1.5253(6)
C(9)–C(11)	1.5388(7)	1.5408(7)
C(11)–C(12)	1.5409(7)	1.5441(7)
C(12)–C(13)	1.5325(7)	1.5313 (7)
C(13)–C(14)	1.5508(7)	1.5415(7)
C(13)–C(17)	1.5360(7)	1.5462(7)
C(13)–C(18)	1.5368(8)	1.5334(7)
C(14)–C(15)	1.5400(7)	1.5360(7)
C(14)–C(8)	1.5235(7)	1.5172(7)
C(15)–C(16)	1.5529(7)	1.5499(7)
C(16)–(17)	1.5413(7)	1.5463(7)
C(16)–O(3)	1.4387(9)	1.4278(8)
C(17)–O(2)	1.4293(7)	1.4168(8)

[a] *m1*-molecule 1 and *m2*-molecule 2

Bond angles (deg)

Bond	*m1*	*m2*
C(1)–C(2)–C(3)	119.3(1)	199.1(1)
O(1)–C(3)–C(2)	118.4(1)	118.1(1)
O(1)–C(3)–C(4)	121.9(1)	121.8(1)
C(2)–C(3)–C(4)	119.6(1)	120.0(1)
C(3)–C(4)–C(5)	121.0(1)	120.6(1)
C(4)–C(5)–C(6)	118.1(1)	117.2(1)
C(4)–C(5)–C(10)	120.3(1)	120.4(1)
C(6)–C(5)–C(10)	121.6(1)	122.4(1)
C(5)–C(6)–C(7)	113.1(1)	113.6(1)
C(6)–C(7)–C(8)	110.2(1)	110.7(1)
C(7)–C(8)–C(9)	109.0(1)	108.4(1)
C(7)–C(8)–C(14)	112.7(1)	111.9(1)
C(9)–C(8)–C(14)	107.8(1)	109.4(1)
C(8)–C(9)–C(10)	112.2(1)	109.9(1)
C(8)–C(9)–C(11)	111.3(1)	112.5(1)
C(10)–C(9)–C(11)	114.8(1)	114.3(1)
C(1)–C(10)–C(5)	117.6(1)	117.7(1)
C(1)–C(10)–C(9)	121.1(1)	121.8(1)
C(5)–C(10)–C(9)	121.0(1)	120.5(1)
C(9)–C(11)–C(12)	111.9(1)	112.7(1)
C(11)–C(12)–C(13)	111.4(1)	110.6(1)
C(12)–C(13)–C(14)	108.5(1)	108.4(1)
C(12)–C(13)–C(17)	115.4(1)	117.1(1)
C(12)–C(13)–C(18)	110.6(1)	109.8(1)
C(14)–C(13)–C(17)	97.6(1)	98.6(1)
C(14)–C(13)–C(18)	113.6(1)	113.5(1)
C(17)–C(13)–C(18)	110.7(1)	109.1(1)
C(8)–C(14)–C(13)	113.7(1)	113.8(1)
C(8)–C(14)–C(15)	120.6(1)	118.1(1)
C(13)–C(14)–C(15)	103.5(1)	103.8(1)
C(14)–C(15) –C(16)	104.0(1)	104.2(1)
O(3)–C(16)–C(15)	113.9(1)	113.1(1)
O(3)–C(16)–C(17)	111.6(1)	113.0(1)
C(15)–C(16)–C(17)	104.8(1)	105.6(1)
O(2)–C(17)–C(13)	119.7(1)	116.6(1)
O(2)–C(17)–C(16)	112.0(1)	110.2(1)
C(13)–C(17)–C(16)	104.6(1)	103.2(1)
C(3)–O(1)–H(1A)	110.4(2)	108.4(2)
C(17)–O(2) –H(2A)	112.7(2)	103.8(2)
C(16)–O(3)–H(3A)	116.9(1)	109.6(2)

Torsion angles (deg)

Bond	*m1*	*m2*
A-ring		
C(10)–C(1)–C(2)–C(3)	-0.5(2)	-0.5(2)
C(1)–C(2)–C(3)–C(4)	2.1(2)	0.8(2)
C(2)–C(3)–C(4)–C(5)	-2.1(2)	-0.3(2)
C(3)–C(4)–C(5)–C(10)	0.5(2)	-0.4(2)
C(4)–C(5)–C(10)–C(1)	1.1(2)	0.7(2)
C(5)–C(10)–C(1)–C(2)	-1.1(2)	-0.3(2)
B-ring		
C(10)–C(5)–C(6)–C(7)	-19.3(2)	-10.5(2)
C(5)–C(6)–C(7)–C(8)	48.4(2)	41.1(2)
C(6)–C(7)–C(8)–C(9)	-65.0(2)	-66.0(2)
C(7)–C(8)–C(9)–C(10)	50.7(2)	57.8(2)
C(8)–C(9)–C(10)–C(5)	-22.2(2)	-27.9(2)
C(9)–C(10)–C(5)–C(6)	6.2(2)	4.3(2)
C-ring		
C(8)–C(9)–C(11)–C(12)	56.2(2)	51.8(2)
C(9)–C(11)–C(12)–C(13)	-55.2(2)	-54.7(2)
C(11)–C(12)–C(13)–C(14)	54.4(2)	56.8(2)
C(12)–C(13)–C(14)–C(8)	-58.7(2)	-60.2(2)
C(13)–C(14)–C(8)–C(9)	59.3(2)	56.9(2)
C(14)–C(8)–C(9)–C(11)	-56.6(2)	-51.4(2)
D-ring		
C(13)–C(14)–C(15)–C(16)	-33.3(2)	-31.2(2)
C(14)–C(15)–C(16)–C(17)	4.2(2)	2.0(2)
C(15)–C(16)–C(17)–C(13)	26.7(2)	27.6(2)
C(16)–C(17)–C(13)–C(14)	-45.9(2)	-45.8(2)
C(17)–C(13)–C(14)–C(15)	48.6(2)	47.7(2)
C(13)–C(17)–C(16)–O(3)	150.4(2)	151.8(2)
C(15)–C(16)–C(17)–O(2)	157.7(2)	152.9(2)
C(13)–C(17)–O(2)–H(2A)	-4.7(2)	-78.1(2)
C(15)–C(16)–O(3)–H(3A)	84.4(2)	50.8(2)
C(2)–C(3)–O(1)–H(1A)	169.7(2)	-176.3(2)
C(4)–C(3)–O(1)–H(1A)	-8.5(2)	3.6(2)

Table 3. Hydrogen bonds[a]

bond	O–H (Å)	O···O (Å)	H···O (Å)	O–H···O (deg)
m1				
O(1)–H(1A)···O(3)[a]	0.97	2.646(2)	1.682(2)	171.7(1)
O(2)–H(2A)···O(1)[b]	0.97	2.773(2)	1.851(1)	158.6(1)
O(3)–H(3A)···O(1')[c]	0.97	2.890(1)	1.930(1)	170.5(1)
m2				
O(1')–H(1'A)···O(3')[d]	0.97	2.640(2)	1.684(1)	169.9(1)
O(2')–H(2'A)···O(1')[e]	0.97	2.884(1)	1.927(1)	169.2(1)
O(3')–H(3'A)···O(2)[f]	0.97	2.736(1)	1.857(1)	149.9(1)

[a] Symmetry codes: (a) -x+2, y-½, -z+1; (b) -x+1, y+½, -z+1; (c) x, y, z-1 ; (d) -x+1, y+½, -z+2; (e) -x+2, y-½, -z+2; (f) -x+1, y-½, -z+1

Table 4. Analysis of the properties of the bond critical points for the molecule 1 (first row) and 2 (second row)[a]

bond	λ_1	λ_2	λ_3	$\rho(r_c)$ (eÅ^{-3})	$\nabla^2\rho(r_c)$ (eÅ^{-5})	R_{ij} (Å)	d_1 (Å)	d_2 (Å)	ε	Δd (Å)
A-ring										
C(1)–C(2)	-15.07	-12.99	9.95	2.14(1)	-18.1(1)	1.3939	0.7040	0.6899	0.16	0.01
C(2)–C(3)	-16.61	-14.18	8.67	2.19(2)	-22.1(1)	1.3967	0.6846	0.7121	0.17	0.03
C(3)–C(4)	-15.88	-13.36	8.29	2.15(1)	-21.0(1)	1.3947	0.7607	0.6340	0.19	0.02
C(4)–C(5)	-14.72	-12.60	9.51	2.04(1)	-17.8(1)	1.3993	0.6975	0.7017	0.17	0.01
C(5)–C(10)	-14.47	-12.27	9.74	2.05(1)	-17.0(1)	1.4087	0.7253	0.6834	0.18	0.01
C(10)–C(1)	-13.89	-11.35	10.12	2.04(1)	-15.1(1)	1.4065	0.7349	0.6716	0.22	0.01
C(1)–H(1)	-15.65	-14.68	16.05	1.80(1)	-14.3(1)	1.0817	0.7067	0.3750	0.07	0.01
C(2)–H(2)	-17.65	-15.99	11.59	1.90(1)	-22.1(1)	1.0832	0.6889	0.3943	0.10	0.02
C(4)–H(4)	-16.16	-15.03	11.97	1.78(4)	-19.2(1)	1.0849	0.6950	0.3900	0.07	0.002
C(3)–O(1)	-18.17	-14.42	11.28	2.05(3)	-21.3(1)	1.3708	0.8343	0.5365	0.26	0.03
	-17.65	-16.46	12.08	2.16(2)	-22.0(1)	1.3787	0.8627	0.5159	0.07	0.01
O(1)–H(1A)	-43.38	-42.37	27.52	2.08(8)	-58.2(8)	0.9700	0.8205	0.1495	0.02	0.004
	-40.29	-39.52	31.58	2.18(8)	-48.2(7)	0.9661	0.7967	0.1694	0.02	0.004
B-ring										
C(5)–C(6)	-11.20	-10.55	10.64	1.71(1)	-11.1(1)	1.5148	0.7741	0.7408	0.06	0.01
C(6)–C(7)	-11.48	-10.65	10.97	1.74(1)	-11.2(1)	1.5258	0.7633	0.7625	0.08	0.02
C(7)–C(8)	-11.20	-10.26	10.40	1.67(1)	-11.1(1)	1.5293	0.7806	0.7487	0.09	0.004
C(8)–C(9)	-11.94	-11.08	9.82	1.71(1)	-13.2(1)	1.5453	0.7704	0.7749	0.08	0.03
C(9)–C(10)	-11.36	-10.41	10.20	1.69(1)	-11.6(1)	1.5284	0.7911	0.7373	0.09	0.02
C(6)–H(6A)	-15.34	-13.61	12.99	1.82(4)	-16.0(1)	1.0944	0.6649	0.4295	0.13	0.01
C(6)–H(6B)	-13.83	-13.29	18.21	1.64(4)	-8.9(2)	1.0919	0.7474	0.3446	0.04	0.02
C(7)–H(7A)	-17.50	-16.33	15.29	1.86(4)	-18.6(1)	1.0933	0.7508	0.3425	0.07	0.004
C(7)–H(7B)	-16.31	-15.14	14.93	1.83(4)	-16.5(1)	1.0922	0.7205	0.3717	0.08	0.01
C(8)–H(8)	-16.79	-15.76	15.69	1.76(4)	-16.9(2)	1.0990	0.7745	0.3245	0.07	0.01
C(9)–H(9)	-16.14	-15.65	14.21	1.81(4)	-17.6(1)	1.0984	0.7295	0.3688	0.0	0.01
C-ring										
C(9)–C(11)	-10.75	-10.54	10.25	1.65(2)	-11.0(1)	1.5389	0.7555	0.7834	0.02	0.01
C(11)–C(12)	-10.95	-9.56	10.61	1.63(1)	-9.9(1)	1.5410	0.7595	0.7816	0.14	0.01
C(12)–C(13)	-12.33	-10.71	9.98	1.73(1)	-13.1(1)	1.5328	0.7586	0.7742	0.15	0.02
C(13)–C(14)	-11.29	-10.42	9.46	1.62(1)	-12.3(1)	1.5510	0.7749	0.7761	0.08	0.01
C(14)–C(8)	-12.98	-11.80	8.96	1.73(1)	-15.8(1)	1.5236	0.7627	0.7609	0.10	0.01
C(11)–H(11A)	-14.98	-14.54	15.54	1.75(4)	-14.0(1)	1.0938	0.7228	0.3710	0.03	0.02
C(11)–H(11B)	-16.06	-15.38	14.43	1.80(4)	-17.0(1)	1.0909	0.7187	0.3722	0.04	0.01
C(12)–H(12A)	-15.92	-15.31	17.02	1.77(4)	-14.2(2)	1.0917	0.7602	0.3315	0.04	0.004
C(12)–H(12B)	-15.35	-14.45	13.31	1.79(4)	-16.5(1)	1.0901	0.6871	0.4031	0.06	0.01
C(14)–H(14)	-16.50	-16.13	15.31	1.75(4)	-17.3(2)	1.1011	0.7792	0.3219	0.02	0.02
D-ring										
C(14)–C(15)	-10.27	-10.19	10.12	1.57(1)	-10.4(1)	1.5409	0.7816	0.7593	0.01	0.03
C(15)–C(16)	-12.10	-11.18	9.38	1.71(1)	-13.9(1)	1.5544	0.7375	0.8169	0.08	0.035
C(16)–C(17)	-12.71	-12.07	9.51	1.79(1)	-15.3(1)	1.5416	0.7916	0.7499	0.05	0.014
C(17)–C(13)	-11.13	-10.28	9.56	1.65(1)	-11.9(1)	1.5386	0.7199	0.8187	0.08	0.044
C(15)–H(15A)	-17.40	-15.51	12.54	1.82(4)	-20.4(1)	1.0927	0.7242	0.3684	0.12	0.01
C(15)–H(15B)	-16.14	-15.14	16.09	1.68(5)	-15.2(2)	1.0948	0.7847	0.3101	0.07	0.02
C(16)–H(16)	-19.35	-18.60	13.23	1.94(5)	-24.7(2)	1.0968	0.7741	0.3227	0.04	0.01
C(17)–H(17)	-17.41	-16.91	15.27	1.78(4)	-19.1(2)	1.1009	0.7915	0.3094	0.03	0.014
C(17)–O(2)	-14.85	-14.05	13.75	1.96(2)	-15.2(1)	1.4308	0.8536	0.5772	0.06	0.03
	-13.95	-12.67	14.94	1.91(3)	-11.7(1)	1.4170	0.8319	0.5852	0.10	0.01
O(2)–H(2A)	-47.97	-45.24	24.28	2.26(6)	-68.9(7)	0.9665	0.8117	0.1548	0.06	0.01
	-46.44	-43.87	23.04	2.34(8)	-67.3(7)	0.9683	0.8000	0.1683	0.06	0.005
C(16)–O(3)	-14.32	-13.65	14.11	1.87(2)	-13.9(6)	1.4389	0.8588	0.5800	0.05	0.01
	-13.64	-12.59	14.89	1.83(2)	-11.3(1)	1.4301	0.8364	0.5937	0.08	0.04
O(3)–H(3A)	-35.31	-34.33	40.97	2.34(7)	-28.7(5)	0.9694	0.7599	0.2095	0.03	0.01
	-41.18	-39.53	34.28	2.22(7)	-46.4(6)	0.9680	0.7983	0.1698	0.04	0.02
C(13)–C(18)	-11.30	-10.73	10.44	1.71(1)	-11.6(1)	1.5369	0.7892	0.7477	0.05	0.01
C(18)–H(18A)	-16.71	-15.95	15.99	1.89(5)	-16.7(2)	1.0629	0.7085	0.3544	0.05	0.004
C(18)–H(18B)	-16.28	-15.68	13.80	1.88(5)	-18.2(2)	1.0549	0.6779	0.3771	0.04	0.01
C(18)–H(18C)	-16.05	-14.81	15.84	1.85(5)	-15.0(1)	1.0577	0.6869	0.3708	0.08	0.015

[a] λ_1, λ_2 and λ_3 are the eigenvalues of Hessian matix. $\rho(r_c)$ is the electron density; $\nabla^2\rho(r_c)$ is the Laplacian at the CP; d_1 and d_2 are the distances from the critical point; R_{ij} is the sum of d_1 & d_2; ε is the bond ellipticity. Δd is the deviation of CP from the internuclear axis

Table 5. Topological Characteristics of the electron density at the hydrogen bondcritical points[a]

bond	$\rho(\mathbf{r}_c)$ (eÅ^{-3})	$\nabla^2\rho(\mathbf{r}_c)$ (eÅ^{-5})	R_{ij} (Å)	d_1 (Å)	d_2 (Å)
m1					
O(1)–H(1A)···O(3)[a]	0.23(5)	5.07(7)	1.6869	1.1526	0.5343
O(2)–H(2A)···O(1)[b]	0.11(2)	3.00(1)	1.9287	1.2551	0.6737
O(3)–H(3A)···O(1')[c]	0.20(3)	3.00(2)	1.9328	1.2381	0.6947
m2					
O(1')–H(1'A)···O(3')[d]	0.24(5)	5.02(5)	1.6863	1.1299	0.5664
O(2')–H(2'A)···O(1')[e]	0.05(2)	2.31(1)	2.0748	1.3544	0.7204
O(2')–H(2'A)···O(2)[f]	0.20(3)	3.41(2)	1.8682	1.2186	0.6496

[a] Symmetry codes: (a) -x+2, y-½, -z+1; (b) -x+1, y+½, -z+1; (c) x, y, z-1 ; (d) -x+1, y+½, -z+2; (e) -x+2, y-½, -z+2; (f) -x+1, y-½, -z+1

Table 6a. Net atomic charges (e) for the molecule 1 (first row) and 2 (second row)

Atom	charge	Atom	charge
C(1)	-0.21(3)	H(6A)	0.20(2)
C(2)	-0.06(3)	H(6B)	0.12(2)
C(3)	0.16(3)	H(7A)	0.20(2)
C(4)	-0.06(3)	H(7B)	0.24(2)
C(5)	0.00	H(8)	0.16(2)
C(10)	-0.04(2)	H(9)	0.20(2)
C(6)	-0.36(3)	H(11A)	0.20(2)
C(7)	-0.48(3)	H(11B)	0.22(2)
C(8)	-0.12(3)	H(12A)	0.08(2)
C(9)	-0.29(3)	H(12B)	0.26(2)
C(11)	-0.31(3)	H(14)	0.17(2)
C(12)	-0.47(3)	H(15A)	0.30(2)
C(13)	0.00	H(15B)	0.21(2)
C(14)	-0.07(3)	H(16)	0.21(2)
C(15)	-0.24(3)	H(17)	0.16(2)
C(16)	0.05(3)	H(18A)	0.20(2)
C(17)	-0.08(3)	H(18B)	0.27(2)
C(18)	-0.61(3)	H(18C)	0.19(2)
O(1)	-0.63(3)	H(1A)	0.43(3)
	-0.79(3)		0.35(3)
O(2)	-0.86(3)	H(2A)	0.48(2)
	-0.87(3)		0.46(2)
O(3)	-0.84(3)	H(3A)	0.25(2)
	-0.77(3)		0.46(2)
H(1)	0.16(2)		
H(2)	0.29(2)		
H(4)	0.31(2)		

Table 6b. Group charge(e) calculation for the molecule 1 (first row) and 2 (second row)

Atoms	charge(e)
C(3), O(1), H(1A)	-0.04
	-0.20
C(17), H(17), O(2A), H(2A)	-0.30
	-0.33
C(16), H(16), O(3A), H(3A)	-0.33
	-0.05
C(1), H(1), C(10)	-0.05
C(2), H(2)	0.23
C(4), H(4)	0.28
C(6), C(7), H(6A), H(6B)	-0.08
H(7A), H(7B)	
C(11), C(12), H(11A), H(11B)	-0.02
H(12A), H(12B)	
C(14), H(14), C(15), H(15A), H(15B)	0.37

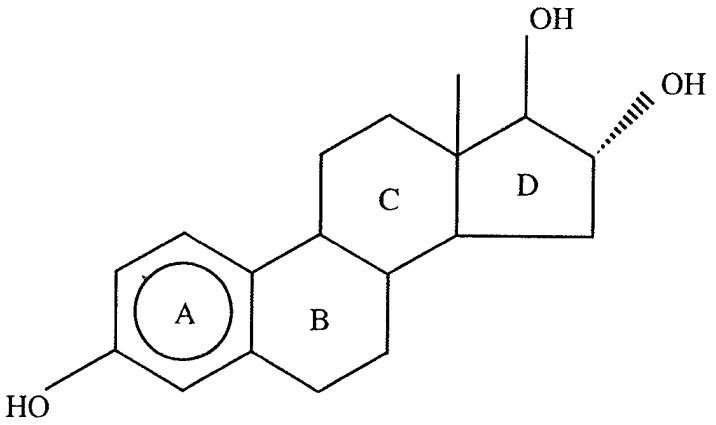

Figure 1. Estriol

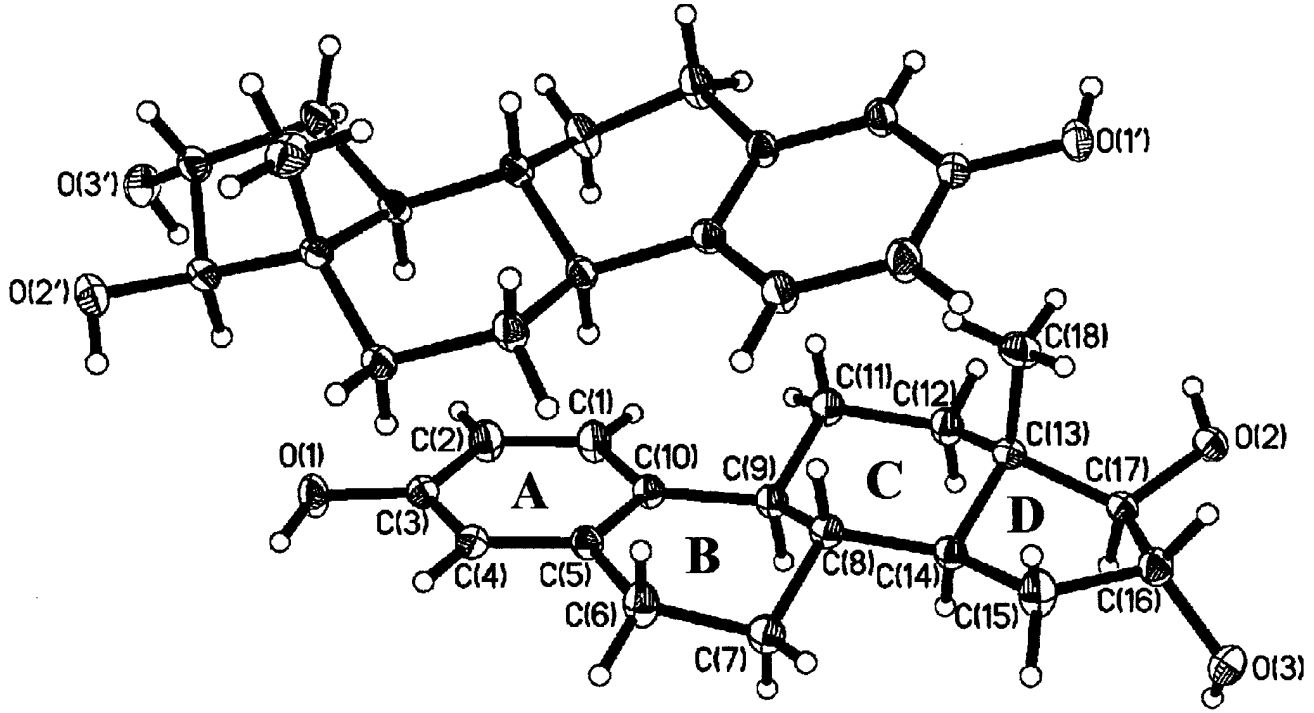

Figure 2. ORTEP view of two molecules in the asymmetric unit showing 75% probability ellipsoids of the atoms and atomic labeling.

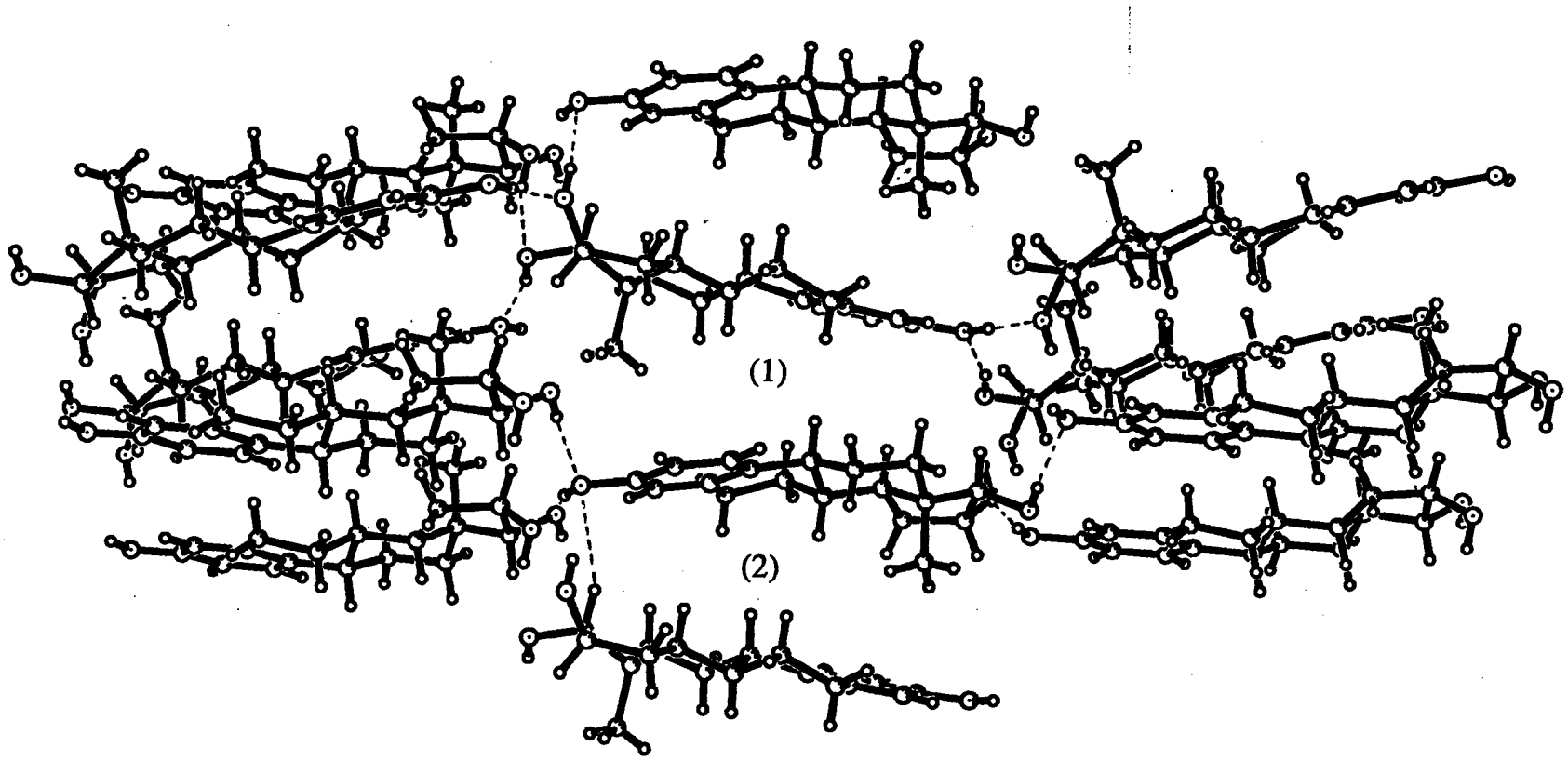

Figure 3. Intermolecular hydrogen bonding view of molecules 1 and 2.

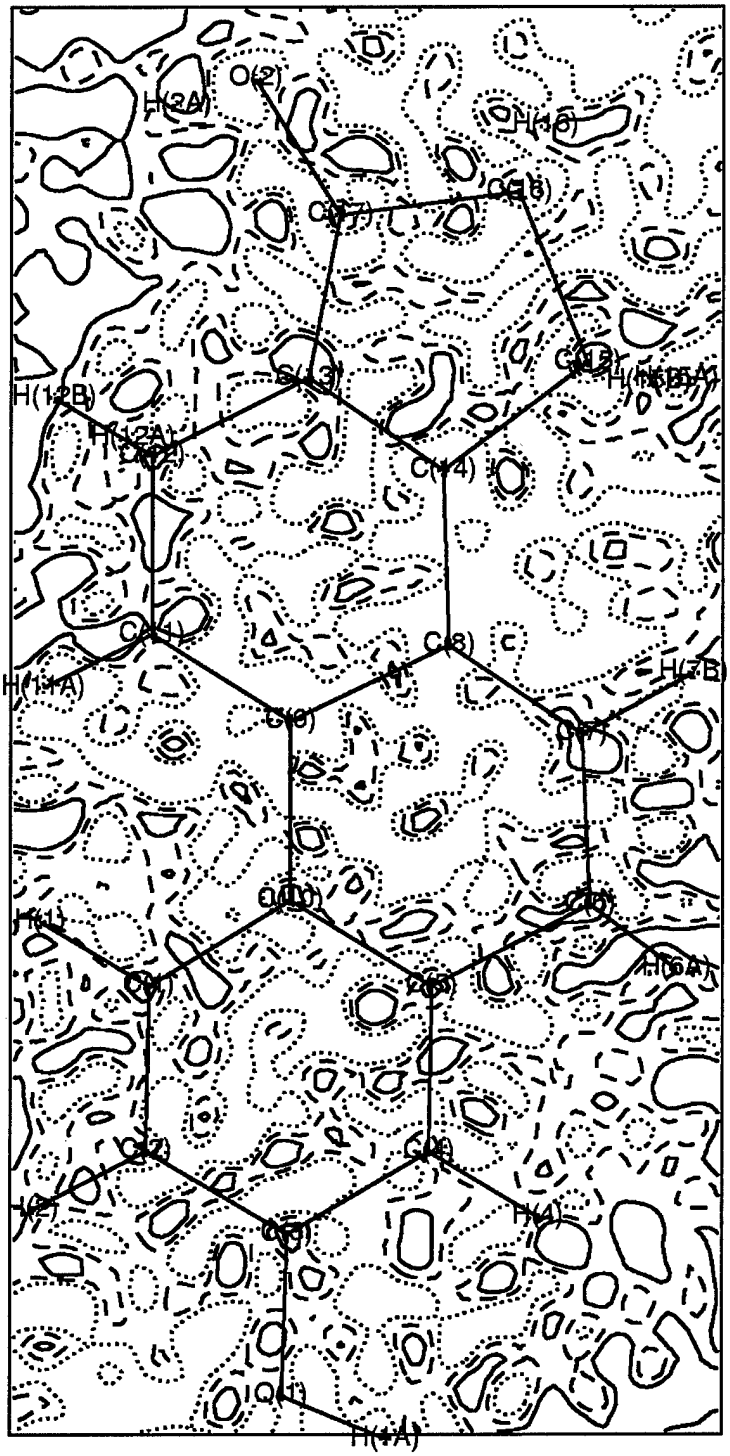

Figure 4a. Residual density maps for molecule 1 in the plane of C(1), C(5) and C(16) . Contour interval 0.05 eÅ^{-3}. Positive, negative and zero contours are drawn as solid, dotted and broken lines respectively.

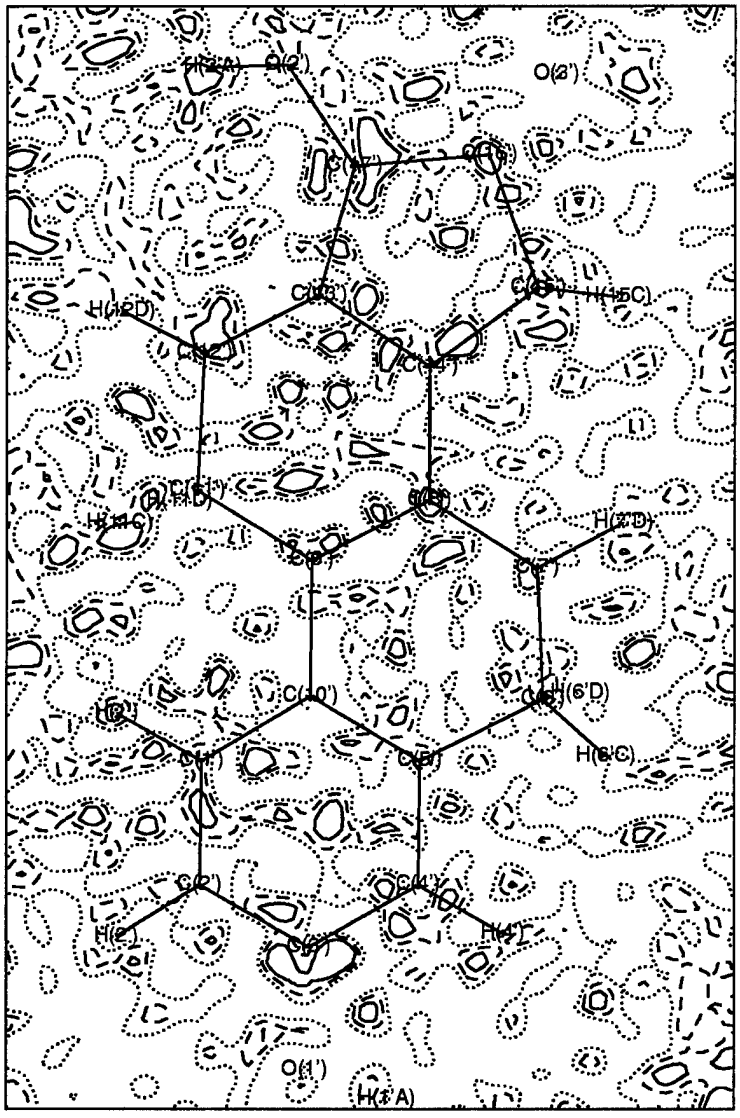

Figure 4b. Residual density maps for molecule 2 in the C(1') C(5') C(16') plane. Contour interval 0.05 eÅ^{-3}. Positive, negative and zero contours are drawn as solid, dotted and broken lines respectively.

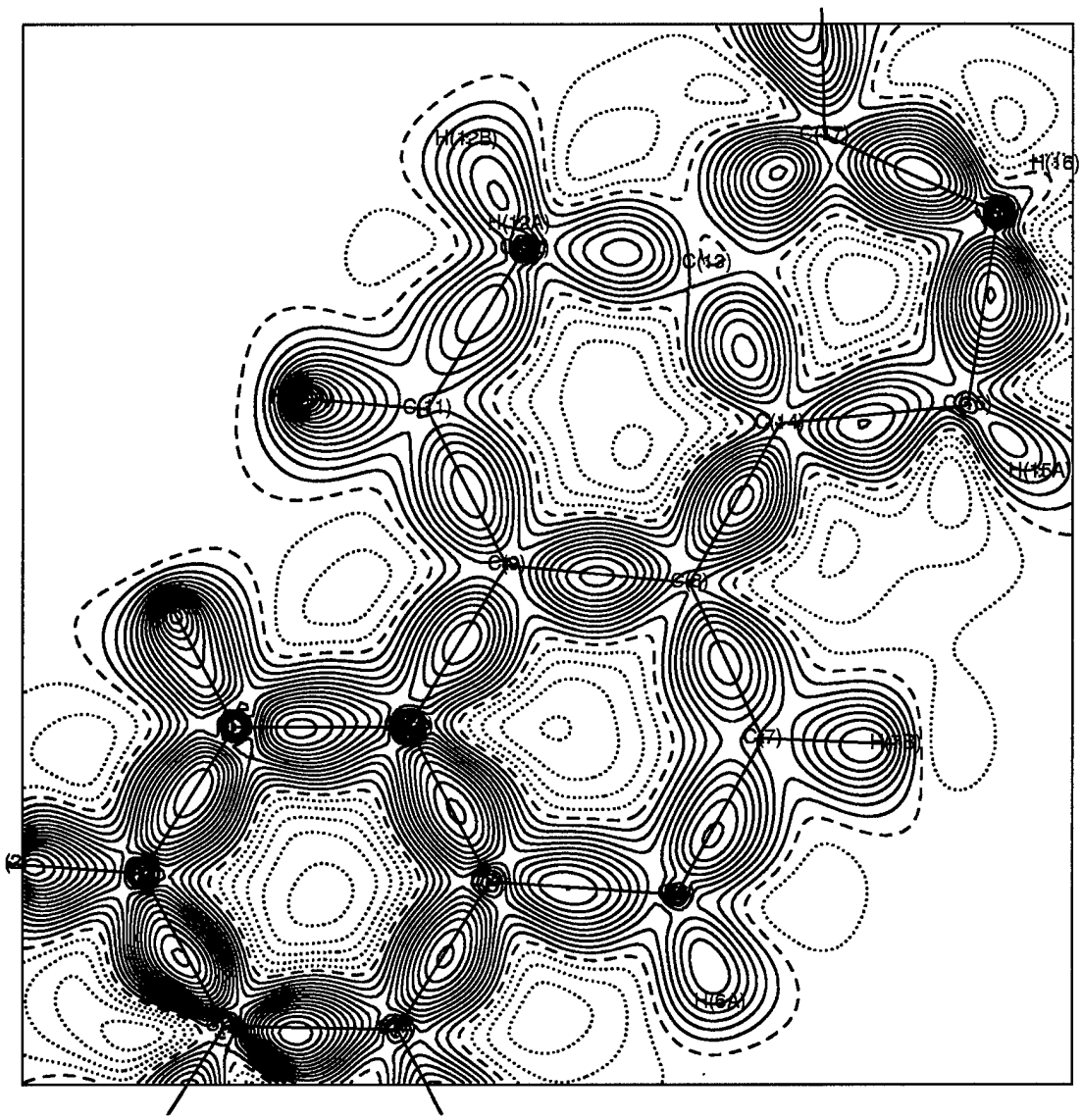

Figure 5. Static deformation density map of molecule 1. Contour intervals 0.05 eÅ^{-3}. Positive solid line, negative dotted line and zero contour broken line.

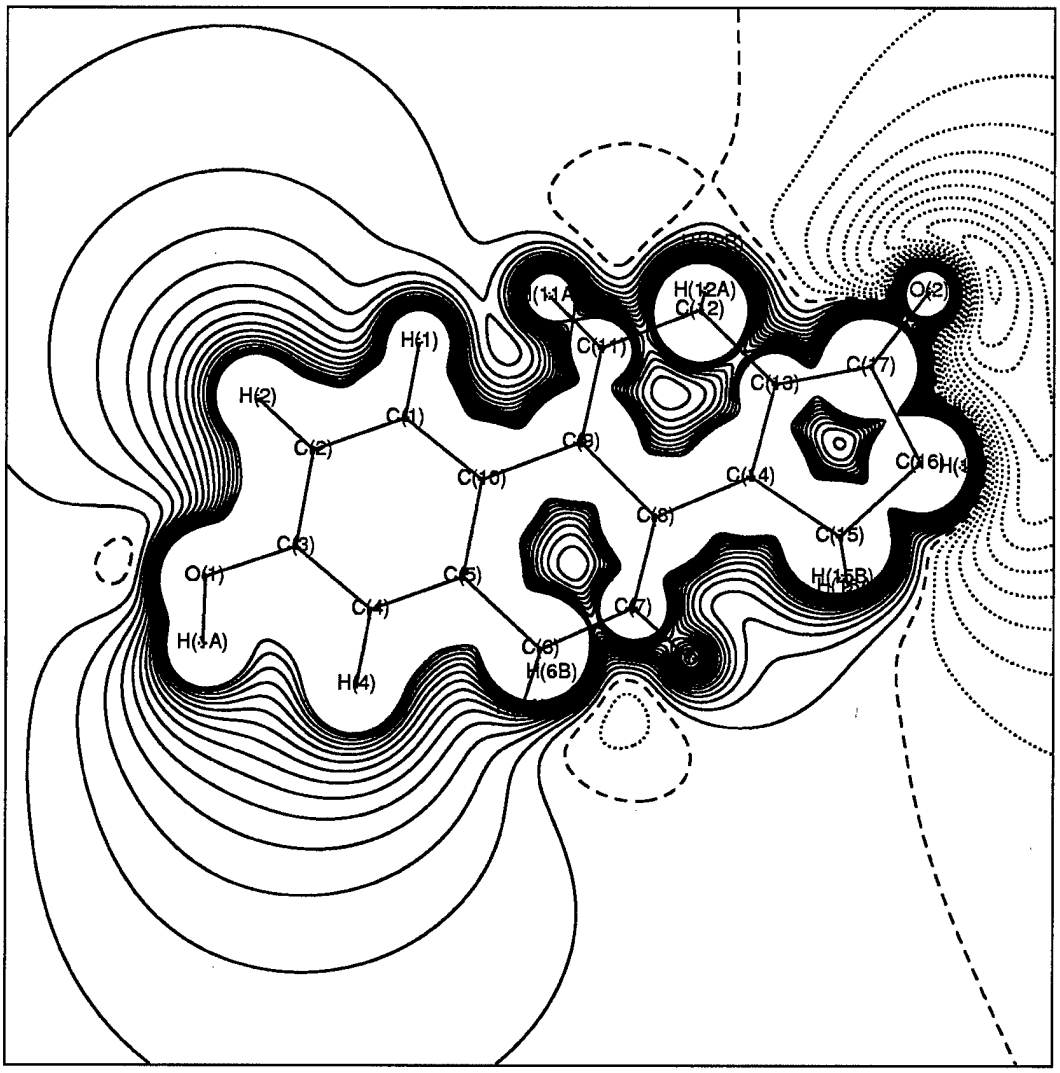

Figure 6a. Electrostatic potential contour map of molecule 1 in the plane of O(1), C(5) and C(16). Contour interval 0.05 eÅ^{-3}; Positive contour is solid line, negative contour is dotted line and zero contour is broken line.

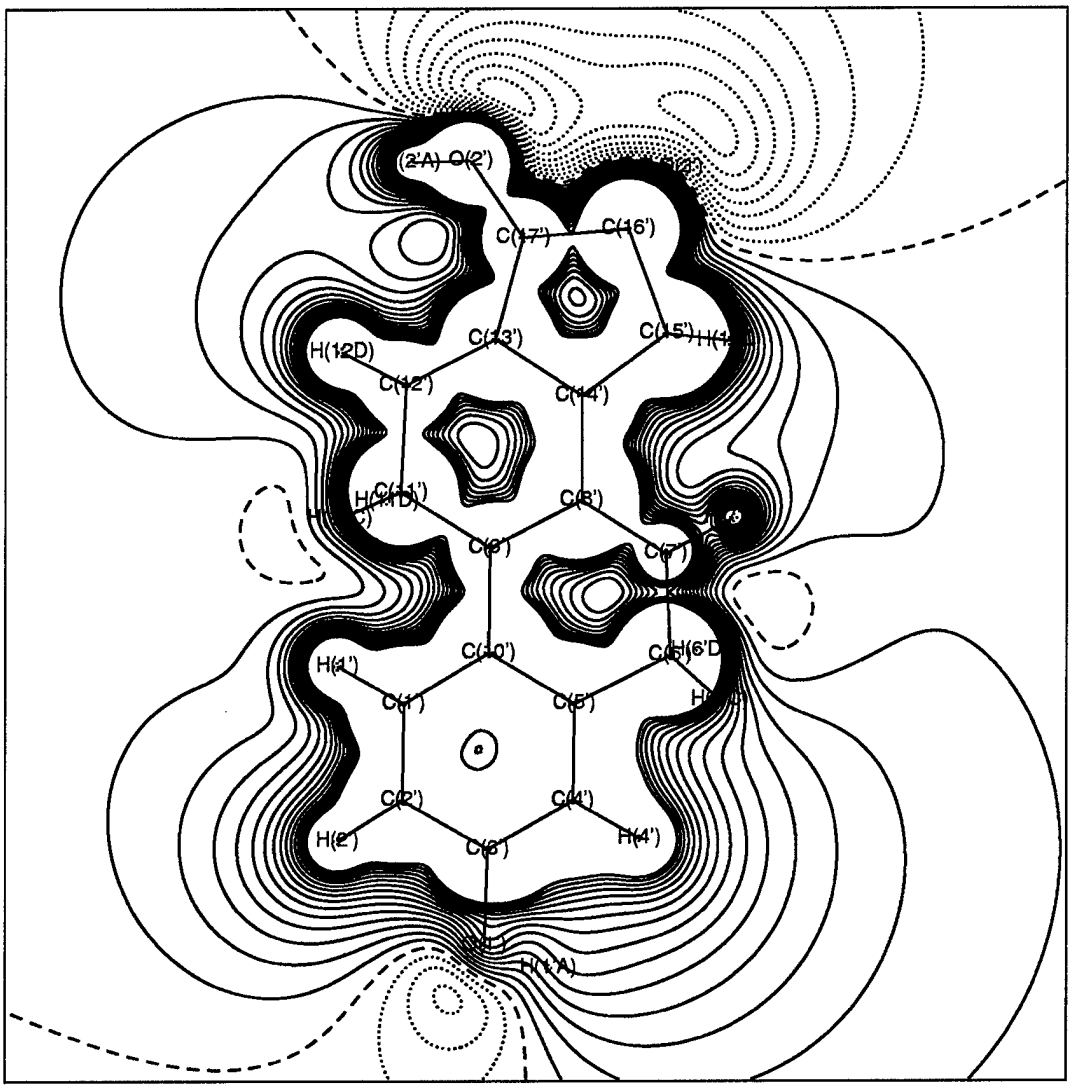

Figure 6b. Electrostatic potential contour map of molecule 2 in the plane of C(1'), C(5') and C(16'). Contour interval 0.05 eÅ^{-3}; Positive contour is solid line, negative contour is dotted line and zero contour is broken line.

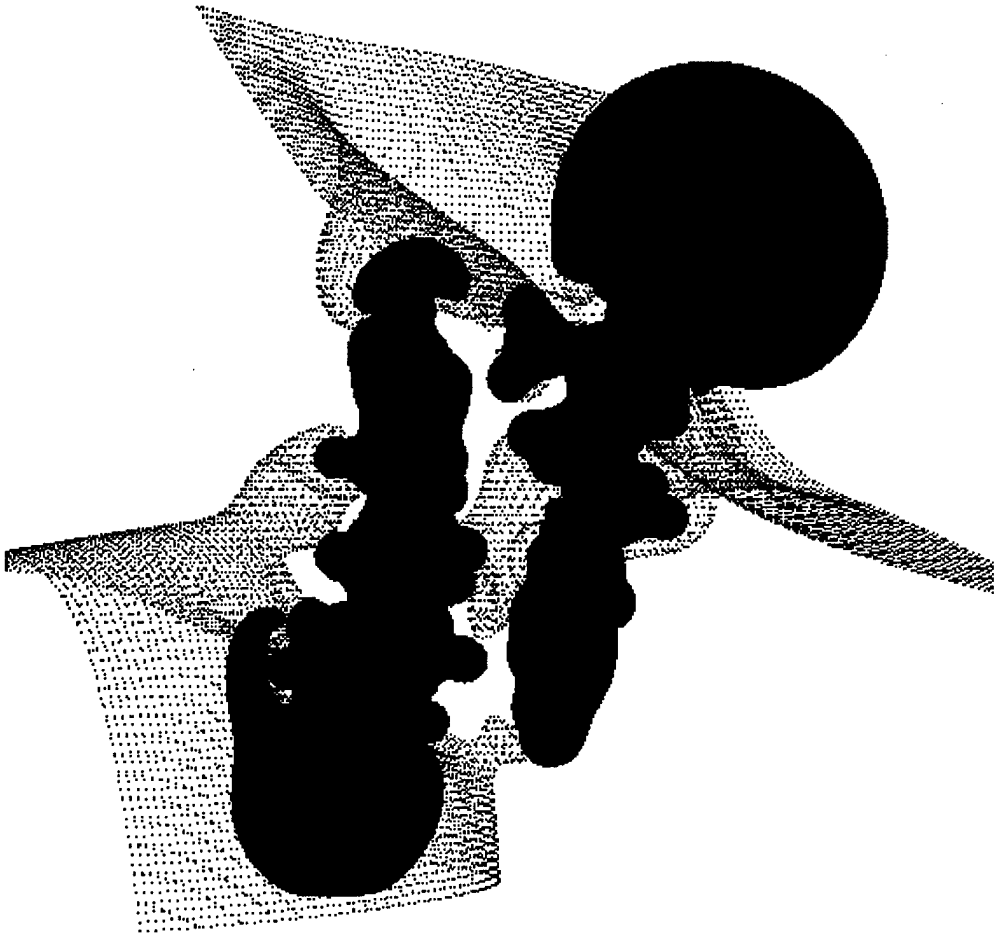

Figure 7. Isosurface representation of electrostatic potential of molecule 1 (right) and 2 (left). Surfaces are drawn at constant positive and negative potentials of 0.5 /e/Å (red) and –0.1 e/Å (green). Grey dots represent zero surface.

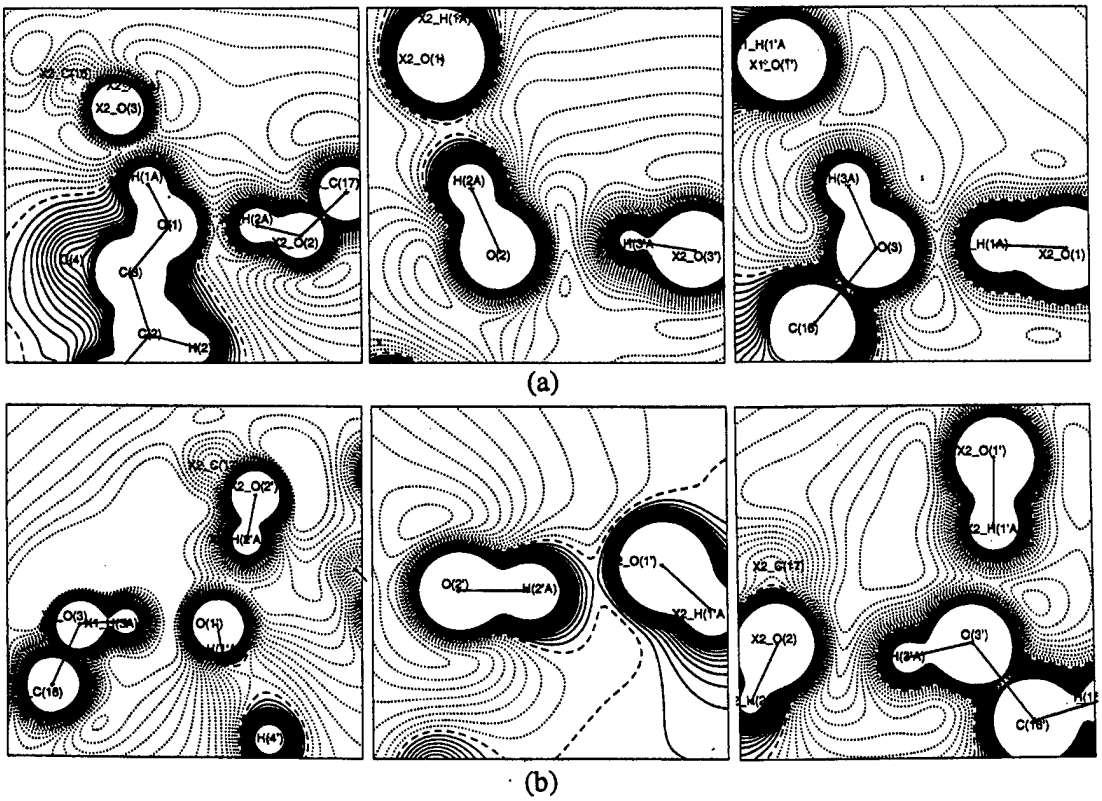

Figure 8. The electrostatic potential in the hydrogen bonding environment of oxygen atoms of (a) molecule 1 and (b) molecule 2. Contour interval 0.05 eÅ^{-3}; Positive solid lines, negative dotted lines and zero contours are broken lines.

Supplementary Tables

Table S1. Fractional coordinates, equivalent displacement parameters (Å^2) after multipole refinement[a]

Atom	x	y	z	U_{eq}
Molecule 1				
O(1)	0.51768(10)	0.85352(11)	0.52120(11)	0.018
O(2)	0.79921(9)	1.32161(11)	0.40944(9)	0.015
O(3)	1.19065(9)	1.28089(11)	0.40369(9)	0.015
C(1)	0.45782(8)	1.00729(11)	0.42503(8)	0.014
C(2)	0.41442(8)	0.94969(11)	0.44370(8)	0.016
C(3)	0.56255(8)	0.91059(11)	0.51231(7)	0.012
C(4)	0.75074(7)	0.93004(11)	0.56560(6)	0.011
C(5)	0.79388(7)	0.98789(11)	0.54672(6)	0.010
C(6)	1.00170(8)	1.00579(11)	0.60531(7)	0.013
C(7)	1.03656(7)	1.06192(11)	0.53178(7)	0.013
C(8)	0.89489(7)	1.10844(11)	0.53900(6)	0.010
C(9)	0.69131(7)	1.08931(11)	0.43663(6)	0.010
C(10)	0.64664(7)	1.02772(11)	0.47414(6)	0.010
C(11)	0.54265(8)	1.13507(11)	0.43759(7)	0.013
C(12)	0.58776(7)	1.19493(11)	0.38487(7)	0.012
C(13)	0.78969(7)	1.21485(11)	0.48383(6)	0.010
C(14)	0.93243(7)	1.16700(11)	0.47888(6)	0.010
C(15)	1.12818(8)	1.19665(11)	0.55149(8)	0.015
C(16)	1.08802(7)	1.26090(11)	0.49990(7)	0.012
C(17)	0.87053(7)	1.26401(11)	0.41297(6)	0.010
C(18)	0.80161(10)	1.23048(11)	0.65010(7)	0.017
H(1A)	0.63209	0.82990	0.55330	0.034
H(2A)	0.69428	1.32373	0.44686	0.012
H(3A)	1.13395	1.27295	0.29273	0.025
H(1)	0.34450	1.03712	0.36414	0.029
H(2)	0.26604	0.93672	0.39812	0.044
H(4)	0.86510	0.89941	0.61941	0.021
H(6A)	1.09283	0.97171	0.58700	0.037
H(6B)	1.04093	1.01387	0.73024	0.020
H(7A)	1.01476	1.05396	0.40896	0.015
H(7B)	1.18207	1.07730	0.59177	0.021
H(8)	0.89840	1.11151	0.65964	0.017
H(9)	0.68554	1.08694	0.31532	0.016
H(11A)	0.40304	1.12061	0.35796	0.024
H(11B)	0.53292	1.13757	0.55336	0.020
H(12A)	0.57626	1.19302	0.26278	0.018
H(12B)	0.48167	1.22649	0.38902	0.019
H(14)	0.90581	1.15747	0.35520	0.014
H(15A)	1.23477	1.17769	0.51002	0.022
H(15B)	1.18913	1.19417	0.67908	0.024
H(16)	1.12808	1.29047	0.60016	0.025
H(17)	0.84636	1.25096	0.29187	0.011
H(18A)	0.76328	1.19583	0.70939	0.033
H(18B)	0.70167	1.26365	0.64136	0.026
H(18C)	0.94099	1.24472	0.71651	0.025
Molecule 2				
O(1')	0.98786(9)	1.26560(11)	1.07236(8)	0.013
O(2')	0.74949(10)	0.79556(11)	1.08083(9)	0.016

O(3')	0.31379(9)	0.81942(11)	0.90942(8)	0.015
C(1')	1.04605(7)	1.10997(11)	1.03189(7)	0.013
C(2')	1.08893(7)	1.16877(11)	1.05868(7)	0.013
C(3')	0.94251(7)	1.20768(11)	1.04700(6)	0.010
C(4')	0.75670(7)	1.18771(11)	1.01090(6)	0.010
C(5')	0.71459(7)	1.12874(11)	0.98527(6)	0.009
C(6')	0.51022(7)	1.11043(11)	0.95313(8)	0.013
C(7')	0.47065(7)	1.04728(11)	0.90310(7)	0.012
C(8')	0.63563(7)	1.00865(11)	0.99989(6)	0.009
C(9')	0.81329(7)	1.02453(11)	0.96109(6)	0.009
C(10')	0.86001(7)	1.08860(11)	0.99460(6)	0.010
C(11')	0.98227(7)	0.98340(11)	1.03926(7)	0.012
C(12')	0.92732(7)	0.91892(11)	1.00723(7)	0.012
C(13')	0.75705(7)	0.90425(11)	1.05525(6)	0.009
C(14')	0.59061(7)	0.94487(11)	0.96631(6)	0.009
C(15')	0.41989(8)	0.91948(11)	0.99963(8)	0.014
C(16')	0.46119(8)	0.85355(11)	1.01718(7)	0.012
C(17')	0.65666(8)	0.84557(11)	0.99892(6)	0.011
C(18')	0.81622(9)	0.90814(11)	1.23340(6)	0.015
H(1'A)	0.87426	1.28653	1.06698	0.027
H(2'A)	0.84956	0.78829	1.03968	0.022
H(3'A)	0.28464	0.83420	0.80471	0.020
H(1')	1.15901	1.07987	1.03660	0.026
H(2')	1.23032	1.18590	1.08056	0.026
H(4')	0.64298	1.21784	1.00111	0.021
H(6'A)	0.41147	1.14015	0.87102	0.027
H(6'B)	0.48205	1.11487	1.06167	0.014
H(7'A)	0.44868	1.04194	0.77938	0.024
H(7'B)	0.33470	1.03427	0.91168	0.021
H(8')	0.66573	1.01546	1.12513	0.012
H(9')	0.77340	1.01922	0.83423	0.011
H(11'A)	1.09205	0.99035	0.98873	0.020
H(11'B)	1.04447	0.99134	1.16493	0.017
H(12'A)	0.89389	0.91066	0.88280	0.018
H(12'B)	1.05438	0.89402	1.07392	0.029
H(14')	0.56308	0.93793	0.84142	0.012
H(15'A)	0.28167	0.92827	0.90891	0.023
H(15'A)	0.40421	0.93935	1.10220	0.016
H(16')	0.48007	0.83935	1.13620	0.015
H(17')	0.62869	0.84147	0.87314	0.014
H(18'A)	0.86807	0.94995	1.27305	0.017
H(18'B)	0.92207	0.87636	1.28493	0.022
H(18'C)	0.70244	0.89942	1.27329	0.032

[a] $U_{eq} = \frac{1}{2} (\Sigma_i \Sigma_j U_{ij} a_i^* a_j^* \mathbf{a_i} . \mathbf{a_j})$

Table S2. Anisotropic thermal parameters of non-Hydrogen atoms ($Å^2$) and estimated standard deviations.

Atom	U_{11}	U_{22}	U_{33}	U_{12}	U_{13}	U_{23}
Molecule 1						
O(1)	0.0125(2)	0.0088(2)	0.0312(3)	-0.0001(2)	0.0108(2)	0.0023(2)
O(2)	0.0146(2)	0.0087(2)	0.0217(3)	0.0028(1)	0.0102(2)	0.0011(2)
O(3)	0.0113(2)	0.0137(2)	0.0187(2)	-0.0034(2)	0.0066(2)	-0.0017(2)
C(1)	0.0083(2)	0.0111(2)	0.0211(2)	0.0005(1)	0.0039(2)	0.0019(2)
C(2)	0.0094(2)	0.0109(2)	0.0250(3)	-0.0003(1)	0.0062(2)	0.0016(2)
C(3)	0.0109(2)	0.0089(1)	0.0164(2)	0.0002(1)	0.0071(1)	0.0008(1)
C(4)	0.0103(2)	0.0096(1)	0.0120(2)	0.0005(1)	0.0048(1)	0.0009(1)
C(5)	0.0087(1)	0.0086(1)	0.0102(2)	0.0005(1)	0.0029(1)	0.0007(1)
C(6)	0.0085(2)	0.0104(2)	0.0167(2)	0.0010(1)	0.0015(1)	0.0032(1)
C(7)	0.0083(2)	0.0104(2)	0.0170(2)	0.0018(1)	0.0041(1)	0.0024(1)
C(8)	0.0080(1)	0.0089(1)	0.0104(2)	0.0008(1)	0.0024(1)	0.0010(1)
C(9)	0.0076(1)	0.0087(1)	0.0108(2)	0.0011(1)	0.0022(1)	0.0008(1)
C(10)	0.0080(1)	0.0090(1)	0.0112(2)	0.0004(1)	0.0026(1)	0.0007(1)
C(11)	0.0085(2)	0.0099(2)	0.0194(2)	0.0014(1)	0.0054(1)	0.0017(1)
C(12)	0.0086(2)	0.0094(2)	0.0163(2)	0.0014(1)	0.0034(1)	0.0016(1)
C(13)	0.0092(1)	0.0085(1)	0.0106(2)	0.0005(1)	0.0042(1)	-0.0005(1)
C(14)	0.0078(1)	0.0086(1)	0.0111(2)	0.0010(1)	0.0029(1)	0.0007(1)
C(15)	0.0081(2)	0.0115(2)	0.0214(2)	0.0006(1)	0.0020(2)	0.0023(2)
C(16)	0.0097(2)	0.0096(2)	0.0147(2)	-0.0005(1)	0.0041(1)	-0.0009(1)
C(17)	0.0097(2)	0.0080(1)	0.0123(2)	0.0010(1)	0.0048(1)	0.0001(1)
C(18)	0.0216(2)	0.0145(2)	0.0123(2)	-0.0001(2)	0.0089(2)	-0.0018(2)
Molecule 2						
O(1')	0.0118(2)	0.0071(1)	0.0182(2)	-0.0011(1)	0.0073(2)	-0.0007(1)
O(2')	0.0171(2)	0.0093(2)	0.0201(3)	0.0029(2)	0.0096(2)	0.0024(2)
O(3')	0.0145(2)	0.0111(2)	0.0167(2)	-0.0051(2)	0.0065(2)	-0.0028(2)
C(1')	0.0082(1)	0.0087(1)	0.0217(2)	0.0000(1)	0.0066(1)	-0.0009(2)
C(2')	0.0092(2)	0.0083(2)	0.0211(2)	-0.0007(1)	0.0067(2	-0.0005(1)
C(3')	0.0097(1)	0.0073(1)	0.0128(2)	-0.0004(1)	0.0053(1)	-0.0003(1)
C(4')	0.0089(1)	0.0069(1)	0.0134(2)	0.0002(1)	0.0041(1)	0.0002(1)
C(5')	0.0074(1)	0.0070(1)	0.0125(2)	0.0004(1)	0.0032(1)	0.0001(1)
C(6')	0.0071(1)	0.0089(1)	0.0212(2)	0.0007(1)	0.0034(1)	-0.0006(1)
C(7')	0.0075(1)	0.0087(2)	0.0175(2)	0.0003(1)	0.0008(1)	-0.0020(1)
C(8')	0.0072(1)	0.0073(1)	0.0115(2)	-0.0001(1)	0.0034(1)	-0.0016(1)
C(9')	0.0084(1)	0.0067(1)	0.0114(2)	0.0003(1)	0.0041(1)	-0.0006(1)
C(10')	0.0078(1)	0.0076(1)	0.0123(2)	0.0004(1)	0.0040(1)	0.0000(1)
C(11')	0.0080(1)	0.0085(1)	0.0175(2)	0.0008(1)	0.0047(1)	0.0005(1)
C(12')	0.0103(2)	0.0084(1)	0.0157(2)	0.0014(1)	0.0069(1)	0.0002(1)
C(13')	0.0090(1)	0.0083(1)	0.0089(1)	0.0000(1)	0.0040(1)	-0.0007(1)
C(14')	0.0080(1)	0.0073(1)	0.0113(2)	-0.0003(1)	0.0032(1)	-0.0020(1)
C(15')	0.0099(2)	0.0091(2)	0.0220(2)	-0.0015(1)	0.0078(2)	-0.0035(2)
C(16')	0.0119(2)	0.0080(1)	0.0144(2)	-0.0017(1)	0.0066(1)	-0.0019(1)
C(17')	0.0117(2)	0.0076(1)	0.0121(2)	-0.0003(1)	0.0060(1)	-0.0013(1)
C(18')	0.0175(2)	0.0149(2)	0.0095(2)	-0.0022(2)	0.0044(2)	-0.0009(1)

The thermal parameters are listed in the form of $\exp\{-2\pi^2(U_{11}h^2a^{*2}+2U_{12}hka^*b^*+\cdots)\}$

Table S3. Bond angles (deg)

bond	m 1	m2
C(2)–C(1)–H(1)	119.7(2)	119.2(2)
C(10)–C(1)–H(1)	117.9(2)	118.7(2)
C(1)–C(2)–H(2)	118.0(2)	122.5(2)
C(3)–C(2)–H(2)	122.6(2)	118.3(2)
C(3)–C(4)–H(4)	119.2(2)	120.1(2)
C(5)–C(4)–H(4)	119.8(2)	119.2(2)
C(5)–C(6)–H(6A)	111.8(1)	110.5(2)
C(5)–C(6)–H(6B)	106.0(1)	108.0(1)
C(7)–C(6)–H(6A)	109.1(1)	112.5(2)
C(7)–C(6)–H(6B)	107.1(2)	106.4(2)
H(6A)–C(6)–H(6B)	109.6(2)	105.3(2)
C(6)–C(7)–H(7A)	109.0(2)	111.1(2)
C(6)–C(7)–H(7B)	110.6(2)	109.1(2)
C(8)–C(7)–H(7A)	108.2(1)	109.1(1)
C(8)–C(7)–H(7B)	109.6(2)	112.5(2)
H(7A)–C(7)–H(7B)	109.1(1)	104.2(1)
C(7)–C(8)–H(8)	108.8(1)	110.1(1)
C(9)–C(8)–H(8)	107.0(1)	109.6(1)
C(14)–C(8)–H(8)	111.4(2)	107.4(2)
C(8)–C(9)–H(9)	107.5(1)	106.6(1)
C(10)–C(9)–H(9)	104.4(2)	106.1(2)
C(11)–C(9)–H(9)	105.9(1)	106.9(1)
C(9)–C(11)–H(11A)	108.1(2)	109.5(2)
C(9)–C(11)–H(11B)	110.1(2)	110.9(2)
C(12)–C(11)–H(11A)	109.3(2)	104.6(2)
C(12)–C(11)–H(11B)	110.9(2)	110.3(2)
H(11A)–C(11)–H(11B)	106.5(1)	108.2(1)
C(11)–C(12)–H(12A)	109.8(2)	108.3(2)
C(11)–C(12)–H(12B)	110.1(2)	106.3(2)
C(13)–C(12)–H(12A)	108.5(1)	110.9(1)
C(13)–C(12)–H(12B)	111.1(1)	112.0(1)
H(12A)–C(12)–H(12B)	105.8(2)	108.7(2)
C(8)–C(14)–H(14)	101.9(2)	107.3(2)
C(13)–C(14)–H(14)	107.4(1)	106.1(1)
C(15)–C(14)–H(14)	109.1(1)	107.0(1)
C(14)–C(15)–H(15A)	112.1(1)	114.3(1)
C(14)–C(15)–H(15B)	114.1(1)	111.5(1)
C(16)–C(15)–H(15A)	111.3(2)	111.2(2)
C(16)–C(15)–H(15B)	109.7(2)	113.8(2)
H(15A)–C(15)–H(15B)	105.8(1)	102.2(2)
O(3)–C(16)–H(16)	105.5(1)	108.4(2)

C(15)–C(16)–H(16)	120.0(2)	110.2(2)
C(17)–C(16)–H(16)	109.0(1)	106.4(1)
O(2)–C(17)–H(17)	107.8(2)	111.0(2)
C(13)–C(17)–H(17)	106.1(2)	108.2(2)
C(16)–C(17)–H(17)	105.6(1)	106.9(1)
C(13)–C(18)–H(18A)	113.5(1)	110.5(1)
C(13)–C(18)–H(18B)	107.9(1)	108.6(1)
C(13)–C(18)–H(18C)	109.8(1)	113.1(1)
H(18A)–C(18)–H(18B)	105.6(1)	110.7(1)
H(18A)–C(18)–H(18C)	109.4(2)	107.3(2)
H(18B)–C(18)–H(18C)	110.4(3)	106.4(2)

Table S4. Multipole population coefficients for the atoms of molecule 1 (first row) and 2 (second row)[a].

Atom	M1	D0	D1+	D1-	Q0	Q1+	Q1-	Q2+	Q2-
O(1)	6.51(4)	-0.04(2)	-0.09(2)	-0.01(2)	0.04(2)	-0.02(2)	-0.04(2)	-0.06(2)	- 0.01(2)
	6.68(4)	-0.05(2)	-0.06(2)	-0.04(2)	0.04(2)	0.01(2)	0.01(2)	-0.05(2)	0.00
O(2)	6.71(4)	0.08(2)	-0.03(2)	-0.05(2)	0.07(2)	0.00	-0.08(2)	-0.07(2)	-0.02(2)
	6.69(4)	0.03(2)	-0.06(2)	-0.06(2)	0.08(2)	0.05(2)	0.04(2)	-0.05(2)	0.02(2)
O(3)	6.82(4)	-0.03(2)	-0.06(2)	-0.03(2)	-0.02(2)	0.00	0.00	-0.06(2)	-0.03(2)
	6.74(4)	0.01(2)	-0.09(2)	-0.03(2)	0.04(2)	0.05(2)	-0.08(2)	-0.08(2)	-0.07(2)
C(1)	4.21(6)	-0.11(3)	0.00	0.05(4)	-0.25(3)	-0.03(3)	0.05(3)	0.00	-0.02(3)
C(2)	3.80(6)	0.03(3)	-0.05(4)	0.00	-0.24(3)	0.00	0.04(2)	0.05(3)	-0.08(3)
C(3)	3.87(6)	0.00	0.23(4)	0.13(4)	-0.33(2)	0.00	-0.06(2)	0.00	-0.07(3)
C(4)	3.65(6)	0.16(3)	0.14(4)	0.00	-0.21(2)	-0.03(2)	0.00	0.00	0.01(3)
C(5)	3.88(6)	0.00	0.09(4)	-0.02(4)	-0.31(3)	-0.03(3)	-0.01(3)	-0.01(3)	-0.01(3)
C(6)	4.25(6)	0.09(3)	-0.10(3)	-0.15(3)	0.00	-0.10(2)	0.00	0.03(2)	0.04(2)
C(7)	4.48(6)	0.00	-0.12(3)	0.01(3)	0.00	0.05(2)	-0.04(2)	0.07(2)	-0.05(2)
C(8)	4.07(6)	0.13(3)	-0.05(3)	-0.12(3)	0.06(2)	-0.09(2)	-0.08(2)	0.01(2)	0.04(2)
C(9)	4.11(6)	0.01(2)	0.12(3)	0.02(2)	0.00	0.00	0.01(2)	-0.01(2)	-0.05(2)
C(10)	3.69(6)	-0.04(3)	0.07(4)	0.00	-0.13(3)	0.01(3)	0.05(2)	-0.04(3)	-0.08(3)
C(11)	4.25(5)	-0.08(3)	-0.08(3)	0.02(3)	0.00	-0.03(2)	-0.06(2)	0.00	0.04(2)
C(12)	4.29(6)	-0.14(3)	-0.12(3)	0.08(3)	0.04(2)	0.05(2)	-0.03(2)	0.06(2)	-0.05(2)
C(13)	3.86(6)	0.05(3)	0.04(3)	-0.03(3)	-0.04(2)	-0.15(2)	0.00	0.05(2)	0.04(2)
C(14)	4.06(6)	-0.10(3)	-0.13(3)	0.08(3)	0.00	0.06(2)	-0.08(2)	-0.08(2)	0.06(2)
C(15)	4.08(5)	0.00	-0.12(3)	-0.07(3)	-0.04(2)	-0.03(2)	-0.17(3)	0.00	0.09(2)
C(16)	4.23(5)	0.09(3)	0.07(3)	-0.10(3)	0.05(2)	-0.11(2)	-0.03(2)	0.00	0.13(2)
C(17)	4.23(5)	-0.16(3)	-0.06(3)	0.09	0.03(2)	0.05(2)	-0.03(2)	0.00	-0.13(2)
C(18)	4.35(6)	-0.14(3)	0.10(3)	0.03(3)	0.05(2)	-0.03(3)	0.02(3)	-0.06(2)	-0.03(3)
H(1A)	0.64(4)	0.13(3)							
	0.73(3)	0.13(3)							
H(2A)	0.69(3)	0.21(2)							
	0.73(3)	0.25(3)							
H(3A)	0.94(3)	0.10(2)							
	0.76(3)	0.12 (2)							
H(1)	1.00(4)	0.10(2)							
H(2)	0.80(3)	0.25(2)							
H(4)	0.79(3)	0.21(2)							
H(6A)	1.00(4)	0.22(2)							
H(6B)	0.94(3)	0.01(2)							
H(7A)	0.85(3)	0.11(2)							
H(7B)	0.92(3)	0.13(3)							
H(8)	0.81(3)	0.03(2)							
H(9)	0.89(3)	0.11(2)							
H(11A)	0.96(3)	0.07(2)							
H(11B)	0.90(3)	0.13(2)							
H(12A)	0.88(3)	0.02(2)							
H(12B)	0.91(3)	0.20(2)							
H(14)	0.79(3)	0.05(2)							
H(15A)	0.79(3)	0.18(2)							
H(15B)	0.76(3)	0.03(2)							
H(16)	0.74(3)	0.14(2)							
H(17)	0.75(30	0.05(2)							
H(18A)	0.94(4)	0.10(2)							
H(18B)	0.90(4)	0.19(2)							
H(18C)	1.00(4)	0.10(2)							

All the ring (A, B, C, D) atoms of the molecule 1 has been constrained equal to molecule 2.

Atom	O0	O1+	O1-	O2+	O2-	O3+	O3-	H0	H1+	H1-	H2+	H2-	H3+	H3-	H4+	H4-
O(1)	-0.05(2)	0.03(2)	-0.03(2)	0.03(2)	-0.05(2)	0.05(2)	-0.02(2)	0.03(3)	0.01(2)	0.03(2)	0.06(2)	0.04(2)	-0.02(2)	0.02(2)	0.04(2)	0.06(2)
	-0.02(2)	-0.03(2)	-0.03(2)	0.00	-0.01(2)	0.11(2)	-0.06(2)	0.06 (2)	0.01(2)	-0.04(2)	-0.04(2)	0.03(2)	0.00	0.03(2)	0.04(2)	0.00
O(2)	-0.02(2)	0.00	0.00	0.03(2)	0.01(2)	0.122)	0.02(2)	0.00	-0.03(2)	-0.01(2)	-0.03(2)	-0.01(2)	-0.02(2)	0.06(2)	-0.03(2)	0.08(2)
	-0.04(2)	-0.01(2)	-0.02(2)	0.01(2)	0.04(2)	0.08(2)	-0.04(2)	-0.05(2)	0.00	-0.06(2)	0.06(2)	0.02(2)	-0.07(2)	-0.05(2)	0.00	0.01(2)
O(3)	0.03(2)	-0.01(2)	0.06(2)	-0.01(2)	-0.02(2)	0.06(2)	-0.08(2)	0.01(2)	0.07(2)	0.04(2)	0.01(2)	0.06(2)	-0.03(2)	0.01(2)	0.04(2)	-0.03(2)
	0.05(2)	-0.04(2)	0.01(2)	0.03(2)	0.01(2)	0.09(2)	-0.05(2)	-0.05(2)	-0.06(2)	0.03(2)	0.01(2)	0.02(2)	-0.06(2)	0.07(2)	-0.02(2)	0.04(2)
C(1)	0.03(3)	0.01(3)	-0.02(3)	0.03(3)	0.00	0.51(4)	0.04(3)	0.05(3)	0.00	0.03(3)	-0.03(3)	0.02(4)	0.00	0.00	0.08(3)	0.07(4)
C(2)	-0.01(3)	0.00	0.06(3)	0.03(3)	0.00	0.46(4)	-0.10(4)	0.06(4)	0.06(3)	0.00	0.03(4)	0.00	0.11(3)	0.03(3)	0.01(4)	-0.22(3)
C(3)	0.00	0.00	0.05(3)	0.00	0.00	0.58(4)	-0.07(3)	0.12(3)	0.00	0.00	0.02(3)	0.04(3)	-0.06(4)	0.06(4)	-0.01(4)	-0.14(4)
C(4)	0.07(3)	0.00	0.00	0.05(3)	-0.06(3)	0.41(4)	-0.01(4)	0.07(3)	-0.03(3)	0.00	-0.03(3)	-0.06(3)	-0.01(3)	0.00	-0.02(4)	-0.07(3)
C(5)	0.00	0.00	0.06(3)	0.00	-0.05(3)	0.45(4)	-0.02(4)	0.09(3)	-0.06(3)	-0.04(3)	-0.06(4)	0.01(4)	-0.11(4)	-0.06(4)	-0.07(5)	0.00
C(6)	0.02(3)	0.06(3)	0.05(3)	0.01(2)	0.36(3)	-0.01(3)	0.00	-0.08(3)	-0.02(3)	-0.04(3)	0.03(3)	-0.09(3)	-0.10(3)	0.00	0.04(3)	-0.03(3)
C(7)	-0.02(3)	0.00	0.04(2)	0.02(3)	0.47(3)	0.02(3)	0.02(3)	-0.21(3)	-0.06(3)	-0.01(3)	-0.09(3)	0.03(3)	-0.06(3)	-0.04(3)	-0.03(3)	0.02(3)
C(8)	0.03(3)	0.00	0.00	0.01(3)	0.56(3)	0.00	0.02(3)	-0.24(4)	-0.09(3)	-0.01(3)	0.05(3)	-0.02(3)	0.08(3)	-0.03(3)	-0.14(3)	-0.05(3)
C(9)	0.01(2)	-0.07(3)	-0.01(3)	0.01(3)	0.46(3)	-0.11(3)	0.02(2)	-0.12(4)	0.00	-0.07(3)	-0.02(3)	0.00	0.00	0.02(3)	-0.16(3)	0.00
C(10)	-0.01(3)	0.00	0.01(3)	0.00	0.00	0.39(4)	-0.01(3)	-0.04(3)	-0.08(3)	0.08(3)	0.07(4)	-0.03(4)	0.04(4)	-0.05(4)	-0.07(4)	0.02(3)
C(11)	0.09(3)	0.08(2)	-0.03(2)	-0.06(2)	0.44(3)	-0.03(2)	0.00	-0.06(4)	0.11(3)	0.00	0.01(3)	0.00	0.02(3)	-0.06(3)	-0.10(3)	-0.07(3)
C(12)	0.09(3)	0.07(2)	0.04(3)	0.02(2)	0.45(3)	-0.01(3)	0.00	-0.14(3)	0.07(3)	0.00	0.00	0.00	-0.02(3)	0.01(3)	-0.06(3)	0.00
C(13)	0.00	-0.01(3)	-0.01(3)	0.03(3)	0.47(3)	-0.03(3)	-0.02(3)	-0.13(4)	-0.01(4)	-0.03(4)	0.12(4)	0.00	0.04(4)	0.03(4)	-0.12(4)	0.07(4)
C(14)	-0.01(3)	0.00	0.00	- 0.02(3)	0..55(3)	0.00	0.00	-0.24(4)	0.09(3)	-0.02(3)	-0.05(3)	0.01(4)	-0.04(3)	-0.04(4)	-0.15(3)	0.03(3)
C(15)	-0.02(3)	-0.04(3)	-0.09(2)	0.00	0.48(3)	0.01(2)	0.03(3)	-0.18(3)	-0.07(3)	-0.02(3)	-0.10(3)	-0.11(3)	0.03(3)	-0.06(3)	0.00	0.00
C(16)	0.00	-0.04 (3)	0.00	0.07(3)	0.69(3)	-0.01(2)	0.00	-0.25(4)	0.04(3)	-0.06(3)	0.05(3)	0.00	0.02(3)	0.00	-0.21(3)	0.00
C(17)	-0.02(3)	0.00	0.04(3)	0.13(3)	0.57(3)	0.06 (3)	-0.08(3)	-0.22(4)	0.02(3)	0.04(3)	-0.03(3)	-0.09(3)	0.01(3)	-0.09(3)	-0.13(3)	0.08(3)
C(18)	0.00	-0.06(2)	-0.05(3)	0.01(2)	0.36(3)	0.02(3)	-0.04(3)	-0.06(3)	0.00	0.00	0.04(3)	0.02(3)	0.00	0.04(3)	-0.06(3)	-0.03(3)

Appendix G.

Parrish, D. & Pinkerton, A.A.

The Experimental Charge Density Study of Estrogens: 17β-Estradiol•Urea

manuscript under revision.

In order to relate molecular electrostatic potential to biological activities of estrogens, a comparative charge density study of different derivatives has been initiated. The first completed charge density analysis of this series for 17β-estradiol•urea is presented here. It has been demonstrated that it is possible to perform a quality experimental charge density study for the big organic system with 56 atoms in the non-centrosymmetric space group. The special tools such as the optimal coordinate system and slow initially constrained refinement have been used to accomplish this study.

Our results for the urea molecule reasonably agree with the previous experimental and theoretical results showing the quality of our data. In the 17β-estradiol molecule, oxygen atoms appeared to be sp^3 in shape, exhibiting two consistent, distinct lone pairs despite of different chemical environments. No interaction of hydroxy group oxygen lone pairs with the π orbitals of the aromatic ring has been observed. The analysis of the electrostatic potential revealed that the negative potential in the lone pair region of the oxygen atoms is quite different. The Bader's topological analysis has been performed, and atomic charges have been estimated. The results are compared and discussed.

Estrogens are known to be responsible for the development of secondary sexual characteristics, as well as they effect growth, differentiation and function of wide range of tissues [1]. It has also been shown [2] that some estrogens are responsible for the initiation and progression of certain types of breast cancer. These molecules have the ability to bind as ligands to the estrogen receptor in the first of many steps which could result in the activation (agonistic effect) or repression (antagonistic effect) of genes critical in the mechanism of tumor growth. While the mechanism by which the estrogens influence cancer is currently unknown, subtle changes in the chemical structure of estradiol and the other estrogens are known to elicit different biological responses in the development of cancer. It has been suggested [3] that the agonistic/antagonistic responses of the different estrogens can be related to such physical properties as their electrostatic potential and charge density distribution.

A comparative charge density study of a series of estrogen derivatives has been initiated in our group, with the primary goal of relating the electronic and physical structure of the molecule to biological action. In addition to molecular properties, charge density studies provide significant

fundamental information about the functional groups and the atoms which make them up, helping to investigate basic chemical principles of small organic molecules in general. This paper will pay particular attention to the hydroxy groups of the estrogen molecule. The hydroxy groups are some of the most chemically interesting portion of the estrogen molecule, and their interaction with the receptor is thought to be mostly responsible for their activity.

Described here is the charge density study of 17β-estradiol•urea. This particular crystal system was chosen to be the first in the series for two reasons. First, 17β-estradiol (E_2) is the most common naturally occurring estrogen and is typically the standard by which all other estrogenic activities are related. E_2 demonstrates an agonistic response in *in vitro* tests which typically utilize the estrogen receptor in either competitive yeast or human cell assays [4-5]. Secondly, it contained a solvated urea molecule which has been extensively studied. Both theoretical and experimental charge density studies have been performed on this molecule [6-7]. This provides a direct means of comparison to test our methods against previous results.

Experimental

Data Collection and Reduction

Crystals were grown by slow evaporation as described by Duax in the original publication of the crystal structure [8]. The clear, colorless crystal of approximate dimensions 0.35 × 0.37 × 0.40 mm was attached to a 30 μm carbon fiber using a small amount of epoxy resin. Data were collected at 100.0(1) K on a Bruker Platform Diffractometer equipped with a SMART 6000 CCD area detector located at 7.12 cm from the goniometer center. The Oxford Cryostream system has been used to cool the crystal. The crystals were irradiated with graphite monochromated Mo K_α radiation (λ = 0.7107 Å). 0.3° omega scans were carried out at four phi settings and three detector positions in 2θ, resulting in more than 7400 frames. A frame time of 60 seconds was used for the low angle setting, and 180 seconds for the medium and high angle settings. A complete experimental protocol is deposited.

The intensities were integrated using the program *SAINT* [9]. After several integrations and preliminary refinements, it was found that different integration parameters were required for each detector setting to obtain the best possible structure factors. The box sizes, profile fitting parameters, and the simple sum perimeter limits were adjusted for each detector setting. The unit cell parameters have been finally refined in *SAINT*.

Lorentz-polarization and $\lambda/2$ corrections were applied to the integrated intensities with a $\lambda/2$ correction factor of 0.0012, this value being taken from the earlier study [10]. The program

SORTAV [11] was used for outlier determination, averaging, and applying the absorption correction. Only reflections with $I > 3\sigma(I)$ and below 1.00 $Å^{-1}$ were used during the multipole refinements.

Table 1. The crystal information and experimental details.

Formula	$C_{19}H_{28}N_2O_3$
Formula Weight	332.43
Crystal System	Orthorhombic
Space Group	$P2_12_12_1$
a	7.9022(9) Å
b	9.2228(10) Å
c	24.5890(28) Å
$\alpha = \beta = \gamma$	90.0°
Volume	1792.06 $Å^3$
Z	4
T	100.0 K
λ	0.7107 Å
$(\sin\theta/\lambda)_{max}$	1.180 $Å^{-1}$
Reflections Collected	110999
Rejected Outliers	779
Unique Reflections	13187
Included in the Refinement [$I > 3\sigma(I)$]	7626
Data completeness	98.6 %
Average redundancy	8.4
R_{int}	0.0411
R_1 (spherical)	0.065
wR_2 (spherical)	0.145
$R(F^2)$ [$I > 3\sigma(I)$] (multipole)	0.029
$R(F^2)$ all data (multipole)	0.036
wR (F^2)	0.045
Weighting scheme	$1/\sigma^2$
Goodness of Fit	1.393

Least-Squares Refinements

The crystal structure was re-solved, and the spherical atom model was refined using the program *SHELXL-97* [12]. 17β-estradiol and urea molecules are shown in Figure 1. All hydrogen atoms were located from the difference Fourier map. The results of this refinement served as the starting point for the aspherical atom refinements that were performed using the *XD* software package [13].

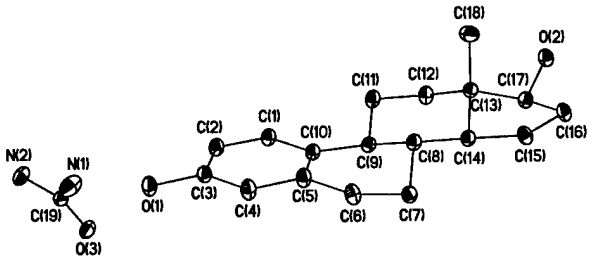

Figure 1. 17β-estradiol and urea molecules showing 50% probability thermal ellipsoids as at 100K. Hydrogen atoms are omitted for clarity.

The aspherical atom model [14], used in further refinements consists of three components. The first and second describe spherically averaged core and valence densities normalized to one electron, while the third one describes the aspherical valence density. $\rho(\mathbf{r})$ is the electron density, P_c, P_v, and P_{lm} are population coefficients, the core population (P_c) was fixed in this study. Asphericity is taken into account by expanding of the electron density over real combinations of spherical harmonics, y_{lm}, which satisfy local symmetry. The variable radial parameters, κ and κ', allow for expansion or contraction of the valence terms. R_l are normalized Slater-type radial functions.

$$\rho_{atomic}(\mathbf{r}) = P_c\rho_{core} + P_v\kappa^3\rho_{valence}(\kappa\mathbf{r})$$

$$+ \sum_{l=1}^{4} \kappa'^3 R_l(\kappa'\mathbf{r}) \sum_{m=-1}^{1} P_{lm} y_{lm}(\mathbf{r}/\mathbf{r})$$

Because the model is based on atom centered multipoles, a coordinate system is required for each atom in the system. The core structure of the estrogen molecule was set up using the standard estrogen coordinate system to take advantage of the shape of certain multipoles to increase the stability of the initial multipole refinements [15]. The vectors for the oxygen atoms of the estrogen molecule were directed to bound atoms. The coordinate system setup for the urea molecule is deposited.

Before the refinements were begun, the hydrogen atom positions were corrected by extending the X – H distances to their neutron bond lengths ($C_{sp2}H$ = 1.08 Å, $C_{sp3}H$ = 1.10 Å, $C_{sp3}H_2$ = 1.09 Å, $C_{sp3}H_3$ = 1.06 Å, OH = 0.97 Å, $N_{sp2}H_2$ = 1.01 Å). These values were fixed in the refinement. A well known correlation exists between the thermal parameter and the kappa parameters of a hydrogen atom, only allowing the kappa parameters to be refined when the thermal parameters of the hydrogen atom are known [16]. To avoid this problem, fixed kappa values (κ_H = 1.20 and κ'_H = 1.20) were used, while the thermal parameters were allowed to refine [17-18].

Initially, to reduce the number of parameters in the least squares process, chemical constraints and only the most significant multipoles were considered. By the end of the refinement, all non-hydrogen atoms were treated up to the octupole level with no chemical constraints. The hydrogen atoms were refined with only two multipoles having cylindrical symmetry along the X - H bond. Hydrogen atoms bound to the same carbon have been constrained to be equal. The electroneutrality constraint has been imposed on both of two molecules. Complete tables giving the final structural information, such as atomic coordinates, U_{ij}'s, U_{iso}'s, bond lengths, bond angles and multipole parameters are deposited.

Topological Analysis, Atomic Charges and Electrostatic Potential

The topological analysis was performed based on the Atoms in Molecules (AIM) Quantum Theory [19]. The *XD* property assessment program, *XDPROP*, was used to perform a quantitative critical point* analysis on all covalent and hydrogen bonding interactions, as well as oxygen lone pair densities. The atomic basin boundaries were defined and the atomic charges (Bader's charges) were integrated within the basins with the program *TOPXD* [20]. The integrated atomic charge $q(\Omega)$ over the atomic basin Ω is defined as a difference between nuclear Z_Ω and electronic $N(\Omega)$ charges:

* Critical points are special points in the electron density, where $\nabla\rho(\mathbf{r}_{CP})=0$. The saddle (3,-1) point reflects the chemical bonding. In the Laplacian, the (3,+3) minimum point corresponds to the maximum curvature of the electron density in the charge concentration regions. See ref. [19].

$$q(\Omega) = Z_\Omega - N(\Omega), \quad N(\Omega) = \int_\Omega \rho(\mathbf{r})d\tau.$$

This method allows one an exhaustive partitioning of the molecules into the respective atoms, leading to the additivity and transferability of it's properties [21].

The calculation of the electrostatic potential (ESP) was performed using the program *XDPROP*. It can be calculated by the evaluation of

$$V(\mathbf{r}) = \sum_A \frac{Z_A}{|\mathbf{R}_A - \mathbf{r}|} - \int \frac{\rho(\mathbf{r}')d\mathbf{r}'}{|\mathbf{r}' - \mathbf{r}|}$$

where Z_A is the charge on nucleus A located at $\mathbf{R}_A$. The construction assembles positive charges at the nuclei and a continuous distribution of electrons. The calculations were performed based on the isolated from the crystal β-estradiol molecule.

Results and Discussion

Packing

The molecular structure and hydrogen bonding pattern were found to be the same as described by Duax [8]. The packing of this structure results in a formation of six hydrogen bonds ranging in donor-acceptor length from 2.64 – 3.10 Å, these are listed in Table 2. The O(1) atom acts as an acceptor in two hydrogen bonds with hydrogens of two independent urea molecules (H(1NB) and H(2NB)). The H··O vectors of these hydrogen bonds are pointed almost directly at the positions of the lone pairs of O(1). The O(2) atom has a very similar hydrogen bonding structure to O(1) in which it acts as an acceptor in two hydrogen bonds and a donator in one. The hydrogen atoms from the O(1) atom of another independent E_2 molecule and H(2NB) of a urea molecule line up almost directly with the lone pair positions of O(2). Topological analysis yielded in a (3,-1) critical point and a bond path[†] for each hydrogen – acceptor interaction, verifying the true bonding interaction in these hydrogen bonds [22]. The complete table of results from hydrogen bond topology is deposited.

[†] Bond path is a line along which the electron density decreases for any lateral displacement.

Table 2. The geometrical information for the hydrogen bonds.

D—H··A	d (D··A), Å	∠DHA, °
O(2)—H(2O)· ·O(3)	2.6395(7)	169.1(16)
O(1)—H(1O)· ·O(2)	2.6698(7)	171.0(20)
N(1)—H(1NA)· ·O(3)	2.8231(10)	168.6(18)
N(1)—H(1NB)· ·O(1)	2.9783(9)	135.2(16)
N(2)—H(2NB)· ·O(1)	3.0086(9)	161.1(17)
N(2)—H(2NA)· ·O(2)	3.1023(8)	169.1(16)

Kappa Parameters

The coefficients of expansion/contraction of the spherical valence and deformation densities, κ and κ' parameters respectively, are shown in Table 3. The grouping of individual atoms were based on the atom type, hybridization and chemical environment. A total of twelve kappa sets were utilized in order to allow the necessary flexibility while attempting to maintain a minimum number of parameters. As mentioned earlier, the hydrogen atom kappa values were fixed at 1.20. All other kappa values were allowed to refine during the least squares minimization.

Table 3. The expansion/contraction (κ and κ')parameters for the 17β-estradiol•urea crystal

Atoms	Kappa	κ	κ'
O(1), O(2)	1	0.971	0.854
C(3)	2	1.009	0.879
C(17)	3	1.012	0.933
C(1), C(2), C(4)	4	0.976	0.896
C(5), C(10)	5	0.986	0.838
C(6), C(7), C(8), C(9), C(11), C(12), C(13), C(14), C(15), C(16), C(17), C(18)	6	0.985	0.878
all C – H hydrogen atoms	7	1.200	1.200

H(1O), H(2O)	8	1.200	1.200
C(19)	9	0.986	0.818
O(3)	10	0.991	1.080
N(1), N(2)	11	0.996	1.004
all N – H hydrogen atoms	12	1.200	1.200

Atomic Charges

The net atomic charges were derived directly from the monopole populations of the multipole model, as well as from integrating of the electron density within the atomic basins as described by the AIM theory. A complete list of atomic charges determined by both methods are listed in Table 4.

As mentioned earlier, the urea molecule gives us the opportunity to compare our results with previous theoretical and experimental results [6-7]. The atomic charges derived directly from the monopole populations of the multipole model compared favorably to the experimental values reported[‡] by Zavodnik et al. [6], with values matching within one e.s.d. Bader's charges are in a fair agreement with those reported by Gatti et al. [7]. Generally, Bader's charges are significantly bigger than the charges derived from the monopole populations; this is not surprising due to the different ways of calculations. Upon first inspection, a charge of +2.13 e^- for the central carbon seems tremendously high. At the same time, there is evidence in the literature, from both theoretical and experimental data, that this is not unreasonable for a carbon surrounded by electronegative oxygen and nitrogen atoms [7, 23].

The net atomic charges for the atoms of the estrogen molecule derived from the monopole populations of the multipole model were as expected for the given atom types and their chemical neighbors. In addition, like atoms with similar chemical environments exhibited very consistent monopole populations. Again, the charge integrations over atomic basins yielded much greater charges for the oxygen atoms and the atoms directly bound to them, maintaining the consistency between chemically equivalent atoms.

Table 4. Net atomic charges for the atoms of 17β-estradiol • urea

[‡] See the deposition material of Zavodnik et al. (1999) *Acta Crystallogr.* **B55**, 45-54.

Atom	$q(P_v)$	$q(\Omega)$	Atom	$q(P_v)$	$q(\Omega)$
O(1)	-0.534(9)	-1.24	H(1O)	0.401(9)	0.68
O(2)	-0.527(9)	-1.11	H(2O)	0.391(9)	0.67
C(1)	-0.233(16)	-0.19	H(1)	0.206(10)	0.14
C(2)	-0.227(16)	-0.12	H(2)	0.248(9)	0.20
C(3)	0.148(14)	0.49	H(4)	0.249(9)	0.21
C(4)	-0.267(15)	-0.21	H(6A)	0.147(7)	0.15
C(5)	-0.110(15)	-0.09	H(6B)	0.147(7)	0.16
C(6)	-0.265(16)	-0.28	H(7A)	0.146(7)	0.08
C(7)	-0.279(16)	-0.15	H(7B)	0.146(7)	0.10
C(8)	-0.121(14)	-0.12	H(8)	0.180(9)	0.16
C(9)	-0.131(15)	-0.07	H(9)	0.180(9)	0.09
C(10)	-0.106(15)	-0.05	H(11A)	0.147(7)	0.08
C(11)	-0.277(15)	-0.16	H(11B)	0.147(7)	0.09
C(12)	-0.273(15)	-0.14	H(12A)	0.141(7)	0.07
C(13)	-0.158(16)	-0.08	H(12B)	0.141(7)	0.06
C(14)	-0.111(14)	-0.04	H(14)	0.176(8)	0.11
C(15)	-0.294(15)	-0.23	H(15A)	0.141(7)	0.10
C(16)	-0.273(16)	-0.18	H(15B)	0.141(7)	0.13
C(17)	0.168(13)	0.36	H(16A)	0.146(7)	0.11
C(18)	-0.402(17)	-0.24	H(16B)	0.146(7)	0.14
O(3)	-0.234(9)	-1.27	H(17)	0.120(9)	0.14
N(1)	-0.282(12)	-1.41	H(18A)	0.122(6)	0.06
N(2)	-0.286(11)	-1.40	H(18B)	0.122(6)	0.06
C(19)	-0.030(14)	2.13	H(18C)	0.122(6)	0.06
			H(1NA)	0.205(10)	0.49
			H(1NB)	0.209(11)	0.49
			H(2NA)	0.207(10)	0.47
			H(2NB)	0.208(10)	0.49

$q(P_v)$ – net atomic charges derived directly from the monopole populations of the multipole model;
$q(\Omega)$ – Bader's net atomic charges

Topological Analysis

a) urea molecule

Overall values of the electron density at the bond critical points are in a fair agreement with those reported by Zavodnik et al. [6] and Gatti et al. [7], with the exception of the N – H bonds (Table 5). Zavodnik et al. [6] reported significant differences (~0.5 eÅ^{-3}) between the theoretical and experimental electron densities at the (3,-1) critical point for the N – H bond of the urea molecule. The $\rho(r)$ values in this study are much closer to the theoretical values. The difference in the Laplacian values at (3,-1) critical points between experimental and theoretical values is much bigger, showing the sensitivity of the electron density curvature to the different approaches of it's estimation, including the deficiency of the multipole model [24].

Table 5. Topological analysis for the urea molecule.

	this work		Zavodnik, et al. [6]				Gatti, et al. [7]	
	experiment		*experiment*		*theory*		*theory*	
bond	$\rho(r)$	$\nabla^2\rho(r)$	$\rho(r)$	$\nabla^2\rho(r)$	$\rho(r)$	$\nabla^2\rho(r)$	$\rho(r)$	$\nabla^2\rho(r)$
C-O	2.79	-33.15	2.54	-18.86	2.57	-7.92	2.57	-7.95
$(C\text{-}N)_{average}$	2.26	-24.20	2.54	-37.66	2.35	-27.61	2.36	-27.71
$(N\text{-}H)_{average}$	2.22	-28.91	1.82	-31.91	2.34	-47.06	2.34	-47.23

The units for the electron density, $\rho(r)$, are eÅ^{-3}, and for the Laplacian, $\nabla^2\rho(r)$, they are eÅ^{-5}.

A critical point search was also performed in the Laplacian to find the charge density concentration associated with the lone pairs on the urea oxygen. The critical points are (3,+3) in type indicating that $\nabla^2\rho(r)$ is a local minimum at r_c. The critical point information, as well as a plot of the Laplacian in the plane of the lone pairs of the O(3) atom can be seen Table 6 and Fig. 2 respectively. The angle between the lone pairs, being greater that 140°, is much larger than the ideal trigonal planar geometry in agreement with VESPR theory. The inconsistency between the C(3) – O(1) – LP angles are most likely due to the shallow curved shape of the Laplacian in the lone pair region. An extremely small change in $\nabla^2\rho(\mathbf{r})$ could easily move the critical point by 5 – 10°. Gatti et al. [7] also found two (3,+3) critical points in the Laplacian, corresponding to the urea oxygen lone pairs. Although one of their points is very similar to those in Table 6, having the $\nabla^2\rho_c(\mathbf{r}) \cong$ -137 eÅ^{-5} and the O(1)-LP distance of ~0.339 Å, another (3,+3) point is significantly away from the oxygen nucleus (~0.383 Å) having much lower value of the Laplacian (~ -48 eÅ^{-5}). As it has been shown before, the Laplacian values (and it's curvatures) are very 'method-sensitive'.

Table 6. Lone pair Laplacian critical point information for the O(3) atom.

Atom	Lone Pair	$\nabla^2\rho(\mathbf{r}_c)$ ($e\text{Å}^{-5}$)	CP Type	O(1)-LP (Å)	LP1-O(1)-LP2 (°)	C3-O(1)-LP (°)
O(3)	LP1	-149	(3,+3)	0.337	144	118
	LP2	-148	(3,+3)	0.336	144	92

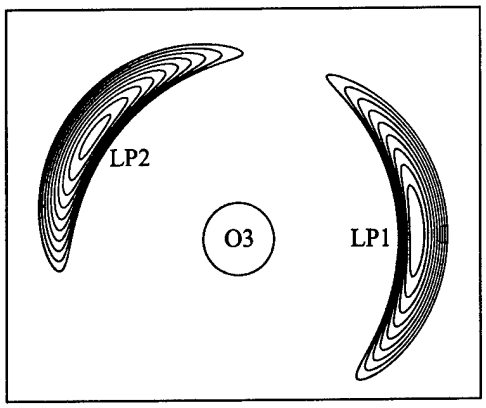

Figure 2. The negative part of the Laplacian in the plane of the O(3) atom lone pairs. Contour interval is -5 $e\text{Å}^{-5}$ starting at -100 $e\text{Å}^{-5}$.

b) E_2 molecule

The critical point analysis of covalent bonds of the estrogen molecule demonstrated the characteristic (3,-1) critical points, with expected $\rho(\mathbf{r}_c)$, $\nabla^2\rho(\mathbf{r}_c)$, and ellipticity values given the hybridization and connectivity. The complete list of all bond critical point properties is deposited. The average $\rho(\mathbf{r}_c)$ values are 1.91 $e\text{Å}^{-3}$ for the C – O bond, 2.17 $e\text{Å}^{-3}$ for C_{ar} – C_{ar}, 1.66 $e\text{Å}^{-3}$ for C – C, 1.91 $e\text{Å}^{-3}$ for C – H and 2.07 $e\text{Å}^{-3}$ for the O – H bond. The critical points are well centered in the homonuclear C – C bonds, and proportionally displaced away from the more electronegative atom in the heteronuclear bonds.

Critical points in the Laplacian corresponding to the lone pairs of both hydroxy oxygen atoms are of the special interest. Table 7 indicates the positions of the lone pair critical points in the Laplacian. The deformation electron density map of the lone pairs of the oxygen O(1), bound to the aromatic ring is presented in Fig. 3, while plot of the Laplacian in the plane of the lone pairs of the O(2) atom is shown in Fig. 4. The finding of two distinct lone pair regions after the

multipole refinement for O(1) was somewhat surprising. We expected that the aromatic hydroxy group, in which hydrogen lies in the plane of the aromatic ring, would be of sp^2 type geometry having some interaction with the π- orbitals of the aromatic ring (the same as in phenol), however, the results of this study indicate that this is not the ground state configuration in the estrogen molecule. The distances of the lone pairs from the oxygen atoms are very consistent. This is believed to be at least partially to due to the fact that the contraction/expansion coefficients for both oxygen atoms are constrained to be equal. Same as in the urea molecule, the angles between the lone pairs agree with VESPR theory in that they are much larger than the ideal tetrahedral value.

Table 7. Lone pair Laplacian critical point information for the O(1) and O(2) atoms.

Atom	Lone Pair	$\nabla^2\rho(r_c)$ ($e\text{Å}^{-5}$)	O-LP (Å)	LP1-O-LP2 (°)	C-O-LP (°)	H-O-LP (°)
O(1)	LP3	-133	0.346	146	104	103
	LP4	-119	0.347	146	90	100
O(2)	LP5	-129	0.346	235	108	115
	LP6	-120	0.346	235	88	101

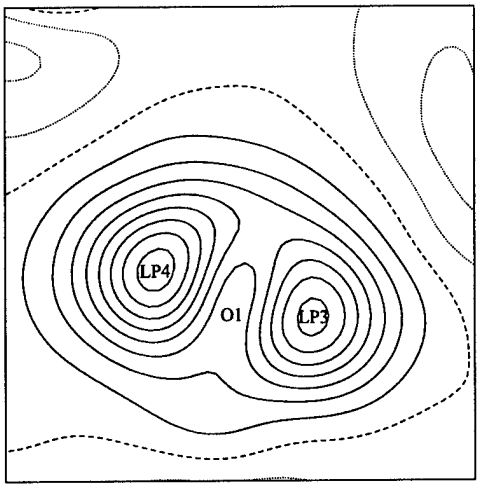

Figure 3. Dynamic model deformation density map in the plane of the lone pairs of the O(1) atom. Contour intervals are 0.05 $e\text{Å}^{-3}$ with solid lines positive, dashed lines zero, and dotted lines negative.

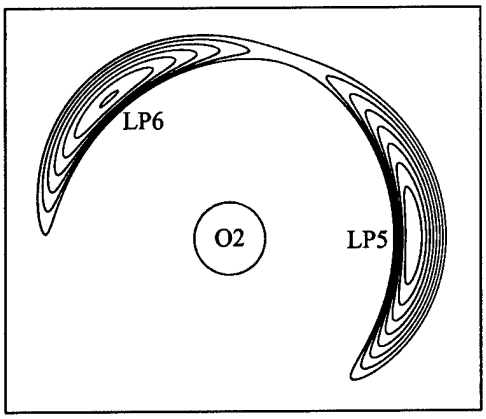

Figure 4. The negative part of the Laplacian in the plane of the lone pairs of the O(2) atom. Contour intervals are -5 $eÅ^{-5}$ starting at -80 $eÅ^{-5}$.

Electrostatic Potential

The core structure of the estrogen molecule generally is hydrophobic and relatively predictable in terms of the electrostatic potential. The ESP plotted on the van der Waals molecular surface for the E_2 molecule with the program package *MOLMOL* [25] is shown in Fig. 6. Since the isolated molecule (taken from the crystal) is calculated in this case, the ESP does not reflect the interactions in the condensed phase, such as hydrogen bonding. The negative potential areas (red) are produced by the aromatic ring, oxygens and some of carbon atoms (Fig. 6), while the hydrogen atoms involved in the hydrogen bonding produce highly positive areas (blue) on the molecular surface.

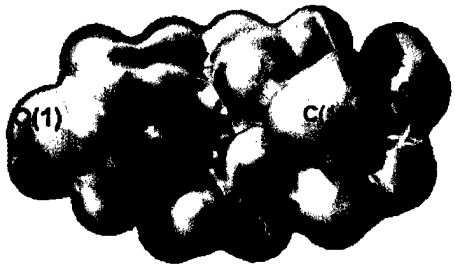

Figure 6. The E_2 electrostatic potential plotted on the van der Waals molecular surface. Negative values are in red, positive are in blue.

The hydroxy groups are of particular interest in the E_2 molecule, offering varying environments being bound to sp^2 and sp^3 type carbons and being involved in several hydrogen

bonds. The consistency in the lone pair density, in shape, size, position, and hydrogen bonding geometry suggested that the electrostatic potential surrounding the oxygen atoms might be relatively consistent in shape and magnitude. This however was not the case. Fig. 7 demonstrates the electrostatic potential of the O(1) hydroxy group lone pair region. The significant portion of the negative ESP extends approximately 180° around the oxygen. A maximum ESP of ~ -0.20 $e\text{Å}^{-1}$ was observed for this hydroxy group. The additional negative regions displayed represent the potential created by the π density of the aromatic ring. The oxygen atom forms a continuum with the negative potential above and below the aromatic ring.

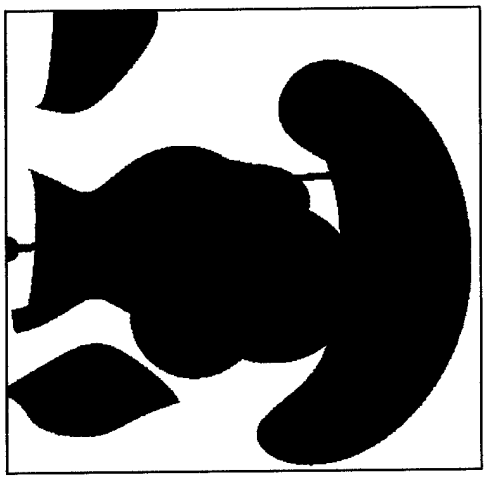

Figure 7. Electrostatic potential isosurface around the O(1) atom. The blue surface represents +1.0 $e\text{Å}^{-1}$, while the red surfaces represent –0.15 $e\text{Å}^{-1}$.

Before discussing the O(2) hydroxy group, it is important to recognize the orientation of the hydrogen atom H(2O). A hydroxy group attached to an aromatic ring almost exclusively has the hydrogen atom in the plane of the ring. Obviously, a hydroxy group bound to an sp^3 carbon can freely rotate. In the solid state, the orientation of the OH group will almost always be defined by the hydrogen bonding scheme. Fig. 8 displays the D-ring[§] of the E_2 molecule and the torsion angle (γ) of 49° between H(2O) and H(17).

[§] The C(13)-C(14)-C(15)-C(16)-C(17) ring.

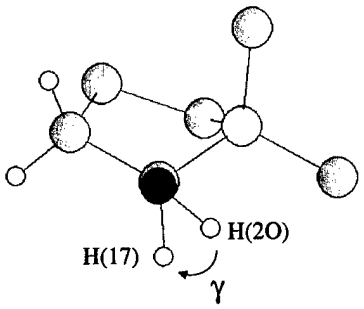

Figure 8. The O(2) hydroxy group geometry showing torsion angle (γ) between the H(2O) and H(17) atoms. The O(2) atom is shown in red.

The negative electrostatic potential around O(2) has much greater maximum value than that of the O(1) hydroxy group, reaching a value of ~ -0.35 eÅ^{-1}. In addition, the ESP does not evenly cover the lone pair region as on the O(1) hydroxy group. A shift toward the lone pair opposite H(17) appears to have taken place (Fig. 9). The coverage area of the negative potential seems smaller, covering near 120°, versus the approximate 180° coverage on O(1).

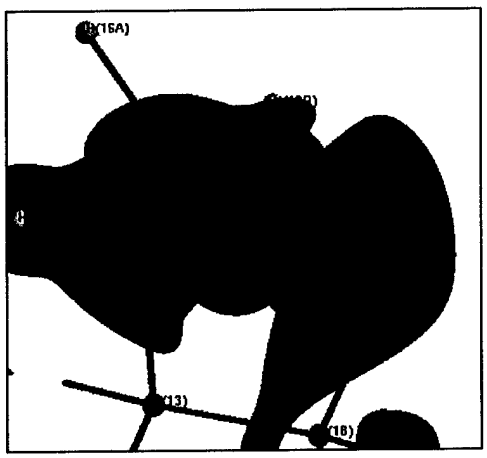

Figure 9. Electrostatic potential isosurface around the O(2) atom. The blue surface represents +1.0 eÅ^{-1}, while the red surfaces represent –0.25 eÅ^{-1}.

It is believed that the agonistic or the antagonistic responses of different estrogens can be related to their electrostatic potential [3]. We intend to construct a database with ESP calculated for estrogens with different biological activities. Once enough data are available, we hope to identify specific topological features in these estrogens that distinguish binding ability of these molecules to the estrogen receptor.

Conclusions

This is one of the first charge density studies accomplished for the big (56 atoms) organic molecules in the non-centrosymmetric unit cell. Our study showed that it is possible to get a quality data for such kind of system; the optimal coordinate system and slow, initially constrained refinement are the necessary tools for this type of study. Since most estrogens are identical in the core structure of the molecule, this study will provide a better starting point for future multipole refinements of other estrogen derivatives. Overall our results pertaining to the urea molecule reasonably agree with the previous literature results showing the quality of our data.

For the E_2 molecule, the lone pair densities of the oxygen atoms, which are an extremely small features of the system, were found to be quite similar. This indicates that the oxygen atom bound at the C(3) position do not have a strong interaction with the π orbitals of the aromatic ring in the ground state configuration. Despite this consistency, the electrostatic potentials in the region of the hydroxy groups differ greatly in both shape and magnitude. Future studies may reveal how the H(17) – C(17) – O(2) – H(20) torsion angle affects the electrostatic potential of the C(17) hydroxy group. Obviously many more estrogen systems must be completed before the comparative portion of the study can take place and real conclusions can be made on the relationship between the electrostatic potential and estrogenic action.

We would like to thank Dr. Samuel Brooks for his contribution. We thank Dr. A.Volkov and Prof. P. Coppens for making *TOPXD* program available for us. We would also like to thank the Department of Defense for their financial support (Grant # DAMD17-00-1-0468 and # DAMD17-99-1-9408).

Supplemental Tables and figures

S1 – experimental protocol

S2 - atomic coordinates

S3, S4 - atomic thermal parameters

S5 - bond lengths

S6 - bond angles

S7,S8,S9 – multipole populations

S10, S11,S12 - topological results

Fig. D1. Local multipole coordinate system for the urea molecule

1. Korach, K.S. (1994) *Science.* **266**, 1524-1527.
2. Lacassagne, A. (1936) *American Journal of Cancer.* **27**, 217-225.
3. VanderKuur, J.A., Wiese, T. & Brooks, S.C. (1993) *Biochemistry.* **32**, 7002-7008.
4. Gutendorf, B. and Westendorf, J. (2001) *Toxicology.* **166**, 79-89.
5. Nishihara, T., Nishikawa, J., Kanayama, T., Dakeyama, F., Saito, K., Imagawa, M., Takatori, S., Kitagawa, Y., Hori, S. & Utsumi, H. (2000) *Journal of Health Science.* **46**, 282-298.
6. Zavodnik, V., Stash, A., Tsirelson, V., De Vries, R. & Feil, D. (1999) *Acta Crystallographica.* **B55**, 45-54.
7. Gatti, C., Saunders, V.R. & Roetti, C. (1994) *Journal of Chemical Physics.* **101**, 10686-10696.
8. Duax, W.L., (1972) *Acta Crystallographica.* **B28**, 1864-1871.
9. BRUKER-AXS, *SAINT Software Package.* 1999, Madison, Wisconsin.
10. Kirschbaum, K., Martin, A. & Pinkerton, A.A. (1997) *Journal of Applied Crystallography.* **30**, 514-516.
11. Blessing, R.H., (1997) *Journal of Applied Crystallography.* **30**, 421-426.
12. Sheldrick, G.M. (1997) *SHELXL-97: Program for Crystal Structure Refinement* (University of Gottingen, Gottingen, Germany).
13. Koritsanszky, T., Howard, S., Mallison, P.R., Su, Z., Richter, T., & Hansen, N.K. (1995) *XD. A Computer Program Package for Mulitpole Refienement and Analysis of Electron Densities from Diffraction Data* (Berlin).
14. Hansen, N. & Coppens, P. (1978) *Acta Crystallographica.* **A34,** 909-921.
15. Chen, Yu.-Sh., Kirschbaum, K., Parrish, D., Pinkerton, A.A., Poomani, K. & Zhurova, E.A. (2003) *Journal of Applied Crystallography* (submitted).
16. Coppens, P., Guru Row, T.N., Leung, P., Stevens, E.D., Becker, P.J. & Yang, Y.W. (1979) *Acta Crystallographica.* **A35**, 63-72.
17. Coppens, P. (1997) *X-Ray Charge Densities and Chemical Bonding* (New York: Oxford University Press).
18. Volkov, A., Abramov, Y.A. & Coppens, P. (2001) *Acta Crystallographica.* **A57,** 272-282.

19. Bader, R.F.W. (1990) *Atoms in Molecules : A Quantum Theory* (Oxford: Oxford University Press).

20. Volkov, A., Gatti, C., Abramov, Yu. & Coppens, P. (2000) *Acta Crystallographica.* **A56**, 252-258.

21. Bader, R.F.W. (1994) *Physical review.* **B49**, 13348-13356.

22. Bader, R.W.F. (1998) *Journal of Physical Chemistry* **A102**, 7314-7323.

23. Li, X., Wu, G., Abramov, Y.A., Volkov, A.V. & Coppens, P. (2002) *Proceedings of the National Academy of Sciences of the United States of America.* **99**, 12132-12137.

24. Volkov, A., Abramov, Yu., Coppens, P. & Gatti C. (2000) *Acta Crystallographica.* **A56**, 332-339.

25. Koradi, R., Billeter, M. & Wüthrich, K. (1996) *Journal of Molecular Graphics.* **14**, 51-55.

	Frame #	2θ	ω	φ	χ	scan axis	scan range	# frames	time, s
1	001	-10.00	0.00	45.00	54.74	2	-0.300	606	60.00
2	001	-10.00	0.00	135.00	54.74	2	-0.300	606	60.00
3	001	-10.00	0.00	225.00	54.74	2	-0.300	606	60.00
4	001	-10.00	0.00	315.00	54.74	2	-0.300	606	60.00
5	001	-10.00	0.00	45.00	54.74	2	-0.300	50	60.00
6	001	-50.00	-40.00	0.00	54.74	2	-0.300	606	180.00
7	001	-50.00	-40.00	90.00	54.74	2	-0.300	606	180.00
8	001	-50.00	-40.00	180.00	54.74	2	-0.300	606	180.00
9	001	-50.00	-40.00	270.00	54.74	2	-0.300	606	180.00
10	001	-50.00	-40.00	0.00	54.74	2	-0.300	50	180.00
11	001	-85.00	-75.00	22.00	54.74	2	-0.300	606	180.00
12	001	-85.00	-75.00	112.00	54.74	2	-0.300	606	180.00
13	001	-85.00	-75.00	202.00	54.74	2	-0.300	606	180.00
14	001	-85.00	-75.00	292.00	54.74	2	-0.300	606	180.00
15	001	-85.00	-75.00	22.00	54.74	2	-0.300	50	180.00

Table S1. Data collection strategy.

Atom	X	Y	Z
O(1)	-0.42062(4)	-0.59512(3)	-0.23303(1)
O(2)	-0.84204(4)	-0.41992(3)	0.18982(1)
C(1)	-0.44199(5)	-0.59436(4)	-0.08495(1)
C(2)	-0.37742(5)	-0.60178(4)	-0.13756(1)
C(3)	-0.4861(5)	-0.58212(4)	-0.18160(1)
C(4)	-0.65570(5)	-0.5501(4)	-0.17217(1)
C(5)	-0.71966(5)	-0.54136(4)	-0.11929(1)
C(6)	-0.90362(5)	-0.50054(6)	-0.11256(2)
C(7)	-0.97328(5)	-0.53272(5)	-0.05589(1)
C(8)	-0.84924(5)	-0.48088(4)	-0.01225(1)
C(9)	-0.68422(5)	-0.57013(4)	-0.01689(1)
C(10)	-0.61318(5)	-0.56619(3)	-0.07448(1)
C(11)	-0.55543(5)	-0.52952(4)	0.02735(1)
C(12)	-0.63107(5)	-0.53975(4)	0.08481(1)
C(13)	-0.79264(5)	-0.44892(3)	0.08952(1)
C(14)	-0.91846(5)	-0.49686(4)	0.04520(1)
C(15)	-1.08391(5)	-0.41990(5)	0.06156(2)
C(16)	-1.07775(5)	-0.41829(5)	0.12479(2)
C(17)	-0.90256(5)	-0.48032(4)	0.13966(1)
C(18)	-0.75011(6)	-0.28658(4)	0.08704(2)
O(3)	-0.04795(4)	-0.97598(3)	-0.22248(1)
N(1)	-0.09666(6)	-0.74923(4)	-0.25469(2)
N(2)	0.16791(5)	-0.85170(4)	-0.26107(2)
C(19)	0.00538(5)	-0.86273(4)	-0.24497(1)

Atom	X	Y	Z
H(1O)	-0.5101(10)	-0.5906(7)	-0.2600(3)
H(2O)	-0.7416(10)	-0.4740(7)	0.2001(3)
H(1)	-0.3549(9)	-0.6099(6)	-0.0516(2)
H(2)	-0.2451(9)	-0.6249(7)	-0.1443(3)
H(4)	-0.7396(8)	-0.5354(6)	-0.2064(2)
H(6A)	-0.9756(9)	-0.5613(7)	-0.1427(3)
H(6B)	-0.9109(9)	-0.3834(7)	-0.1179(3)
H(7A)	-0.9919(9)	-0.6491(6)	-0.0509(2)
H(7B)	-1.0952(9)	-0.4794(6)	-0.0503(2)
H(8)	-0.8208(8)	-0.3661(7)	-0.0204(2)
H(9)	-0.7195(8)	-0.6834(6)	-0.0086(2)
H(11A)	-0.4469(9)	-0.6023(7)	0.0259(2)
H(11B)	-0.5073(8)	-0.4206(6)	0.0198(2)
H(12A)	-0.6641(9)	-0.6524(6)	0.0929(2)
H(12B)	-0.5387(8)	-0.5068(6)	0.1153(2)
H(14)	-0.9373(9)	-0.6139(6)	0.0514(2)
H(15A)	-1.1951(9)	-0.4796(7)	0.0480(3)
H(15B)	-1.0829(9)	-0.3086(6)	0.0467(2)
H(16A)	-1.1754(9)	-0.4876(7)	0.1422(3)
H(16B)	-1.0878(9)	-0.3057(7)	0.1379(2)
H(17)	-0.9087(7)	-0.5986(6)	0.1451(2)
H(18A)	-0.6611(9)	-0.2600(7)	0.1177(3)
H(18B)	-0.8580(9)	-0.2197(7)	0.0921(3)
H(18C)	-0.6965(9)	-0.2566(6)	0.0491(2)
H(1NA)	-0.0502(9)	-0.6532(8)	-0.2676(3)
H(1NB)	-0.2168(11)	-0.7522(7)	-0.2407(3)
H(2NA)	0.2088(9)	-0.7645(7)	-0.2827(3)
H(2NB)	0.2470(9)	-0.9369(7)	-0.2568(2)

Table S2. Fractional atomic coordinates for E_2•urea after final refinement.

Atom	U^{11}	U^{22}	U^{33}	U^{12}	U^{13}	U^{23}
O(1)	0.01222(10)	0.02450(12)	0.01244 (9)	0.00170(11)	0.00137(8)	-0.00125(8)
O(2)	0.01472(11)	0.02039(11)	0.01106(9)	0.00246(10)	-0.00176(8)	-0.00157(8)
C(1)	0.00954(12)	0.01862(13)	0.01229(12)	0.00158(11)	-0.00071(10)	0.00118(10)
C(2)	0.00985(13)	0.02010(14)	0.01343(12)	0.00179(12)	0.00003(10)	0.00045(10)
C(3)	0.01019(13)	0.01714(13)	0.01147(11)	0.00098(12)	0.00044(10)	-0.00054(9)
C(4)	0.01087(13)	0.02638(16)	0.01088(12)	0.00322(13)	-0.00014(10)	-0.00061(10)
C(5)	0.00955(13)	0.02430(15)	0.01111(12)	0.00314(12)	-0.00084(10)	-0.00028(10)
C(6)	0.01116(14)	0.04861(26)	0.01153(13)	0.00856(18)	-0.00124(11)	0.00106(14)
C(7)	0.00924(13)	0.02874(17)	0.01278(12)	0.00086(14)	-0.00142(10)	-0.00273(11)
C(8)	0.00966(12)	0.01630(12)	0.01105(11)	0.00091 (11)	-0.00096(10)	0.00024(9)
C(9)	0.00979(12)	0.01526(12)	0.01152(11)	0.00020(11)	-0.00078(9)	0.00086(9)
C(10)	0.00904(12)	0.01546(12)	0.01142(11)	0.00118(11)	-0.00076(9)	0.00038(9)
C(11)	0.00972(13)	0.02408(16)	0.01227(12)	0.00005(13)	-0.00148(10)	0.00008(11)
C(12)	0.01179(13)	0.02236(15)	0.01170(12)	0.00321(13)	-0.00164(10)	0.00089(10)
C(13)	0.01108(13)	0.01360(12)	0.01124(11)	-0.00012(11)	-0.00106(10)	-0.00013(9)
C(14)	0.01016(13)	0.01701(13)	0.01148(11)	-0.00026(11)	-0.00066(10)	-0.00070(9)
C(15)	0.01225(15)	0.03704(21)	0.01301(13)	0.00644 (16)	-0.00147(11)	-0.00244(13)
C(16)	0.01281(15)	0.03796(21)	0.01288(13)	0.00515(16)	-0.00004(12)	-0.00294(13)
C(17)	0.01247(14)	0.01783(13)	0.01145(11)	0.00010(13)	-0.00039(10)	-0.00020(10)
C(18)	0.02594(21)	0.01516(13)	0.01724(15)	-0.00396(14)	-0.00060(14)	-0.00082(11)
O(3)	0.01601(12)	0.01798(11)	0.02293(12)	-0.00179(11)	0.00589(10)	0.00220(9)
N(1)	0.01699(17)	0.01720(14)	0.04870(23)	0.00432(14)	0.00778(17)	0.00299(14)
N(2)	0.01344(14)	0.01739(13)	0.02783(15)	0.00034(12)	0.00619(12)	0.00421(11)
C(19)	0.01340(15)	0.01471(12)	0.01815(13)	-0.00052(12)	0.00340(12)	-0.00093(10)

Table S3. Anisotropic thermal parameters of non-H atoms for E_2•urea.

Atom	U_{iso}
H(1O)	0.0129(16)
H(2O)	0.0150(17)
H(1)	0.0249(16)
H(2)	0.0200(16)
H(4)	0.0185(15)
H(6A)	0.0436(19)
H(6B)	0.0379(18)
H(7A)	0.0280(16)
H(7B)	0.0259(15)
H(8)	0.0225(15)
H(9)	0.0216(16)
H(11A)	0.0345(17)
H(11B)	0.0239(14)
H(12A)	0.0298(16)
H(12B)	0.0270(15)

Atom	U_{iso}
H(14)	0.0184(14)
H(15A)	0.0381(18)
H(15B)	0.0283(16)
H(16A)	0.0400(19)
H(16B)	0.0324(17)
H(17)	0.0245(14)
H(18A)	0.0371(18)
H(18B)	0.0379(17)
H(18C)	0.0342(17)
H(1NA)	0.0319(18)
H(1NB)	0.0351(19)
H(2NA)	0.0296(17)
H(2NB)	0.0336(17)

Table S4. Isotropic thermal parameters of H atoms for E_2•urea.

Atoms	Bond Length (Å)
O(1) – C(3)	1.3714(4)
O(2) – C(17)	1.4354(4)
C(1) – C(2)	1.3923(5)
C(1) – C(10)	1.4014(5)
C(2) – C(3)	1.3938(5)
C(3) – C(4)	1.3921(5)
C(4) – C(5)	1.3973(5)
C(5) – C(6)	1.5108(6)
C(5) – C(10)	1.4051(5)
C(6) – C(7)	1.5274(5)
C(7) – C(8)	1.5300(5)
C(8) – C(9)	1.5463(5)
C(8) – C(14)	1.5219(5)

Atoms	Bond Length (Å)
C(9) – C(10)	1.5236(5)
C(9) – C(11)	1.5361(5)
C(11) – C(12)	1.5369(5)
C(12) – C(13)	1.5314(5)
C(13) – C(14)	1.5400(5)
C(13) – C(17)	1.5357(5)
C(13) – C(18)	1.5357(5)
C(14) – C(15)	1.5411(6)
C(15) – C(16)	1.5555(5)
C(16) – C(17)	1.5419(6)
O(3) – C(19)	1.2548(5)
N(1) – C(19)	1.3427(6)
N(2) – C(19)	1.3478(5)

Table S5. Bond distances of non-H atoms of E_2•urea.

Atoms	Bond Angle (°)
C(3) – O(1) – H(1O)	110.6 (5)
C(17) – O(2) – H(2O)	107.3(5)
C(2) – C(1) – C(10)	122.2 (1)
C(2) – C(1) – H(1)	117.7 (4)
C(10) – C(1) – H(1)	120.0 (4)
C(1) – C(2) – C(3)	119.3 (1)
C(1) – C(2) – H(2)	120.5 (4)
C(3) – C(2) – H(2)	120.1 (4)
O(1) – C(3) – C(2)	118.2 (1)
O(1) – C(3) – C(4)	122.4 (1)
C(2) – C(3) – C(4)	119.4 (1)
C(3) – C(4) – C(5)	121.0 (1)
C(3) – C(4) – H(4)	119.2 (4)
C(5) – C(4) – H(4)	119.7 (4)
C(4) – C(5) – C(6)	117.7 (1)
C(4) – C(5) – C(10)	120.2 (1)
C(6) – C(5) – C(10)	122.1 (1)
C(5) – C(6) – C(7)	113.5 (1)
C(5) – C(6) – H(6A)	107.4 (4)
C(5) – C(6) – H(6B)	106.5 (4)
C(7) – C(6) – H(6A)	109.4 (4)
C(7) – C(6) – H(6B)	106.5 (4)
H(6A) – C(6) – H(6B)	113.6 (6)
C(6) – C(7) – C(8)	110.4 (1)
C(6) – C(7) – H(7A)	110.0 (4)
C(6) – C(7) – H(7B)	110.3 (3)
C(8) – C(7) – H(7A)	108.4 (4)
C(8) – C(7) – H(7B)	109.7 (4)
H(7A) – C(7) – H(7B)	108.1 (5)
C(7) – C(8) – C(9)	108.8 (1)
C(7) – C(8) – C(14)	113.0 (1)
C(9) – C(8) – C(14)	108.7 (1)
C(7) – C(8) – H(8)	107.7 (4)
C(9) – C(8) – H(8)	109.1 (4)

Atoms	Bond Angle (°)
C(14) – C(8) – H(8)	109.6 (3)
C(8) – C(9) – C(10)	111.5 (1)
C(8) – C(9) – C(11)	112.1 (1)
C(10) – C(9) – C(11)	114.1 (1)
C(8) – C(9) – H(9)	106.2 (4)
C(10) – C(9) – H(9)	106.7(4)
C(11) – C(9) – H(9)	105.5 (4)
C(1) – C(10) – C(5)	117.7 (1)
C(1) – C(10) – C(9)	121.5 (1)
C(5) – C(10) – C(9)	120.8 (1)
C(9) – C(11) – C(12)	112.2 (1)
C(9) – C(11) – H(11A)	110.3 (4)
C(9) – C(11) – H(11B)	109.6(3)
C(12) – C(11) – H(11A)	107.4 (4)
C(12) – C(11) – H(11B)	110.4 (3)
H(11A) – C(11) – H(11B)	106.7 (5)
C(11) – C(12) – C(13)	111.1 (1)
C(11) – C(12) – H(12A)	108.7 (4)
C(11) – C(12) – H(12B)	110.8 (4)
C(13) – C(12) – H(12A)	107.9 (4)
C(13) – C(12) – H(12B)	110.7 (4)
H(12A) – C(12) – H(12B)	107.5 (5)
C(12) – C(13) – C(14)	109.1 (1)
C(12) – C(13) – C(17)	115.4 (1)
C(12) – C(13) – C(18)	110.4 (1)
C(14) – C(13) – C(17)	98.6 (1)
C(14) – C(13) – C(18)	113.1 (1)
C(17) – C(13) – C(18)	109.8 (1)
C(8) – C(14) – C(13)	113.4 (1)
C(8) – C(14) – C(15)	120.2 (1)
C(13) – C(14) – C(15)	103.3 (1)
C(8) – C(14) – H(14)	105.8 (3)
C(13) – C(14) – H(14)	105.8 (4)
C15 – C14 – H14	107.5 (4)

Atoms	Bond Angle (°)
C(14) – C(15) – (C16)	103.8 (1)
C(14) – C(15) – H(15A)	111.8 (4)
C(14) – C(15) – H(15B)	109.9 (4)
C(16) – C(15) – H(15A)	109.7 (4)
C(16) – C(15) – H(15B)	109.0 (4)
H(15A) – C(15) – H(15B)	112.3 (6)
C(15) – C(16) – C(17)	105.2 (1)
C(15) – C(16) – H(16A)	111.4 (4)
C(15) – C(16) – H(16B)	107.6 (4)
C(17) – C(16) – H(16A)	109.0 (4)
C(17) – C(16) – H(16B)	110.4 (4)
H(16A) – C(16) – H(16B)	113.0 (6)
O(2) – C(17) – C(13)	115.4 (1)
O(2) – C(17) – C(16)	111.0 (1)
C(13) – C(17) – C(16)	104.3 (1)
O(2) – C(17) – H(17)	107.1 (3)
C(13) – C(17) – H(17)	108.1 (3)
C(16) – C(17) – H(17)	110.9 (4)
C(13) – C(18) – H(18A)	110.0 (4)
C(13) – C(18) – H(18B)	112.7 (4)
C(13) – C(18) – H(18C)	112.1 (4)
H(18A) – C(18) – H(18B)	108.4 (6)
H(18A) – C(18) – H(18C)	107.4 (6)
H(18B) – C(18) – H(18C)	105.9 (6)
O(3) – C(19) – N(1)	121.7 (1)
O(3) – C(19) – N(2)	120.8 (1)
N(1) – C(19) – N(2)	117.5 (1)
C(19) – N(1) – H(1NA)	121.4 (5)
C(19) – N(1) – H(1NB)	118.9 (5)
H(1NA) – N(1) – H(1NB)	118.2 (6)
C(19) – N(2) – H(2NA)	121.0 (5)
C(19) – N(2) – H(2NB)	120.0 (5)
H(2NA) – N(2) – H(2NB)	118.4 (6)

Table S6. Bond angles of E_2•urea.

Multipoles	O(1)	O(2)	O(3)	N(1)	N(2)
$P_{1,+1}$	-0.017(8)	-0.069(7)	-0.096(6)	0.048(10)	0.0
$P_{1,-1}$	0.0	-0.029(7)	-0.022(6)	-0.009(8)	-0.009(9)
$P_{1,0}$	-0.008(8)	0.023(7)	-0.014(5)	0.049(8)	-0.043(7)
$P_{2,0}$	0.089(8)	0.078(8)	-0.087(7)	-0.053(9)	-0.036(8)
$P_{2,+1}$	-0.013(8)	0.026(8)	0.0	-0.046(10)	0.014(9)
$P_{2,-1}$	-0.023(9)	0.035(7)	0.045(7)	0.0	-0.009(9)
$P_{2,+2}$	-0.036(8)	-0.047(8)	-0.077(7)	0.042(10)	0.012(9)
$P_{2,-2}$	0.0	0.015(8)	-0.022(8)	0.0	0.0
$P_{3,0}$	0.0	0.056(14)	0.028(11)	0.059(13)	-0.043(12)
$P_{3,+1}$	-0.037(10)	-0.010(10)	0.024(10)	0.059(12)	-0.046(12)
$P_{3,-1}$	-0.051(10)	-0.052(10)	-0.040(10)	0.0	0.0
$P_{3,+2}$	0.027(14)	0.011(10)	0.0	-0.085(15)	0.0
$P_{3,-2}$	0.031(14)	-0.010(10)	0.0	-0.022(13)	0.030(12)
$P_{3,+3}$	0.101(10)	0.069(12)	0.0	0.158(11)	0.175(10)
$P_{3,-3}$	-0.058(11)	-0.028(10)	0.018(10)	0.012(11)	0.0
$P_{4,0}$	0.041(13)	-0.031(14)			
$P_{4,+1}$	-0.036(13)	0.022(13)			
$P_{4,-1}$	-0.015(13)	0.016(13)			
$P_{4,+2}$	-0.025(13)	0.038(12)			
$P_{4,-2}$	0.0	-0.017(12)			
$P_{4,+3}$	0.029(14)	-0.025(13)			
$P_{4,-3}$	0.0	0.0			
$P_{4,+4}$	0.020 (12)	0.020(12)			
$P_{4,-4}$	-0.020(12)	-0.042(13)			

Table S7. Multipole populations of Oxygen and Nitrogen atoms of E_2•urea. Populations less than one estimated standard deviation were set to zero.

Multipoles	C(1)	C(2)	C(3)	C(4)	C(5)	C(6)	C(7)	C(8)	C(9)
$P_{1,+1}$	0.061(15)	0.064(14)	0.042(16)	0.0	0.047(16)	-0.088(13)	-0.080(13)	0.0	-0.034(12)
$P_{1,-1}$	-0.014(14)	-0.046(15)	0.072(14)	0.032(16)	0.036(16)	0.0	0.0	0.0	0.0
$P_{1,0}$	-0.012(12)	0.022(13)	0.0	-0.028(13)	-0.064(14)	-0.086(13)	-0.049(12)	0.020(12)	0.078(13)
$P_{2,0}$	-0.227(11)	-0.182(11)	-0.202(11)	-0.190(11)	-0.251(12)	-0.042(15)	0.0	0.0	0.052(13)
$P_{2,+1}$	0.017(13)	-0.018(13)	0.0	0.021(13)	-0.033(14)	-0.042(12)	-0.011(11)	-0.014(13)	-0.048(12)
$P_{2,-1}$	0.037(13)	0.014(13)	0.030(12)	0.0	0.018(13)	0.048(12)	-0.012(12)	-0.014(12)	-0.032
$P_{2,+2}$	0.048(14)	0.0	0.052(14)	0.048(14)	0.047(15)	0.105(12)	0.061(11)	0.014(11)	0.019(12)
$P_{2,-2}$	0.020(14)	0.068(14)	-0.060(14)	-0.029(14)	0.0	0.017(13)	0.0	0.0	0.019(12)
$P_{3,0}$	-0.023(16)	-0.020(16)	0.0	0.0	-0.024(18)	-0.053(17)	0.026(17)	0.033(18)	0.0
$P_{3,+1}$	-0.043(15)	0.0	0.0	0.0	0.043(17)	0.023(18)	-0.185(15)	0.0	-0.018(17)
$P_{3,-1}$	0.024(15)	0.014 (14)	0.025(15)	0.029(16)	0.040(17)	0.032 (15)	0.016(14)	0.0	-0.082 (15)
$P_{3,+2}$	-0.020(20)	0.018(20)	0.0	0.0	0.075(23)	0.0	0.0	0.0	-0.067(16)
$P_{3,-2}$	-0.025(20)	0.028(17)	-0.088(22)	0.039(19)	0.0	0.304(15)	0.282(15)	0.391(15)	0.389(15)
$P_{3,+3}$	0.361(15)	0.342(15)	0.356(15)	0.362(15)	0.316(15)	-0.209(15)	-0.187(16)	0.021(15)	-0.048(15)
$P_{3,-3}$	-0.032(19)	0.0	0.077(22)	0.063(19)	0.0	-0.046(17)	0.0	-0.0170(17)	-0.028(17)

Multipoles	C(10)	C(11)	C(12)	C(13)	C(14)	C(15)	C(16)	C(17)	C(18)	C(19)
$P_{1,+1}$	0.068(18)	-0.094(13)	-0.030(12)	0.015(12)	-0.076(14)	-0.074(14)	-0.052(14)	-0.020(11)	0.063(11)	0.154(14)
$P_{1,-1}$	-0.042(15)	-0.059(11)	-0.053(13)	0.058(13)	-0.048(12)	0.069(12)	-0.016(13)	-0.060(12)	0.029(12)	-0.028(16)
$P_{1,0}$	-0.028(13)	0.015(11)	0.0	-0.033(12)	0.059(13)	-0.068(12)	-0.094(12)	-0.067(12)	-0.012(12)	-0.070(13)
$P_{2,0}$	-0.221(11)	0.017(11)	0.0	-0.025(12)	-0.024(12)	-0.032(13)	-0.087(11)	0.0	-0.045(12)	-0.383(12)
$P_{2,+1}$	0.0	-0.060(12)	0.022(11)	-0.023(12)	0.0	0.028(11)	0.0	0.038(11)	0.033(12)	0.0
$P_{2,-1}$	0.029(13)	0.0	0.013(13)	0.0	-0.051	0.016(12)	0.0	0.0	0.0	-0.030(13)
$P_{2,+2}$	0.057(15)	0.069(11)	0.038(12)	0.0	-0.037(11)	0.086(12)	0.083(12)	0.013(11)	0.016(10)	0.175(15)
$P_{2,-2}$	-0.032(15)	-0.024(11)	0.039(12)	0.0	0.027(13)	0.0	0.0	0.075(11)	-0.014(11)	0.0
$P_{3,0}$	0.059(16)	0.028(15)	0.022(14)	0.0	0.0	0.046(19)	-0.040(16)	-0.039(15)	-0.036(15)	0.0
$P_{3,+1}$	-0.024(17)	-0.135(16)	-0.114(14)	-0.024(15)	-0.025(16)	0.0	0.0	-0.095(14)	0.0	-0.092(16)
$P_{3,-1}$	0.044(15)	-0.022(14)	-0.042(17)	0.0	0.032(16)	0.050(16)	0.056(17)	-0.030(16)	0.0	-0.046(18)
$P_{3,+2}$	0.0	-0.050(16)	0.034(16)	0.075(17)	0.0	0.0	-0.019(18)	0.065(15)	0.0	-0.034(19)
$P_{3,-2}$	-0.090(24)	0.346(16)	0.384(15)	0.464(15)	0.383(14)	0.342(15)	0.347(15)	-0.333(14)	0.283(14)	0.036(19)
$P_{3,+3}$	0.358(16)	-0.170(14)	-0.091(16)	0.027(17)	-0.027(17)	-0.176(16)	-0.131(16)	-0.017(16)	0.060(13)	0.499(18)
$P_{3,-3}$	0.0	0.0	0.0	-0.026(18)	0.0	0.0	0.013(16)	0.062(15)	-0.057(13)	0.035(14)

Table S8. Multipole populations of Carbon atoms of E_2•urea. Populations less than one estimated standard deviation were set to zero.

Atoms	$P_{1,0}$	$P_{2,0}$
H(1O)	0.131(11)	0.066(14)
H(2O)	0.125(11)	0.098(14)
H(1)	0.125(13)	0.0
H(2)	0.097(13)	0.018(15)
H(4)	0.140(12)	0.0
H(6A)	0.104(9)	0.040(10)
H(6B)	0.104(9)	0.040(10)
H(7A)	0.097(9)	0.023(10)
H(7B)	0.097(9)	0.023(10)
H(8)	0.135(11)	0.085(15)
H(9)	0.074(12)	0.0
H(11A)	0.098(8)	0.030(11)
H(11B)	0.098(8)	0.030(11)
H(12A)	0.114(8)	0.0
H(12B)	0.114(8)	0.0
H(14)	0.064(11)	0.030(13)
H(15A)	0.094(8)	0.019(11)
H(15B)	0.094(8)	0.019(11)
H(16A)	0.116(8)	0.022(11)
H(16B)	0.116(8)	0.022(11)
H(17)	0.163(11)	0.062(15)
H(18A)	0.112(6)	-0.020(9)
H(18B)	0.112(6)	-0.020(9)
H(18C)	0.112(6)	-0.020(9)
H(1NA)	0.152(14)	0.077(17)
H(1NB)	0.164(15)	0.025(18)
H(2NA)	0.162(13)	0.0
H(2NB)	0.189(13)	0.097(19)

Table S9. Multipole populations of Hydrogen atoms of E_2•urea. Populations less than one estimated standard deviation were set to zero.

Bond	$\rho(r_c)$, eÅ^{-3}	$\nabla^2\rho(r_c)$, eÅ^{-5}	R_{ij}, Å	d_1, Å	d_2, Å	λ_1, eÅ^{-5}	λ_2, eÅ^{-5}	λ_3, eÅ^{-5}	ε
O(1) – C(3)	2.098	-18.857	1.3735	0.8416	0.5319	-16.54	-15.32	13.01	0.08
O(1) – H(1O)	2.082	-45.739	0.9701	0.7919	0.1782	-39.04	-38.76	32.06	0.01
O(2) – C(17)	1.730	-7.141	1.4361	0.8238	0.6123	-12.57	-11.54	16.97	0.09
O(2) – H(2O)	2.047	-43.332	0.9702	0.7870	0.1831	-37.90	-37.81	32.37	0.00
C(1) – C(2)	2.180	-21.211	1.3924	0.7506	0.6418	-16.19	-13.27	8.25	0.22
C(1) – C(10)	2.162	-19.986	1.4015	0.6760	0.7255	-16.00	-12.89	8.90	0.24
C(1) – H(1)	1.803	-16.859	1.0804	0.7148	0.3657	-16.99	-15.59	15.72	0.09
C(2) – C(3)	2.202	-20.649	1.3945	0.6937	0.7009	-16.90	-13.39	9.64	0.26
C(2) – H(2)	1.792	-17.541	1.0801	0.7367	0.3434	-17.68	-16.19	16.33	0.09
C(3) – C(4)	2.233	-21.385	1.3922	0.7022	0.6900	-17.48	-13.46	9.55	0.30
C(4) – C(5)	2.149	-19.523	1.3974	0.7239	0.6735	-15.61	-12.90	8.98	0.21
C(4) – H(4)	1.771	-17.492	1.0801	0.7149	0.3652	-16.77	-15.48	14.76	0.08
C(5) – C(6)	1.749	-12.453	1.5108	0.7609	0.7499	-11.79	-10.83	10.17	0.09
C(5) – C(10)	2.065	-17.595	1.4058	0.7293	0.6765	-14.99	-11.80	9.20	0.27
C(6) – C(7)	1.676	-10.645	1.5288	0.7855	0.7433	-10.86	-10.20	10.42	0.07
C(6) – H(6A)	1.679	-12.422	1.0907	0.7045	0.3862	-15.18	-12.92	15.68	0.18
C(6) – H(6B)	1.671	-13.218	1.0957	0.7117	0.3840	-15.24	-14.10	16.12	0.08
C(7) – C(8)	1.665	-10.244	1.5304	0.7717	0.7587	-10.52	-10.09	10.37	0.04
C(7) – H(7A)	1.789	-15.317	1.0904	0.7168	0.3736	-16.18	-15.35	16.22	0.05
C(7) – H(7B)	1.734	-14.552	1.0910	0.7109	0.3800	-15.54	-14.88	15.86	0.04
C(8) – C(9)	1.621	-9.895	1.5468	0.7797	0.7670	-10.12	-10.01	10.24	0.01
C(8) – C(14)	1.659	-10.990	1.5222	0.7693	0.7529	-10.84	-10.13	9.98	0.07
C(8) – H(8)	1.801	-18.734	1.1000	0.7139	0.3862	-16.60	-16.08	13.94	0.03
C(9) – C(10)	1.657	-10.454	1.5240	0.7446	0.7793	-10.86	-9.74	10.14	0.12
C(9) – C(11)	1.687	-11.499	1.5365	0.7502	0.7863	-11.15	-10.61	10.25	0.05
C(9) – H(9)	1.754	-14.686	1.1001	0.7386	0.3614	-16.07	-15.31	16.69	0.05

Table S10. Topological properties of bond critical points in E_2•urea.

Bond	$\rho(r_c)$	$\nabla^2\rho(r_c)$	R_{ij}	d_1	d_2	λ_1	λ_2	λ_3	ε
C(11) – C(12)	1.625	-10.516	1.5370	0.7473	0.7897	-10.55	-9.99	10.02	0.06
C(11) – H(11A)	1.741	-15.198	1.0910	0.7090	0.3819	-15.71	-14.96	15.47	0.05
C(11) – H(11B)	1.831	-16.318	1.0900	0.7223	0.3677	-16.92	-15.93	16.53	0.06
C(12) – C(13)	1.732	-11.974	1.5316	0.7636	0.7680	-11.50	-10.84	10.36	0.06
C(12) – H(12A)	1.739	-14.601	1.0903	0.7011	0.3891	-15.10	-14.78	15.28	0.02
C(12) – H(12B)	1.794	-15.750	1.0901	0.7073	0.3828	-16.06	-15.27	15.59	0.05
C(13) – C(14)	1.683	-10.928	1.5407	0.7776	0.7631	-10.65	-10.49	10.21	0.02
C(13) – C(17)	1.649	-10.407	1.5358	0.7916	0.7443	-11.02	-10.06	10.67	0.10
C(13) – C(18)	1.648	-10.737	1.5358	0.7775	0.7583	-10.55	-10.39	10.21	0.02
C(14) – C(15)	1.582	-9.329	1.5422	0.7477	0.7945	-10.49	-9.05	10.21	0.16
C(14) – H(14)	1.713	-14.051	1.1000	0.7367	0.3634	-15.48	-15.16	16.58	0.02
C(15) – C(16)	1.625	-10.658	1.5559	0.7830	0.7730	-10.72	-10.17	10.23	0.05
C(15) – H(15A)	1.773	-14.401	1.0910	0.7210	0.3700	-16.49	-14.64	16.73	0.13
C(15) – H(15B)	1.589	-11.136	1.0925	0.6989	0.3936	-13.94	-12.59	15.40	0.11
C(16) – C(17)	1.641	-9.595	1.5420	0.7793	0.7627	-11.05	-9.81	11.26	0.13
C(16) – H(16A)	1.763	-14.754	1.0907	0.7080	0.3827	-16.11	-14.34	15.70	0.12
C(16) – H(16B)	1.650	-12.737	1.0941	0.7002	0.3939	-14.47	-13.65	15.38	0.06
C(17) – H(17)	1.904	-19.411	1.1003	0.7162	0.3842	-18.18	-17.30	16.07	0.05
C(18) – H(18A)	1.775	-13.392	1.0605	0.6782	0.3823	-15.20	-14.30	16.11	0.06
C(18) – H(18B)	1.808	-13.845	1.0601	0.6825	0.3776	-15.81	-14.51	16.47	0.09
C(18) – H(18C)	1.787	-13.862	1.0601	0.6785	0.3816	-15.56	-14.39	16.09	0.08
O(3) – C(19)	2.787	-33.153	1.2549	0.8140	0.4409	-24.40	-23.77	15.02	0.03
N(1) – C(19)	2.250	-23.973	1.3436	0.8764	0.4672	-17.80	-16.46	10.29	0.08
N(2) – C(19)	2.276	-24.418	1.3479	0.8762	0.4717	-18.03	-15.72	9.33	0.15
N(1) – H(1NA)	2.208	-29.694	1.0101	0.7501	0.2600	-30.17	-28.94	29.42	0.04
N(1) – H(1NB)	2.190	-26.490	1.0101	0.7472	0.2629	-29.09	-27.32	29.92	0.06
N(2) – H(2NA)	2.172	-24.824	1.0100	0.7452	0.2648	-28.46	-26.60	30.24	0.07
N(2) – H(2NB)	2.299	-34.625	1.0100	0.7533	0.2567	-32.37	-30.74	28.49	0.05

Table S11. Topological properties of bond critical points in E_2•urea continued.

Bond	$\rho(r_c)$, eÅ^{-3}	$\nabla^2\rho(r_c)$,eÅ^{-5}	R_{ij}, Å	d_1, Å	d_2, Å	λ_1, eÅ^{-5}	λ_2, eÅ^{-5}	λ_3, eÅ^{-5}	ε
O(2)-H(2O)...O(3)	0.284	2.78	1.691	1.136	0.556	-2.03	-1.95	6.76	0.04
O(1)-H(1O)...O(2)	0.253	3.42	1.702	1.151	0.552	-1.65	-1.56	6.63	0.06
N(1)-H(1NA)...O(3)	0.212	2.78	1.826	1.177	0.648	-1.29	-1.26	5.34	0.02
N(1)-H(1NB)...O(1)	0.092	1.72	2.174	1.361	0.834	-0.44	-0.36	2.52	0.24
N(2)-H(2NB)...O(1)	0.131	1.70	2.018	1.297	0.721	-0.76	-0.70	3.15	0.08
N(2)-H(2NA)...O(2)	0.072	2.00	2.116	1.368	0.752	-0.34	-0.28	2.62	0.22

Table S12. Topological properties of hydrogen bond critical points.

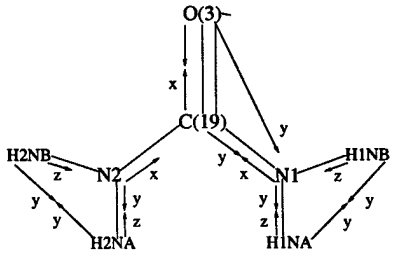

Figure D1. Local multipole coordinate system for the urea molecule.

Appendix H.

Crystal structure and charge density analysis of 17β-estradiol•½ MeOH

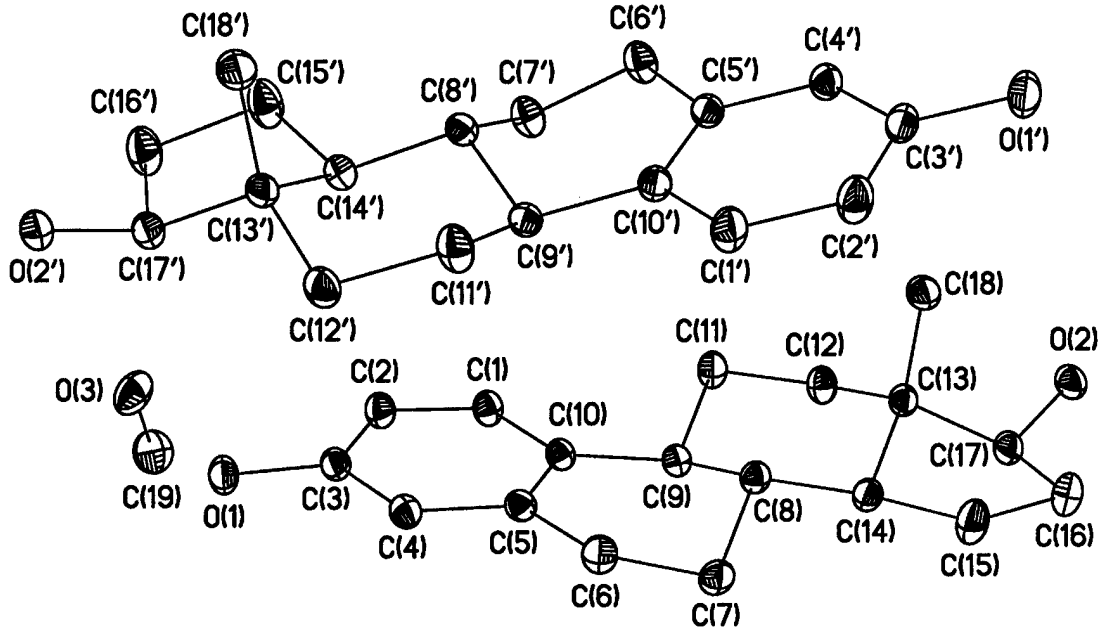

Figure 1. Thermal ellipsoid plot of 17β-estradiol•½methanol where ellipsoids represent 50% probability electron density of the atom. Hydrogen atoms are omitted for clarity.

Run	2θ	ω	ϕ	Scan Width (°)	# of Frames	Frame Times (sec)
1	-40	-46	22	-0.15	1100	16
2	-40	-46	112	-0.15	1100	16
3	-40	-46	202	-0.15	1100	16
4	-40	-46	292	-0.15	1100	16
5	-80	-86	67	-0.15	1100	32
6	-80	-86	157	-0.15	1100	32
7	-80	-86	247	-0.15	1100	32
8	-80	-86	337	-0.15	1100	32
9	-102	-108	22	-0.15	1100	64
10	-102	-108	112	-0.15	1100	64
11	-102	-108	202	-0.15	1100	64
12	-102	-108	292	-0.15	1100	64

Table 1. Data collection parameters for 17β-estradiol•½methanol.

Crystal Data			
Chemical Formula	$C_{37}H_{52}O_5$		
Temperature	100.0(1) K		
Crystal Dimensions	0.22 x 0.26 x 0.42 mm		
Space Group	P1		
A	7.2910(1) Å		
B	9.2768(1) Å		
C	12.3873(2) Å		
α	89.4704(6)		
β	87.8577(6)		
γ	70.7607(7)		
Volume	790.489(33) $Å^3$		
Z (Crystallographic)	2		
Integration Parameters			
	Box Size (°)	Profile Fitting (I/σ)	Simple Sum Perimeter Limit
Low Angle	1.5 x 1.5 x 1.0	20 20	0.02
Medium Angle	1.2 x 1.2 x 0.8	20 20	0.02
High Angle	1.0 x 1.0 x 0.6	10 10	0.02
Reflection Statistics (from SORTAV)			
Total Reflections	86369		
Rejected Outliers	33		
Unique Reflections	29051		
Average Redundancy	3.0		
Resolution	1.329 $Å^{-1}$		
Completeness	91.9 %		
R_1	5.77 %		
R_2	5.34 %		
R_w	15.25 %		
Z (Refinement)	1.219		

Table 2. Selected crystal, integration, and reflection data for 17β-estradiol•½methanol.

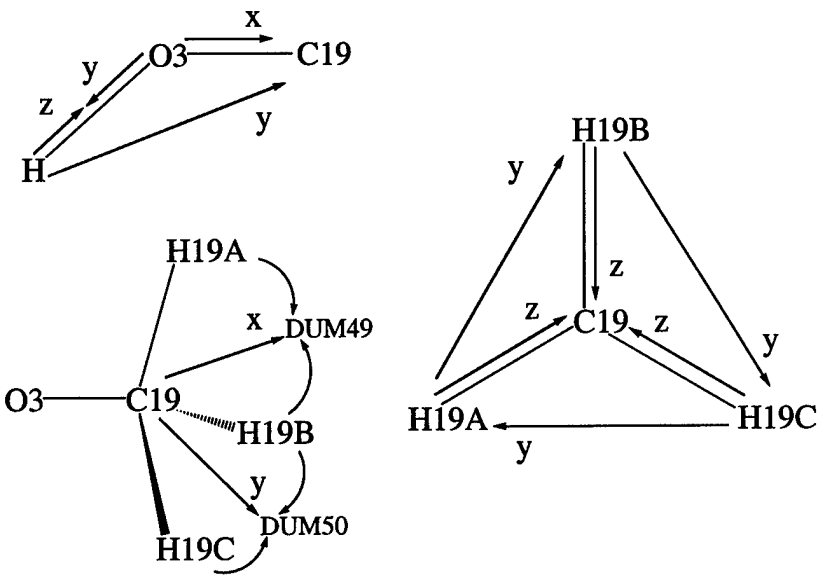

Figure 2. Coordinate system for the methanol molecule.

	n	m	$\langle n \rangle$	R_1	R_2	R_w	Z	V
Q < -4	0	0	0.0	0.0000	0.0000	0.0000	0.000	0.000
-4 < Q < -3	0	0	0.0	0.0000	0.0000	0.0000	0.000	0.000
-3 < Q < -2	8	4	2.0	0.3321	0.3844	0.3018	1.034	0.263
-2 < Q < -1	173	74	2.3	0.5492	0.6949	0.3870	0.761	0.455
-1 < Q < 0	2508	941	2.7	1.1243	1.1755	1.0245	1.183	2.153
0 < Q < 1	7959	2832	2.8	1.0254	1.0485	0.9274	1.329	1.501
1 < Q < 2	7845	2724	2.9	0.5759	0.6902	0.4618	1.252	0.519
2 < Q < 3	6736	2209	3.0	0.3661	0.4556	0.2863	1.194	0.322
3 < Q < 4	5725	1806	3.2	0.2602	0.3270	0.2132	1.220	0.235
4 < Q < 6	10058	2909	3.5	0.1800	0.2248	0.1548	1.231	0.170
6 < Q < 8	8497	2264	3.8	0.1266	0.1558	0.1169	1.254	0.127
8 < Q < 10	6921	1723	4.0	*0.0969*	0.1194	0.0927	1.242	0.101
10 < Q < 20	18395	4459	4.1	0.0596	0.0679	0.0645	1.224	0.063
20 < Q < 30	4702	1214	3.9	0.0389	0.0677	0.0370	1.193	0.040
30 < Q < 50	1174	361	3.3	0.0232	0.0273	0.0241	1.141	0.025
50 < Q < 100	212	75	2.8	0.0115	0.0136	0.0142	1.028	0.011
100 < Q	0	0	0.0	0.0000	0.0000	0.0000	0.000	0.000

Table 3. Intensity-Significance Intervals where n is the number of reflections, m is the number of unique reflections, $\langle n \rangle$ is the average measurement multiplicity, and Q=I/Max ($\sigma_{int}/\sigma_{ext}$) respectively for 17$\beta$-estradiol•½methanol.

	n	m	$\langle n \rangle$	R_1	R_2	R_w	Z	V
D > 1.016	4805	1570	3.1	.0345	.0529	.0721	1.568	.035
1.016 > D > 0.806	6705	1582	4.2	.0512	.0579	.0943	1.358	.057
0.806 > D > 0.705	6464	1594	4.1	.0554	.0578	.1004	1.337	.061
0.705 > D > 0.640	7744	1576	4.9	.0711	.0719	.1065	1.271	.075
0.640 > D > 0.594	8049	1558	5.2	.0792	.0777	.1080	1.250	.081
0.594 > D > 0.559	7545	1532	4.9	.1092	.1085	.1249	1.189	.105
0.559 > D > 0.531	6152	1521	4.0	.1373	.1371	.1424	1.155	.124
.531 > D > 0.508	4376	1441	3.0	.1334	.1241	.1677	1.274	.135
.508 > D > 0.488	4098	1401	2.9	.1508	.1428	.1755	1.245	.148
.488 > D > 0.472	4118	1436	2.9	.1593	.1445	.1895	1.280	.155
.472 > D > 0.457	3747	1354	2.8	.1854	.1681	.1988	1.230	.177
.457 > D > 0.444	3746	1387	2.7	.2289	.2205	.2122	1.192	.215
.444 > D > 0.432	3456	1331	2.6	.3003	.3007	.2497	1.183	.270
.432 > D > 0.422	3298	1303	2.5	.3737	.3823	.2719	1.167	.333
.422 > D > 0.412	2886	1194	2.4	.3703	.3773	.2801	1.166	.321
.412 > D > 0.403	1376	641	2.1	.3296	.3234	.3198	1.396	.309
.403 > D > 0.395	986	493	2.0	.3404	.3040	.3670	1.502	.352
.395 > D > 0.388	754	377	2.0	.4069	.3446	.4136	1.574	.431
.388 > D > 0.381	500	250	2.0	.4569	.4011	.4303	1.430	.486
.381 > D > 0.374	108	54	2.0	.5333	.4996	.5168	1.417	.584

Table 4. Equal-Volume Resolution Shells where n is the number of reflections, m is the number of unique reflections, $\langle n \rangle$ is the average measurement multiplicity, and S=sinθ/λ (Å^{-1}) respectively for 17β-estradiol•½methanol.

	Monopole	sp^2		sp^3
		20	33+	32-
O1	-0.50			
O2	-0.49			
C1	-0.30	-0.22	0.34	
C2	-0.38	-0.19	0.37	
C3	0.27	-0.21	0.38	
C4	-0.33	-0.17	0.36	
C5	-0.18	-0.22	0.33	
C6	-0.26			0.31
C7	-0.31			0.34
C8	-0.21			0.39
C9	-0.17			0.31
C10	-0.25	-0.18	0.37	
C11	-0.31			0.35
C12	-0.28			0.31
C13	-0.16			0.38
C14	-0.20			0.38
C15	-0.26			0.33
C16	-0.35			0.42
C17	0.20			0.38
C18	-0.32			0.27

	Monopole
H1O	0.40
H2O	0.38
H1	0.23
H2	0.22
H4	0.26
H6x	0.20
H7x	0.17
H8	0.20
H9	0.16
H11x	0.17
H12x	0.16
H14	0.19
H15x	0.16
H16x	0.18
H17	0.13
H18x	0.18

Atoms	Kappa	κ	κ'
O1, O2, O3	1	0.97	1.16
C3	2	1.01	0.92
C17	3	1.02	0.95
C1, C2, C4	4	0.97	0.92
C5, C10	5	0.98	0.87
C6, C7, C8, C9, C11, C12, C13, C14, C15, C16, C17, C18, C19	6	0.98	0.95
all C-H hydrogen atoms	7	1.20	1.29
H1O, H2O, H3O	8	1.20	1.29

Table 5. Starting values entered into the model for the multipole refinement for 17β-estradiol•½methanol. Units for multipole populations are e^-.

Atom	X	Y	Z
O1	0.08240(13)	0.21162(10)	0.936405(8)
O2	0.10594(13)	-0.05126(10)	0.06557(7)
C1	-0.06613(13)	0.15097(10)	0.66487(7)
C2	-0.08242(13)	0.19541(10)	0.77285(7)
C3	0.08629(14)	0.17723(11)	0.82894(7)
C4	0.26644(14)	0.12231(11)	0.77447(7)
C5	0.28180(13)	0.08148(10)	0.66531(7)
C6	0.48051(13)	0.03222(10)	0.60930(8)
C7	0.49100(12)	-0.05741(10)	0.50539(7)
C8	0.32007(13)	0.02383(10)	0.43507(7)
C9	0.12862(13)	0.02870(10)	0.49496(7)
C10	0.11375(14)	0.09174(11)	0.60917(7)
C11	-0.04837(13)	0.10675(10)	0.42644(7)
C12	-0.03113(14)	0.03067(11)	0.31502(7)
C13	0.15891(13)	0.02225(10)	0.25505(6)
C14	0.33043(13)	-0.05715(10)	0.32756(7)
C15	0.51074(13)	-0.08784(11)	0.25121(7)
C16	0.43778(12)	-0.11963(10)	0.14061(7)
C17	0.21795(13)	-0.09091(10)	0.15990(8)
C18	0.15271(14)	0.18231(10)	0.21808(7)

Atom	X	Y	Z
H1O	-0.0503(22)	0.2510(18)	0.9652(12)
H2O	0.1284(24)	0.0361(18)	0.0311(12)
H1	-0.2009(20)	0.1644(16)	0.6260(11)
H2	-0.2242(21)	0.2411(16)	0.8125(11)
H4	0.3944(20)	0.1116(16)	0.8194(10)
H6A	0.5897(19)	-0.0323(15)	0.6651(11)
H6B	0.5127(20)	0.1370(16)	0.5919(11)
H7A	0.4844(20)	-0.1709(16)	0.5233(11)
H7B	0.6269(20)	-0.0687(15)	0.4609(11)
H8	0.3190(21)	0.1410(16)	0.4195(11)
H9	0.1338(19)	-0.0908(15)	0.5028(10)
H11A	-0.1825(20)	0.1042(16)	0.4670(11)
H11B	-0.0617(20)	0.2269(16)	0.4192(11)
H12A	-0.0363(20)	-0.0845(16)	0.3270(11)
H12B	-0.1555(20)	0.0952(15)	0.2685(11)
H14	0.3164(20)	-0.1689(16)	0.3477(11)
H15A	0.6267(22)	-0.1869(17)	0.2797(12)
H15B	0.5532(22)	0.0144(17)	0.2507(12)
H16A	0.5101(21)	-0.2360(16)	0.1119(11)
H16B	0.4559(22)	-0.0401(17)	0.0791(12)
H17	0.1966(20)	-0.1975(15)	0.1875(11)
H18A	0.0354(21)	0.2267(16)	0.1658(11)
H18B	0.1336(20)	0.2577(16)	0.2845(11)
H18C	0.2817(22)	0.1811(17)	0.1751(12)

Table 6. Fractional atomic coordinates for molecule 1 of 17β-estradiol•½methanol.

Atom	X	Y	Z
O1'	0.44563(13)	0.49573(10)	0.14404(8)
O2'	0.15712(13)	0.64715(11)	1.02254(7)
C1'	0.50368(13)	0.44528(10)	0.43452(7)
C2'	0.54823(14)	0.44473(10)	0.32415(8)
C3'	0.39817(13)	0.49586(10)	0.25199(7)
C4'	0.20597(13)	0.54530(10)	0.29149(7)
C5'	0.16168(13)	0.54570(11)	0.40252(7)
C6'	-0.05026(14)	0.60488(10)	0.43907(7)
C7'	-0.08644(13)	0.56878(10)	0.55668(8)
C8'	0.06136(13)	0.60192(10)	0.62803(7)
C9'	0.26559(13)	0.49008(11)	0.59721(7)
C10'	0.31159(13)	0.49584(10)	0.47642(7)
C11'	0.42220(13)	0.51079(10)	0.66974(7)
C12'	0.37063(14)	0.50141(10)	0.79075(8)
C13'	0.17009(14)	0.61553(11)	0.82063(7)
C14'	0.01990(13)	0.58481(10)	0.74798(7)
C15'	-0.17643(13)	0.68090(10)	0.79979(7)
C16'	-0.13940(13)	0.66862(10)	0.92246(7)
C17'	0.08319(13)	0.59214(11)	0.93220(7)
C18'	0.17533(13)	0.77899(10)	0.81232(8)
O3	-0.28167(13)	0.29338(10)	1.01529(7)
C19	-0.35895(13)	0.17109(11)	1.02075(7)
H3O	-0.35307(25)	0.37300(22)	1.06225(17)
H19A	-0.29199(24)	0.08909(21)	0.95875(15)
H19B	-0.51182(24)	0.21209(20)	1.00791(15)
H19C	-0.34233(23)	0.11940(20)	1.09895(15)

Atom	X	Y	Z
H1O'	0.3341(22)	0.5447(17)	0.1007(12)
H2O'	0.1344 (23)	0.7561(17)	1.0186(12)
H1'	0.6239 (21)	0.4062(16)	0.4879(11)
H2'	0.6958(21)	0.4029(16)	0.2915(11)
H4'	0.0906(20)	0.5827(15)	0.2349(11)
H6C	-0.1306(20)	0.5579(15)	0.3848(11)
H6D	-0.1013(21)	0.7288(17)	0.4312(12)
H7C	-0.0741(20)	0.4489(16)	0.5651(11)
H7D	-0.2360(19)	0.6359(15)	0.5793(10)
H8'	0.0560(19)	0.7196(15)	0.6101(10)
H9'	0.2574(20)	0.3759(16)	0.6148(11)
H11C	0.5588(21)	0.4192(17)	0.6528(11)
H11D	0.4370(20)	0.6218(16)	0.6521(11)
H12C	0.3708 (21)	0.3860(16)	0.8082(11)
H12D	0.4841(20)	0.5202(16)	0.8379(11)
H14'	0.0331(20)	0.4644(16)	0.7608(11)
H15C	-0.2902(21)	0.6352(16)	0.7785(11)
H15D	-0.2110(22)	0.8005(17)	0.7772(12)
H16C	-0.2159(21)	0.6001(17)	0.9642(12)
H16D	-0.1856(22)	0.7791(17)	0.9632(13)
H17'	0.1173(20)	0.4698(15)	0.9497(10)
H18D	0.2891(21)	0.7876(16)	0.8599(11)
H18E	0.2046(20)	0.8088(16)	0.7323(11)
H18F	0.0440(23)	0.8618(18)	0.8405(12)

Table 7. Fractional atomic coordinates for molecule 2 and methanol of 17β-estradiol•½methanol.

Atom	U^{11}	U^{22}	U^{33}	U^{12}	U^{13}	U^{23}
O1	0.02315(12)	0.01838(11)	0.01172(8)	-0.00821(9)	0.00038(8)	-0.00143(7)
O2	0.02742(14)	0.01660(10)	0.01237(8)	-0.00827(10)	-0.00257(8)	-0.00055(7)
C1	0.01183(10)	0.02079(13)	0.01240(9)	-0.00540(9)	0.00016(8)	-0.00046(9)
C2	0.01489(11)	0.01999(13)	0.01241(10)	-0.00567(10)	0.00116(8)	-0.00063(9)
C3	0.01715(12)	0.01344(10)	0.01130(9)	-0.00612(9)	-0.00016(8)	0.00036(8)
C4	0.01523(11)	0.01497(11)	0.01220(9)	-0.00595(9)	-0.00180(8)	0.00039(8)
C5	0.01212(10)	0.01365(10)	0.01193(9)	-0.00438(8)	-0.00169(8)	0.00091(8)
C6	0.01108(10)	0.02189(14)	0.01563(11)	-0.00391(10)	-0.00226(8)	-0.00091(10)
C7	0.01153(10)	0.01874(13)	0.01690(11)	-0.00068(9)	-0.00173(9)	-0.00146(10)
C8	0.01108(9)	0.01379(10)	0.01239(9)	-0.00381(8)	-0.00023(7)	-0.00045(8)
C9	0.01150(10)	0.01434(11)	0.01169(9)	-0.00501(8)	-0.00072(7)	0.00044(8)
C10	0.01091(9)	0.01456(11)	0.01085(9)	-0.00475(8)	-0.00064(7)	0.00068(8)
C11	0.01118(10)	0.02348(15)	0.01289(10)	-0.00428(10)	-0.00113(8)	-0.00183(9)
C12	0.01433(11)	0.02257(15)	0.01333(10)	-0.00799(10)	-0.00128(8)	-0.00153(9)
C13	0.01540(11)	0.01279(10)	0.01145(9)	-0.00557(9)	-0.00003(8)	-0.00079(7)
C14	0.01351(10)	0.01445(11)	0.01285(9)	-0.00400(9)	0.00044(8)	-0.00125(8)
C15	0.01524(13)	0.02956(19)	0.01735(13)	-0.00556(13)	0.00290(10)	-0.00514(12)
C16	0.02131(15)	0.02492(17)	0.01594(12)	-0.00703(13)	0.00430(11)	-0.00569(11)
C17	0.02088(13)	0.01382(11)	0.01227(10)	-0.00648(15)	-0.00006(11)	-0.00162(13)
C18	0.02731(16)	0.01397(12)	0.01504(11)	-0.00815(11)	-0.00065(11)	0.00034(9)
O1'	0.02050(12)	0.02548(14)	0.01264(9)	-0.00112(10)	0.00182(8)	-0.00266(9)
O2'	0.02908(14)	0.01675(10)	0.01253(8)	-0.00712(10)	-0.00434(9)	-0.00013(7)
C1'	0.01201(11)	0.02698(17)	0.01402(11)	0.00007(11)	-0.00084(13)	-0.00137(10)
C2'	0.01366(12)	0.02877(18)	0.01463(11)	-0.00027(11)	0.00023(9)	-0.00244(11)
C3'	0.01544(12)	0.01728(12)	0.01231(10)	-0.00199(10)	0.00038(9)	-0.00223(9)
C4'	0.01434(11)	0.01596(11)	0.01173(9)	-0.00340(9)	-0.00136(8)	-0.00047(8)
C5'	0.01218(10)	0.01417(10)	0.01179(9)	-0.00328(8)	-0.00185(8)	0.00034(8)
C6'	0.01206(11)	0.02589(16)	0.01333(10)	-0.00459(10)	-0.00254(8)	0.00307(10)
C7'	0.01301(11)	0.02461(15)	0.01363(10)	-0.00787(10)	-0.00229(8)	0.00273(10)
C8'	0.01167(9)	0.01277(10)	0.01186(9)	-0.00365(8)	-0.00136(7)	0.00172(7)
C9'	0.01227(10)	0.01343(10)	0.01241(9)	-0.00207(8)	-0.00242(8)	0.00063(8)
C10'	0.01146(10)	0.01537(11)	0.01218(9)	-0.00169(8)	-0.00187(8)	-0.00036(8)
C11'	0.01272(11)	0.02953(18)	0.01384(11)	-0.00590(12)	-0.00282(9)	0.00010(11)
C12'	0.01563(12)	0.02041(14)	0.01340(10)	-0.00364(11)	-0.00403(10)	0.00092(9)
C13'	0.01718(11)	0.01090(9)	0.01195(9)	-0.00572(9)	-0.00183(8)	0.00114(7)
C14'	0.01426(11)	0.01539(11)	0.01184(9)	-0.00583(9)	-0.00107(8)	0.00163(8)
C15'	0.01570(13)	0.03738(24)	0.01515(12)	-0.00321(14)	0.00057(10)	0.00073(13)
C16'	0.02051(15)	0.03456(22)	0.01457(12)	-0.00670(15)	0.00243(11)	-0.00056(13)
C17'	0.02185(14)	0.01486(11)	0.01165(9)	-0.00722(10)	-0.00124(9)	0.00096(8)
C18'	0.03705(22)	0.01437(12)	0.01709(12)	-0.01337(14)	-0.00299(13)	0.00180(10)
O3	0.02682(15)	0.02440(15)	0.02598(14)	-0.00745(12)	0.01130(12)	-0.00554(12)
C19	0.02730(20)	0.03127(23)	0.02636(19)	-0.01196(18)	0.00339(15)	0.00142(16)

Table 8. Anisotropic thermal parameters of non-H atoms for 17β-estradiol•½methanol.

Atom	U_{iso}
H1O	0.0320(26)
H2O	0.0353(29)
H1	0.0453(25)
H2	0.0460(26)
H4	0.0429(24)
H6A	0.0404(21)
H6B	0.0491(26)
H7A	0.0495(25)
H7B	0.0475(24)
H8	0.0457(24)
H9	0.0386(21)
H11A	0.0488(25)
H11B	0.0493(25)
H12A	0.0519(26)
H12B	0.0462(24)
H14	0.0414(22)
H15A	0.0601(29)
H15B	0.0558(28)
H16A	0.0592(28)
H16B	0.0602(29)
H17	0.0505(23)
H18A	0.0572(27)
H18B	0.0554(26)
H18C	0.0658(31)

Atom	U_{iso}
H1O'	0.0326(27)
H2O'	0.0316(26)
H1'	0.0470(24)
H2'	0.0495(26)
H4'	0.0393(22)
H6C	0.0478(24)
H6D	0.0580(29)
H7C	0.0512(26)
H7D	0.0428(22)
H8'	0.0422(23)
H9'	0.0479(25)
H11C	0.0550(28)
H11D	0.0519(26)
H12C	0.0515(26)
H12D	0.0505(25)
H14'	0.0450(23)
H15C	0.0578(29)
H15D	0.0600(30)
H16C	0.0636(31)
H16D	0.0657(31)
H17'	0.0553(24)
H18D	0.0590(28)
H18E	0.0611(29)
H18F	0.0749(36)

H3O	0.0402(30)
H19A	0.0770(36)
H19B	0.0837(40)
H19C	0.0903(43)

Table 9. Isotropic thermal parameters of H atoms for 17β-estradiol•½methanol.

Atoms	Bond Length (Å)
O1 – C3	1.3688(4)
O2 – C17	1.4259(5)
C1 – C2	1.3926(5)
C1 – C10	1.4009(4)
C2 – C3	1.3961(5)
C3 – C4	1.3925(5)
C4 – C5	1.3981(5)
C5 – C6	1.5111(5)
C5 – C10	1.4069(4)
C6 – C7	1.5247(5)
C7 – C8	1.5264(5)
C8 – C9	1.5435(4)
C8 – C14	1.5222(5)
C9 – C10	1.5223(5)
C9 – C11	1.5377(5)
C11 – C12	1.5381(5)
C12 – C13	1.5266(5)
C13 – C14	1.5421(5)
C13 – C17	1.5374(5)
C13 – C18	1.5366(5)
C14 – C15	1.5392(5)
C15 – C16	1.5532(6)
C16 – C17	1.5453(6)

Atoms	Bond Length (Å)
O1' – C3'	1.3687(4)
O2' – C17'	1.4284(5)
C1' – C2'	1.3930(5)
C1' – C10'	1.4029(5)
C2' – C3'	1.3944(5)
C3' – C4'	1.3938(5)
C4' – C5'	1.4007(4)
C5' – C6'	1.5124(5)
C5' – C10'	1.4073(4)
C6' – C7'	1.5247(5)
C7' – C8'	1.5270(5)
C8' – C9'	1.5447(4)
C8' – C14'	1.5225(4)
C9' – C10'	1.5254(4)
C9' – C11'	1.5404(5)
C11' – C12'	1.5405(5)
C12' – C13'	1.5304(5)
C13' – C14'	1.5408(5)
C13' – C17'	1.5421(5)
C13' – C18'	1.5319(5)
C14' – C15'	1.5351(5)
C15' – C16'	1.5499(6)
C16' – C17'	1.5511(6)

O3 – C19	1.4234(8)

Table 10. Bond distances of non-H atoms of 17β-estradiol•½methanol.

Atoms	Bond Angle (°)
C3 – O1 – H1O	110.8(8)
C17 – O2 – H2O	109.5(8)
C2 – C1 – C10	122.4(1)
C2 – C1 – H1	116.1(6)
C10 – C1 – H1	121.4(6)
C1 – C2 – C3	119.1(1)
C1 – C2 – H2	119.9(6)
C3 – C2 – H2	120.9(6)
O1 – C3 – C2	122.5(1)
O1 – C3 – C4	118.1(1)
C2 – C3 – C4	119.4(1)
C3 – C4 – C5	121.2(1)
C3 – C4 – H4	117.9(6)
C5 – C4 – H4	120.9(6)
C4 – C5 – C6	118.5(1)
C4 – C5 – C10	120.0(1)
C6 – C5 – C10	121.5(1)
C5 – C6 - C7	113.4(1)
C5 – C6 – H6A	109.9(6)
C5 – C6 – H6B	105.9(6)
C7 – C6 – H6A	111.1(6)
C7 – C6 – H6B	110.2(6)
H6A – C6 – H6B	106.1(9)
C6 – C7 – C8	110.5(1)
C6 – C7 – H7A	110.7(6)
C6 – C7 – H7B	109.5(6)
C8 – C7 – H7A	107.7(6)
C8 – C7 – H7B	109.4(6)
H7A – C7 – H7B	109.0(8)
C7 – C8 – C9	109.3(1)
C7 – C8 – C14	112.3(1)

Atoms	Bond Angle (°)
C9 – C8 – C14	107.7(1)
C7 – C8 – H8	109.1(6)
C9 – C8 – H8	109.5(6)
C14 – C8 – H8	108.9(6)
C8 – C9 – C10	112.1(1)
C8 – C9 – C11	111.4(1)
C10 – C9 – C11	114.5(1)
C8 – C9 – H9	106.0(6)
C10 – C9 – H9	106.7(6)
C11 – C9 – H9	105.4(6)
C1 – C10 – C5	117.7(1)
C1 – C10 – C9	121.2(1)
C5 – C10 – C9	120.9(1)
C9 – C11 – C12	112.0(1)
C9 – C11 – H11A	111.2(6)
C9 – C11 – H11B	107.7(6)
C12 – C11 – H11A	108.2(6)
C12 – C11 – H11B	111.5(6)
H11A – C11 – H11B	106.0(8)
C11 – C12 – C13	111.5(1)
C11 – C12 – H12A	108.2(6)
C11 – C12 – H12B	108.6(6)
C13 – C12 – H12A	109.3(6)
C13 – C12 – H12B	110.7(6)
H12A – C12 – H12B	108.5(9)
C12 – C13 – C14	109.1(1)
C12 – C13 – C17	115.2(1)
C12 – C13 – C18	110.2(1)
C14 – C13 – C17	97.9(1)
C14 – C13 – C18	113.5(1)
C17 – C13 – C18	110.5(1)

Atoms	Bond Angle (°)
C8 – C14 – C13	113.4(1)
C8 – C14 – C15	120.3(1)
C13 – C14 – C15	103.9(1)
C8 – C14 – H14	105.8(6)
C13 – C14 – H14	105.6(6)
C15 – C14 – H14	106.8(6)
C14 – C15 – C16	103.6(1)
C14 – C15 – H15A	109.4(6)
C14 – C15 – H15B	107.5(6)
C16 – C15 – H15A	111.6(6)
C16 – C15 – H15B	112.9(6)
H15A – C15 – H15B	111.4(10)
C15 – C16 – C17	105.2(1)
C15 – C16 – H16A	112.9(6)
C15 – C16 – H16B	111.3(6)
C17 – C16 – H16A	110.1(6)
C17 – C16 – H16B	108.3(6)
H16A – C16 – H16B	109.0(9)
O2 – C17 – C13	117.1(1)
O2 – C17 – C16	114.7(1)
C13 – C17 – C16	104.4(1)
O2 – C17 – H17	104.1(6)
C13 – C17 – H17	107.2(6)
C16 – C17 – H17	109.0(6)
C13 – C18 – H18A	108.9(7)
C13 – C18 – H18B	111.6(6)
C13 – C18 – H18C	112.4(7)
H18A – C18 – H18B	109.0(9)
H18A – C18 – H18C	107.7(9)
H18B – C18 – H18C	107.1(10)

Table 11. Bond angles for molecule 1 of 17β-estradiol•½methanol.

Atoms	Bond Angle (°)
C3' – O1' – H1O'	112.9(8)
C17' – O2' – H2O'	112.3(8)
C2' – C1' – C10'	122.2(1)
C2' – C1' – H1'	117.3(6)
C10' – C1' – H1'	120.4(6)
C1' – C2' – C3'	119.5(1)
C1' – C2' – H2'	122.4(6)
C3' – C2' – H2'	118.1(6)
O1' – C3' – C2'	118.4(1)
O1' – C3' – C4'	122.2(1)
C2' – C3' – C4'	119.4(1)
C3' – C4' – C5'	121.0(1)
C3' – C4' – H4'	118.9(6)
C5' – C4' – H4'	120.1(6)
C4' – C5' – C6'	117.7(1)
C4' – C5' – C10'	120.3(1)
C6' – C5' – C10'	122.0(1)
C5' – C6' – C7'	113.6(1)
C5' – C6' – H6C	107.7(6)
C5' – C6' – H6D	108.1(6)
C7' – C6' – H6C	111.4(6)
C7' – C6' – H6D	107.2(6)
H6C – C6' – H6D	108.7(9)
C6' – C7' – C8'	110.3(1)
C6' – C7' – H7C	110.3(6)
C6' – C7' – H7D	107.5(6)
C8' – C7' – H7C	108.9(6)
C8' – C7' – H7D	112.8(6)
H7C – C7' – H7D	107.1(8)
C7' – C8' – C9'	108.7(1)
C7' – C8' – C14'	112.9(1)
C9' – C8' – C14'	108.7(1)
C7' – C8' – H8'	106.6(6)

Atoms	Bond Angle (°)
C'9 – C8' – H8'	109.6(6)
C14' – C8' – H8'	110.3(6)
C8' – C9' – C10'	111.2(1)
C8' – C9' – C11'	111.9(1)
C10' – C9' – C11'	114.2(1)
C8' – C9' – H9'	105.1(6)
C10' – C9' – H9'	107.3(6)
C11' – C9' – H9'	106.4(6)
C1' – C10' – C5'	117.6(1)
C1' – C10' – C9'	121.4(1)
C5' – C10' – C9'	120.9(1)
C9' – C11' – C12'	112.2(1)
C9' – C11' – H11C	109.0(6)
C9' – C11' – H11D	108.1(6)
C12' – C11' – H11C	107.0(6)
C12' – C11' – H11D	109.7(6)
H11C – C11' – H11D	110.9(9)
C11' – C12' – C13'	111.1(1)
C11' – C12' – H12C	108.4(6)
C11' – C12' – H12D	108.9(6)
C13' – C12' – H12C	109.4(6)
C13' – C12' – H12D	111.8(6)
H12C – C12' – H12D	107.1(9)
C12' – C13' – C14'	108.4(1)
C12' – C13' – C17'	115.6(1)
C12' – C13' – C18'	110.1(1)
C14' – C13' – C17'	99.4(1)
C14' – C13' – C18'	113.5(1)
C17' – C13' – C18'	109.6(1)
C8' – C14' – C13'	113.3(1)
C8' – C14' – C15'	119.6(1)
C13' – C14' – C15'	103.7(1)
C8' – C14' – H14'	106.6(6)

Atoms	Bond Angle (°)
C13' – C14' – H14'	105.9(6)
C15' – C14' – H14'	106.8(6)
C14' – C15' – C16'	103.5(1)
C14' – C15' – H15C	110.5(6)
C14' – C15' – H15D	110.5(6)
C16' – C15' – H15C	112.2(6)
C16' – C15' – H15D	107.6(6)
H15C – C15' – H15D	112.1(9)
C15' – C16' – C17'	106.0(1)
C15' – C16' – H16C	112.1(6)
C15' – C16' – H16D	113.1(6)
C17' – C16' – H16C	110.0(6)
C17' – C16' – H16D	109.3(6)
H16C – C16' – H16D	106.4(10)
O2' – C17' – C13'	115.7(1)
O2' – C17' – C16'	112.8(1)
C13' – C17' – C16'	104.6(1)
O2' – C17' – H17'	103.2(6)
C13' – C17' – H17'	110.7(6)
C16' – C17' – H17'	109.9(6)
C13' – C18' – H18D	108.4(7)
C13' – C18' – H18E	112.6(7)
C13' – C18' – H18F	112.9(8)
H18D – C18' – H18E	107.1(9)
H18D – C18' – H18F	108.1(10)
H18E – C18' – H18F	107.6(10)
C19 – O3 – H3O	110.4(9)
O3 – C19 – H19A	110.0(5)
O3 – C19 – H19B	110.5(5)
O3 – C19 – H19C	111.3(5)
H19A – C19 – H19B	107.4(8)
H19A – C19 – H19C	111.3(8)
H19B – C19 – H19C	106.1(8)

Table 12. Bond angles for molecule 2 and methanol of 17β-estradiol•½methanol.

Atom	Monopole Population ($P_{0,0}$)
O1	6.536(20)
O2	6.533(20)
C1	4.200(34)
C2	4.241(36)
C3	3.857(34)
C4	4.279(36)
C5	4.107(32)
C6	4.216(37)
C7	4.211(37)
C8	4.124(36)
C9	4.101(35)
C10	4.123(36)
C11	4.205(36)
C12	4.187(37)
C13	4.232(32)
C14	4.131(33)
C15	4.313(37)
C16	4.366(36)
C17	3.874(34)
C18	4.355(37)
O3	6.491(20)
C19	4.264(35)

Atom	Monopole Population ($P_{0,0}$)
O1'	6.539(21)
O2'	6.543(21)
C1'	4.194(36)
C2'	4.256(35)
C3'	3.875(34)
C4'	4.295(34)
C5'	4.123(34)
C6'	4.222(35)
C7'	4.199(34)
C8'	4.115(35)
C9'	4.115(33)
C10'	4.090(35)
C11'	4.215(36)
C12'	4.215(36)
C13'	4.220(34)
C14'	4.120(35)
C15'	4.309(37)
C16'	4.344(37)
C17'	3.852(33)
C18'	4.365(36)

Table 13. Monopole populations (e^-) of non-H atoms of 17β-estradiol•½methanol.

Atom	Monopole Population ($P_{0,0}$)
H1O	0.665(19)
H2O	0.636(19)
H1	0.783(19)
H2	0.769(19)
H4	0.776(19)
H6A	0.826(14)
H6B	0.826(14)
H7A	0.842(14)
H7B	0.842(14)
H8	0.819(19)
H9	0.833(17)
H11A	0.833(14)
H11B	0.833(14)
H12A	0.837(14)
H12B	0.837(14)
H14	0.820(18)
H15A	0.857(15)
H15B	0.857(15)
H16A	0.872(14)
H16B	0.872(14)
H17	0.916(20)
H18A	0.887(13)
H18B	0.887(13)
H18C	0.887(13)
H3O	0.696(20)
H19A	0.850(12)
H19B	0.850(12)
H19C	0.850(12)

Atom	Monopole Population ($P_{0,0}$)
H1O'	0.638(18)
H2O'	0.651(18)
H1'	0.796(19)
H2'	0.788(21)
H4'	0.790(19)
H6C	0.832(15)
H6D	0.832(15)
H7C	0.842(14)
H7D	0.842(14)
H8'	0.803(18)
H9'	0.829(20)
H11C	0.827(15)
H11D	0.827(15)
H12C	0.841(14)
H12D	0.841(14)
H14'	0.821(19)
H15C	0.841(15)
H15D	0.841(15)
H16C	0.870(15)
H16D	0.870(15)
H17'	0.939(20)
H18D	0.879(13)
H18E	0.879(13)
H18F	0.879(13)

Table 14. Monopole populations (e^-) of H atoms of 17β-estradiol•½methanol.

Multipoles	O1	O1'	O2	O2'	O3
$P_{1,+1}$	-0.025(17)	-0.033(17)	-0.043(17)	-0.028(18)	-0.046(20)
$P_{1,-1}$	0.030(19)	0.0	0.0	0.0	0.0
$P_{1,0}$	0.0	0.0	0.0	0.0	-0.068(19)
$P_{2,0}$	0.117(12)	0.127(13)	0.083(12)	0.089(12)	0.063(14)
$P_{2,+1}$	-0.033(11)	-0.016(12)	-0.021(11)	-0.018(11)	-0.038(14)
$P_{2,-1}$	-0.047(11)	-0.027(12)	0.0	-0.021(12)	-0.014(13)
$P_{2,+2}$	-0.042(11)	-0.035(11)	-0.077(11)	-0.046(11)	0.0
$P_{2,-2}$	-0.017(11)	0.0	0.0	0.0	0.0
$P_{3,0}$	-0.029(20)	0.0	0.0	0.050(22)	-0.040(25)
$P_{3,+1}$	-0.029(19)	0.0	0.0	0.0	-0.026(24)
$P_{3,-1}$	-0.028(20)	0.0	-0.024(20)	0.0	0.027(21)
$P_{3,+2}$	0.0	0.0	0.0	0.0	0.0
$P_{3,-2}$	0.0	0.034(21)	0.0	0.0	0.0
$P_{3,+3}$	0.083(18)	0.095(18)	0.075(19)	0.102(19)	0.073(20)
$P_{3,-3}$	-0.019(19)	0.0	0.0	-0.038(19)	-0.037(21)
$P_{4,0}$	0.037(19)	0.057(22)	0.0	0.025(20)	0.0
$P_{4,+1}$	0.0	-0.035(20)	0.0	0.0	0.0
$P_{4,-1}$	0.053(18)	0.0	0.025(18)	0.040(18)	0.0
$P_{4,+2}$	0.0	0.0	0.0	0.023(19)	0.023(22)
$P_{4,-2}$	0.0	0.0	0.0	0.021(19)	0.067(23)
$P_{4,+3}$	0.0	0.0	-0.039(18)	0.0	0.0
$P_{4,-3}$	0.0	-0.022(18)	0.020(18)	0.0	0.0
$P_{4,+4}$	0.024(16)	0.038(16)	0.0	0.0	0.020(18)
$P_{4,-4}$	0.0	0.036(17)	0.0	-0.020(16)	-0.030(20)

Table 15. Multipole populations (e^-) of Oxygen atoms of 17β-estradiol•½methanol.

Multipoles	C1	C1'	C2	C2'	C3	C3'	C4	C4'	C5	C5'
$P_{1,+1}$	0.031(29)	0.051(29)	0.0	0.125(29)	0.0	0.082(23)	-0.056(28)	-0.036(28)	0.037(31)	0.0
$P_{1,-1}$	0.0	0.129(31)	-0.040(28)	0.0	0.080(22)	0.0	0.0	0.0	0.087(28)	-0.029(29)
$P_{1,0}$	0.0	0.032(29)	0.0	-0.049(29)	0.032(21)	-0.031(23)	0.0	0.0	0.0	-0.027(27)
$P_{2,0}$	-0.154(19)	-0.150(21)	-0.178(19)	-0.147(21)	-0.118(15)	-0.122(16)	-0.142(18)	-0.176(19)	-0.198(18)	-0.127(18)
$P_{2,+1}$	0.060(19)	0.045(20)	0.044(19)	0.0	-0.031(15)	-0.037(16)	-0.025(18)	0.0	-0.026(18)	0.065(18)
$P_{2,-1}$	0.029(19)	0.0	0.0	0.0	-0.018(15)	0.0	-0.068(18)	0.026(18)	0.027(18)	0.0
$P_{2,+2}$	0.039(18)	0.041(19)	0.0	0.064(19)	0.077(15)	0.039(16)	0.0	0.033(18)	0.033(18)	0.0
$P_{2,-2}$	0.019(18)	-0.054(19)	-0.041(19)	0.0	-0.048(15)	-0.024(15)	-0.058(18)	-0.028(19)	-0.048(19)	-0.035(18)
$P_{3,0}$	0.0	0.0	0.058(31)	0.0	-0.039(25)	0.0	0.0	0.0	0.0	0.0
$P_{3,+1}$	0.0	0.051(31)	0.0	0.0	0.045(24)	0.0	0.030(29)	0.0	0.0	0.0
$P_{3,-1}$	0.0	-0.042(31)	0.0	0.0	-0.036(23)	0.048(24)	-0.042(30)	0.047(30)	0.016(29)	0.052(29)
$P_{3,+2}$	0.0	0.0	0.0	0.0	0.032(24)	0.0	0.0	0.0	0.0	0.0
$P_{3,-2}$	0.0	0.0	0.0	0.0	0.0	0.0	0.0	-0.030(30)	0.0	0.0
$P_{3,+3}$	0.271(27)	0.298(27)	0.315(28)	0.318(28)	0.270(22)	0.222(22)	0.280(27)	0.294(27)	0.313(27)	0.288(29)
$P_{3,-3}$	0.0	0.082(31)	0.0	-0.006(30)	-0.029(26)	0.0	0.0	0.0	-0.068(31)	0.0

Multipoles	C6	C6'	C7	C7'	C8	C8'	C9	C9'	C10	C10'
$P_{1,+1}$	0.0	-0.071(26)	-0.033(25)	-0.091(27)	0.0	0.052(27)	0.0	0.0	0.066(29)	-0.062(29)
$P_{1,-1}$	0.038(25)	0.0	-0.043(25)	0.047(25)	-0.030(26)	0.0	0.056(27)	0.0	0.0	0.091(28)
$P_{1,0}$	-0.030(24)	-0.043(26)	-0.083(25)	-0.037(24)	-0.033(27)	0.035(26)	0.0	-0.055(27)	0.0	0.0
$P_{2,0}$	0.0	0.055(19)	0.022(18)	0.0	0.047(17)	-0.028(16)	0.034(17)	0.0	-0.213(19)	-0.133(19)
$P_{2,+1}$	-0.063(18)	0.0	0.0	0.020(17)	-0.047(17)	-0.017(16)	0.023(16)	0.017(17)	-0.021(18)	0.0
$P_{2,-1}$	0.0	-0.036(19)	0.0	0.0	-0.063(17)	-0.029(16)	0.049(17)	0.053(17)	0.048(18)	-0.020(19)
$P_{2,+2}$	0.055(17)	0.018(16)	0.025(17)	0.025(17)	0.0	-0.017(16)	-0.067(16)	-0.020(15)	0.0	0.0
$P_{2,-2}$	0.018(17)	0.0	-0.058(16)	0.0	0.0	0.076(17)	0.023(16)	0.072(17)	0.0	-0.023(18)
$P_{3,0}$	-0.048(30)	0.0	0.0	-0.035(28)	0.036(30)	0.057(29)	0.035(29)	0.0	0.0	-0.053(31)
$P_{3,+1}$	0.0	-0.088(28)	-0.071(28)	0.0	-0.053(28)	0.088(28)	0.067(26)	0.0	0.0	0.052(30)
$P_{3,-1}$	0.0	-0.060(28)	0.0	0.078(26)	0.0	0.080(26)	0.0	0.0	0.0	0.0
$P_{3,+2}$	-0.029(28)	0.0	0.073(29)	0.0	0.050(28)	-0.069(28)	-0.161(27)	-0.036(28)	0.0	0.0
$P_{3,-2}$	0.313(27)	0.241(29)	0.209(27)	0.256(28)	0.341(27)	0.295(28)	0.272(26)	-0.288(28)	-0.049(30)	0.0
$P_{3,+3}$	-0.113(27)	-0.165(25)	-0.151(25)	-0.153(28)	0.0	0.074(26)	0.053(26)	0.0	0.334(28)	0.295(27)
$P_{3,-3}$	-0.053(27)	0.0	0.080(27)	0.0	0.0	-0.037(27)	0.0	-0.032(26)	0.0	0.0

Table 16. Multipole populations (e^-) of Carbon atoms of 17β-estradiol•½methanol.

Multipoles	C11	C11'	C12	C12'	C13	C13'	C14	C14'	C15	C15'
$P_{1,+1}$	-0.097(26)	0.0	-0.074(27)	0.0	-0.026(24)	0.0	0.0	0.0	0.0	-0.070(27)
$P_{1,-1}$	0.038(26)	0.0	0.0	0.049(25)	0.0	0.105(26)	0.032(25)	0.0	0.026(24)	0.076(26)
$P_{1,0}$	0.0	0.0	-0.039(23)	0.0	-0.027(26)	0.026(24)	-0.094(27)	0.0	0.034(24)	-0.053(25)
$P_{2,0}$	0.0	0.0	-0.044(18)	0.041(18)	0.026(18)	-0.031(17)	0.031(18)	0.020(17)	0.030(19)	-0.054(20)
$P_{2,+1}$	0.0	-0.045(18)	0.073(17)	0.067(17)	-0.052(17)	-0.095(17)	0.066(17)	-0.081(17)	0.0	-0.021(19)
$P_{2,-1}$	-0.095(17)	0.0	-0.034(17)	0.0	-0.024(17)	0.0	-0.023(17)	0.0	-0.071(18)	-0.059(19)
$P_{2,+2}$	0.0	0.047(17)	0.0	0.047(17)	0.0	0.0	0.0	0.0	0.070(18)	0.029(17)
$P_{2,-2}$	0.020(16)	-0.024(17)	-0.080(17)	-0.018(17)	0.0	0.058(17)	-0.025(16)	0.0	0.021(18)	-0.022(19)
$P_{3,0}$	-0.028(28)	0.036(30)	0.0	0.067(30)	0.044(30)	0.055(28)	-0.044(29)	0.064(26)	-0.039(30)	0.0
$P_{3,+1}$	-0.098(26)	-0.069(29)	-0.031(27)	-0.035(27)	-0.061(27)	0.085(27)	-0.094(28)	-0.042(28)	0.0	-0.048(29)
$P_{3,-1}$	0.0	-0.037(28)	0.044(27)	0.045(27)	0.0	0.099(26)	0.0	-0.113(27)	0.028(27)	0.0
$P_{3,+2}$	-0.042(28)	0.0	0.058(27)	0.0	0.096(28)	-0.036(28)	0.067(28)	0.0	-0.039(29)	0.0
$P_{3,-2}$	0.272(27)	0.295(28)	0.283(28)	0.267(27)	0.329(27)	0.332(27)	0.296(27)	0.307(27)	0.289(28)	0.236(30)
$P_{3,+3}$	-0.139(27)	-0.127(26)	-0.115(26)	-0.075(26)	-0.037(26)	0.034(26)	-0.099(25)	-0.077(28)	-0.115(28)	-0.181(28)
$P_{3,-3}$	0.0	0.049(27)	0.0	-0.033(26)	0.0	-0.077(28)	0.026(26)	0.060(27)	0.0	0.0

Multipoles	C16	C16'	C17	C17'	C18	C18'	C19
$P_{1,+1}$	0.0	-0.034(26)	0.028(20)	0.039(19)	-0.028(25)	-0.078(26)	-0.085(24)
$P_{1,-1}$	-0.031(25)	0.0	0.0	0.0	0.034(24)	0.097(24)	-0.028(26)
$P_{1,0}$	-0.061(26)	-0.049(24)	-0.067(18)	0.0	-0.034(24)	0.046(24)	0.025(25)
$P_{2,0}$	0.033(20)	0.0	-0.018(13)	0.028(14)	-0.017(17)	0.020(17)	0.080(21)
$P_{2,+1}$	0.0	-0.025(19)	0.052(13)	0.014(13)	-0.039(17)	0.0	0.0
$P_{2,-1}$	0.0	-0.050(20)	0.0	0.0	-0.016(16)	0.055(17)	0.020(19)
$P_{2,+2}$	0.0	0.0	0.0	0.0	0.054(18)	0.0	0.020(19)
$P_{2,-2}$	-0.019(18)	-0.030(18)	-0.078(13)	-0.031(13)	0.023(17)	0.059(18)	0.0
$P_{3,0}$	0.041(30)	0.059(30)	-0.074(22)	-0.066(21)	-0.028(29)	0.054(27)	0.177(32)
$P_{3,+1}$	-0.091(29)	0.0	-0.080(21)	-0.087(21)	0.0	0.110(28)	0.109(30)
$P_{3,-1}$	0.034(28)	0.022(29)	0.0	0.0	0.0	0.0	0.0
$P_{3,+2}$	0.0	-0.070(29)	0.074(22)	0.0	0.039(27)	0.072(28)	0.0
$P_{3,-2}$	0.274(28)	0.205(28)	0.212(21)	0.224(21)	0.212(26)	-0.229(28)	0.299(31)
$P_{3,+3}$	-0.135(25)	-0.116(28)	-0.076(21)	0.0	0.0	0.078(27)	0.091(30)
$P_{3,-3}$	0.061(26)	-0.039(27)	0.0	-0.021(20)	0.0	0.044(26)	0.0

Table 17. Multipole populations (e^-) of Carbon atoms of 17β-estradiol•½methanol continued.

Atoms	$P_{1,0}$	$P_{2,0}$
H1O	0.121(19)	0.005(28)
H2O	0.125(21)	0.002(28)
H1	0.109(24)	-0.007(31)
H2	0.107(22)	0.066(32)
H4	0.127(23)	-0.018(30)
H6A	0.105(15)	-0.010(19)
H6B	0.105(15)	-0.010(19)
H7A	0.134(15)	0.034(20)
H7B	0.134(15)	0.034(20)
H8	0.150(23)	-0.029(31)
H9	0.089(22)	0.028(29)
H11A	0.110(16)	-0.015(21)
H11B	0.110(16)	-0.015(21)
H12A	0.099(16)	0.019(20)
H12B	0.099(16)	0.019(20)
H14	0.118(24)	-0.006(29)
H15A	0.070(17)	0.018(22)
H15B	0.070(17)	0.018(22)
H16A	0.132(16)	-0.005(22)
H16B	0.132(16)	-0.005(22)
H17	0.167(24)	0.041(33)
H18A	0.106(13)	-0.035(17)
H18B	0.106(13)	-0.035(17)
H18C	0.106(13)	-0.035(17)

Atoms	$P_{1,0}$	$P_{2,0}$
H1O'	0.127(19)	0.018(27)
H2O'	0.129(20)	0.012(28)
H1'	0.191(23)	0.006(29)
H2'	0.150(23)	0.043(34)
H4'	0.112(22)	0.049(28)
H6C	0.138(16)	0.024(22)
H6D	0.138(16)	0.024(22)
H7C	0.137(15)	0.051(21)
H7D	0.137(15)	0.051(21)
H8'	0.148(22)	0.056(30)
H9'	0.127(24)	0.065(32)
H11C	0.139(16)	0.033(22)
H11D	0.139(16)	0.033(22)
H12C	0.140(16)	-0.026(20)
H12D	0.140(16)	-0.026(20)
H14'	0.176(24)	0.058(31)
H15C	0.075(17)	0.062(23)
H15D	0.075(17)	0.062(23)
H16C	0.094(17)	-0.033(22)
H16D	0.094(17)	-0.033(22)
H17'	0.219(23)	0.062(35)
H18D	0.102(13)	0.012(17)
H18E	0.102(13)	0.012(17)
H18F	0.102(13)	0.012(17)
H3O	0.088(19)	-0.043(30)
H19A	0.183(13)	-0.036(19)
H19B	0.183(13)	-0.036(19)
H19C	0.183(13)	-0.036(19)

Table 18. Multipole populations (e^-) of Hydrogen atoms of 17β-estradiol•½methanol.

Bond	$\rho(r_c)$	$\nabla^2\rho(r_c)$	R_{ij}	d_1	d_2	λ_1	λ_2	λ_3	ε
O1 – C3	1.992	-18.666	1.3731	0.8342	0.5389	-17.30	-13.85	12.49	0.25
O1' – C3'	2.101	-18.114	1.3692	0.8106	0.5586	-17.16	-15.42	14.46	0.11
O1 – H1O	2.379	-31.187	0.9702	0.7400	0.2302	-37.16	-36.51	42.48	0.02
O1' – H1O'	2.308	-28.991	0.9701	0.7502	0.2199	-37.32	-35.43	43.76	0.05
O2 – C17	1.734	-8.541	1.4259	0.8182	0.6078	-13.32	-11.42	16.21	0.17
O2' – C17'	1.863	-10.326	1.4294	0.8159	0.6136	-14.80	-13.62	18.10	0.09
O2 – H2O	2.303	-30.051	0.9704	0.7491	0.2213	-37.23	-35.63	42.80	0.05
O2' – H2O'	2.311	-26.715	0.9701	0.7415	0.2286	-35.18	-34.78	43.25	0.01
C1 – C2	2.160	-20.204	1.3930	0.7046	0.6884	-16.25	-12.87	8.92	0.26
C1' – C2'	2.111	-19.897	1.3934	0.7349	0.6585	-15.99	-12.24	8.32	0.31
C1 – C10	2.088	-18.453	1.4011	0.6823	0.7187	-15.30	-12.20	9.06	0.25
C1' – C10'	2.097	-19.229	1.4036	0.7295	0.6742	-15.82	-12.35	8.94	0.28
C1 – H1	1.807	-15.039	1.0804	0.6524	0.4280	-16.66	-14.94	16.55	0.12
C1' – H1'	1.785	-16.604	1.0800	0.6082	0.4718	-15.80	-13.51	12.70	0.17
C2 – C3	2.172	-21.192	1.3969	0.6614	0.7355	-16.77	-13.88	9.45	0.21
C2' – C3'	2.103	-18.329	1.3946	0.7454	0.6492	-16.33	-11.74	9.74	0.39
C2 – H2	1.884	-17.271	1.0801	0.6619	0.4182	-17.49	-16.52	16.74	0.06
C2' – H2'	1.891	-18.440	1.0800	0.6345	0.4456	-17.47	-15.48	14.50	0.13
C3 – C4	2.228	-21.634	1.3931	0.7152	0.6779	-17.78	-13.87	10.02	0.28
C3' – C4'	2.156	-19.354	1.3948	0.7118	0.6830	-16.37	-13.24	10.26	0.24
C4 – C5	2.095	-18.890	1.3993	0.6556	0.7437	-15.71	-11.94	8.76	0.32
C4' – C5'	2.078	-18.328	1.4012	0.6942	0.7070	-15.69	-11.90	9.27	0.32
C4 – H4	1.779	-12.634	1.0803	0.6507	0.4295	-15.43	-14.16	16.96	0.09
C4' – H4'	1.932	-18.229	1.0801	0.6569	0.4232	-17.81	-16.99	16.56	0.05
C5 – C6	1.705	-12.450	1.5112	0.7592	0.7520	-11.83	-10.57	9.95	0.12
C5' – C6'	1.694	-11.252	1.5127	0.7635	0.7492	-11.64	-9.88	10.26	0.18

Table 19. Topological properties of bond critical points in 17β-estradiol•½methanol.

Bond	$\rho(r_c)$	$\nabla^2\rho(r_c)$	R_{ij}	d_1	D_2	λ_1	λ_2	λ_3	ε
C5 – C10	2.155	-20.813	1.4072	0.7180	0.6892	-16.33	-13.65	9.17	0.20
C5' – C10'	2.073	-18.203	1.4084	0.6742	0.7342	-15.25	-12.23	9.28	0.25
C6 – C7	1.583	-10.047	1.5249	0.7796	0.7453	-10.69	-9.50	10.14	0.13
C6' – C7'	1.626	-10.314	1.5248	0.7435	0.7813	-10.90	-9.62	10.20	0.13
C6 – H6A	1.691	-10.161	1.0900	0.6479	0.4421	-14.54	-12.47	16.85	0.17
C6 – H6B	1.776	-12.170	1.0923	0.6623	0.4300	-15.70	-14.71	18.24	0.07
C6' – H6C	1.881	-14.581	1.0906	0.6503	0.4403	-16.63	-14.99	17.04	0.11
C6' – H6D	1.872	-14.981	1.0901	0.6465	0.4436	-16.68	-14.86	16.57	0.12
C7 – C8	1.590	-9.180	1.5269	0.7957	0.7312	-10.18	-9.20	10.20	0.11
C7' – C8'	1.625	-9.958	1.5289	0.7494	0.7796	-10.77	-9.54	10.35	0.13
C7 – H7A	1.948	-16.835	1.0900	0.6574	0.4326	-18.12	-16.09	17.38	0.13
C7 – H7B	1.807	-14.807	1.0905	0.6387	0.4518	-15.99	-14.29	15.47	0.12
C7' – H7C	1.964	-17.201	1.0903	0.6551	0.4351	-18.26	-16.04	17.09	0.14
C7' – H7D	1.807	-14.724	1.0912	0.6361	0.4550	-15.79	-14.28	15.35	0.11
C8 – C9	1.581	-9.450	1.5438	0.7668	0.7770	-10.22	-9.47	10.24	0.08
C8' – C9'	1.545	-7.983	1.5457	0.7759	0.7697	-9.94	-8.59	10.54	0.16
C8 – C14	1.682	-11.473	1.5223	0.7540	0.7683	-11.40	-10.29	10.22	0.11
C8' – C14'	1.625	-10.656	1.5235	0.7202	0.8033	-11.05	-9.55	9.94	0.16
C8 – H8	1.813	-12.664	1.1003	0.6650	0.4353	-15.49	-15.16	17.98	0.02
C8' – H8'	1.923	-17.748	1.1009	0.6606	0.4404	-17.42	-16.56	16.23	0.05
C9 – C10	1.688	-11.912	1.5246	0.7404	0.7842	-11.75	-10.36	10.19	0.13
C9' – C10'	1.584	-9.752	1.5281	0.7594	0.7686	-10.43	-9.44	10.12	0.10
C9 – C11	1.489	-8.316	1.5378	0.7931	0.7447	-9.77	-8.35	9.80	0.17
C9' – C11'	1.585	-9.071	1.5412	0.7351	0.8060	-10.51	-9.12	10.56	0.15
C9 – H9	1.879	-15.456	1.1000	0.6783	0.4217	-17.66	-16.23	18.44	0.09
C9' – H9'	1.956	-17.951	1.1001	0.6668	0.4333	-18.16	-16.92	17.12	0.07

Table 20. Topological properties of bond critical points in 17β-estradiol•½methanol continued.

Bond	$\rho(r_c)$	$\nabla^2\rho(r_c)$	R_{ij}	d_1	D_2	λ_1	λ_2	λ_3	ε
C11 – C12	1.589	-10.204	1.5382	0.7492	0.7890	-10.57	-9.72	10.09	0.09
C11' – C12'	1.541	-9.336	1.5408	0.7628	0.7779	-9.91	-9.41	9.98	0.05
C11 – H11A	1.789	-11.786	1.0901	0.6602	0.4299	-15.68	-14.41	18.30	0.09
C11 – H11B	1.813	-12.082	1.0900	0.6636	0.4264	-15.98	-14.81	18.71	0.08
C11' – H11C	1.810	-14.683	1.0924	0.6453	0.4472	-15.97	-14.68	15.96	0.09
C11' – H11D	1.845	-14.612	1.0902	0.6489	0.4413	-16.32	-14.86	16.57	0.10
C12 – C13	1.658	-11.077	1.5275	0.7506	0.7769	-11.03	-10.22	10.17	0.08
C12' – C13'	1.635	-9.576	1.5307	0.7501	0.7806	-11.01	-9.45	10.89	0.16
C12 – H12A	1.960	-16.160	1.0903	0.6768	0.4135	-18.65	-17.02	19.50	0.10
C12 – H12B	1.698	-12.630	1.0914	0.6421	0.4493	-14.77	-13.44	15.58	0.10
C12' – H12C	1.897	-14.894	1.0903	0.6570	0.4333	-17.33	-15.47	17.90	0.12
C12' – H12D	1.693	-10.342	1.0908	0.6354	0.4554	-14.31	-12.11	16.08	0.18
C13 – C14	1.538	-8.278	1.5423	0.7589	0.7834	-9.58	-8.85	10.15	0.08
C13' – C14'	1.643	-9.762	1.5434	0.7891	0.7543	-10.34	-9.90	10.48	0.04
C13 – C17	1.624	-8.277	1.5379	0.7470	0.7909	-10.54	-9.99	12.26	0.06
C13' – C17'	1.510	-6.686	1.5423	0.7449	0.7974	-9.53	-8.74	11.58	0.09
C13 – C18	1.668	-9.648	1.5368	0.7767	0.7602	-10.68	-10.13	11.16	0.05
C13' – C18'	1.715	-10.914	1.5332	0.7625	0.7707	-11.10	-10.93	11.11	0.01
C14 – C15	1.580	-9.879	1.5414	0.7578	0.7836	-10.46	-9.46	10.04	0.11
C14' – C15'	1.586	-9.229	1.5363	0.7506	0.7858	-10.41	-9.10	10.28	0.14
C14 – H14	1.910	-15.081	1.1001	0.6761	0.4240	-17.45	-16.21	18.58	0.08
C14' – H14'	2.006	-20.475	1.1000	0.6528	0.4472	-18.50	-17.49	15.51	0.06
C15 – C16	1.525	-8.303	1.5532	0.7550	0.7982	-10.05	-8.63	10.38	0.17
C15' – C16'	1.492	-7.757	1.5508	0.8012	0.7496	-9.89	-8.13	10.26	0.22
C15 – H15A	1.763	-11.798	1.0901	0.6645	0.4256	-16.19	-14.26	18.65	0.14
C15 – H15B	1.777	-10.781	1.0909	0.6711	0.4198	-15.74	-14.73	19.69	0.07

Table 21. Topological properties of bond critical points in 17β-estradiol•½methanol continued.

Bond	$\rho(r_c)$	$\nabla^2\rho(r_c)$	R_{ij}	d_1	D_2	λ_1	λ_2	λ_3	ε
C15' – H15C	1.882	-15.052	1.0903	0.6688	0.4216	-18.03	-15.33	18.32	0.18
C15' – H15D	1.751	-13.044	1.0913	0.6552	0.4361	-15.90	-14.21	17.07	0.12
C16 – C17	1.638	-9.824	1.5461	0.7828	0.7633	-11.30	-10.29	11.77	0.10
C16' – C17'	1.542	-7.493	1.5512	0.7795	0.7717	-9.98	-9.31	11.80	0.07
C16 – H16A	1.906	-15.286	1.0901	0.6486	0.4414	-16.96	-15.61	17.28	0.09
C16 – H16B	1.797	-13.408	1.0905	0.6364	0.4541	-14.93	-14.58	16.11	0.02
C16' – H16C	1.703	-8.472	1.0901	0.6520	0.4381	-14.36	-12.68	18.56	0.13
C16' – H16D	1.678	-8.319	1.0901	0.6487	0.4414	-13.95	-12.55	18.18	0.11
C17 – H17	2.018	-17.771	1.1000	0.6630	0.4371	-19.36	-18.82	20.41	0.03
C17' – H17'	2.067	-20.809	1.1006	0.6409	0.4597	-20.06	-18.79	18.05	0.07
C18 – H18A	1.812	-11.307	1.0600	0.6184	0.4416	-14.71	-13.64	17.05	0.08
C18 – H18B	1.844	-14.261	1.0605	0.6164	0.4441	-15.77	-14.74	16.25	0.07
C18 – H18C	1.850	-13.230	1.0603	0.6200	0.4403	-15.57	-14.56	16.90	0.07
C18' – H18D	1.762	-12.273	1.0691	0.6267	0.4424	-15.13	-14.29	17.15	0.06
C18' – H18E	1.910	-16.290	1.0611	0.6251	0.4360	-17.09	-15.73	16.53	0.09
C18' – H18F	1.933	-14.147	1.0610	0.6344	0.4265	-17.57	-14.76	18.18	0.19
O3 – C19	1.964	-12.936	1.4239	0.8367	0.5872	-14.50	-13.07	14.64	0.11
O3 – H3O	2.346	-19.388	0.9417	0.7160	0.2257	-35.13	-33.93	49.67	0.04
C19 – H19A	1.785	-12.350	1.0820	0.6237	0.4583	-15.47	-13.65	16.77	0.13
C19 – H19B	1.970	-19.275	1.0731	0.6177	0.4554	-18.20	-15.96	14.88	0.14
C19 – H19C	1.911	-14.353	1.0702	0.6159	0.4543	-17.14	-12.99	15.78	0.32

Table 22. Topological properties of bond critical points in 17β-estradiol•½methanol continued.

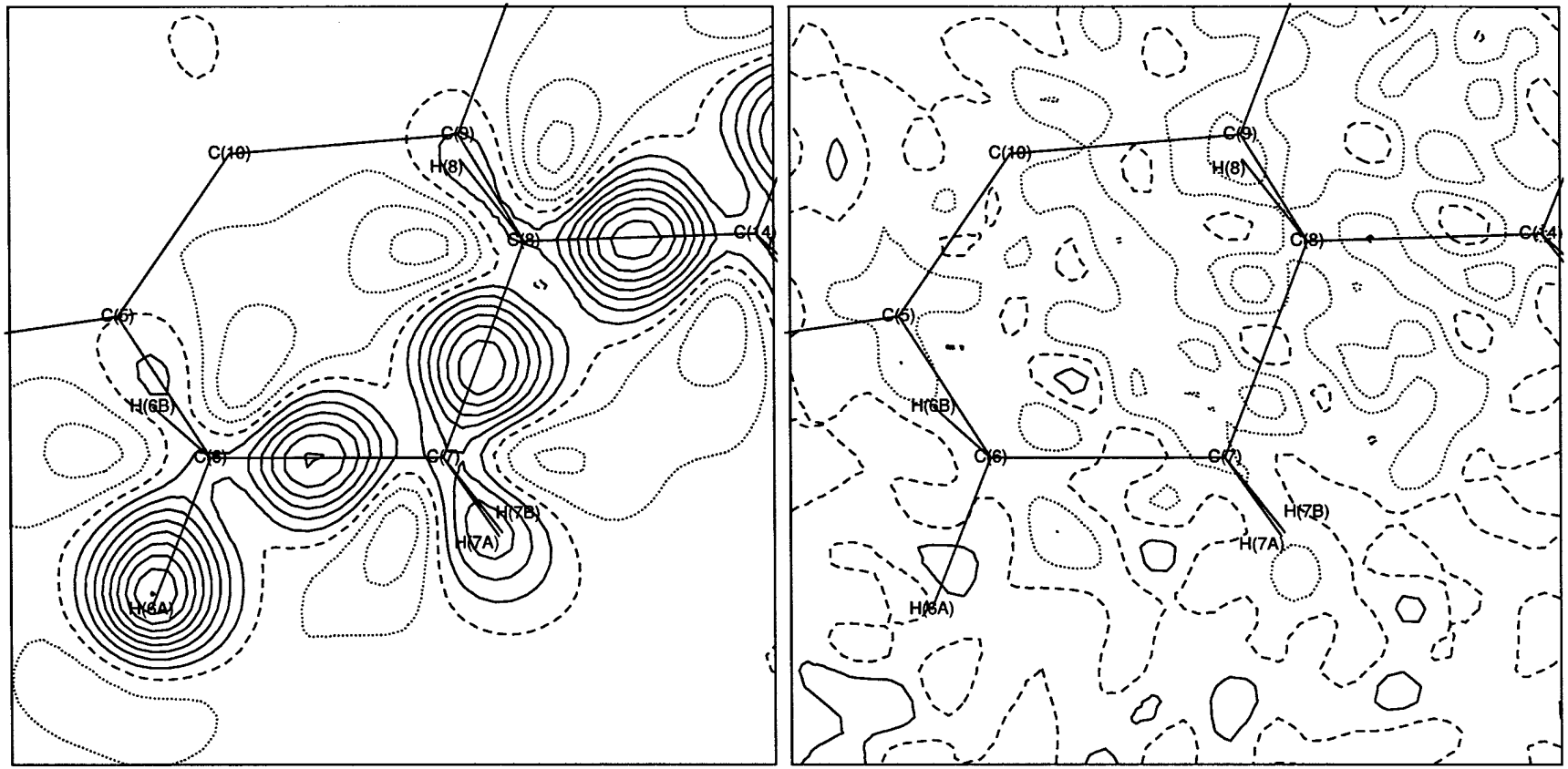

Figure 3. Dynamic model map and residual map in the C6 – C7 – C8 plane of 17β-estradiol•½methanol. Contour intervals are 0.05 eÅ^{-3} with solid lines positive, dashed lines zero, and dotted lines negative.

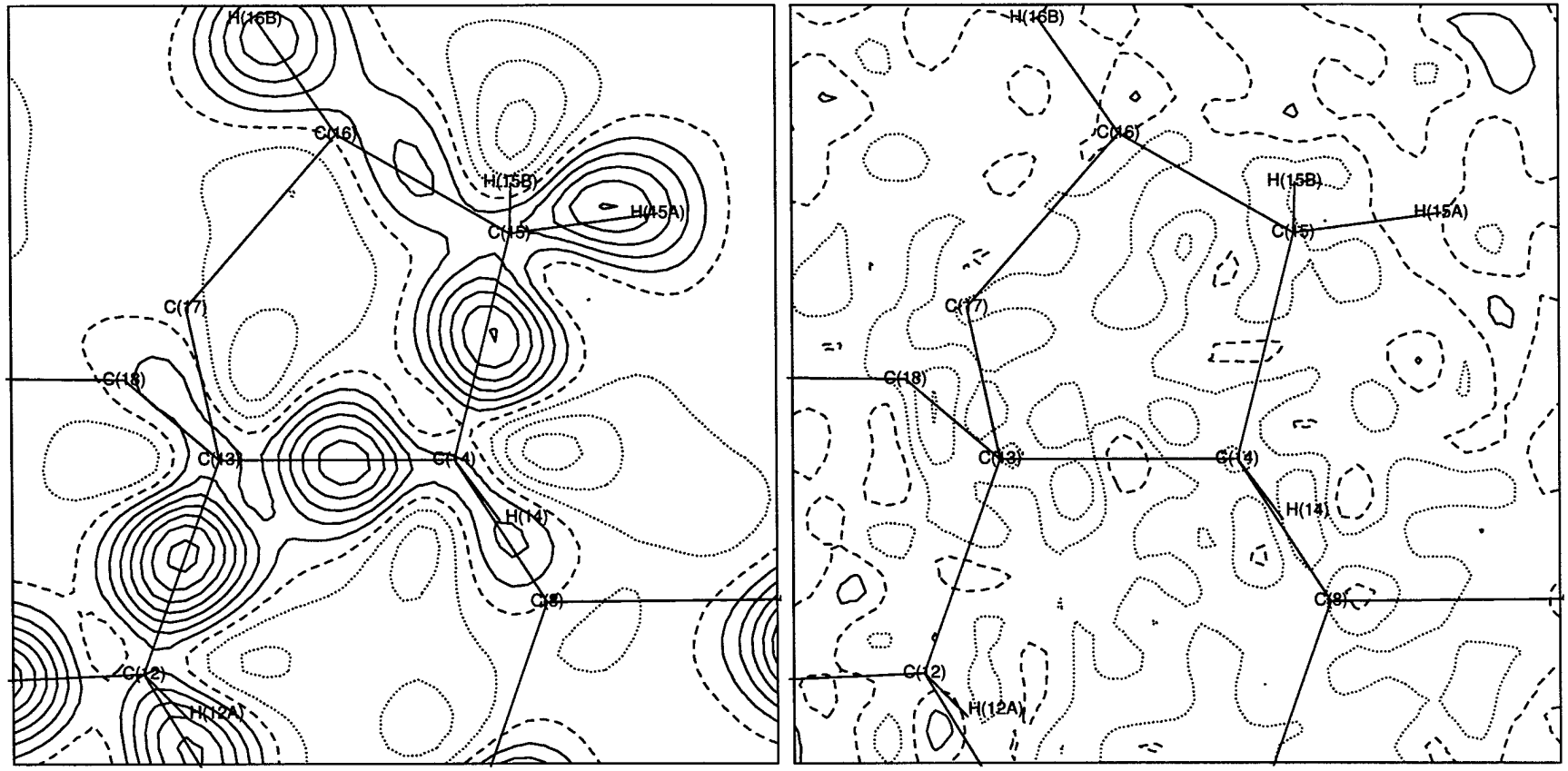

Figure 4. Dynamic model map and residual map in the C13 – C14 – C15 plane of 17β-estradiol•½methanol. Contour intervals are 0.05 eÅ^{-3} with solid lines positive, dashed lines zero, and dotted lines negative.

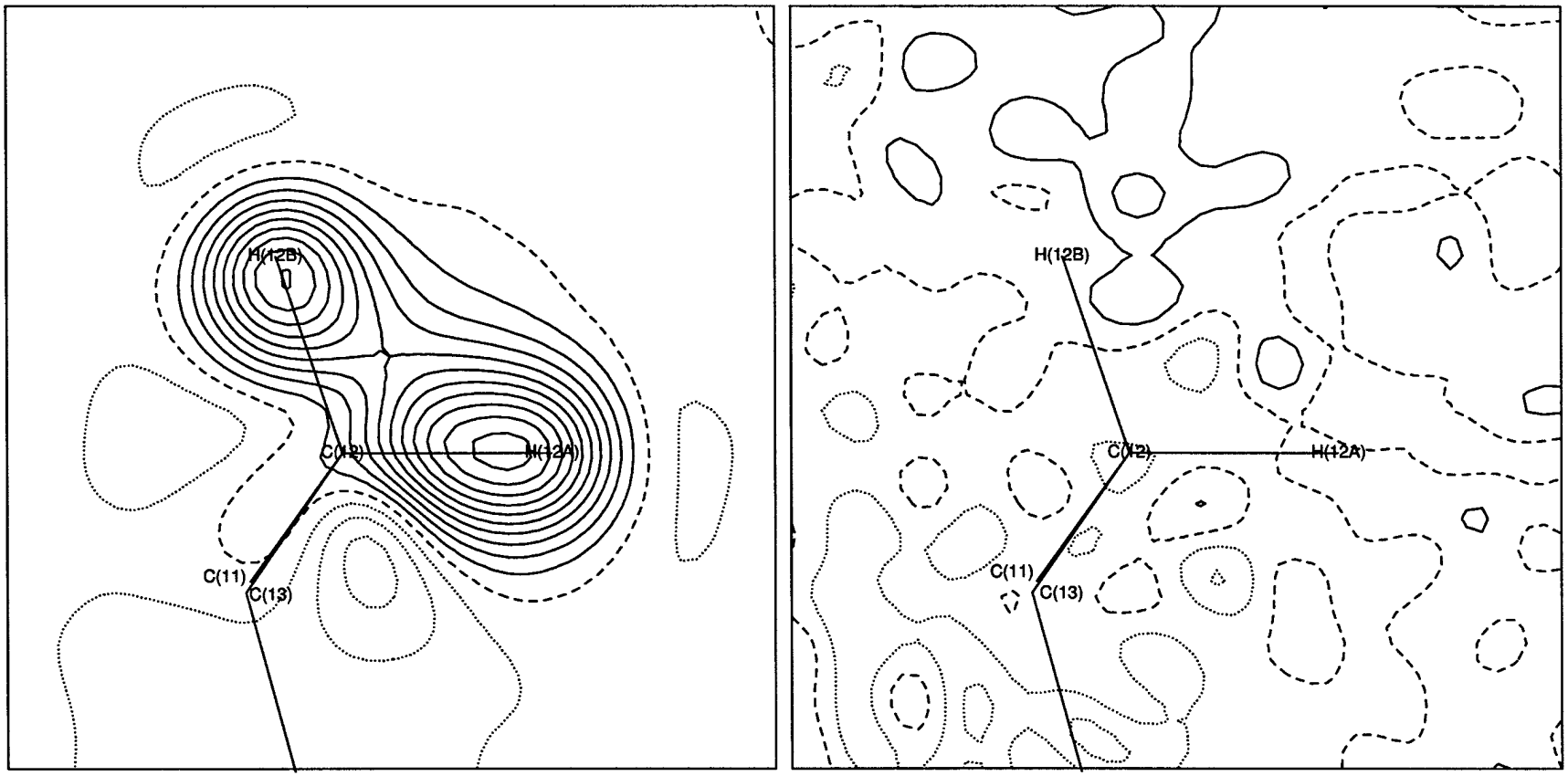

Figure 5. Dynamic model map and residual map in the C12 – H12A – H12B plane of 17β-estradiol•½methanol. Contour intervals are 0.05 eÅ^{-3} with solid lines positive, dashed lines zero, and dotted lines negative.

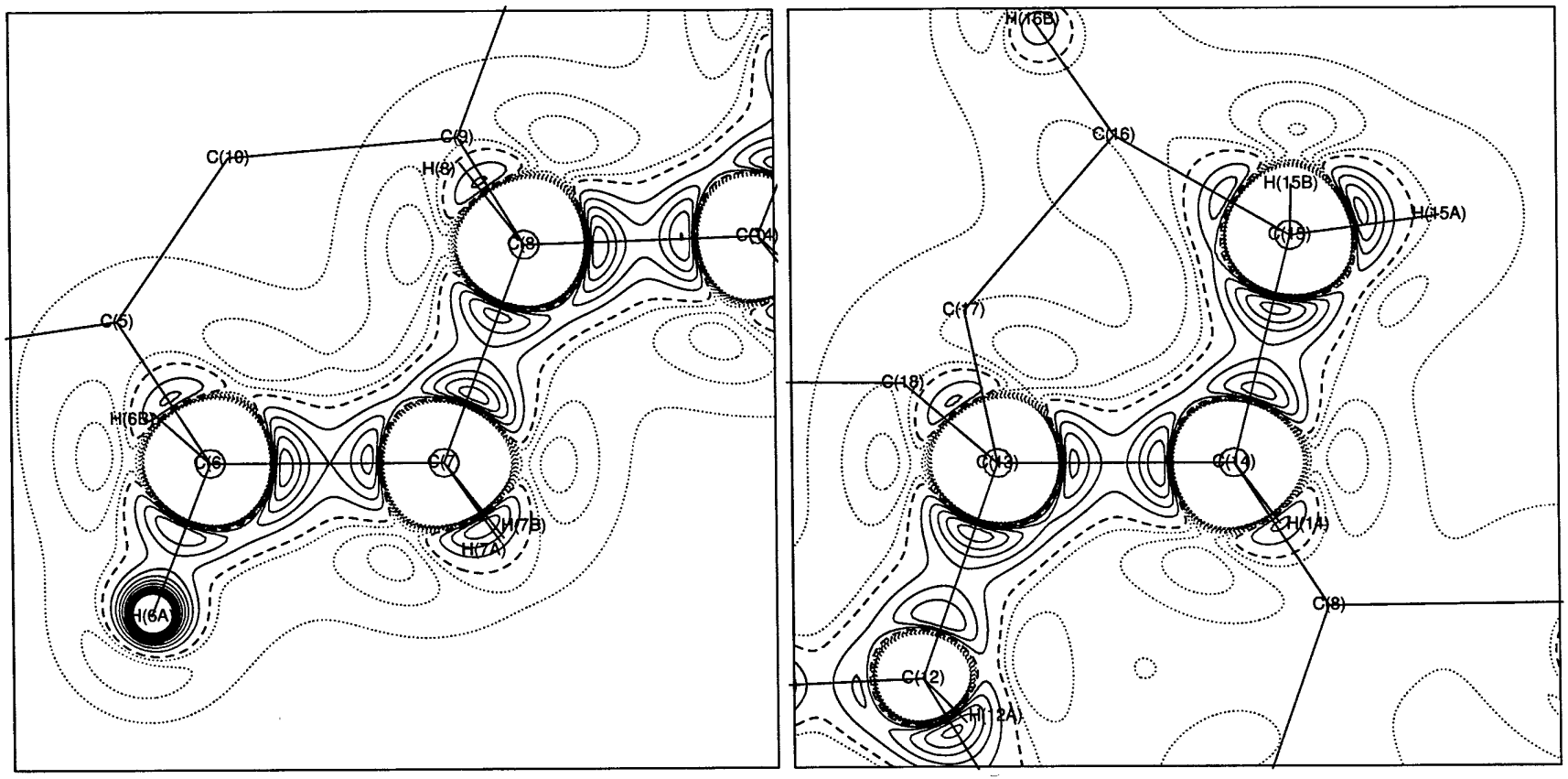

Figure 6. The Laplacian of the total electron density of atoms at rest in the C6 – C7 – C8 and C13 – C14 – C15 planes of 17β-estradiol•½methanol. Contour intervals are 5 eÅ^{-5} starting at 5 eÅ^{-5} (solid blue lines), -2 eÅ^{-5} starting at -2 eÅ^{-5} (dotted red lines), and the dashed line equals 0 eÅ^{-5}.

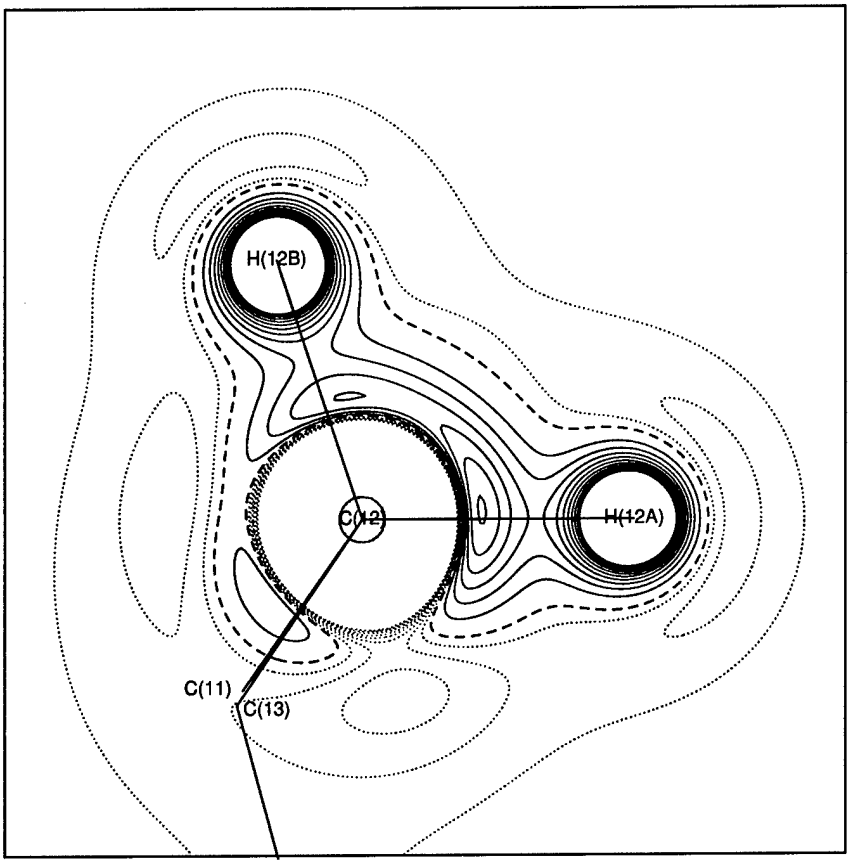

Figure 7. The Laplacian of the total electron density of atoms at rest in the H12A – C12 – H12B plane of 17β-estradiol•½methanol. Contour intervals are 5 eÅ^{-5} starting at 5 eÅ^{-5} (solid blue lines), -2 eÅ^{-5} starting at -2 eÅ^{-5} (dotted red lines), and the dashed line plots 0 eÅ^{-5}.

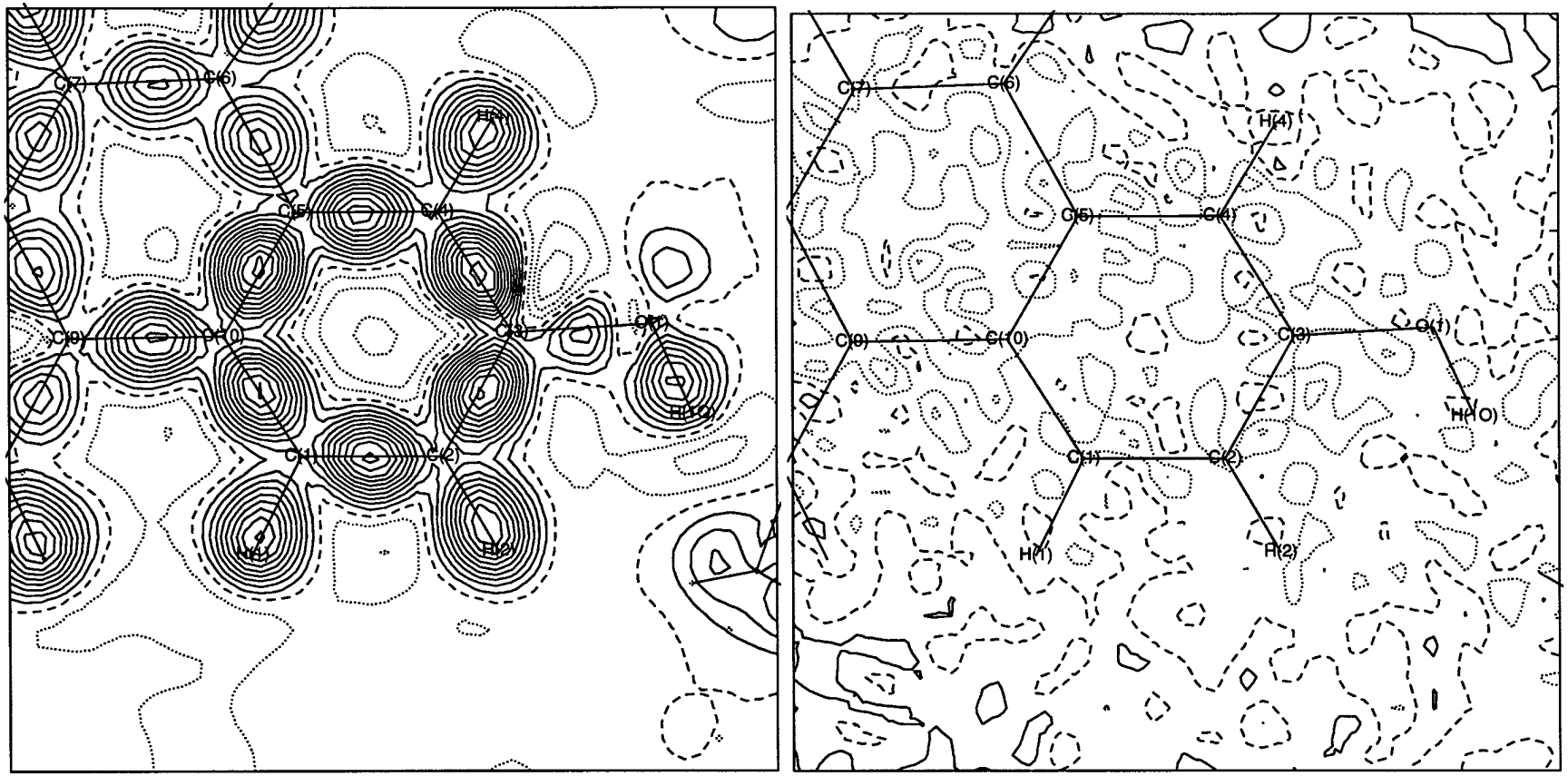

Figure 8. Dynamic model map and residual map in the plane of the aromatic ring of molecule 1 of 17β-estradiol•½methanol. Contour intervals are 0.05 eÅ^{-3} with solid lines positive, dashed lines zero, and dotted lines negative.

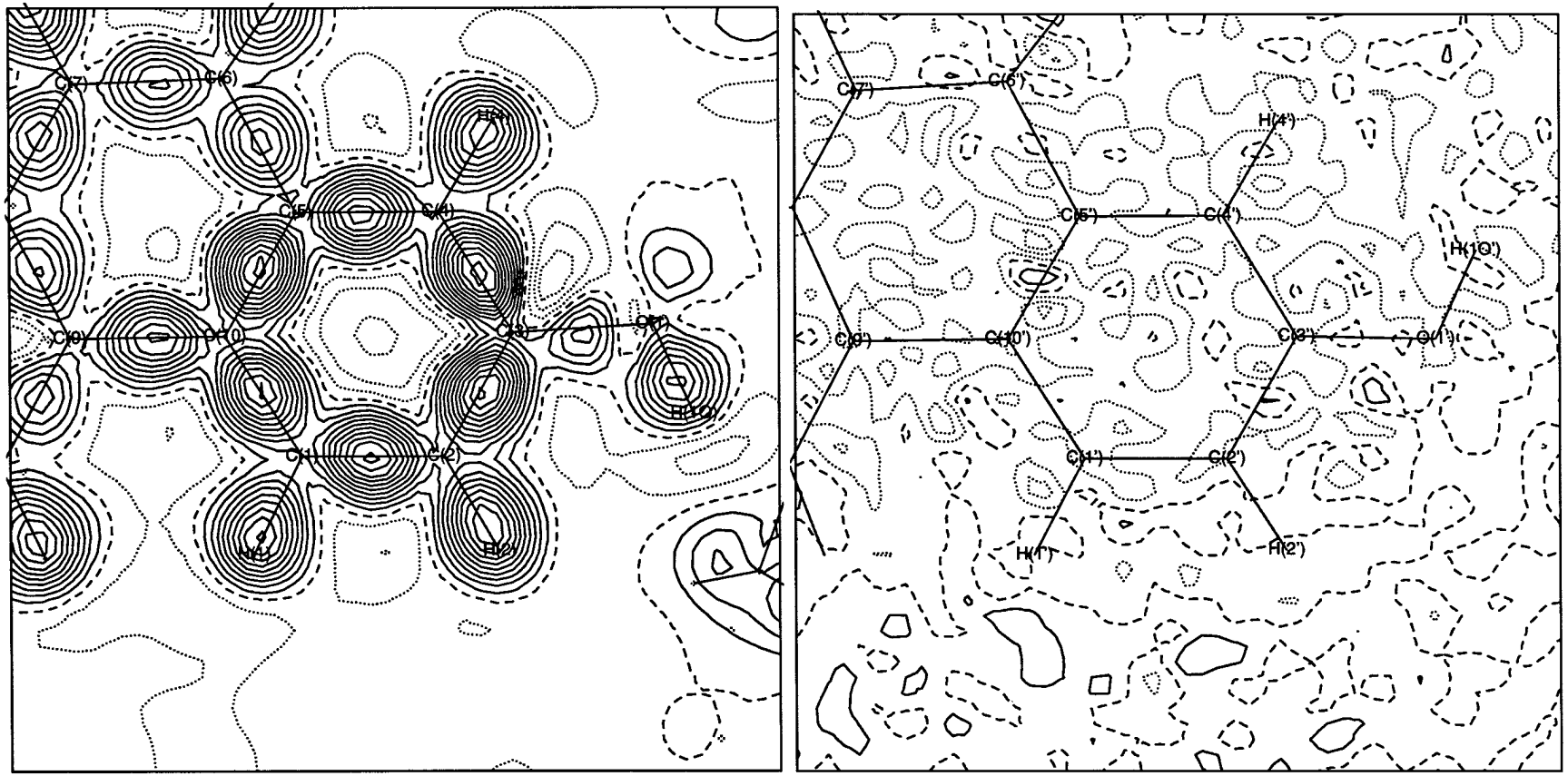

Figure 9. Dynamic model map and residual map in the plane of the aromatic ring of molecule 2 of 17β-estradiol•½methanol. Contour intervals are 0.05 eÅ^{-3} with solid lines positive, dashed lines zero, and dotted lines negative.

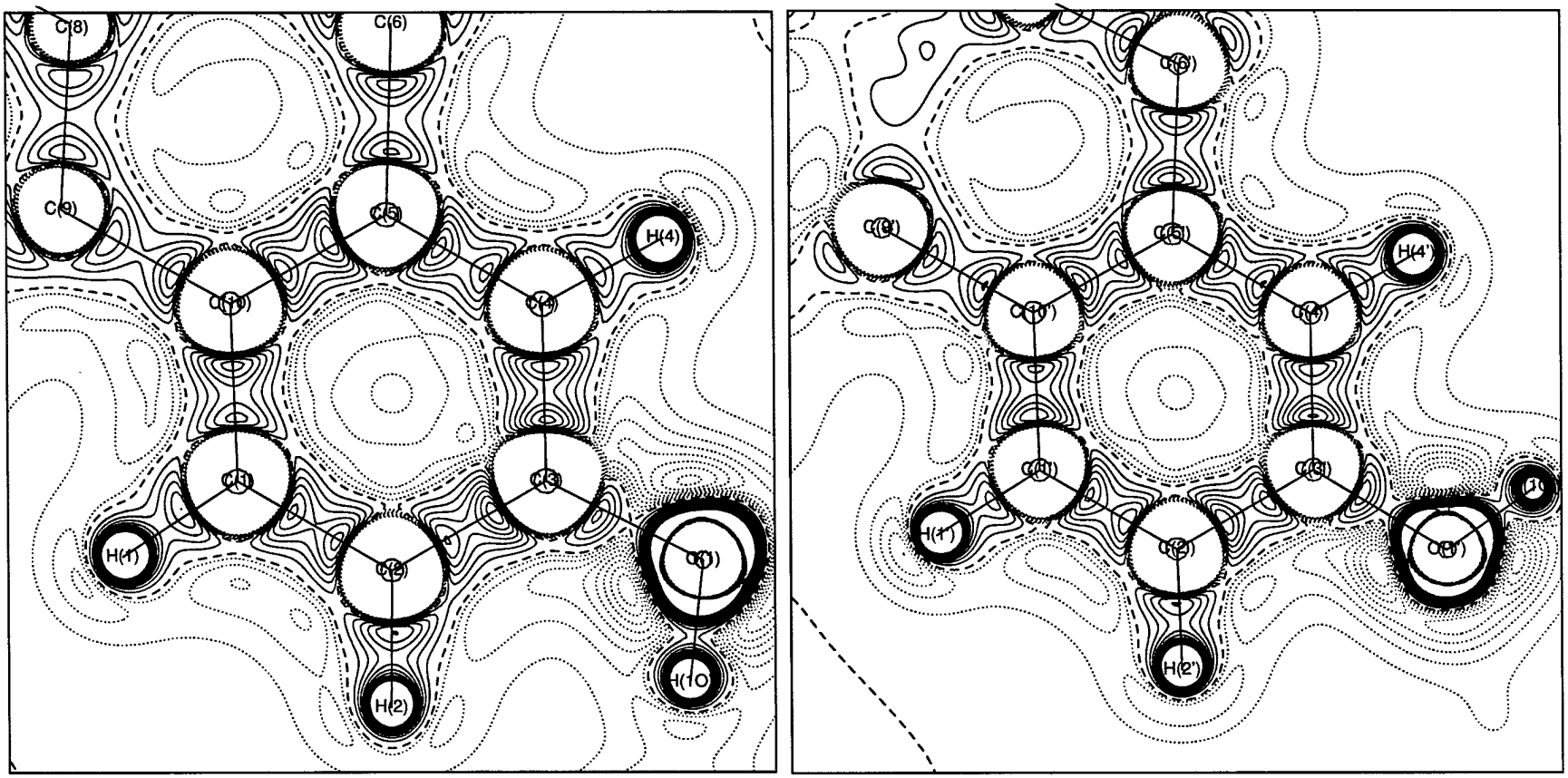

Figure 10. The Laplacian of the total electron density of atoms at rest in the plane of the aromatic rings of 17β-estradiol•½methanol. Contour intervals are 5 eÅ^{-5} starting at 5 eÅ^{-5} (solid blue lines), -2 eÅ^{-5} starting at -2 eÅ^{-5} (dotted red lines), and the dashed line plots 0 eÅ^{-5}.

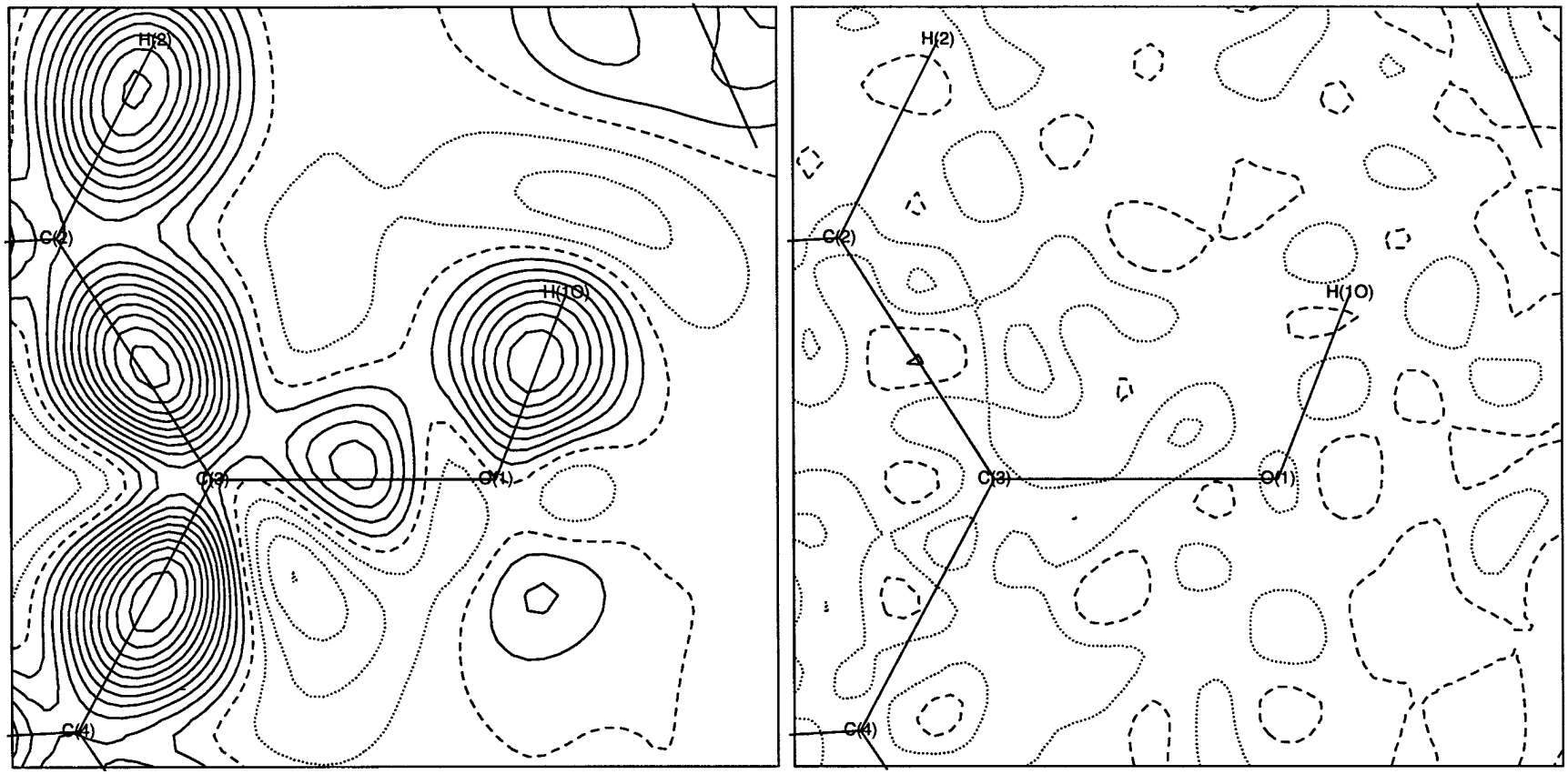

Figure 11. Dynamic model map and residual map in the C3 – O1 – H1O plane of 17β-estradiol•½methanol. Contour intervals are 0.05 eÅ^{-3} with solid lines positive, dashed lines zero, and dotted lines negative.

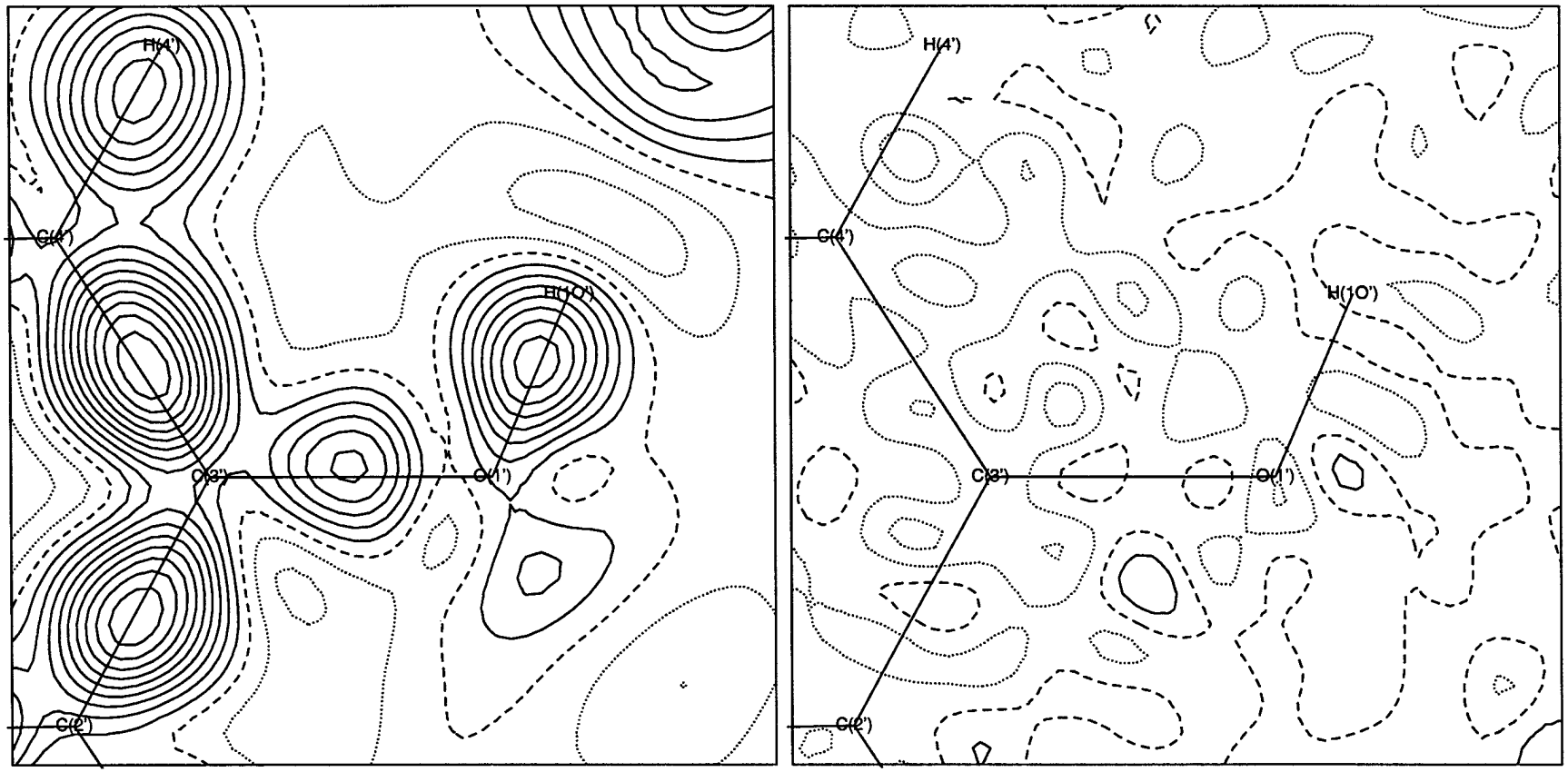

Figure 12. Dynamic model map and residual map in the C3' – O1' – H1O' plane of 17β-estradiol•½methanol. Contour intervals are 0.05 eÅ^{-3} with solid lines positive, dashed lines zero, and dotted lines negative.

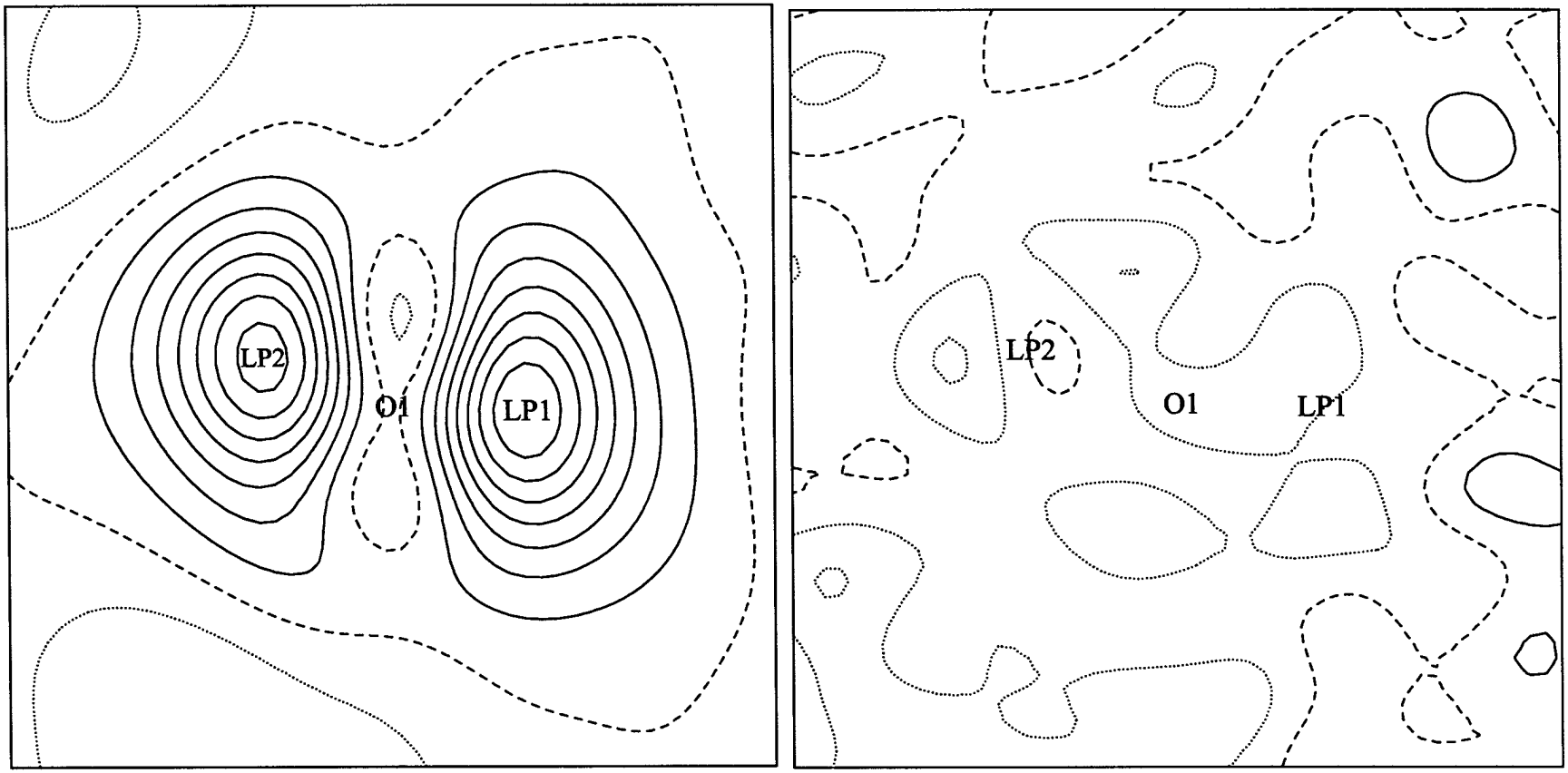

Figure 13. Dynamic model map and residual map in the plane of the lone pairs of O1 of 17β-estradiol•½methanol. Contour intervals are 0.05 eÅ^{-3} with solid lines positive, dashed lines zero, and dotted lines negative.

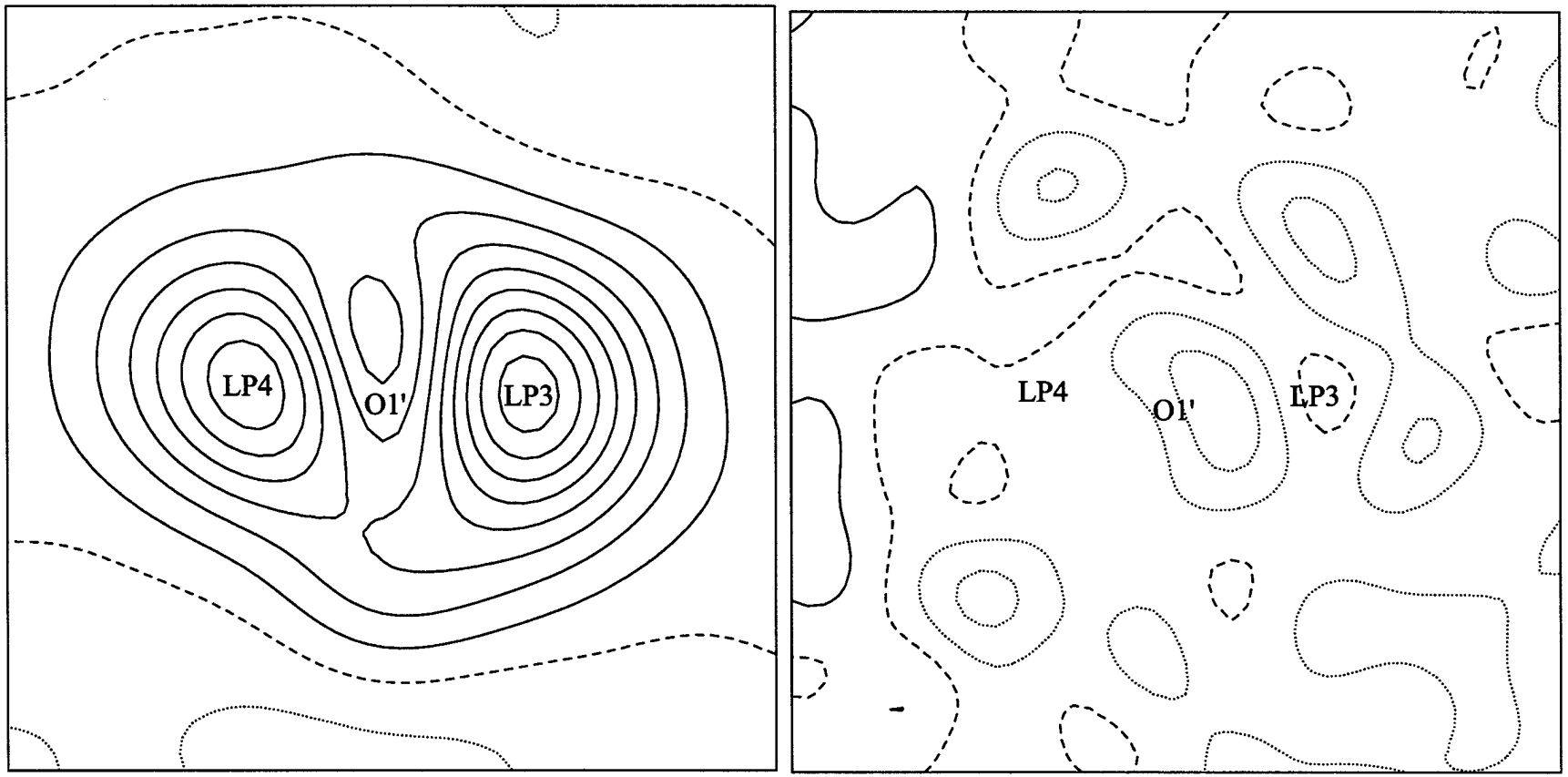

Figure 14. Dynamic model map and residual map in the plane of the lone pairs of O1' of 17β-estradiol•½methanol. Contour intervals are 0.05 eÅ^{-3} with solid lines positive, dashed lines zero, and dotted lines negative.

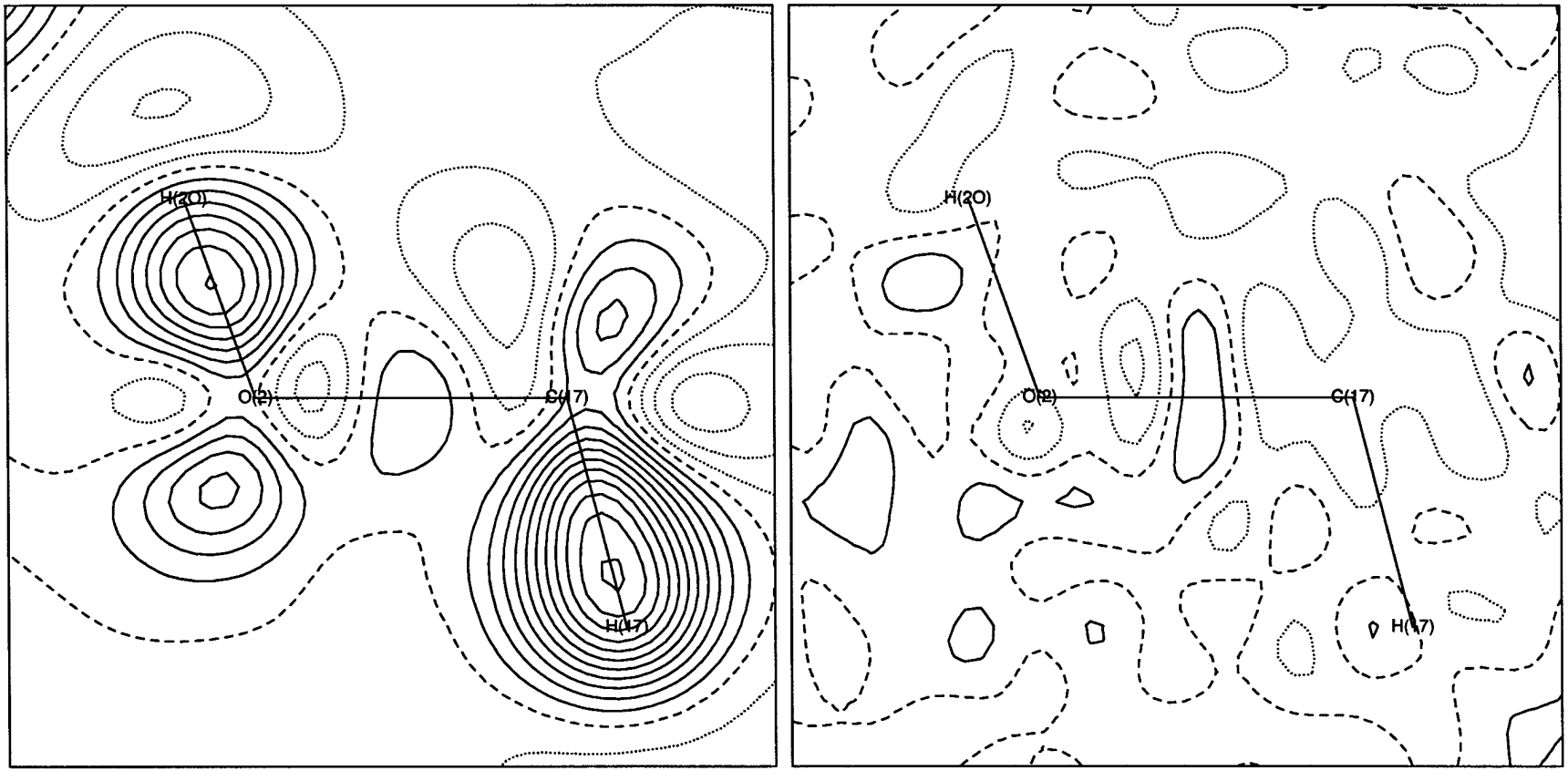

Figure 15. Dynamic model map and residual map in the C17 – O2 – H2O plane of 17β-estradiol•½methanol. Contour intervals are 0.05 eÅ^{-3} with solid lines positive, dashed lines zero, and dotted lines negative.

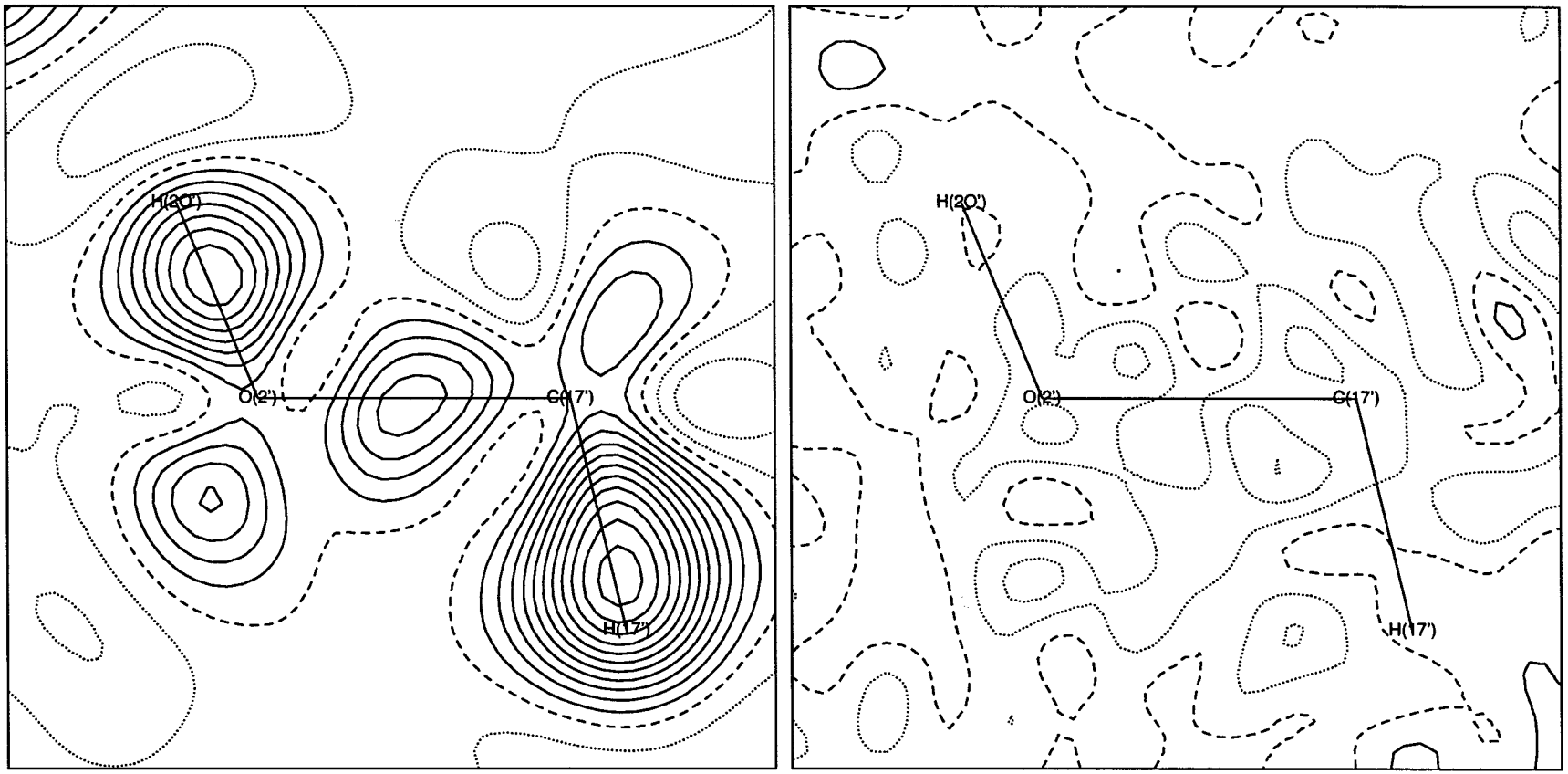

Figure 16. Dynamic model map and residual map in the C17' – O2' – H2O' plane of 17β-estradiol•½methanol. Contour intervals are 0.05 eÅ^{-3} with solid lines positive, dashed lines zero, and dotted lines negative.

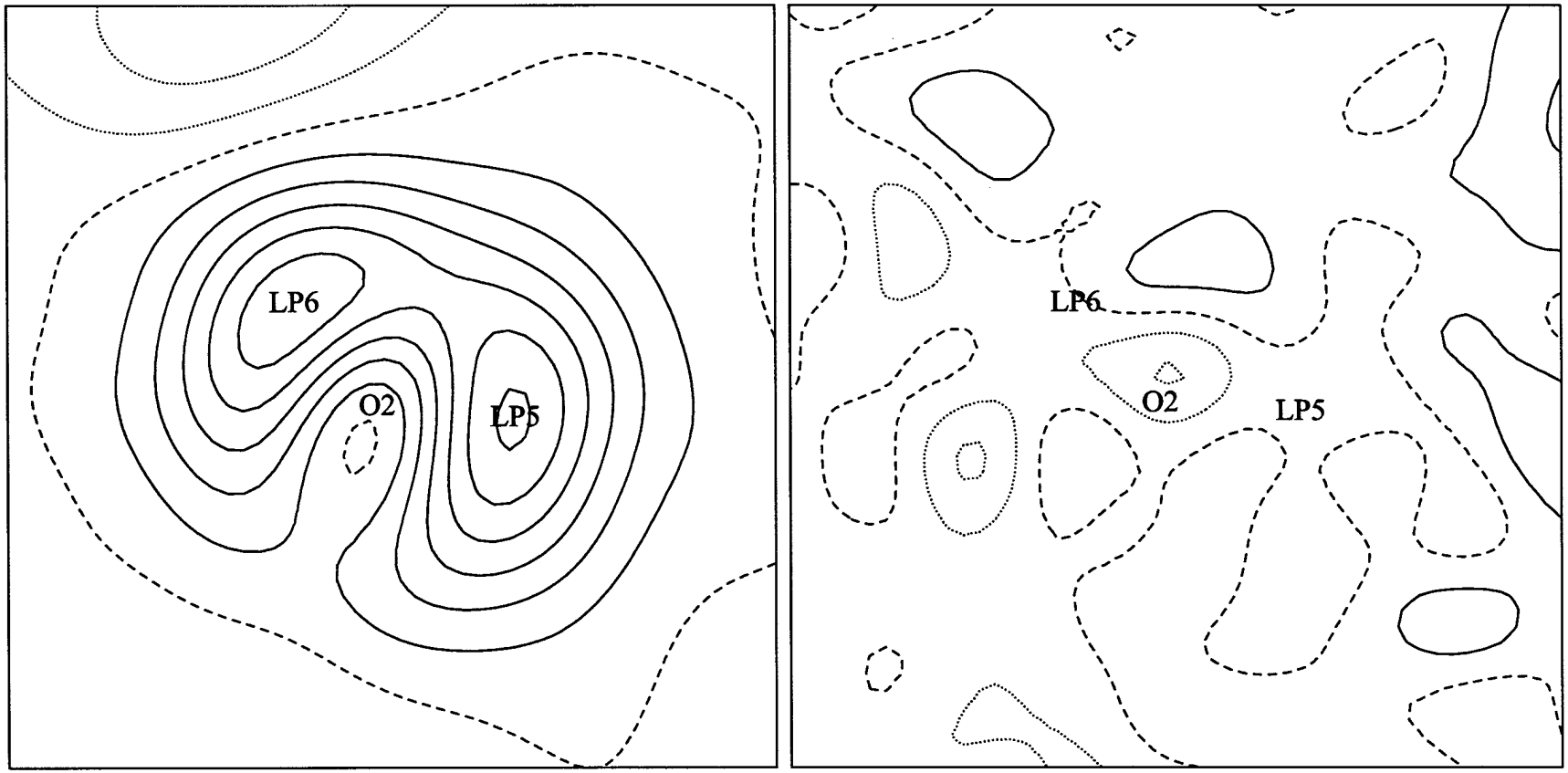

Figure 17. Dynamic model map and residual map in the plane of the lone pairs of O2 of 17β-estradiol•½methanol. Contour intervals are 0.05 e$\mathring{A}^{-3}$ with solid lines positive, dashed lines zero, and dotted lines negative.

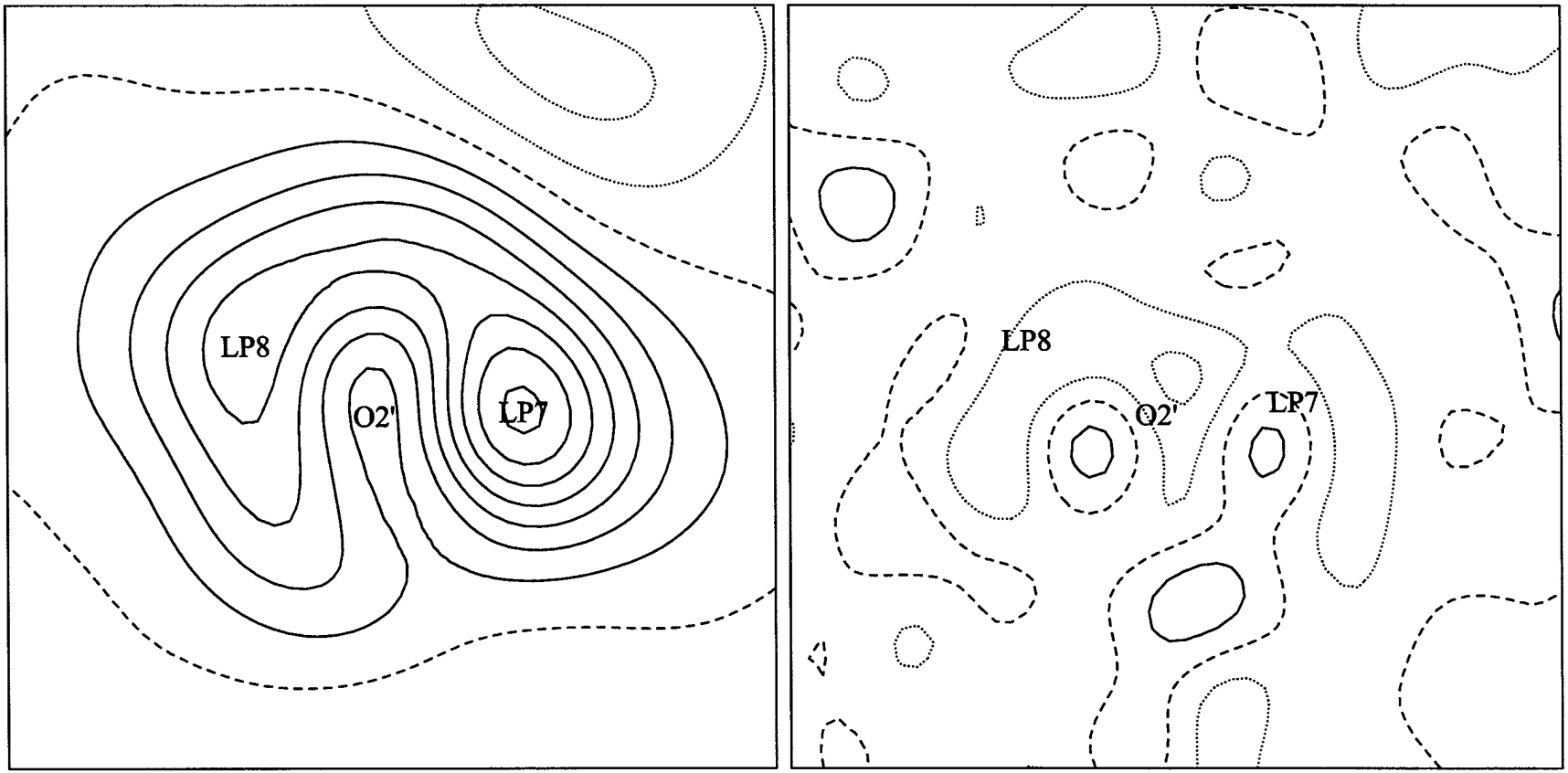

Figure 18. Dynamic model map and residual map in the plane of the lone pairs of O2' of 17β-estradiol•½methanol. Contour intervals are 0.05 e$\AA^{-3}$ with solid lines positive, dashed lines zero, and dotted lines negative.

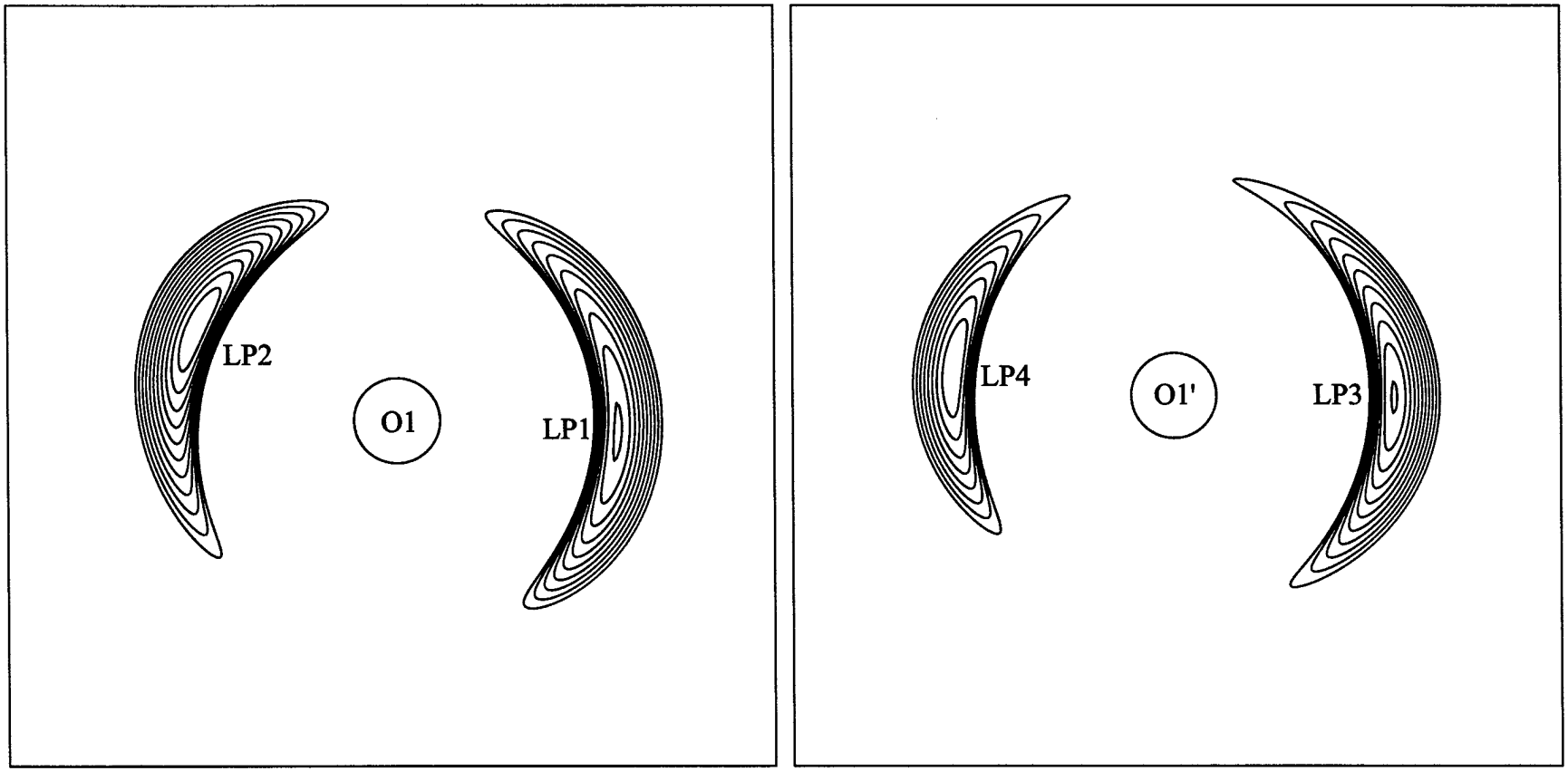

Figure 19. The Laplacian of the total electron density of atoms at rest in the plane of the lone pairs of the O1 and O1' of 17β-estradiol•½methanol. Contour intervals are 5 eÅ^{-5} starting at 80 eÅ^{-5}.

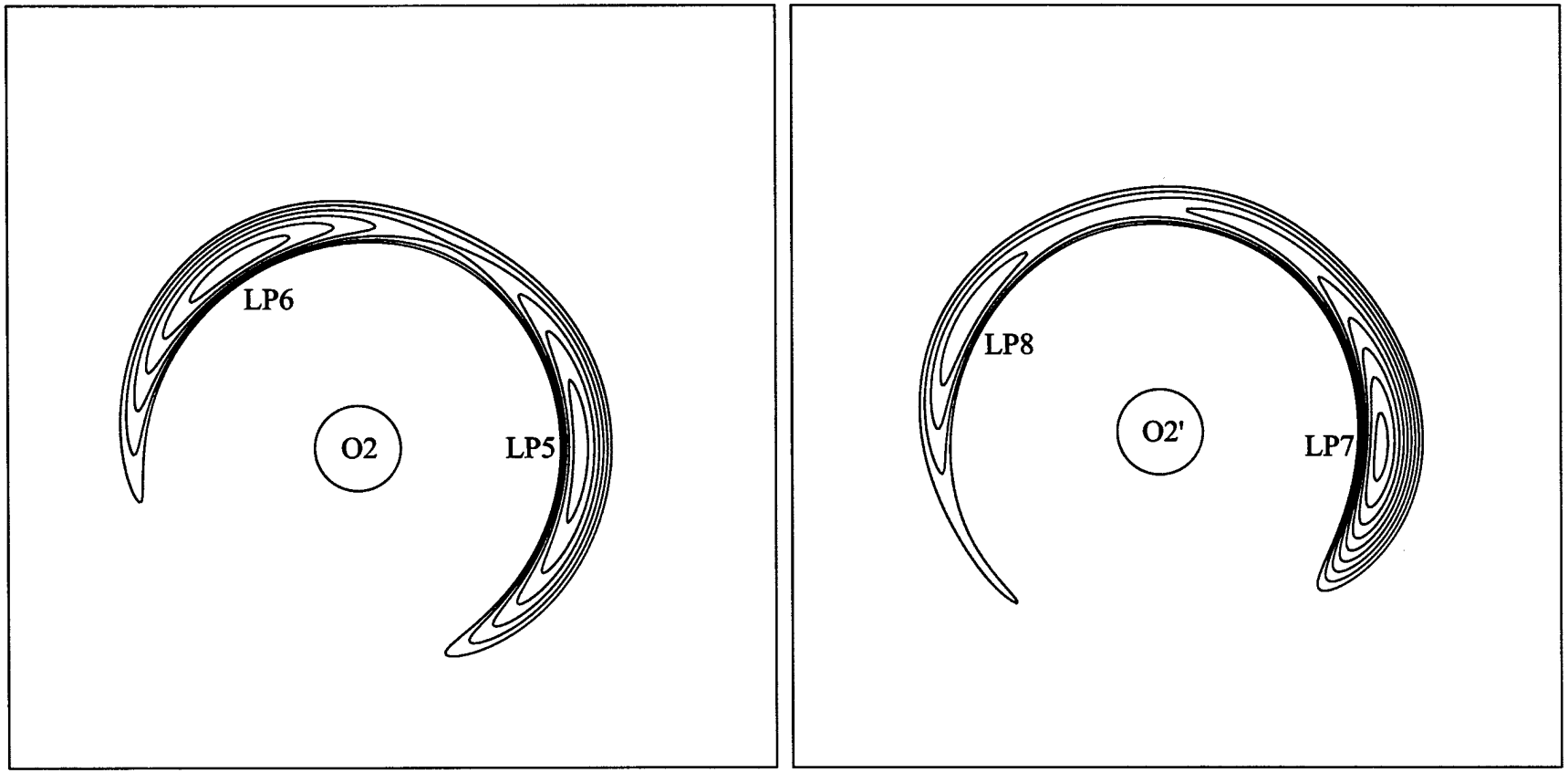

Figure 20. The Laplacian of the total electron density of atoms at rest in the plane of the lone pairs of the O2 and O2' of 17β-estradiol•½methanol. Contour intervals are 5 eÅ^{-5} starting at 90 eÅ^{-5}.

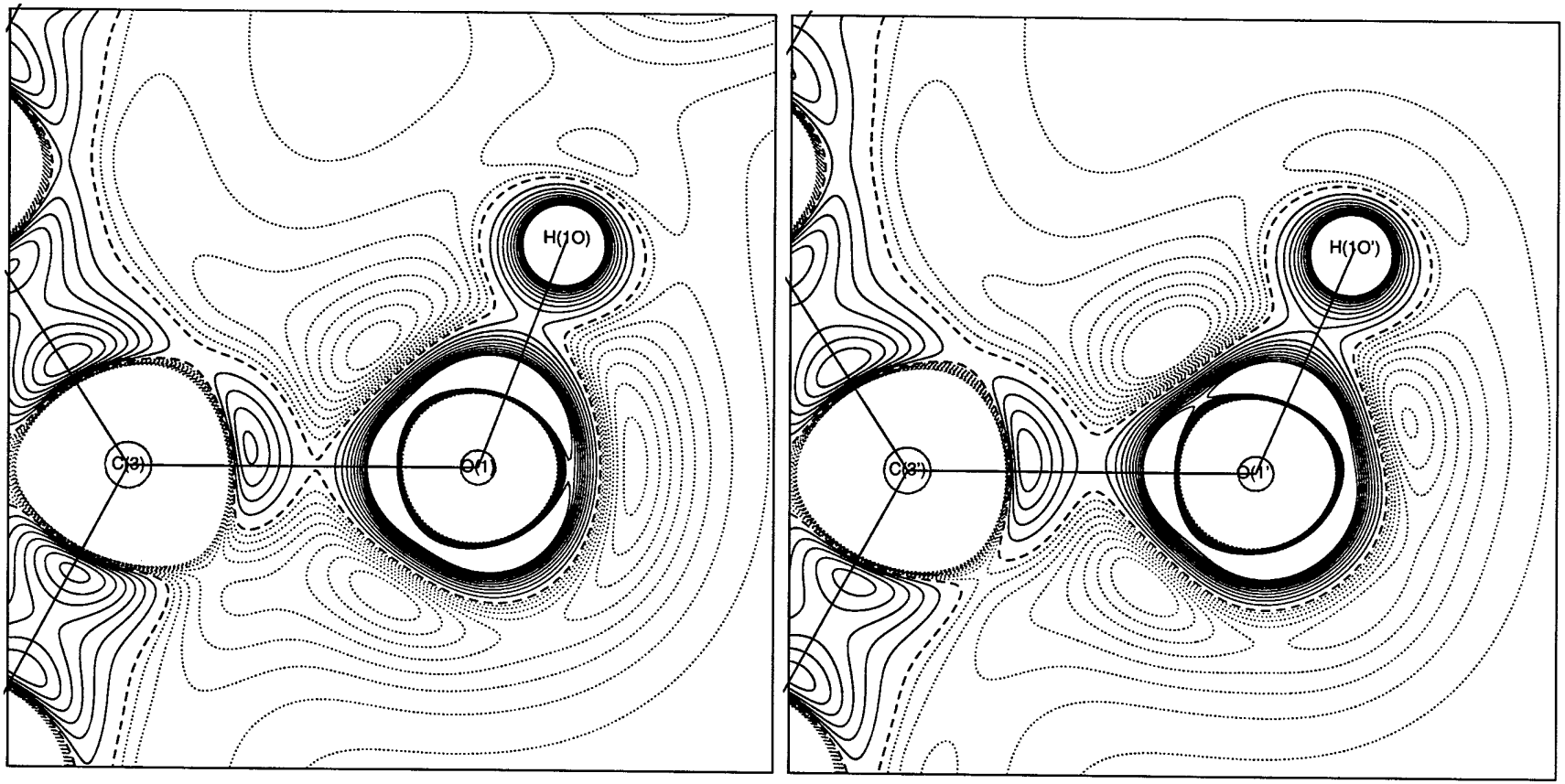

Figure 21. The Laplacian of the total electron density of atoms at rest in the C3–O1–H1O plane and C3'–O1'–H1O' of 17β-estradiol•½methanol. Contour intervals are 5 eÅ^{-5} starting at 5 eÅ^{-5} (solid blue lines), -2 eÅ^{-5} starting at -2 eÅ^{-5} (dotted red lines), and the dashed line plots 0 eÅ^{-5}.

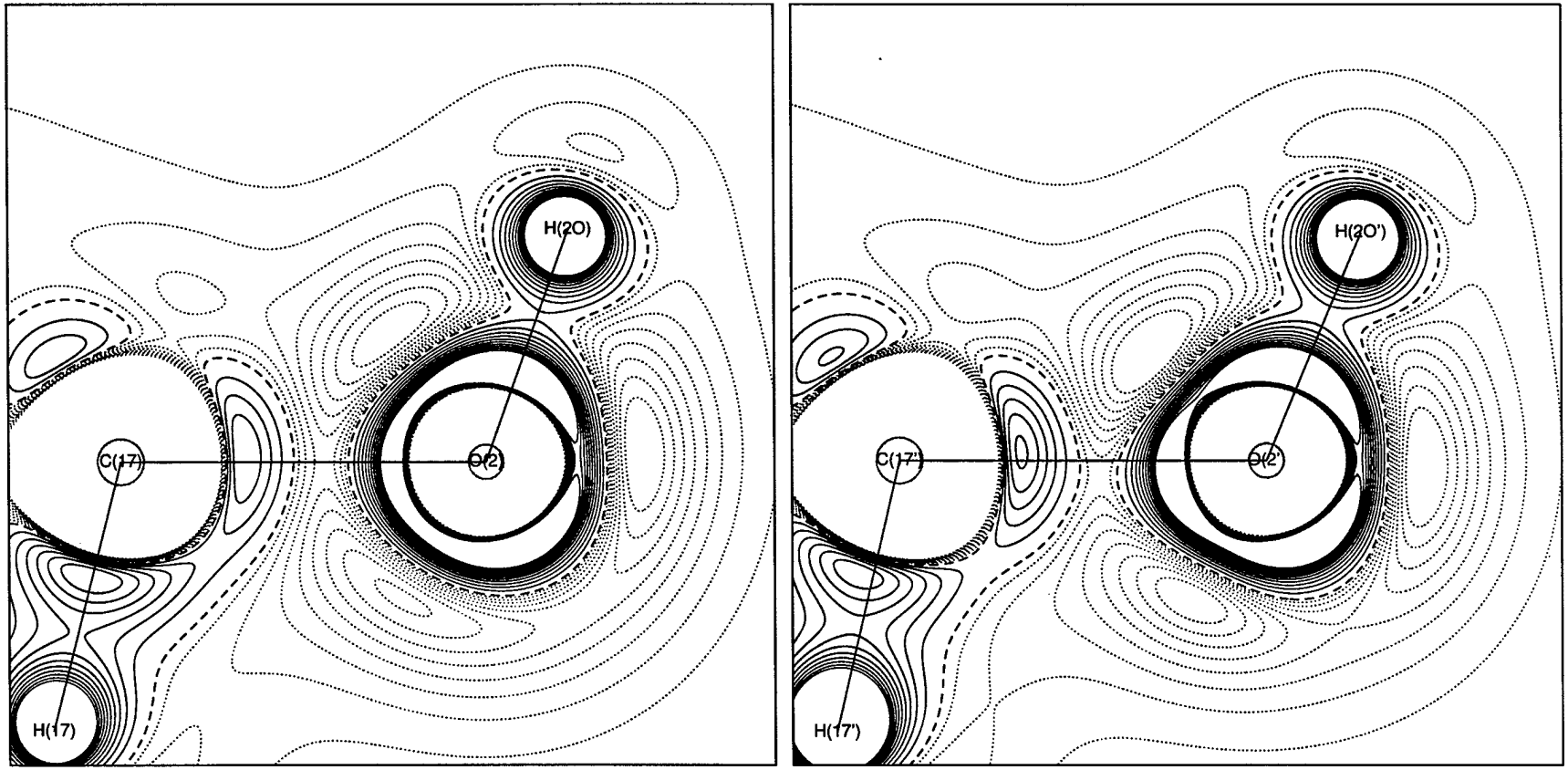

Figure 22. The Laplacian of the total electron density of atoms at rest in the C17–O2–H2O plane and C17'–O2'–H2O' of 17β-estradiol•½methanol. Contour intervals are 5 eÅ^{-5} starting at 5 eÅ^{-5} (solid blue lines), -2 eÅ^{-5} starting at -2 eÅ^{-5} (dotted red lines), and the dashed line plots 0 eÅ^{-5}.

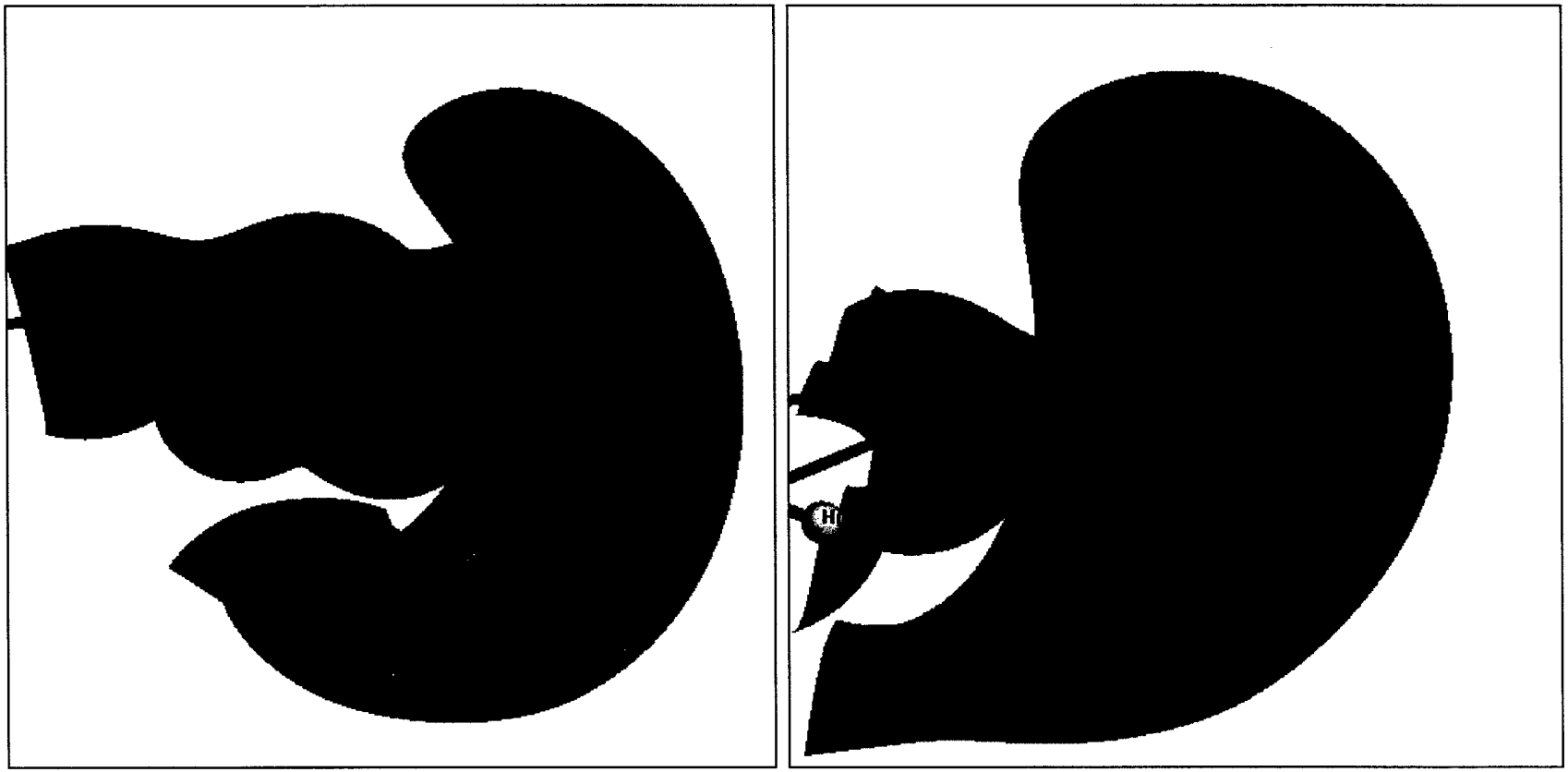

Figure 23. 17β-estradiol•½methanol, molecule 1 C3 hydroxy, red –0.15 eÅ^{-1}, blue 1.0 eÅ^{-1}.

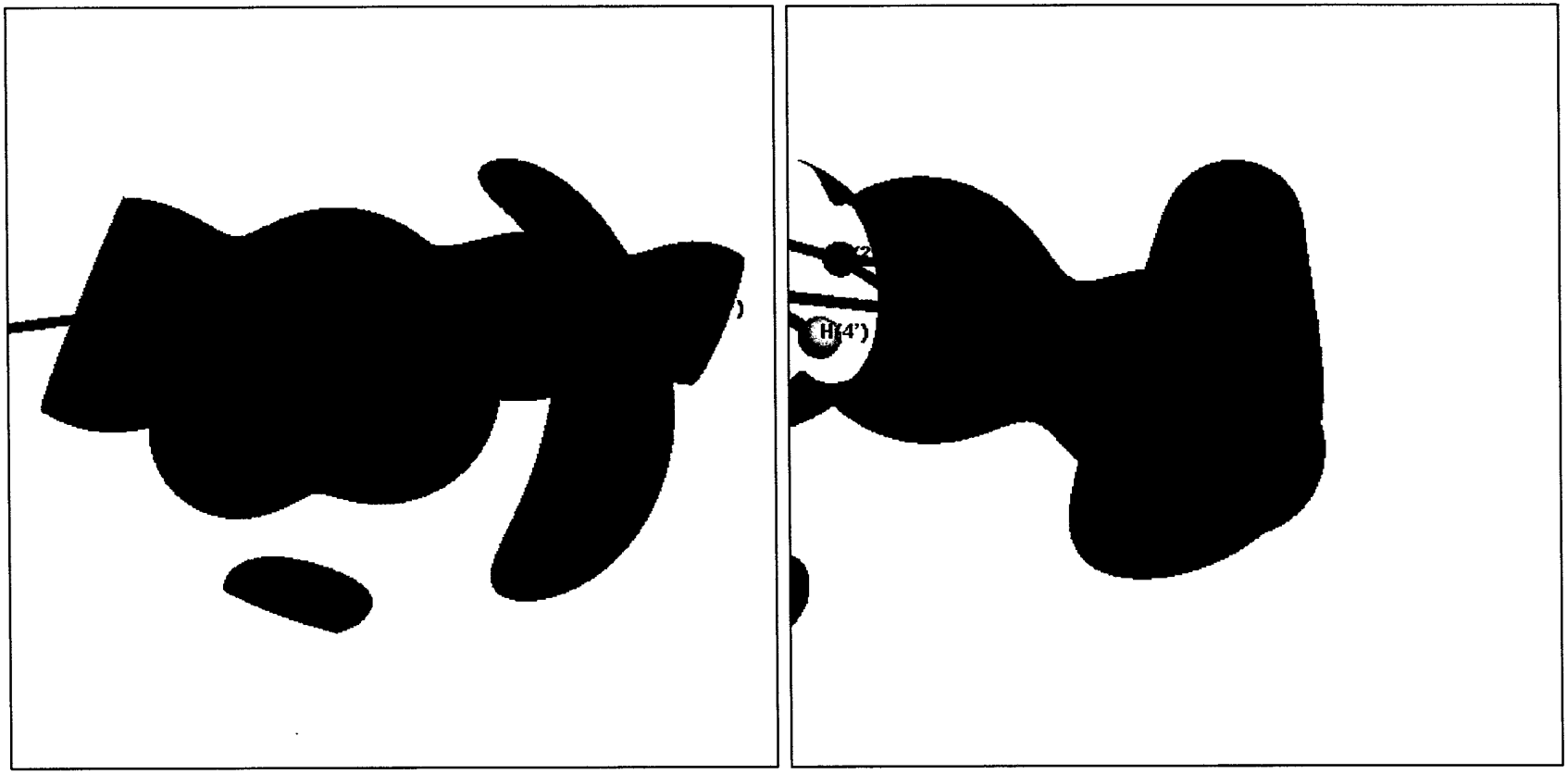

Figure 24. 17β-estradiol•½methanol, molecule 2 C3' hydroxy, red –0.15 eÅ^{-1}, blue 1.0 eÅ^{-1}.

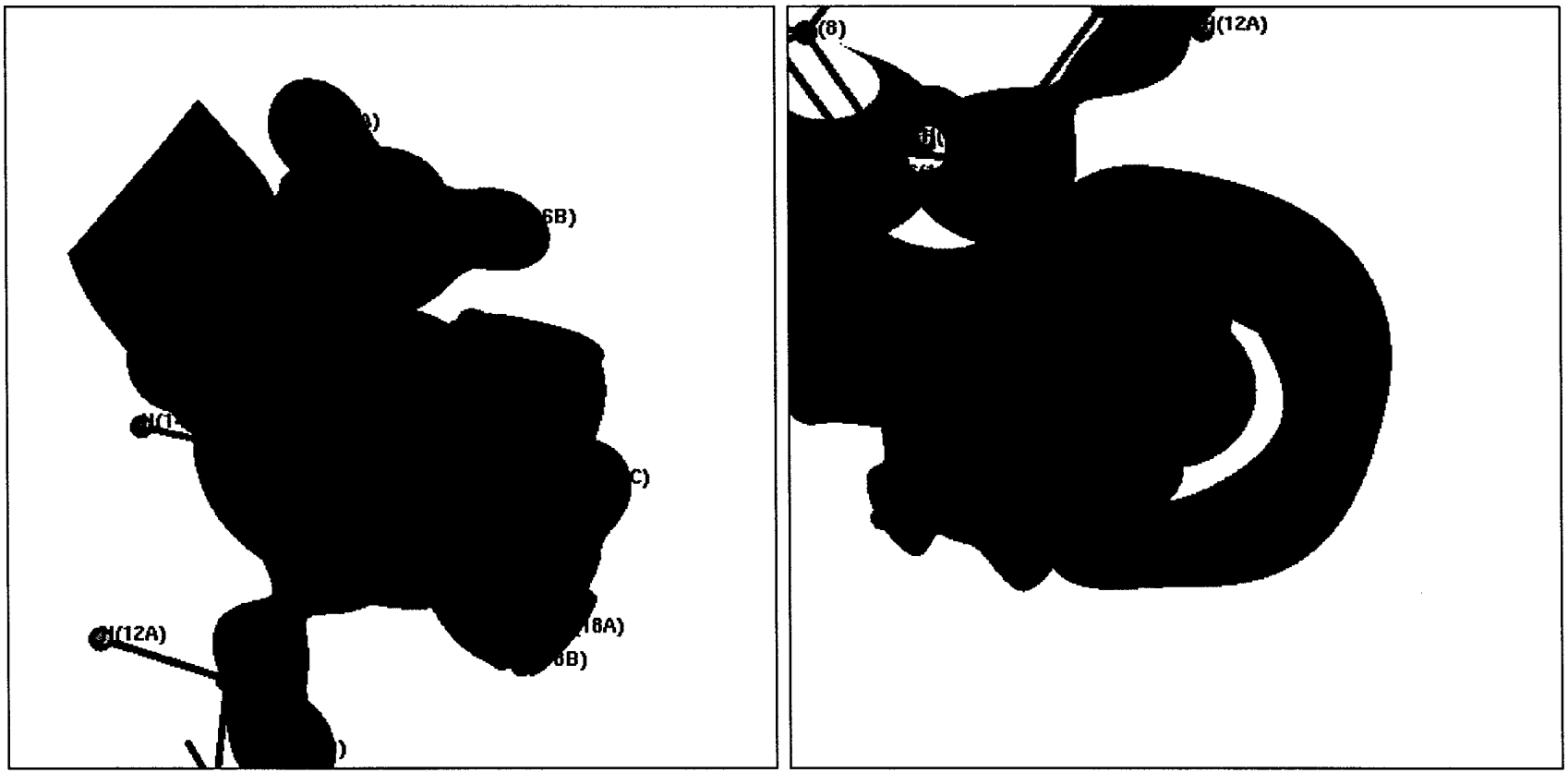

Figure 25. 17β-estradiol•½methanol, molecule 1 C17 hydroxy, red –0.15 eÅ^{-1}, blue 1.0 eÅ^{-1}.

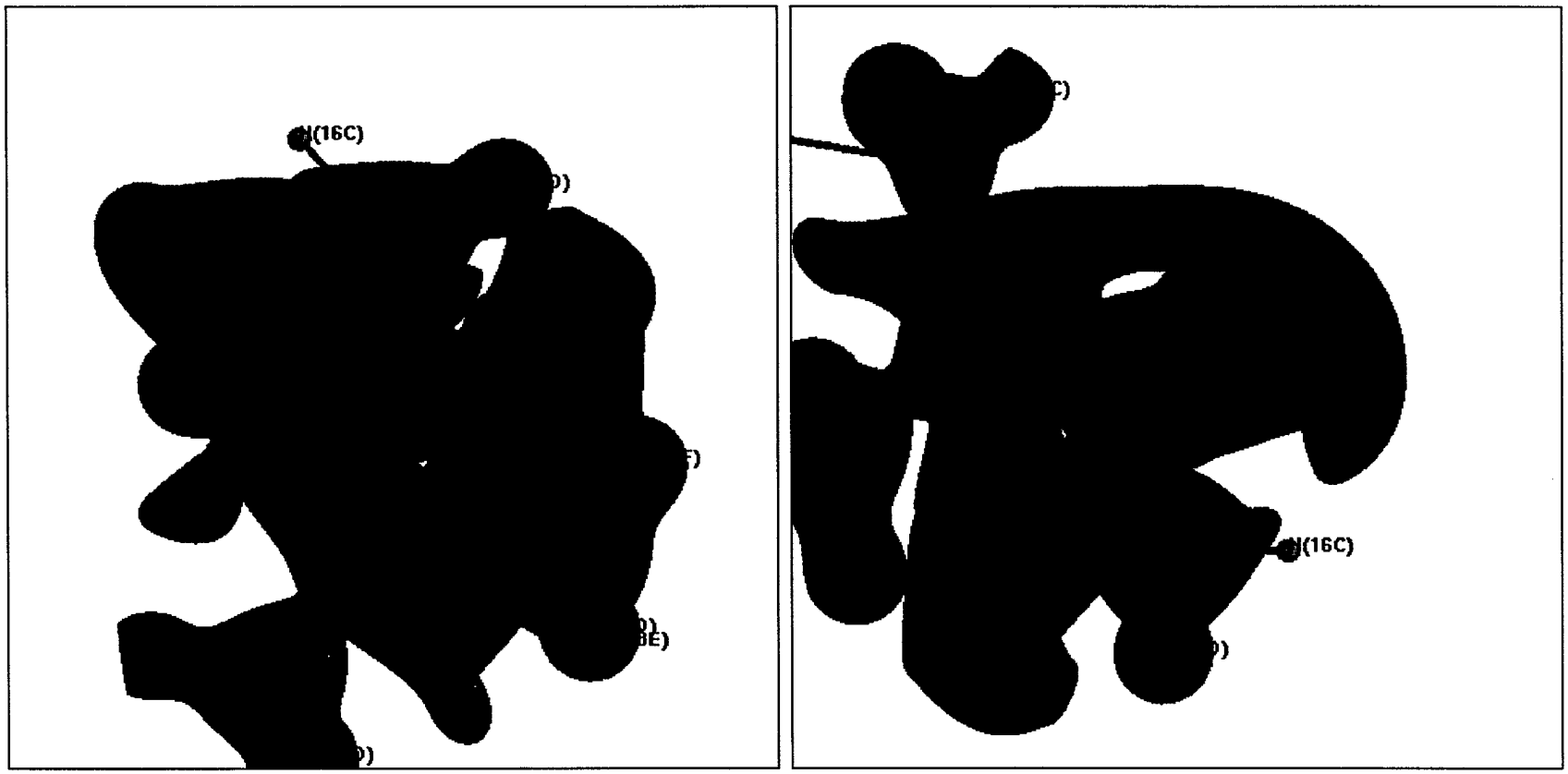

Figure 26. 17β-estradiol•½methanol, molecule 2 C17' hydroxy, red –0.15 eÅ^{-1}, blue 1.0 eÅ^{-1}.

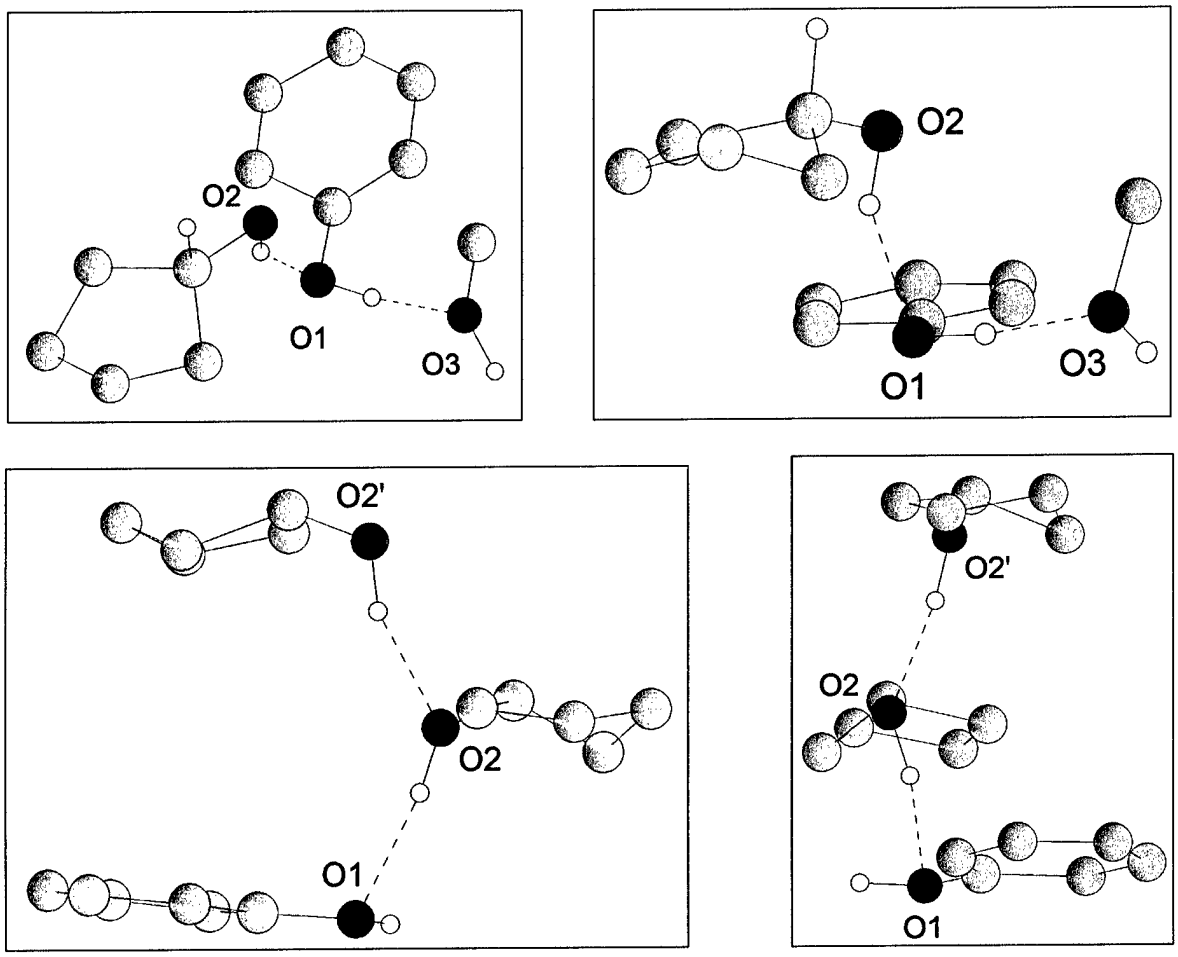

Figure 27. Geometry of hydrogen bonding interactions of molecule 1 of 17β-estradiol•½methanol.

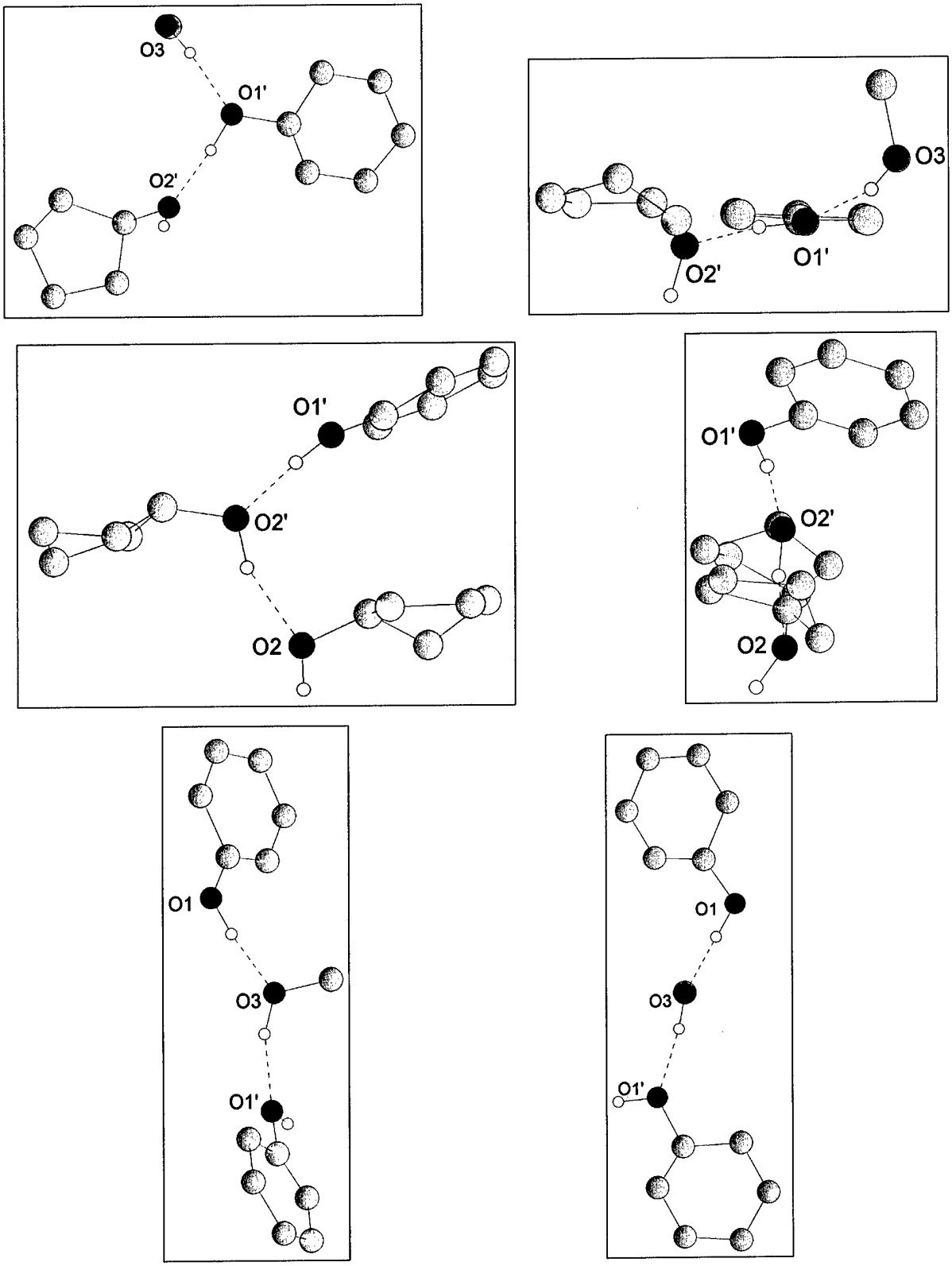

Figure 28. Geometry of hydrogen bonding interactions of molecule 2 and the methanol of 17β-estradiol•½methanol

Appendix I.

Crystal structure and charge density analysis of estrone

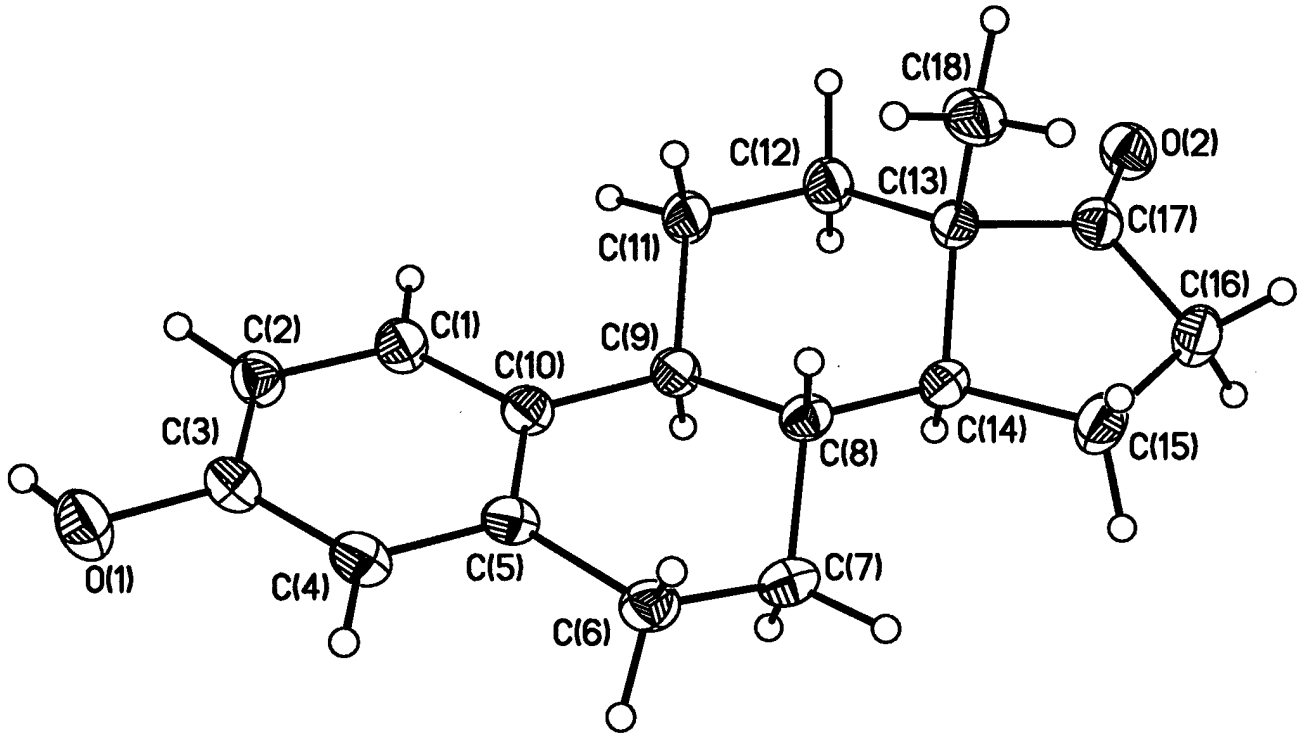

Figure 1a. The estrone molecule with 50% probability thermal ellipsoids for non-hydrogen atoms.

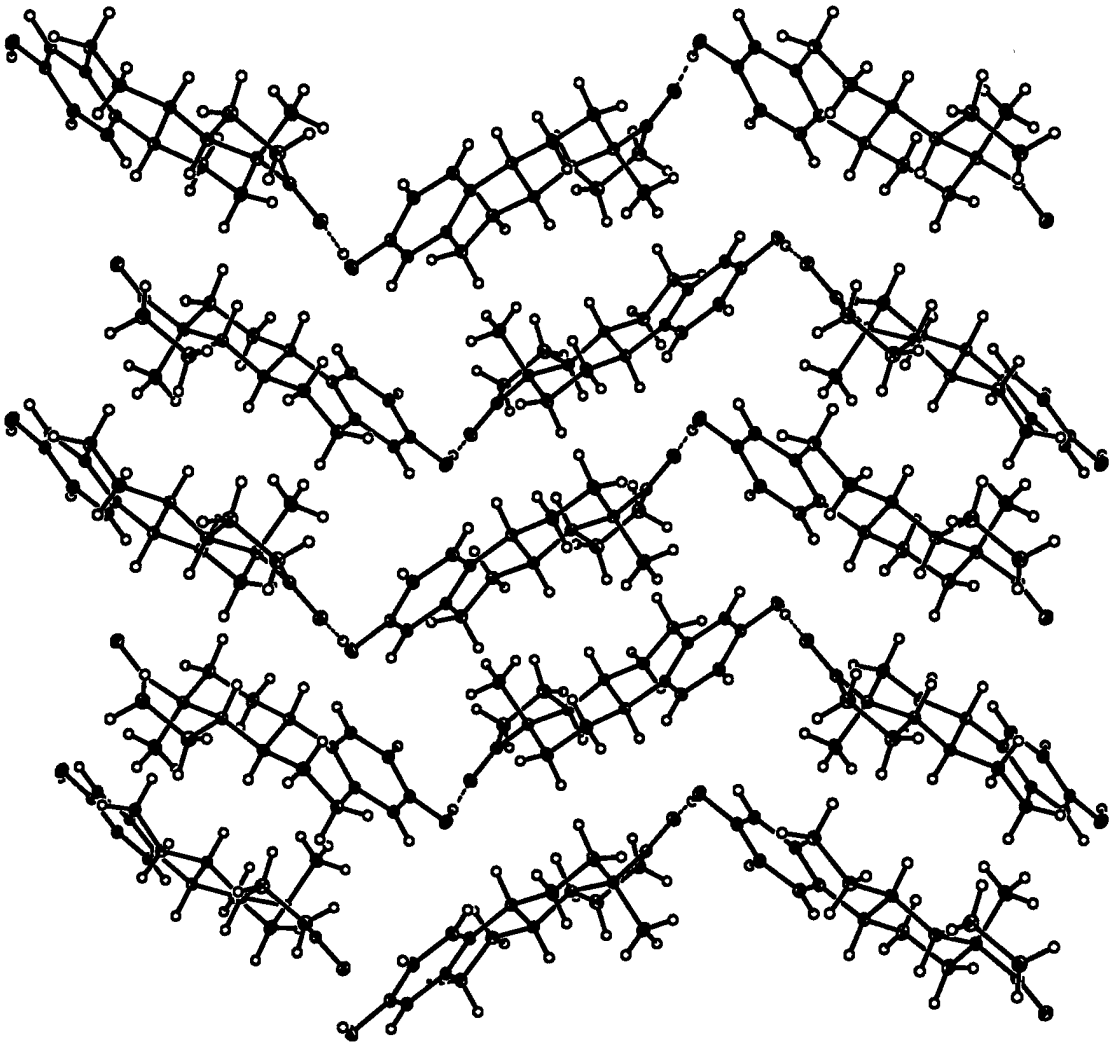

Figure 1b. Packing diagram showing the hydrogen bonds.

Experimental

Compound name:	estrone
Chemical formula:	$C_{18}H_{22}O_2$
Chemical formula weight:	270.36
Crystal density:	1.263
Crystal size, mm	0.2×0.25×0.30
μ, mm^{-1}	0.05
Unit cell parameters:	
a (Å)	7.7618(1)
b (Å)	9.9536(1)
c (Å)	18.4055(1)
V (Å)	1421.97(2)
Z	4
F(000)	584
Space group	$P2_12_12_1$
Temperature:	92.0(2)
Radiation(Å):	Ag K_α (λ=0.56086 Å)
h_{min}/h_{max}	-20/20
k_{min}/k_{max}	-26/25
l_{min}/l_{max}	-48/48
$\theta_{min}/\theta_{max}$	1.75/48.26
Intensity decay	0 %
Total No. of reflections	90695
No. of independent reflections	16278
R_{int}	0.0231
No. of reflections used	8875
Criterion	$I>3\sigma$
Refinement on	F^2
Total No. of parameters	810
Weighting scheme	$w=1/\sigma^2$
Multipole refinement:	
$R(F^2)$	0.0279
$R_w(F^2)$	0.0366
S	1.3337
κ- refinement:	
R	0.0445
R_w	0.0611
S	1.54

Atomic coordinates and U_{iso} in estrone

Atom	x	y	x	U_{iso}
O(1)	-1.34702(4)	-0.80621(3)	-0.31144(2)	0.022
O(2)	-0.81887(4)	-0.28634(3)	0.15628(2)	0.021
C(1)	-1.27691(5)	-0.55423(4)	-0.16813(2)	0.017
C(2)	-1.35941(5)	-0.62550(4)	-0.22323(2)	0.018
C(3)	-1.27233(5)	-0.73037(4)	-0.25798(2)	0.017
C(4)	-1.10329(5)	-0.76064(4)	-0.23767(2)	0.017
C(5)	-1.02040(5)	-0.68873(4)	-0.18217(2)	0.015
C(6)	-0.83709(5)	-0.72801(4)	-0.16266(2)	0.017
C(7)	-0.74637(5)	-0.62131(4)	-0.11661(2)	0.017
C(8)	-0.86413(4)	-0.57930(3)	-0.05415(2)	0.014
C(9)	-1.02082(5)	-0.50316(4)	-0.08568(2)	0.015
C(10)	-1.10798(5)	-0.58421(4)	-0.14580(2)	0.015
C(11)	-1.14594(5)	-0.45811(4)	-0.02538(2)	0.019
C(12)	-1.05678(5)	-0.37607(4)	0.03510(2)	0.019
C(13)	-0.90195(5)	-0.45307(4)	0.06482(2)	0.015
C(14)	-0.77799(5)	-0.48930(4)	0.00219(2)	0.015
C(15)	-0.61274(5)	-0.53505(4)	0.04134(2)	0.020
C(16)	-0.59941(5)	-0.43575(4)	0.10593(2)	0.021
C(17)	-0.78054(5)	-0.37816(4)	0.11509(2)	0.017
C(18)	-0.96009(6)	-0.57650(4)	0.10964(2)	0.022
H(1A)	-1.4610(9)	-0.7709(7)	-0.3207(3)	0.038(2)
H(1)	-1.3493(8)	-0.4749(6)	-0.1419(3)	0.049(2)
H(2)	-1.4904(9)	-0.6010(7)	-0.2387(3)	0.045(2)
H(4)	-1.0358(9)	-0.8413(7)	-0.2651(4)	0.052(2)
H(6A)	-0.8420(9)	-0.8227(6)	-0.1328(3)	0.054(2)
H(6B)	-0.7634(8)	-0.7498(7)	-0.2118(3)	0.052(2)
H(7A)	-0.6238(8)	-0.6610(6)	-0.0970(3)	0.057(2)
H(7B)	-0.7152(8)	-0.5326(6)	-0.1490(3)	0.049(2)
H(8)	-0.9113(8)	-0.6713(7)	-0.0278(3)	0.052(2)
H(9)	-0.9648(8)	-0.4117(6)	-0.1094(3)	0.052(2)
H(11A)	-1.2105(8)	-0.5456(7)	-0.0021(3)	0.043(2)
H(11B)	-1.2491(9)	-0.3978(7)	-0.0491(4)	0.054(2)
H(12A)	-1.1501(8)	-0.3501(6)	0.0772(3)	0.049(2)
H(12B)	-1.0124(8)	-0.2810(6)	0.0121(3)	0.047(2)
H(14)	-0.7469(7)	-0.3938(7)	-0.0248(3)	0.048(2)
H(15A)	-0.6236(9)	-0.6387(7)	0.0602(3)	0.051(2)
H(15B)	-0.5003(10)	-0.5324(7)	0.0057(4)	0.056(2)
H(16A)	-0.5572(9)	-0.4816(7)	0.1568(3)	0.052(2)
H(16B)	-0.5107(9)	-0.3521(7)	0.0974(4)	0.063(2)
H(18A)	-1.0328(8)	-0.6461(6)	0.0787(3)	0.057(2)
H(18B)	-1.0397(8)	-0.5423(7)	0.1525(3)	0.058(2)
H(18C)	-0.8571(9)	-0.6322(7)	0.1324(3)	0.065(2)

U_{ij} values

Atom	U_{11}	U_{22}	U_{33}	U_{12}	U_{13}	U_{23}
O(1)	0.0251(1)	0.0223(1)	0.0180(1)	0.0028(1)	-0.0043(1)	-0.0046(1)
O(2)	0.0215(1)	0.0207(1)	0.0200(1)	-0.0004(1)	-0.0016(1)	-0.0030(1)
C(1)	0.0162(1)	0.0177(1)	0.0170(1)	0.0038(1)	-0.0016(1)	-0.0022(1)
C(2)	0.0175(2)	0.0190(1)	0.0164(1)	0.0031(1)	-0.0018(1)	-0.0018(1)
C(3)	0.0194(2)	0.0174(1)	0.0132(1)	0.0020(1)	-0.0008(1)	-0.0007(1)
C(4)	0.0192(2)	0.0177(1)	0.0142(1)	0.0034(1)	0.0007(1)	-0.0009(1)
C(5)	0.0156(1)	0.0164(1)	0.0137(1)	0.0024(1)	0.0014(1)	0.0004(1)
C(6)	0.0157(2)	0.0181(1)	0.0176(1)	0.0035(1)	0.0020(1)	-0.0009(1)
C(7)	0.0140(1)	0.0175(1)	0.0198(1)	0.0014(1)	0.0032(1)	0.0004(1)
C(8)	0.0130(1)	0.0143(1)	0.0152(1)	0.0011(1)	0.0011(1)	0.0013(1)
C(9)	0.0146(1)	0.0153(1)	0.0144(1)	0.0028(1)	0.0001(1)	-0.0002(1)
C(10)	0.0150(1)	0.0153(1)	0.0146(1)	0.0031(1)	0.0002(1)	-0.0003(1)
C(11)	0.0140(1)	0.0254(2)	0.0171(1)	0.0049(1)	-0.0015(1)	-0.0043(1)
C(12)	0.0175(2)	0.0228(2)	0.0177(2)	0.0061(1)	-0.0021(1)	-0.0045(1)
C(13)	0.0140(1)	0.0160(1)	0.0147(1)	0.0000(1)	-0.0003(1)	0.0016(1)
C(14)	0.0129(1)	0.0154(1)	0.0163(1)	0.0000(1)	0.0003(1)	0.0015(1)
C(15)	0.0146(2)	0.0231(2)	0.0237(2)	0.0031(1)	-0.0030(1)	-0.0022(1)
C(16)	0.0158(2)	0.0238(2)	0.0224(2)	0.0000(1)	-0.0040(1)	-0.0015(1)
C(17)	0.0163(1)	0.0174(1)	0.0166(1)	-0.0013(1)	-0.0011(1)	0.0016(1)
C(18)	0.0243(2)	0.0222(2)	0.0182(2)	-0.0070(1)	0.0012(1)	0.0037(1)

Bond lengths

O(1)	C(3)	1.3691(4)
O(1)	H(1A)	0.967(7)
O(2)	C(17)	1.2242(5)
C(1)	C(2)	1.3934(5)
C(1)	C(10)	1.4062(5)
C(1)	H(1)	1.083(6)
C(2)	C(3)	1.3984(5)
C(2)	H(2)	1.083(7)
C(3)	C(4)	1.3971(5)
C(4)	C(5)	1.4035(5)
C(4)	H(4)	1.083(7)
C(5)	C(6)	1.5186(5)
C(5)	C(10)	1.4115(5)
C(6)	C(7)	1.5304(5)
C(6)	H(6A)	1.092(6)
C(6)	H(6B)	1.092(6)
C(7)	C(8)	1.5270(5)
C(7)	H(7A)	1.092(6)
C(7)	H(7B)	1.092(6)
C(8)	C(14)	1.5247(5)
C(8)	H(8)	1.099(7)
C(9)	C(10)	1.5274(5)
C(9)	H(9)	1.099(6)
C(11)	H(11A)	1.092(7)
C(11)	H(11B)	1.092(7)
C(12)	C(13)	1.5268(5)
C(12)	H(12A)	1.092(6)
C(12)	H(12B)	1.092(6)
C(13)	C(17)	1.5165(5)
C(14)	H(14)	1.099(7)
C(15)	H(15A)	1.092(7)
C(15)	H(15B)	1.092(7)
C(16)	C(17)	1.5276(5)
C(16)	H(16A)	1.092(7)
C(16)	H(16B)	1.092(7)
C(18)	H(18A)	1.059(6)
C(18)	H(18B)	1.059(6)
C(18)	H(18C)	1.059(7)

Bond angles

C(3) - O(1) - H(1A)	108.3(5)
C(2) - C(1) - C(10)	122.2(1)
C(2) - C(1) - H(1)	117.2(4)
C(10) - C(1) - H(1)	120.5(4)
C(1) - C(2) - C(3)	119.4(1)
C(1) - C(2) - H(2)	120.5(4)
C(3) - C(2) - H(2)	120.1(4)
O(1) - C(3) - C(2)	122.4(1)
O(1) - C(3) - C(4)	118.1(1)
C(2) - C(3) - C(4)	119.5(1)
C(3) - C(4) - C(5)	121.0(1)
C(3) - C(4) - H(4)	119.3(4)
C(5) - C(4) - H(4)	119.7(4)
C(4) - C(5) - C(6)	118.1(1)
C(4) - C(5) - C(10)	120.0(1)
C(6) - C(5) - C(10)	121.9(1)
C(5) - C(6) - C(7)	112.5(1)
C(5) - C(6) - H(6A)	108.0(4)
C(5) - C(6) - H(6B)	110.2(4)
C(7) - C(6) - H(6A)	109.7(4)
C(7) - C(6) - H(6B)	110.8(4)
H(6A) - C(6) - H(6B)	105.3(5)
C(6) - C(7) - C(8)	109.4(1)
C(6) - C(7) - H(7A)	109.5(4)
C(6) - C(7) - H(7B)	111.2(4)
C(8) - C(7) - H(7A)	111.8(4)
C(8) - C(7) - H(7B)	108.8(4)
H(7A) - C(7) - H(7B)	106.3(5)
C(7) - C(8) - C(14)	114.2(1)
C(7) - C(8) - H(8)	107.7(4)
C(14) - C(8) - H(8)	109.6(4)
C(10) - C(9) - H(9)	108.9(4)
C(1) - C(10) - C(5)	117.8(1)
C(1) - C(10) - C(9)	120.8(1)
C(5) - C(10) - C(9)	121.3(1)
H(11A) - C(11) - H(11B)	105.0(5)
C(13) - C(12) - H(12A)	112.7(4)
C(13) - C(12) - H(12B)	109.0(4)
H(12A) - C(12) - H(12B)	106.2(5)
C(12) - C(13) - C(17)	117.4(1)
C(8) - C(14) - H(14)	107.3(3)
H(15A) - C(15) - H(15B)	106.0(6)
C(17) - C(16) - H(16A)	109.8(4)
C(17) - C(16) - H(16B)	108.1(4)
H(16A) - C(16) - H(16B)	104.6(5)
O(2) - C(17) - C(13)	126.4(1)
O(2) - C(17) - C(16)	124.9(1)
C(13) - C(17) - C(16)	108.7(1)
H(18A) - C(18) - H(18B)	107.5(5)
H(18A) - C(18) - H(18C)	105.8(5)
H(18B) - C(18) - H(18C)	108.3(5)

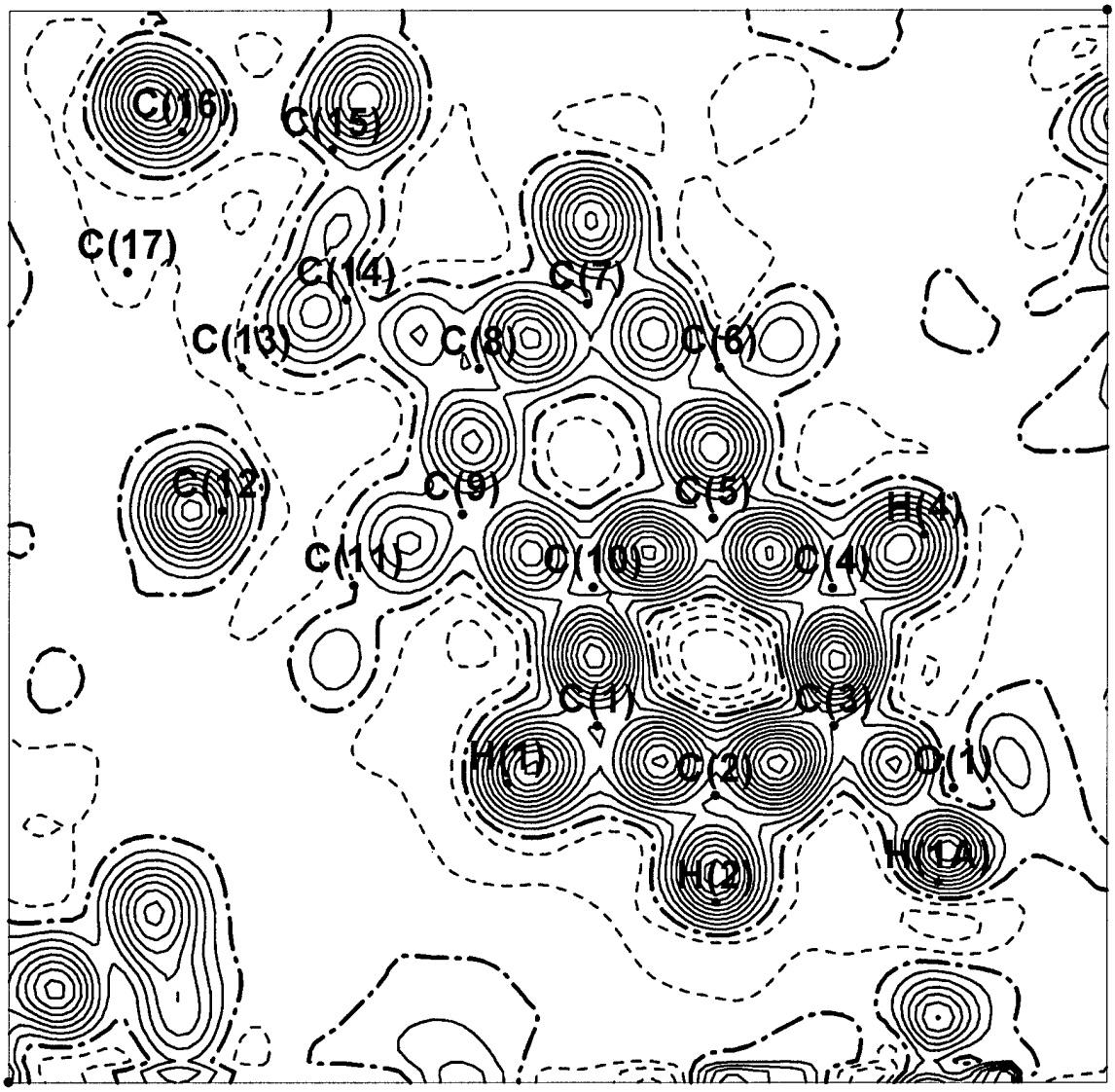

Figure 2a. Dynamic Fourier multipole map in the aromatic ring plane.

Contour interval is 0.05 eÅ^{-3}.

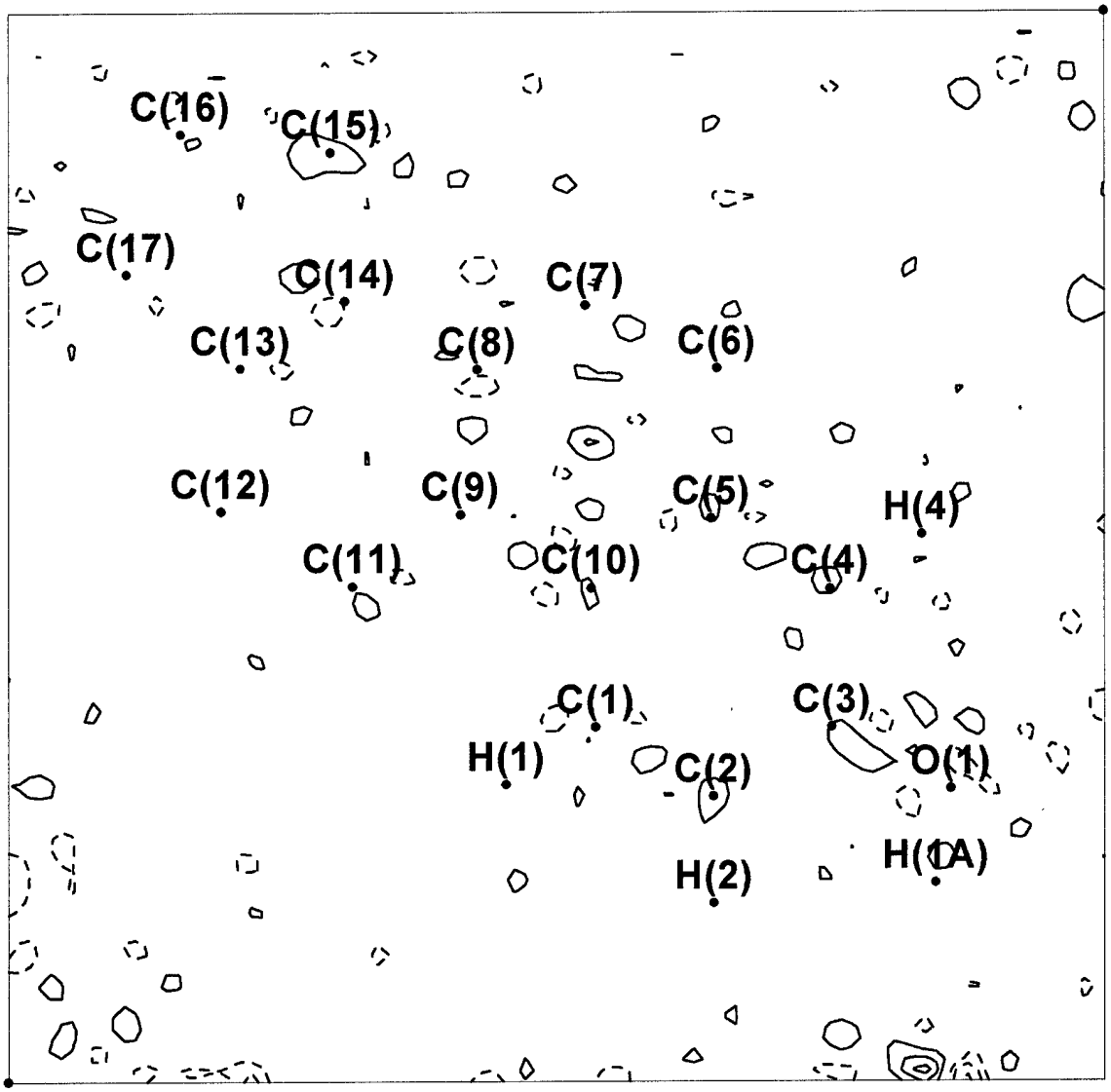

Figure 2b. Residual map in the aromatic ring plane.

Contour interval is 0.05 eÅ^{-3}.

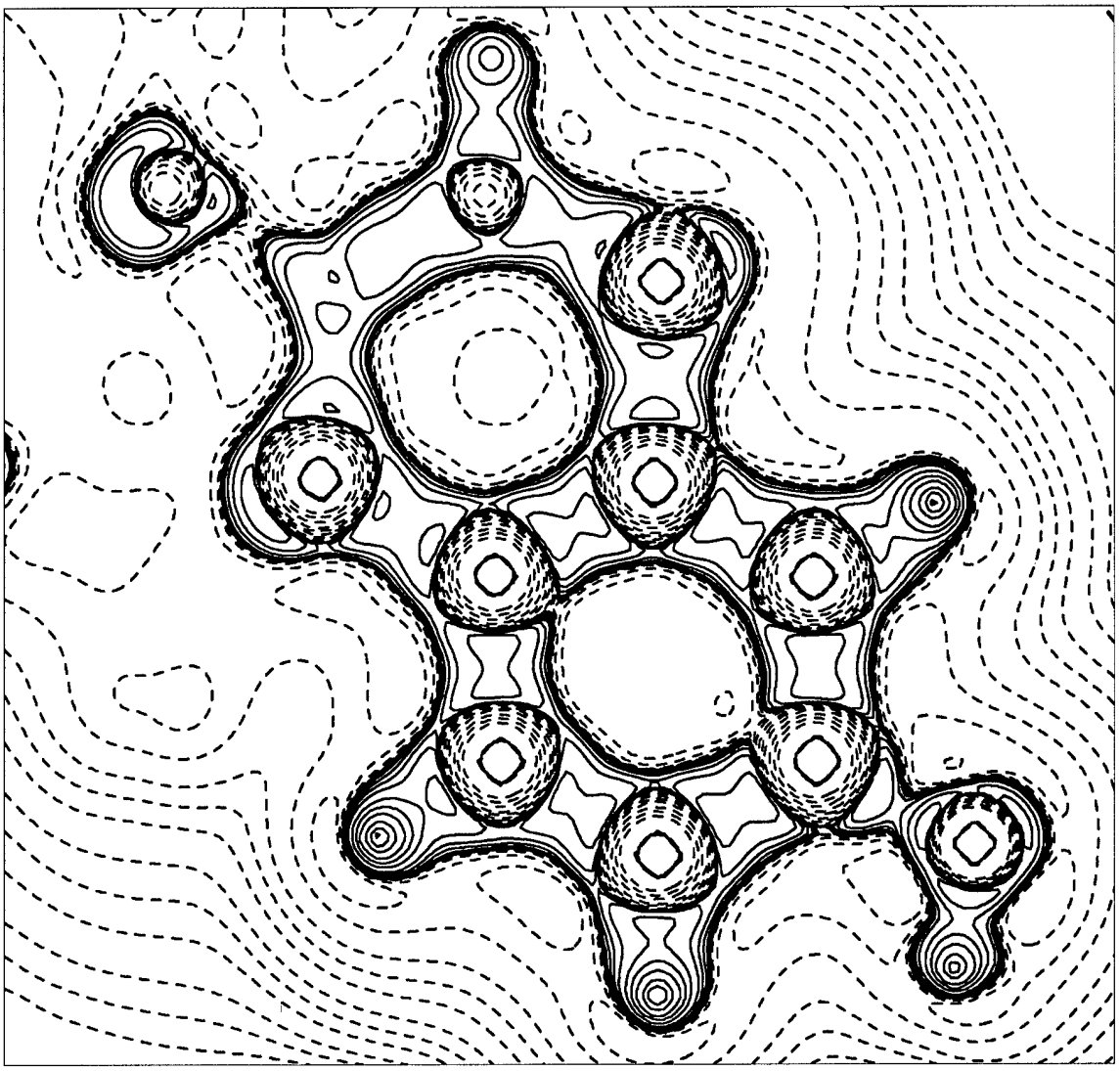

Figure 2c. The Laplacian of the electron density in the aromatic ring plane. Contour interval is 2,4,8 x 10^{-3-+3} eÅ^{-5}.

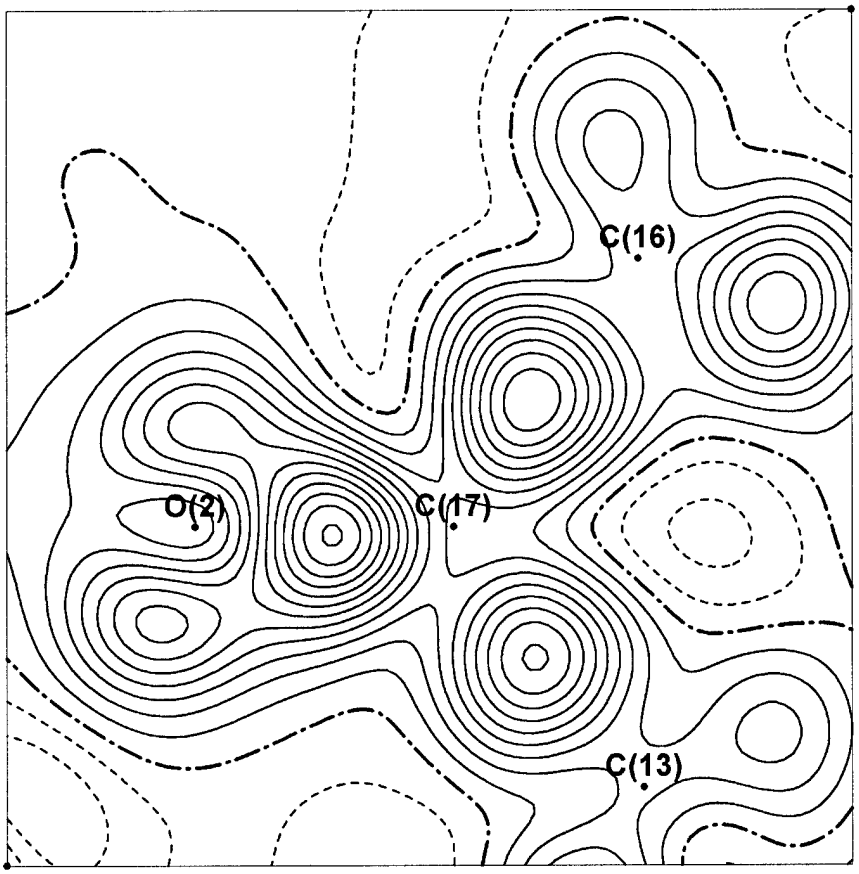

Figure 3a. Dynamic Fourier multipole electron density map in the O(2)-C(17)-C(16) plane. Contour interval is 0.05 eÅ^{-3}.

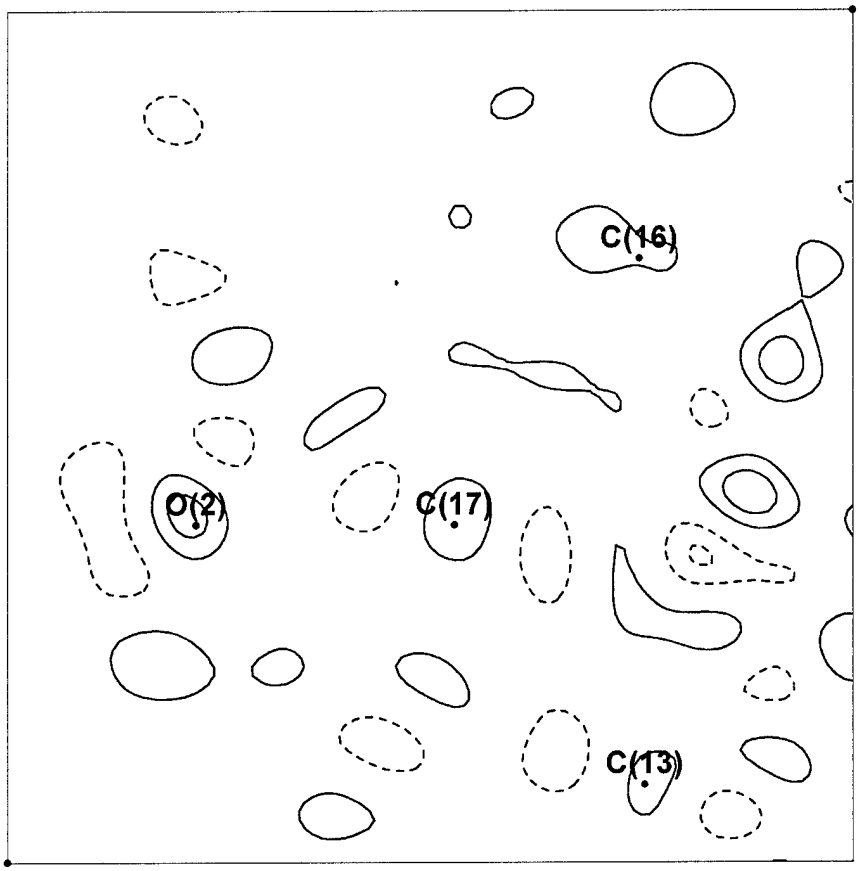

Figure 3b. The residual map in the O(2)-C(17)-C(16) plane.
Contour interval is 0.05 eÅ^{-3}.

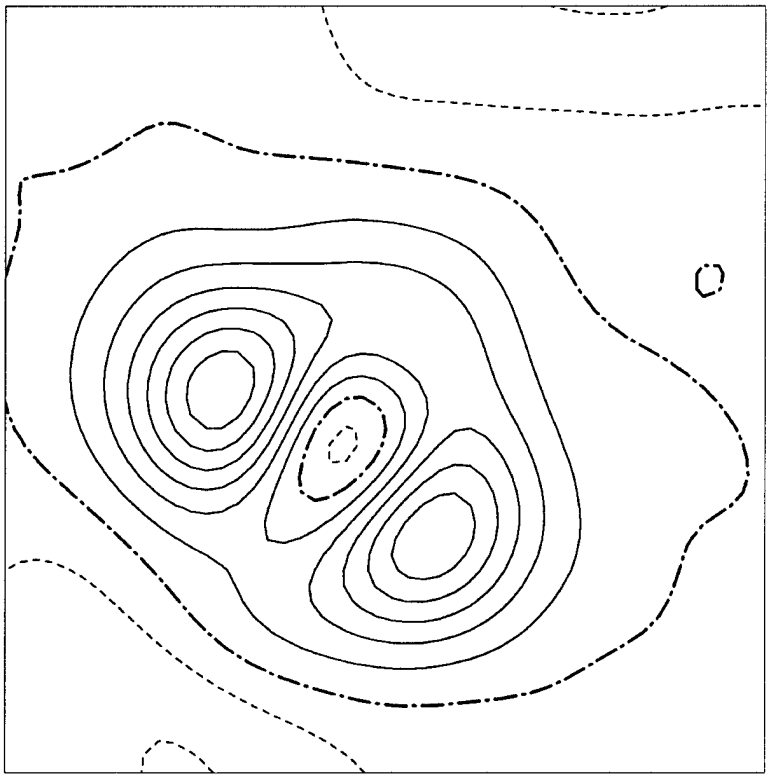

Figure 4a. Dynamic Fourier multipole electron density map showing the O(1) lone pairs. Contour interval is 0.05 eÅ^{-3}.

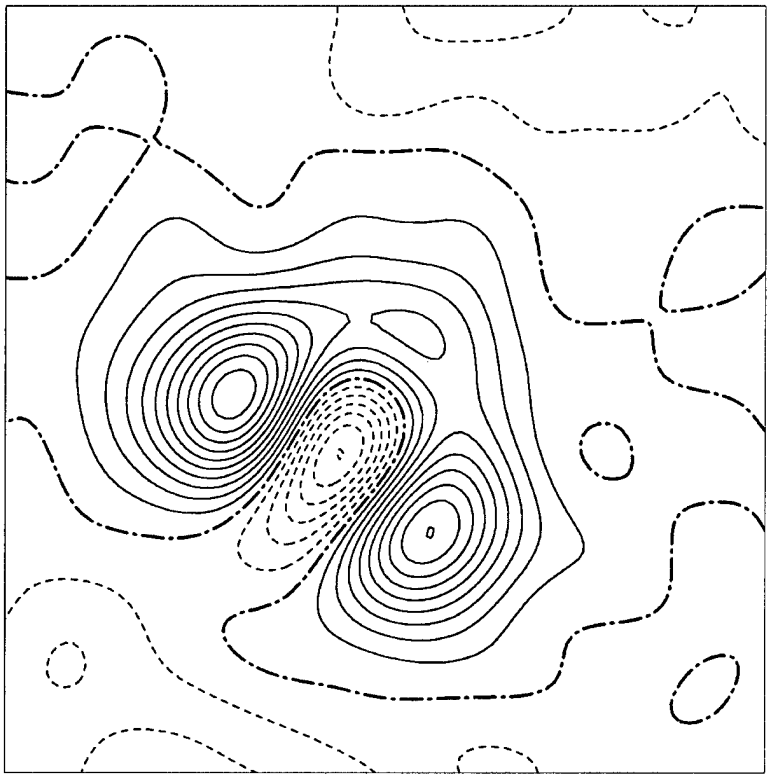

Figure 4b. Static Fourier multipole electron density map showing the O(1) lone pairs. Contour interval is 0.05 eÅ^{-3}.

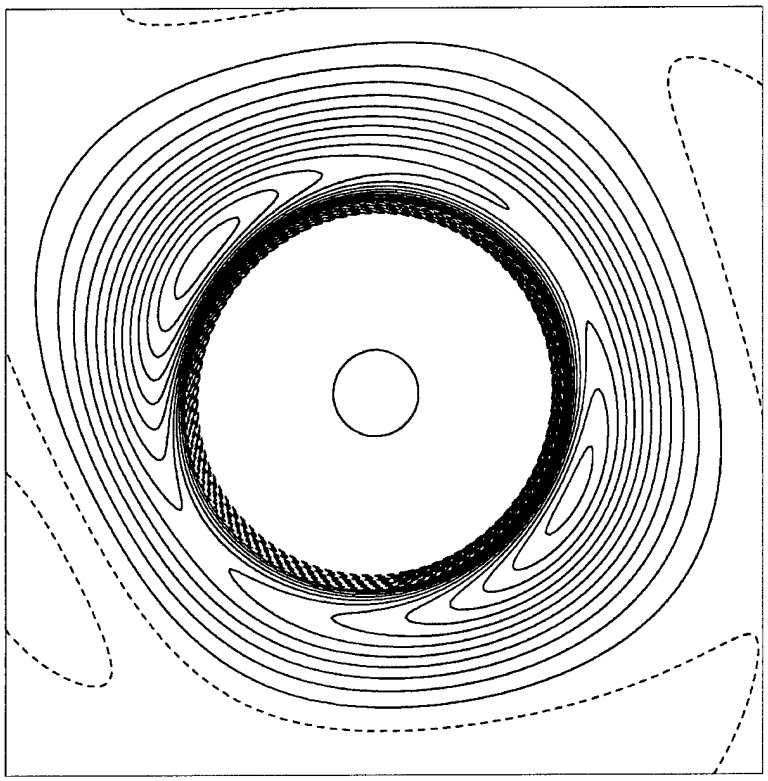

Figure 4c. The Laplacian of the electron density showing the O(1) lone pairs. Contours are from –130 to 130 eÅ^{-5} with interval 10 eÅ^{-3}.

(3,+3) minimum critical points in the Laplacian around the O(1) atom. These points reflect two Laplacian minima accosiated with O(1) lone pairs.

x	y	z	$\nabla^2\rho$, eÅ^{-5}
-1.3160	-0.7855	-0.3193	-120.2
-1.3909	-0.7981	-0.3139	-116.6

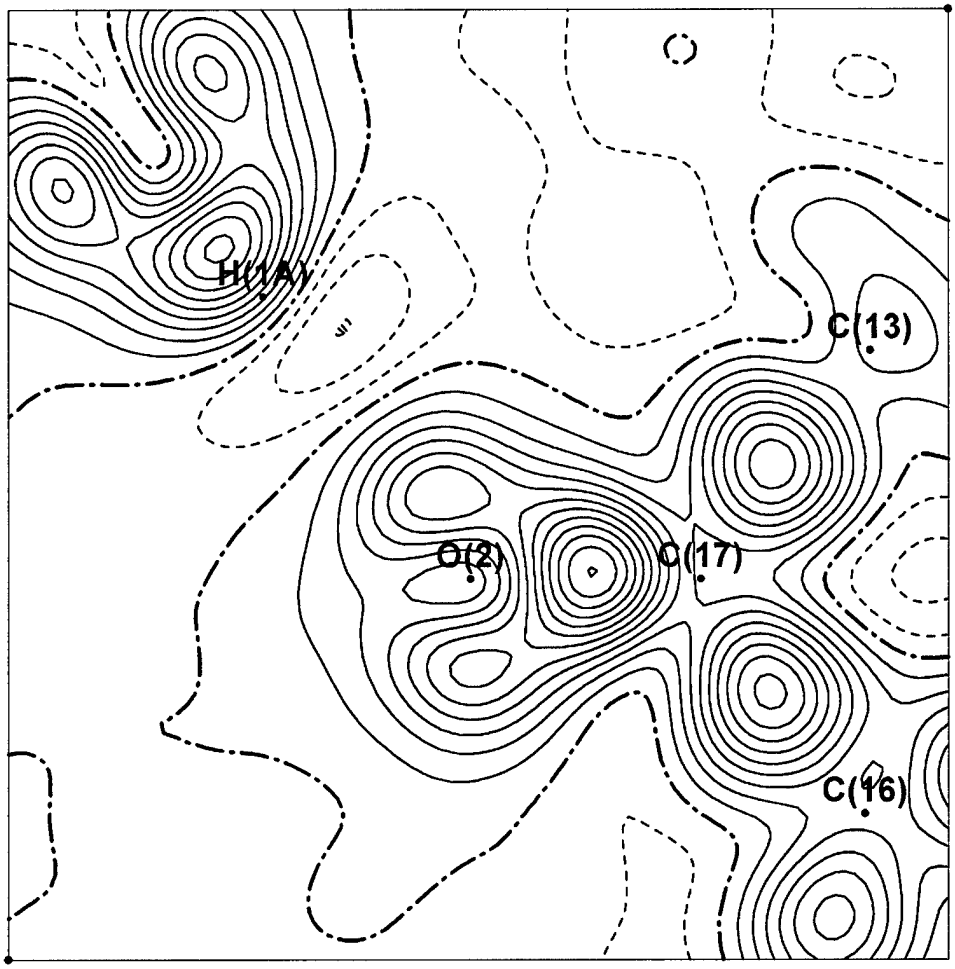

Figure 5a. The dynamic Fourier multipole electron density map in the O(2)-C(17)-$H(1A)_{next\_molecule}$ plane. The contour interval is 0.05 $eÅ^{-3}$. The hydrogen bonding region is shown.

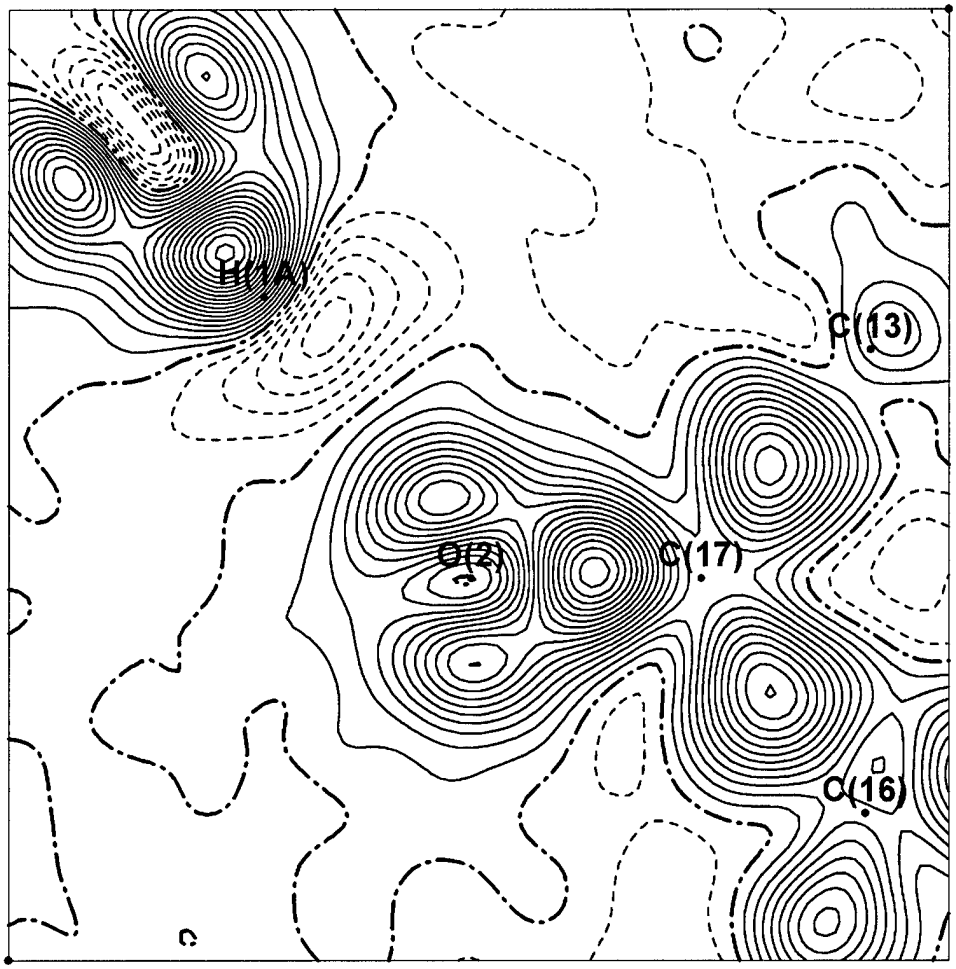

Figure 5b. The static Fourier multipole electron density map in the O(2)-C(17)-$H(1A)_{next\_molecule}$ plane. The contour interval is 0.05 eÅ^{-3}. The hydrogen bonding region is shown.

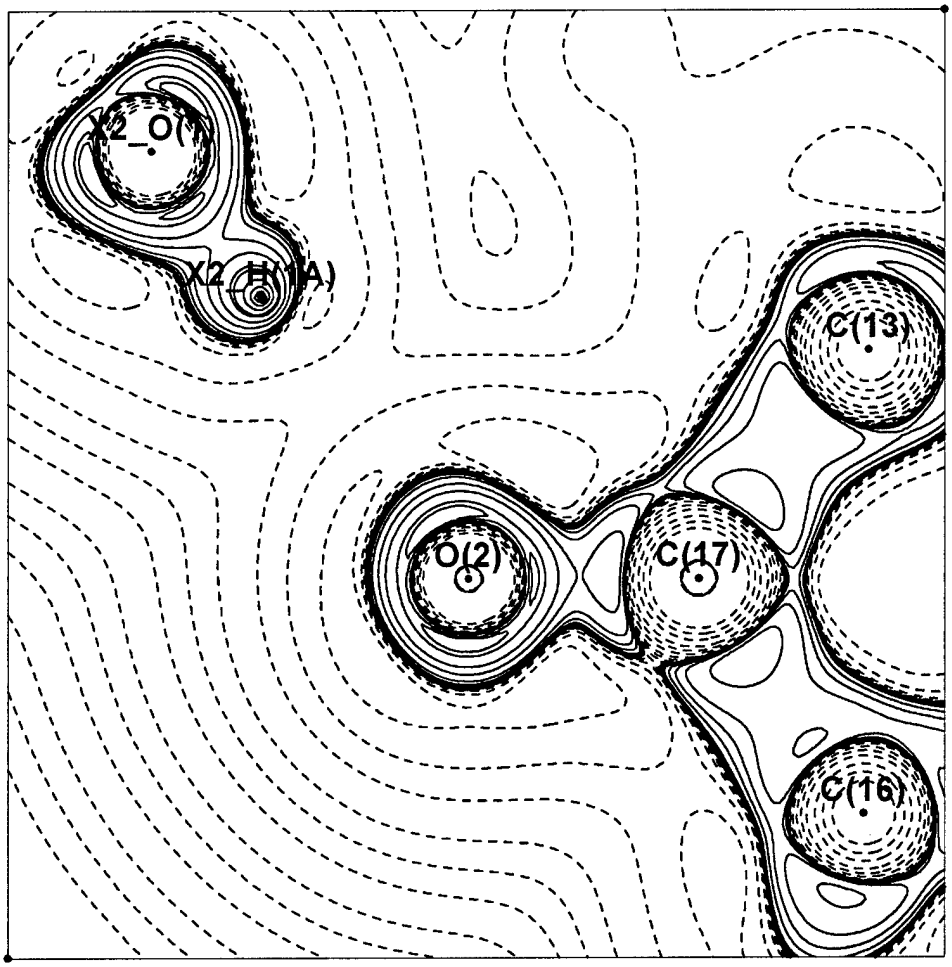

Figure 5c. The Laplacian of the electron density map in the $O(2)\text{-}C(17)\text{-}H(1A)_{next\_molecule}$ plane. The contour interval is 2,4,8 x 10^{-3-+3} eÅ^{-5} plus 100 eÅ^{-5} contour. The hydrogen bonding region is shown.

The (3,-1) bond critical points in the estrone crystal.

Bond		f	del2f	Rij	d1	d2	ellip
				Hessian Eigenvalues			
O(1)	-C(3)	2.128(17)	-22.849(77)	1.3699	0.8687	0.5011	
				-16.62	-15.70	9.48	0.06
O(1)	-H(1A)	2.669(116)	-59.134(1000)	0.9671	0.7522	0.2149	
				-46.46	-45.05	32.37	0.03
O(2)	-C(17)	2.913(22)	-12.730(144)	1.2241	0.8171	0.4070	
				-27.00	-26.48	40.75	0.02
O(2)	-X2_H(1A)	0.182(73)	2.369(137)	1.8539	1.2475	0.6064	
				-1.18	-1.12	4.67	0.05
C(1)	-C(2)	2.193(12)	-21.895(34)	1.3935	0.6485	0.7450	
				-14.52	-13.45	6.08	0.08
C(1)	-C(10)	2.191(15)	-21.866(41)	1.4058	0.6923	0.7135	
				-15.62	-13.14	6.90	0.19
C(1)	-H(1)	1.994(92)	-19.166(313)	1.0832	0.6547	0.4285	
				-17.77	-15.89	14.49	0.12
C(2)	-C(3)	2.269(14)	-23.462(38)	1.3987	0.6897	0.7089	
				-15.97	-14.39	6.90	0.11
C(2)	-H(2)	1.974(75)	-20.394(253)	1.0831	0.6546	0.4285	
				-17.87	-16.09	13.56	0.11
C(3)	-C(4)	2.291(14)	-25.008(37)	1.3969	0.7006	0.6963	
				-17.16	-14.32	6.47	0.20
C(4)	-C(5)	2.161(14)	-20.909(40)	1.4034	0.6505	0.7529	
				-14.59	-12.88	6.56	0.13
C(4)	-H(4)	1.943(82)	-20.414(281)	1.0831	0.6521	0.4310	
				-17.16	-16.51	13.25	0.04
C(5)	-C(6)	1.807(14)	-14.477(38)	1.5192	0.7928	0.7264	
				-11.85	-11.00	8.37	0.08
C(5)	-C(10)	2.140(15)	-21.026(52)	1.4120	0.6668	0.7451	
				-14.91	-13.24	7.13	0.13
C(6)	-C(7)	1.767(12)	-13.974(31)	1.5310	0.7622	0.7687	
				-11.55	-10.63	8.21	0.09
C(6)	-H(6A)	1.835(61)	-17.158(182)	1.0922	0.6344	0.4578	
				-15.17	-14.70	12.72	0.03
C(6)	-H(6B)	1.829(14)	-16.441(51)	1.0922	0.6366	0.4556	
				-15.28	-14.13	12.97	0.08
C(7)	-C(8)	1.717(12)	-12.733(33)	1.5272	0.7334	0.7938	
				-10.61	-10.24	8.11	0.04
C(7)	-H(7A)	1.949(59)	-19.054(185)	1.0923	0.6447	0.4475	
				-17.04	-15.46	13.44	0.10
C(7)	-H(7B)	1.873(14)	-16.504(51)	1.0921	0.6457	0.4464	
				-15.74	-14.80	14.04	0.06
C(8)	-C(9)	1.708(12)	-13.492(30)	1.5463	0.7668	0.7795	
				-11.45	-10.11	8.06	0.13
C(8)	-C(14)	1.791(13)	-15.780(32)	1.5249	0.7587	0.7662	
				-12.24	-11.35	7.81	0.08
C(8)	-H(8)	1.966(88)	-20.355(275)	1.0995	0.6504	0.4491	
				-17.16	-16.46	13.26	0.04

C(9)	-C(10)	1.718(13)	-14.351(37)	1.5278	0.7474	0.7804	
				-11.47	-11.01	8.12	0.04
C(9)	-C(11)	1.693(12)	-12.141(32)	1.5417	0.8041	0.7376	
				-10.58	-10.00	8.44	0.06
C(9)	-H(9)	1.962(80)	-20.120(222)	1.0999	0.6184	0.4815	
				-16.02	-15.24	11.13	0.05
C(11)	-C(12)	1.702(12)	-13.554(32)	1.5445	0.7764	0.7681	
				-11.03	-10.65	8.13	0.04
C(11)	-H(11A)	1.872(65)	-17.184(226)	1.0923	0.6670	0.4254	
				-16.61	-15.39	14.82	0.08
C(11)	-H(11B)	1.888(14)	-17.405(50)	1.0927	0.6703	0.4224	
				-16.82	-15.66	15.08	0.07
C(12)	-C(13)	1.781(12)	-15.139(34)	1.5272	0.7660	0.7612	
				-12.42	-10.73	8.01	0.16
C(12)	-H(12A)	1.908(55)	-18.213(170)	1.0922	0.6317	0.4605	
				-16.57	-14.45	12.81	0.15
C(12)	-H(12B)	1.905(14)	-17.500(53)	1.0921	0.6322	0.4599	
				-15.97	-14.42	12.89	0.11
C(13)	-C(14)	1.662(11)	-12.633(33)	1.5444	0.8016	0.7428	
				-10.50	-10.08	7.95	0.04
C(13)	-C(17)	1.786(13)	-15.569(41)	1.5180	0.7252	0.7927	
				-12.04	-11.64	8.12	0.03
C(13)	-C(18)	1.700(13)	-13.624(34)	1.5475	0.8162	0.7314	
				-11.00	-10.63	8.01	0.04
C(14)	-C(15)	1.712(13)	-12.844(33)	1.5409	0.7822	0.7587	
				-10.81	-10.39	8.36	0.04
C(14)	-H(14)	1.975(73)	-23.180(208)	1.0992	0.6150	0.4842	
				-16.70	-16.27	9.80	0.03
C(15)	-C(16)	1.674(13)	-12.768(33)	1.5499	0.7390	0.8109	
				-11.15	-10.03	8.42	0.11
C(15)	-H(15A)	1.857(65)	-14.108(227)	1.0924	0.6784	0.4140	
				-15.75	-15.05	16.70	0.05
C(15)	-H(15B)	1.847(15)	-14.898(51)	1.0921	0.6730	0.4191	
				-16.49	-14.54	16.13	0.13
C(16)	-C(17)	1.813(14)	-15.402(37)	1.5286	0.7264	0.8022	
				-12.08	-11.97	8.65	0.01
C(16)	-H(16A)	1.920(60)	-19.765(177)	1.0922	0.6327	0.4595	
				-16.60	-15.25	12.08	0.09
C(16)	-H(16B)	1.993(14)	-21.179(52)	1.0940	0.6410	0.4530	
				-17.58	-15.98	12.38	0.10
C(18)	-H(18A)	1.899(59)	-16.059(183)	1.0591	0.6195	0.4396	
				-16.23	-14.12	14.29	0.15
C(18)	-H(18B)	1.864(12)	-14.601(52)	1.0591	0.6169	0.4422	
				-15.16	-13.46	14.02	0.13
C(18)	-H(18C)	1.878(12)	-14.871(51)	1.0595	0.6195	0.4400	
				-15.60	-13.62	14.35	0.15

Figure 6. The electrostatic potential of the estrone molecule. Surfaces are +0.5 $eÅ^{-1}$ (blue) and –0.15 $eÅ^{-1}$ (red).

The multipole population parameters for the non-hydrogen atoms in estrone

Atom	P_v	κ'	κ''	D1+	D1-	D0	Q0	Q1+	Q1-	Q2+	Q2-	O0	O1+	O1-
O(1)	6.4184	0.9605	0.8732	-0.0094	0.0028	-0.0065	0.1163	-0.0092	0.0006	-0.0139	-0.0047	0.0229	0.0362	-0.0575
O(2)	6.2740	0.9771	0.8630	-0.0301	-0.0038	0.0051	-0.1364	0.0211	-0.0101	-0.0606	0.0238	-0.0105	0.0058	-0.0017
C(1)	4.2794	0.9552	0.7712	-0.0987	-0.0124	-0.0303	-0.2752	0.1253	-0.0323	-0.0521	0.0102	0.0103	-0.0173	0.0084
C(2)	4.4375	0.9552	0.7712	-0.0547	0.0629	0.0292	-0.3250	0.0371	-0.0825	0.0157	-0.0179	0.0451	-0.0319	0.0055
C(3)	3.7663	0.9844	0.8112	0.0032	0.0639	-0.0058	-0.2626	0.0219	-0.031	0.0452	-0.0932	-0.0205	0.0729	0.1016
C(4)	4.2846	0.9552	0.7712	-0.0829	0.0345	-0.0028	-0.2843	-0.0266	-0.0316	-0.0070	-0.0294	0.0241	0.1023	-0.0779
C(5)	4.2047	0.9567	0.8476	-0.0525	0.0672	-0.0318	-0.2366	-0.0603	0.0455	-0.0470	0.0063	0.0436	0.0115	-0.0520
C(6)	4.3544	0.9532	0.7973	-0.0249	0.0218	0.0157	-0.0462	0.0292	-0.0113	0.0173	-0.0185	0.0478	-0.0594	0.0245
C(7)	4.4117	0.9532	0.7973	-0.0905	0.0210	-0.0142	-0.0815	-0.0411	0.0612	0.0113	0.0369	-0.0166	0.0419	0.0494
C(8)	4.3339	0.9532	0.7973	0.0182	-0.0137	0.0150	0.0414	-0.0088	-0.0358	0.0076	0.0682	-0.0672	-0.0115	0.0556
C(9)	4.3135	0.9532	0.7973	-0.0918	-0.0315	-0.0291	0.0162	-0.0402	-0.0109	0.1001	-0.0192	0.0315	-0.0350	-0.0083
C(10)	4.1575	0.9567	0.8476	0.0010	0.0602	0.0721	-0.2216	0.0455	0.0785	0.0161	-0.0864	-0.0372	-0.0067	0.0312
C(11)	4.4237	0.9532	0.7973	-0.0755	0.0614	-0.0402	-0.0072	0.0026	0.0988	0.0762	0.0149	0.0052	0.0378	-0.0115
C(12)	4.3349	0.9532	0.7973	-0.0517	-0.0149	-0.0084	-0.0326	-0.0372	0.0149	0.0869	0.0182	0.0104	0.0717	-0.0216
C(13)	4.2497	0.9532	0.7973	-0.0146	0.0252	0.0166	0.0513	-0.0674	0.0175	-0.0330	0.0433	-0.0448	-0.0502	-0.0495
C(14)	4.0905	0.9532	0.7973	-0.0563	0.0512	0.0383	-0.0429	-0.0639	0.0135	-0.0699	0.0255	0.0408	0.0164	0.0010
C(15)	4.5093	0.9532	0.7973	-0.1772	0.0368	-0.0202	-0.0901	-0.0314	0.0906	0.0964	0.0105	-0.0278	-0.0391	0.0404
C(16)	4.4526)	0.9532	0.7973	-0.0252	0.0287	-0.0683	-0.0511	-0.0033	0.0025	0.0170	0.0214	0.0426	-0.0260	-0.0878
C(17)	4.0874	0.9793	0.8526	-0.0667	-0.0721	0.0088	-0.2910	0.0322	0.0298	-0.0798	0.0723	-0.0105	-0.0273	0.0417
C(18)	4.4600	0.9532	0.7973	0.1442	0.1494	-0.0717	0.0411	-0.0116	0.0037	-0.0096	-0.0881	-0.0636	-0.1116	-0.1525

(continued)

Atom	O2+	O2-	O3+	O3-	H0	H1+	H1-	H2+	H2-	H3+	H3-	H4+	H4-
O(1)	-0.0184	-0.0023	0.1121	-0.0111	0.0222	0.0314	-0.0164	0.0142	-0.0570	0.0315	0.0257	0.0324	0.0475
O(2)	0.0171	-0.0096	0.0500	-0.0147	0.0660	0.0061	-0.0043	-0.0176	-0.0451	-0.0217	0.0102	0.0237	-0.0190
C(1)	0.0356	-0.0619	0.3968	0.0853	0.0408	-0.0974	0.0804	-0.0197	-0.0192	-0.0623	0.0410	-0.0791	0.0504
C(2)	-0.0290	0.0229	0.4780	-0.0036	0.0868	-0.0747	0.0146	-0.0323	0.0758	-0.0574	0.0341	-0.0837	0.0344
C(3)	0.0557	-0.0034	0.4756	0.0234	0.0394	0.0203	0.0662	0.0954	0.0032	0.0426	0.0010	-0.0062	-0.0224
C(4)	0.0113	0.0482	0.4175	-0.0030	0.1128	0.0157	-0.0612	0.0868	0.0452	-0.0640	0.0294	-0.1145	0.0531
C(5)	-0.0326	-0.0319	0.3789	-0.0011	0.0780	-0.0444	-0.0405	0.0213	0.0626	-0.0572	0.0050	-0.0421	0.0265
C(6)	-0.0035	-0.4626	-0.0456	0.0097	-0.2044	0.0267	0.0112	-0.0329	-0.0251	0.0301	0.0439	-0.0605	0.0426
C(7)	-0.0072	-0.4316	-0.0520	0.0275	-0.2003	0.0289	0.0266	0.0182	0.0034	0.0546	0.1088	-0.0471	0.0024
C(8)	-0.0035	0.4666	-0.0003	-0.0140	-0.2974	0.0195	-0.0568	0.0080	-0.0077	0.0071	-0.0778	-0.1052	0.0416
C(9)	0.0859	-0.4763	0.0036	0.0617	-0.1985	-0.0348	0.0540	0.0616	-0.0313	-0.0794	0.0023	-0.1768	-0.1168
C(10)	-0.0091	-0.0445	0.3532	0.0370	0.0882	-0.0623	-0.0113	0.0149	0.0181	0.0115	0.0099	0.0024	0.0188
C(11)	-0.0111	-0.3846	-0.0666	-0.0422	-0.0895	0.0350	-0.0214	0.0300	0.0471	0.1087	-0.0425	-0.0447	0.0185
C(12)	-0.0166	-0.4309	-0.0413	-0.0252	-0.1147	0.0868	-0.0215	-0.0647	-0.0253	0.0193	-0.0784	-0.1276	-0.0223
C(13)	0.0823	0.4474	-0.0573	0.0188	-0.2513	0.0020	-0.0698	0.1336	-0.0481	-0.0814	-0.0744	-0.1422	0.0945
C(14)	0.1395	-0.3972	-0.0346	0.0280	-0.2245	0.1045	0.0201	-0.0071	0.0109	0.0023	0.0392	-0.0825	-0.0487
C(15)	0.0192	-0.4247	-0.0705	-0.0205	-0.1204	-0.1298	0.0312	-0.0067	-0.0006	-0.0299	-0.0142	-0.0530	0.0605
C(16)	0.0304	-0.4580	-0.0499	0.0537	-0.1858	-0.0183	-0.0047	-0.1146	0.0140	-0.0100	0.0111	-0.1016	-0.0674
C(17)	-0.0210	0.0247	0.4198	-0.1109	0.0335	-0.0970	-0.0166	0.0542	0.0111	0.0680	-0.0429	0.0345	0.0521
C(18)	-0.0367	0.3271	0.0065	0.03428	0.0143	-0.0584	0.0049	0.0259	0.0124	0.0661	0.0182	-0.0075	-0.0056

The multipole population parameters for hydrogen atoms in estrone

Atom	H(1A)	H(1)	H(2)	H(4)	H(6A)	H(6B)	H(7A)	H(7B)	H(8)	H(9)	H(11A)
P_v	0.7684	0.7024	0.6562	0.6705	0.7277	0.7277	0.7314	0.7314	0.7441	0.7720	0.7072
κ'	1.2031	1.4278	1.4278	1.4278	1.4278	1.4278	1.4278	1.4278	1.4278	1.4278	1.4278
κ"	1.3496	1.2774	1.2774	1.2774	1.2774	1.2774	1.2774	1.2774	1.2774	1.2774	1.2774
D1+	-0.0215	-0.0384	-0.0238	-0.0009	-0.0130	-0.0130	0.0244	0.0244	0.0204	0.0135	0.0219
D1-	0.0016	-0.0030	-0.0292	-0.0432	-0.0119	-0.0119	-0.0338	-0.0338	-0.0121	0.0097	-0.0207
D0	0.1855	0.1549	0.1751	0.1492	0.1558	0.1558	0.1523	0.1523	0.1417	0.2009	0.1090
Q0	0.0716	0.0395	0.0461	0.0733	-0.0225	-0.0225	0.0013	0.0013	0.0328	0.0102	0.0872
Q1+	0.0129	-	-	-	-	-	-	-	-	-	-
Q1-	-0.0154	-	-	-	-	-	-	-	-	-	-
Q2+	-0.0135	-	-	-	-	-	-	-	-	-	-
Q2-	0.0012	-	-	-	-	-	-	-	-	-	-

(continued)

Atom	H(11B)	H(12A)	H(12B)	H(14)	H(15A)	H(15B)	H(16A)	H(16B)	H(18A)	H(18B)	H(18C)
P_v	0.7072	0.7666	0.7666	0.7715	0.7032	0.7032	0.7155	0.7155	0.7895	0.7895	0.7895
κ'	1.4278	1.4278	1.4278	1.4278	1.4278	1.4278	1.4278	1.4278	1.4278	1.4278	1.4278
κ"	1.2774	1.2774	1.2774	1.2774	1.2774	1.2774	1.2774	1.2774	1.2774	1.2774	1.2774
D1+	0.0219	0.0252	0.0252	0.0050	-0.0323	-0.0323	-0.0108	-0.0108	0.0614	0.0614	0.0614
D1-	-0.0207	-0.0089	-0.0089	-0.0263	-0.0460	-0.0460	-0.0205	-0.0205	-0.0183	-0.0183	-0.0183
D0	0.1090	0.1564	0.1564	0.1515	0.1050	0.1050	0.1795	0.1795	0.1037	0.1037	0.1037
Q0	0.0872	0.0544	0.0544	0.1805	-0.0022	-0.0022	0.0552	0.0552	0.0231	0.0231	0.0231

Appendix J.

Measurement of the Electron Density Distribution of Estrogens – a First Step to Advanced Drug Design

DOD Breast Cancer Research Program Era of Hope Meeting (2002)

MEASUREMENT OF THE ELECTRON DENSITY DISTRIBUTION OF ESTROGENS - A FIRST STEP TO ADVANCED DRUG DESIGN

A. Alan Pinkerton, Kristin Kirschbaum, Poomani Kumaradhas, Damon A. Parrish, Nan Wu, and Elizabeth A. Zhurova

Department of Chemistry, University of Toledo, Toledo, OH 43606

apinker@uoft02.utoledo.edu

The scientific approach to preventing or curing disease requires understanding the mechanism by which the disease state is initiated or propogated. A significant body of knowledge exists to indicate that a large number of breast cancers are initiated by estrogens - the family of female hormones. It has been hypothesized that the mechanism involves first binding of the steroid molecule by the estrogen receptor in the nucleus of target breast cells, followed by secondary interaction which partially reorganizes the receptor pocket. This, in turn, modifies the surface of the protein such that the genes necessary for tumor development are activated. The purpose of the present study is to obtain information on the fundamental properties of estrogen molecules that are responsible for the binding event and for the subsequent reorganization of the receptor.

When two molecules approach one another, be they small organic molecules in solution or a steroid molecule approaching a protein, they sense each other's electrostatic potential. Much as two magnets will feel each other's magnetic field and orient themselves to maximize the attraction, so the two molecules will seek to align themselves in such a way as to approach negative regions to positive regions and vice versa. Perfect complementarity of the potentials will maximize the primary binding interaction and the secondary reorganization step necessary for gene expression. Molecules with different electrostatic potentials will have different binding affinities and different activities with respect to gene expression. These parameters are known for many compounds, whereas the electrostatic potentials are not.

The electrostatic potential is a complicated three dimensional function that is determined by the geometrical structure of a molecule and the distribution of the electrons and nuclei that make up that molecule. By using very accurate X-ray diffraction techniques, the complete description of the geometrical structure and the distribution of all of the electrons in a molecule may be determined. This information may then be used to calculate the electrostatic potential at any point in or around a molecule. We report the first studies of this type on a number of natural and unnatural estrogen derivatives.

The U.S. Army Medical Research and Materiel Command under DAMD17-99-1-9408 supported this work.

Measurement of the Electron Density Distribution of

A. Alan Pinkerton, Kristin Kirschbaum, Poomani Kumaradhas,

Department of Chemistry, University

Please also visit poster P16-16

Abstract

The scientific approach to preventing or curing disease requires understanding the mechanism by which the disease state is initiated or propagated. A significant body of knowledge exists to indicate that a large number of breast cancers are initiated by estrogens - the family of female hormones. It has been hypothesized that the mechanism involves first binding of the steroid molecule by the estrogen receptor in the nucleus of target breast cells, followed by secondary interaction which partially reorganizes the receptor pocket. This, in turn, modifies the surface of the protein such that the genes necessary for tumor development are activated. The purpose of the present study is to obtain information on the fundamental properties of estrogen molecules that are responsible for the binding event and for the subsequent reorganization of the receptor.

When two molecules approach one another, be they small organic molecules in solution or a steroid molecule approaching a protein, they sense each other's electrostatic potential. Much as two magnets will feel each other's magnetic field and orient themselves to maximize the attraction, so the two molecules will seek to align themselves in such a way as to approach negative regions to positive regions and vice versa. Perfect complementarity of the potentials will maximize the primary binding interaction and the secondary reorganization step necessary for gene expression. Molecules with different electrostatic potentials will have different binding affinities and different activities with respect to gene expression. These parameters are known for many compounds, whereas the electrostatic potentials are not.

The electrostatic potential is a complicated three dimensional function that is determined by the geometrical structure of a molecule and the distribution of the electrons and nuclei that make up that molecule. By using very accurate X-ray diffraction techniques, the complete description of the geometrical structure and the distribution of all of the electrons in a molecule may be determined. This information may then be used to calculate the electrostatic potential at any point in or around a molecule. We report the first studies of this type on a number of natural and unnatural estrogen derivatives.

Conclusion

We have developed the methodology and protocols to use modern X-ray crystallographic techniques to obtain data of sufficient quality to reliably determine the electron density distribution in molecules from samples of crystalline estrogens. We have established a standardized method for modeling the electron density and refining the parameters of the model against the X-ray data. Thus, comparisons between molecules may be made with confidence that the same parameters are being compared. From the six compounds reported here, there are clear similarities in the electron density and electrostatic potential at the A-ring. This is encouraging, as this region is far removed from the chemical differences in the D-ring. In contrast, there are significant differences in the D-ring properties. This is in agreement with the observation of three orders of magnitude difference in activities being associated with D-ring properties, but that a one order of magnitude difference in binding affinity is a function of both A- and D-ring properties. In order to fully understand the parameters responsible for binding on the one hand, and activity on the other, we are building a more extensive data-base of natural and synthetic estrogen derivatives such that statistical methods (QSAR) may be brought to bear on this problem.

Acknowledgement

We thank Prof. Samuel C. Brooks for insightful discussions.

17β– estradiol • urea

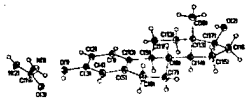

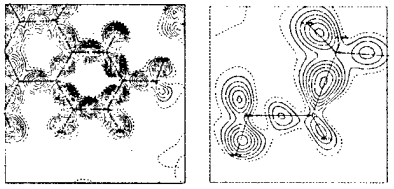

Deformation electron density maps in the plane of the aromatic ring (left) and in the O2-C17-C16 plane (right). Contour intervals are 0.05 eÅ^{-3}.

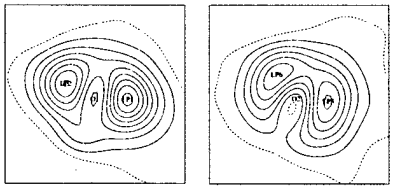

Deformation electron density maps in the plane of the lone pairs of O1 (left) and O2 (right). Contour intervals are 0.05 eÅ^{-3}.

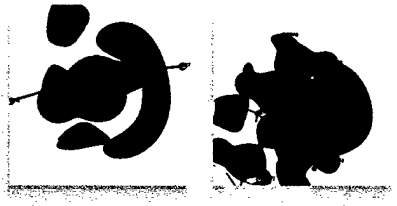

Electrostatic potential isosurfaces for the C3-hydroxy group (left) and C17-hydroxy group (right); red –0.15 eÅ^{-1}, blue 1.0 eÅ^{-1}.

17β– estradiol • ½ methanol

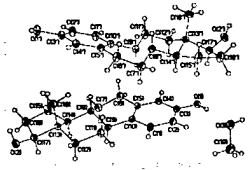

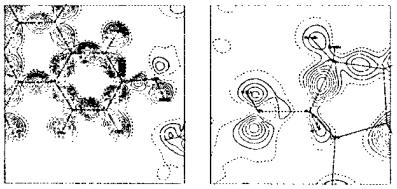

Deformation electron density maps in the plane of the aromatic ring (left) and in the O2-C17-C16 plane (right). Contour intervals are 0.05 eÅ^{-3}.

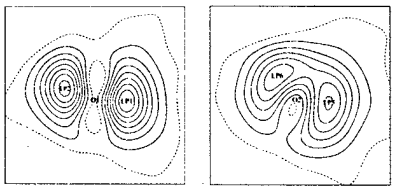

Deformation electron density maps in the plane of the lone pairs of O1 (left) and O2 (right). Contour intervals are 0.05 eÅ^{-3}.

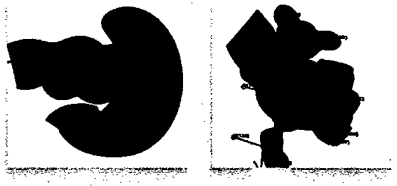

Electrostatic potential isosurfaces for the C3-hydroxy group (left) and C17-hydroxy group (right); red –0.15 eÅ^{-1}, blue 1.0 eÅ^{-1}.

Estrogens – a First Step to Advanced Drug Design

Damon A. Parrish, Nan Wu & Elizabeth A. Zhurova

of Toledo, Toledo, OH 43606, USA

THE UNIVERSITY OF TOLEDO

17α– estradiol • ½ H_2O

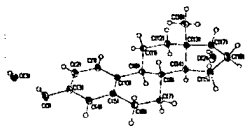

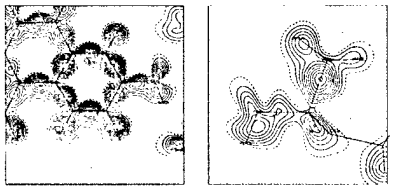

Deformation electron density maps in the plane of the aromatic ring (left) and in the O2-C17-C16 plane (right). Contour intervals are 0.05 eÅ^{-3}.

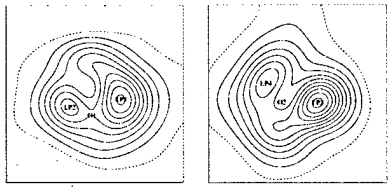

Deformation electron density maps in the plane of the lone pairs of O1 (left) and O2 (right). Contour intervals are 0.05 eÅ^{-3}.

Electrostatic potential isosurfaces for the C3-hydroxy group (left) and C17-hydroxy group (right); blue 1.0 eÅ^{-1}.

red –0.2 eÅ^{-1} red –0.4 eÅ^{-1}

17α– estradiol

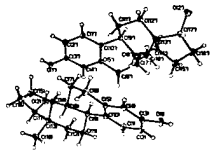

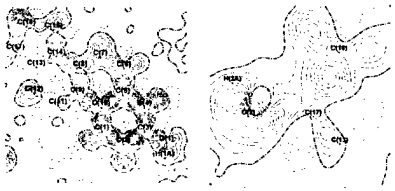

Deformation electron density maps in the plane of the aromatic ring (left) and in the O2-C17-C16 plane (right). Contour intervals are 0.05 eÅ^{-3}.

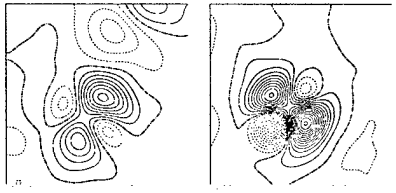

Deformation electron density maps in the plane of the lone pairs of O1 (left) and O1' (right). Contour intervals are 0.05 eÅ^{-3}.

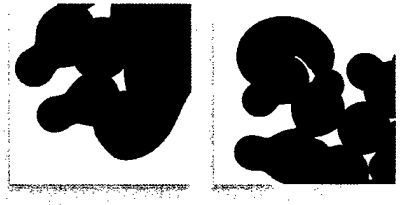

Electrostatic potential isosurfaces for the C3-hydroxy group (left) and C17-hydroxy group (right); blue 0.75 eÅ^{-1}.

red –0.15 eÅ^{-1} red –0.2 eÅ^{-1}

estrone

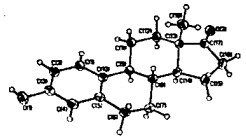

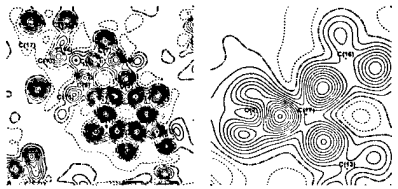

Deformation electron density maps in the plane of the aromatic ring (left) and in the O2-C17-C16 plane (right). Contour intervals are 0.05 eÅ^{-3}.

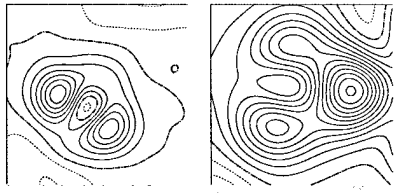

Deformation electron density maps in the plane of the lone pairs of O1 (left) and O2 (right). Contour intervals are 0.05 eÅ^{-3}.

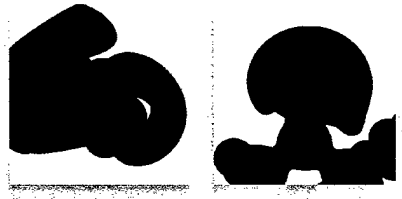

Electrostatic potential isosurfaces for the C3-hydroxy group (left) and C17-carbonyl group (right); red –0.15 eÅ^{-1}, blue 0.5 eÅ^{-1}.

3, 16α, 17β– estriol

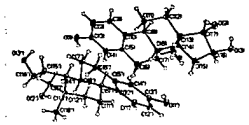

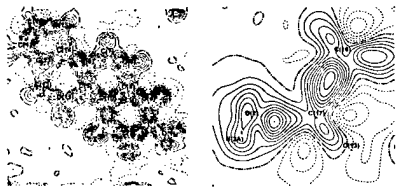

Deformation electron density maps in the plane of the aromatic ring (left) and in the O2-C17-C16 plane (right). Contour intervals are 0.05 eÅ^{-3}.

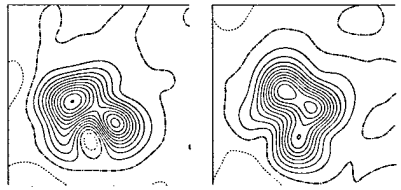

Deformation electron density maps in the plane of the lone pairs of O2 (left) and O2' (right). Contour intervals are 0.05 eÅ^{-3}.

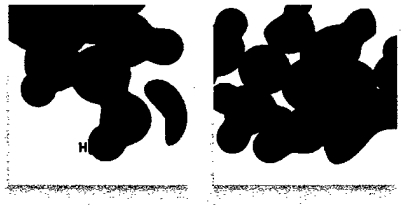

Electrostatic potential isosurfaces for the C3-hydroxy group (left) and C17-carbonyl group (right); blue 0.75 eÅ^{-1}.

red –0.075 eÅ^{-1} red –0.35 eÅ^{-1}

Funding provided by The U.S. Army Medical Research Materiel Command Award Number: DAMD17-99-1-9408

Appendix K.

Electrostatic potential isosurfaces for several hydroxyl groups of selected estrogens

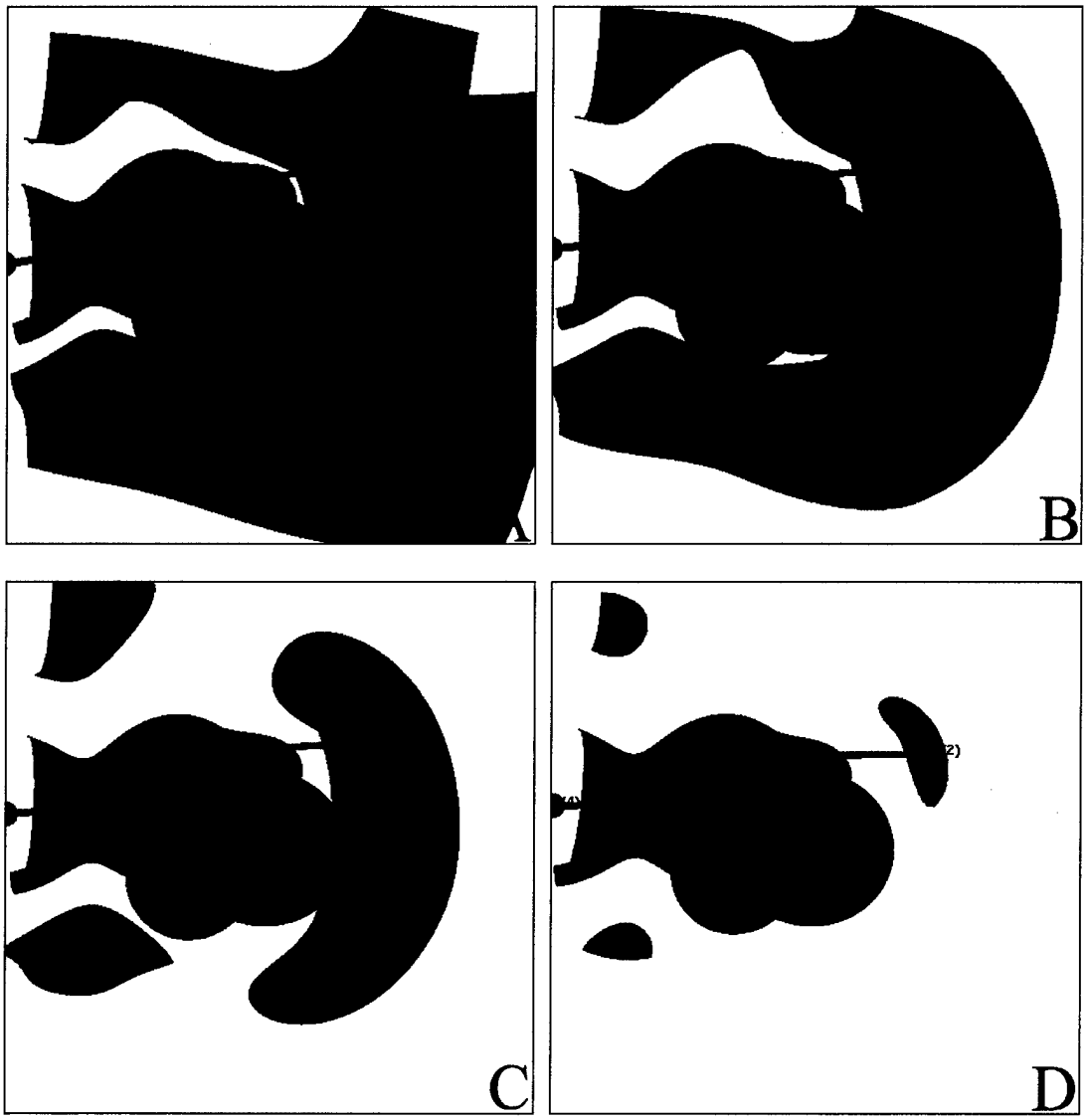

Figure 1. Electrostatic potential isosurfaces of the O1 hydroxy group of 17β-estradiol • urea. The blue surface in each picture represents +1.0 eÅ^{-1}. The red surfaces represent the following potentials: A –0.05 eÅ^{-1}, B –0.10 eÅ^{-1}, C –0.15 eÅ^{-1}, D – 0.20 eÅ^{-1}.

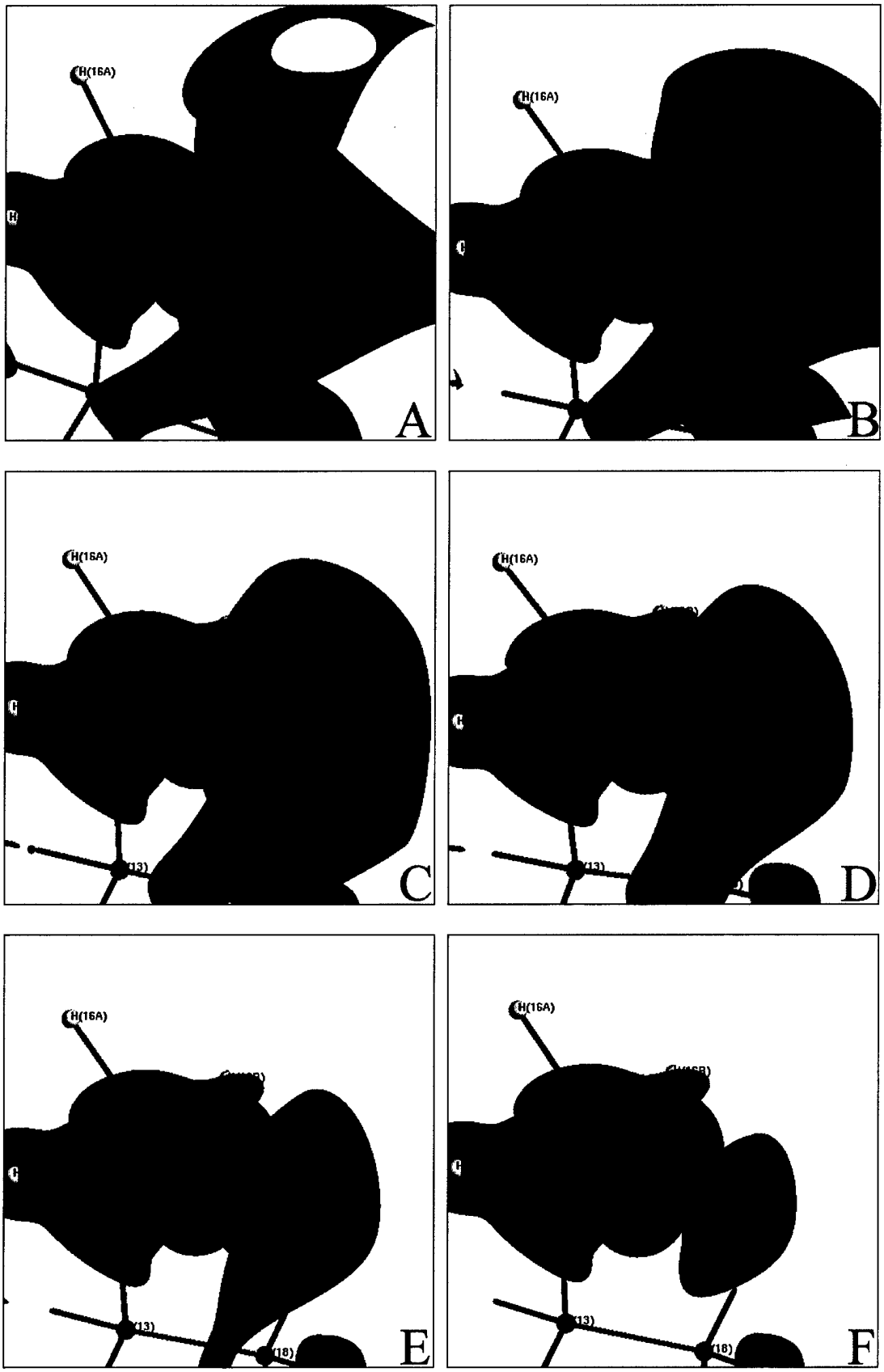
H(16A)
A
H(16A)
B
H(16A)
C
H(16A)
D
H(16A)
E
H(16A)
F

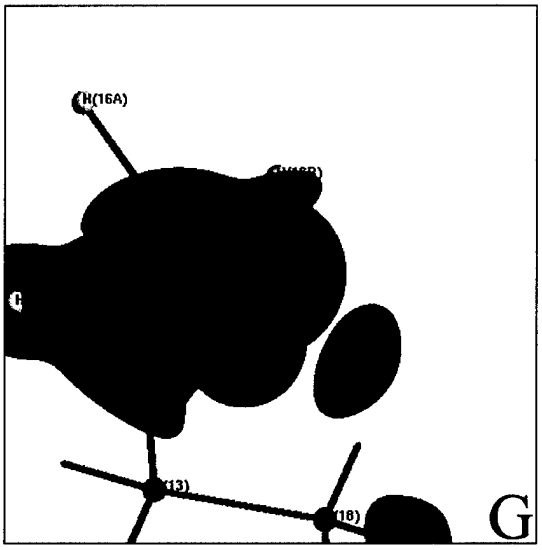

Figure 2. Electrostatic potential isosurfaces of the O2 hydroxy group of 17β-estradiol • urea. The blue surface in each picture represents +1.0 eÅ^{-1}. The red surfaces represent the following potentials: A –0.05 eÅ^{-1}, B –0.10 eÅ^{-1}, C –0.15 eÅ^{-1}, D –0.20 eÅ^{-1}, E –0.25 eÅ^{-1}, F –0.30 eÅ^{-1}, G –0.35 eÅ^{-1}.

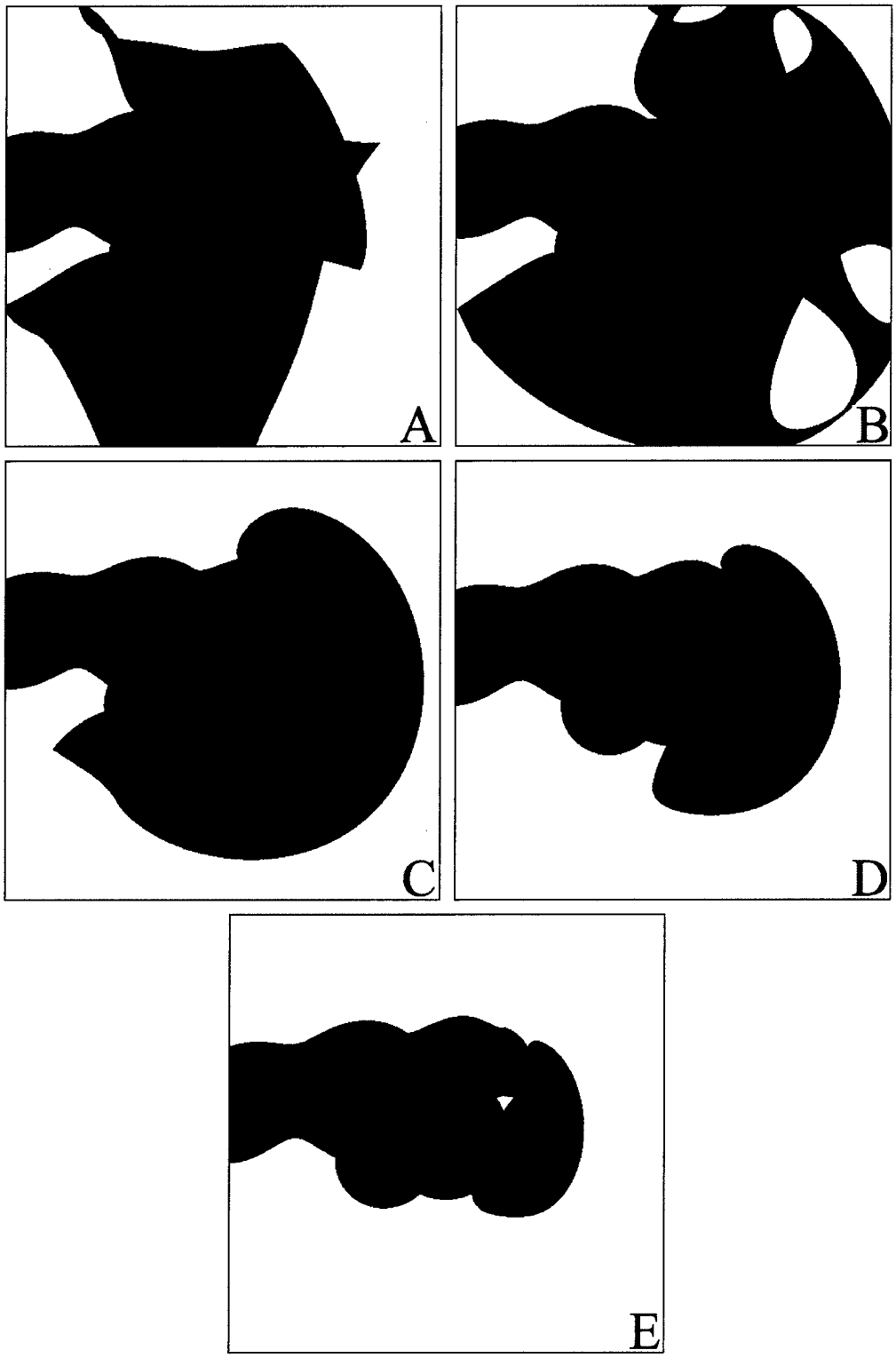

Figure 3. Electrostatic potential isosurfaces of the O1 hydroxy group of 17β-estradiol • methanol. The blue surface in each picture represents +1.0 eÅ^{-1}. The red surfaces represent the following potentials: A –0.05 eÅ^{-1}, B –0.10 eÅ^{-1}, C –0.15 eÅ^{-1}, D – 0.20 eÅ^{-1}.

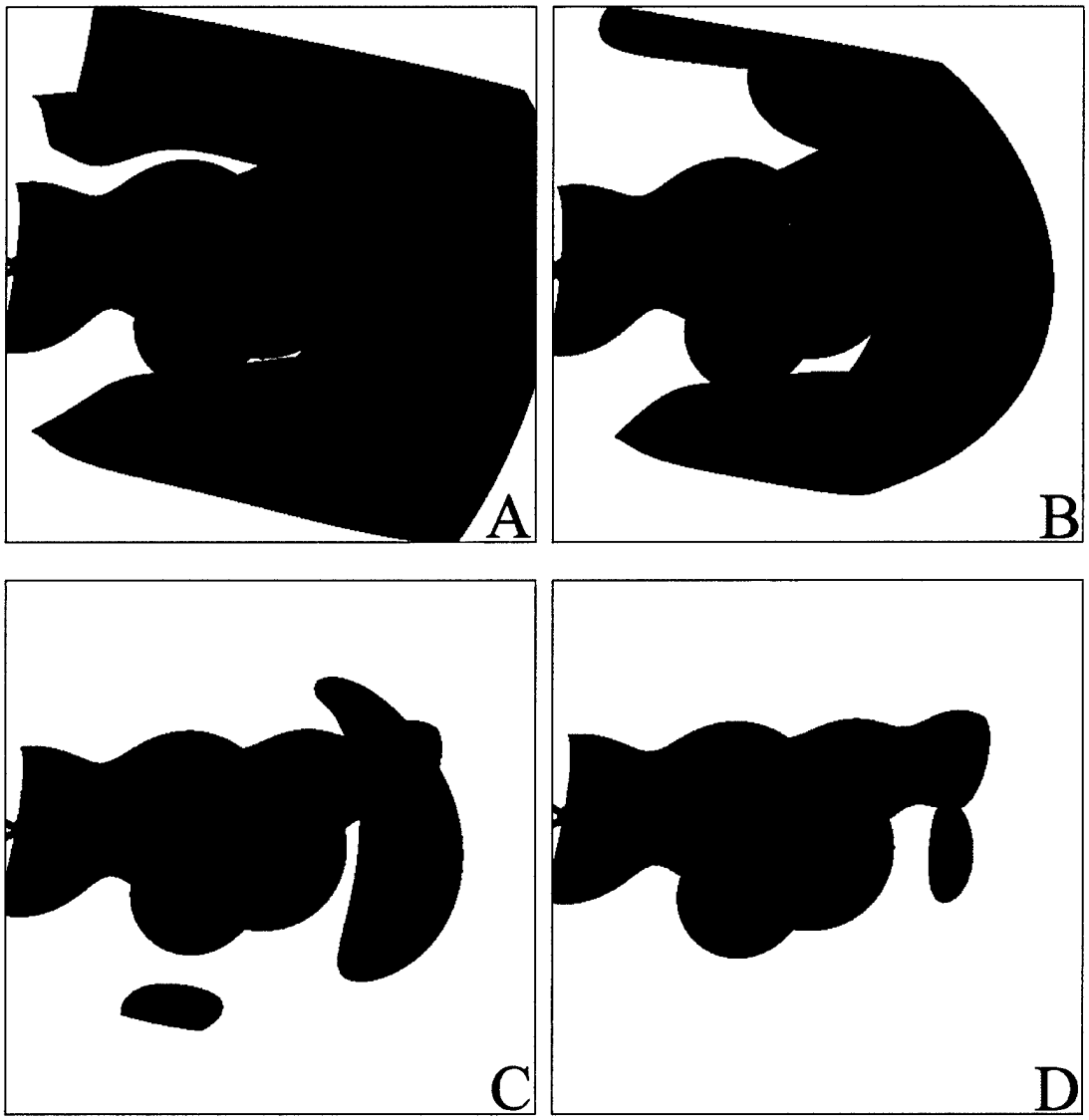

Figure 4. Electrostatic potential isosurfaces of the O1' hydroxy group of 17β-estradiol • methanol. The blue surface in each picture represents +1.0 eÅ^{-1}. The red surfaces represent the following potentials: A –0.05 eÅ^{-1}, B –0.10 eÅ^{-1}, C –0.15 eÅ^{-1}, D –0.20 eÅ^{-1}.

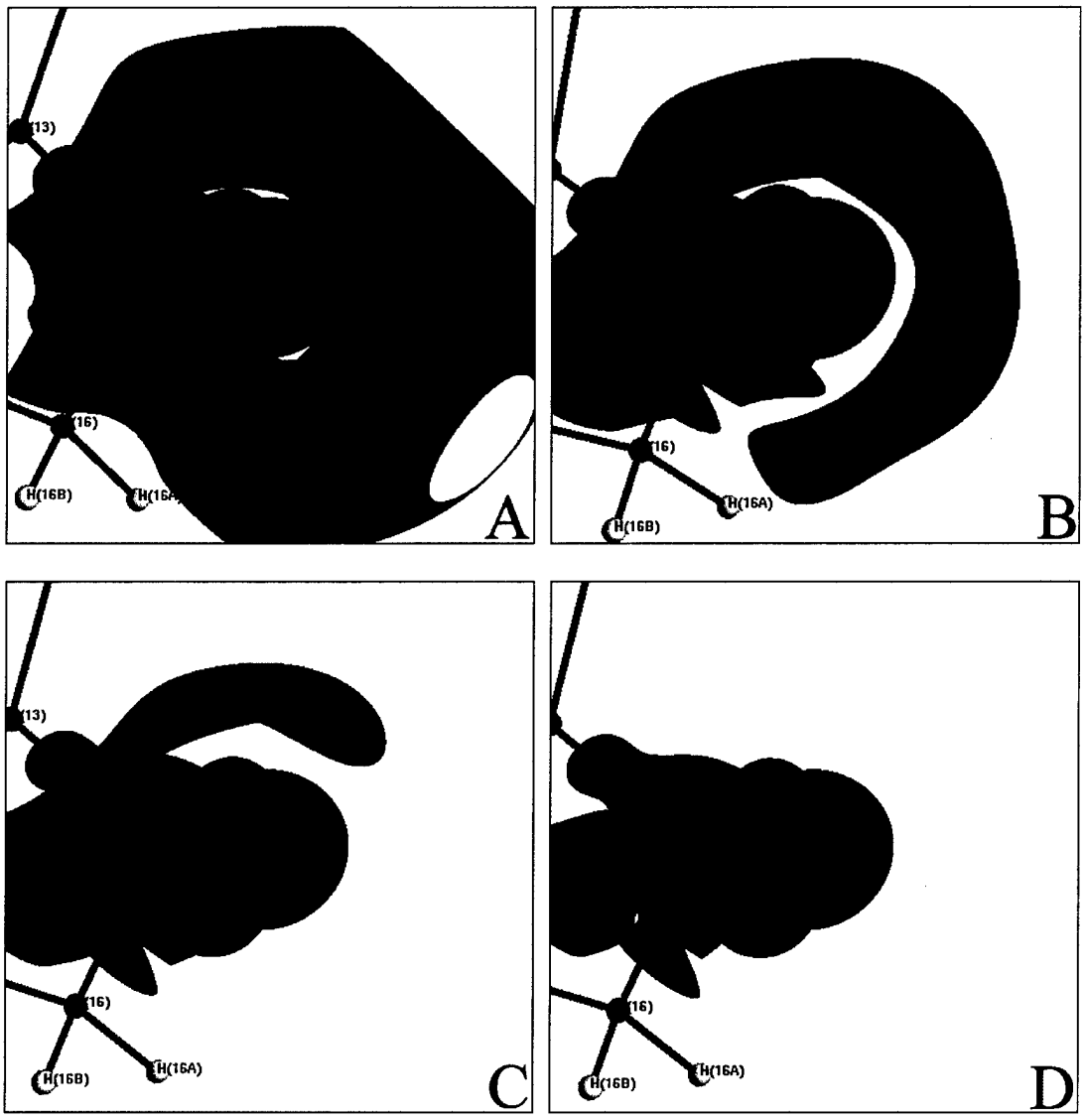

Figure 5. Electrostatic potential isosurfaces of the O2 hydroxy group of 17β-estradiol • methanol. The blue surface in each picture represents +1.0 eÅ^{-1}. The red surfaces represent the following potentials: A –0.05 eÅ^{-1}, B –0.10 eÅ^{-1}, C –0.15 eÅ^{-1}, D – 0.20 eÅ^{-1}.

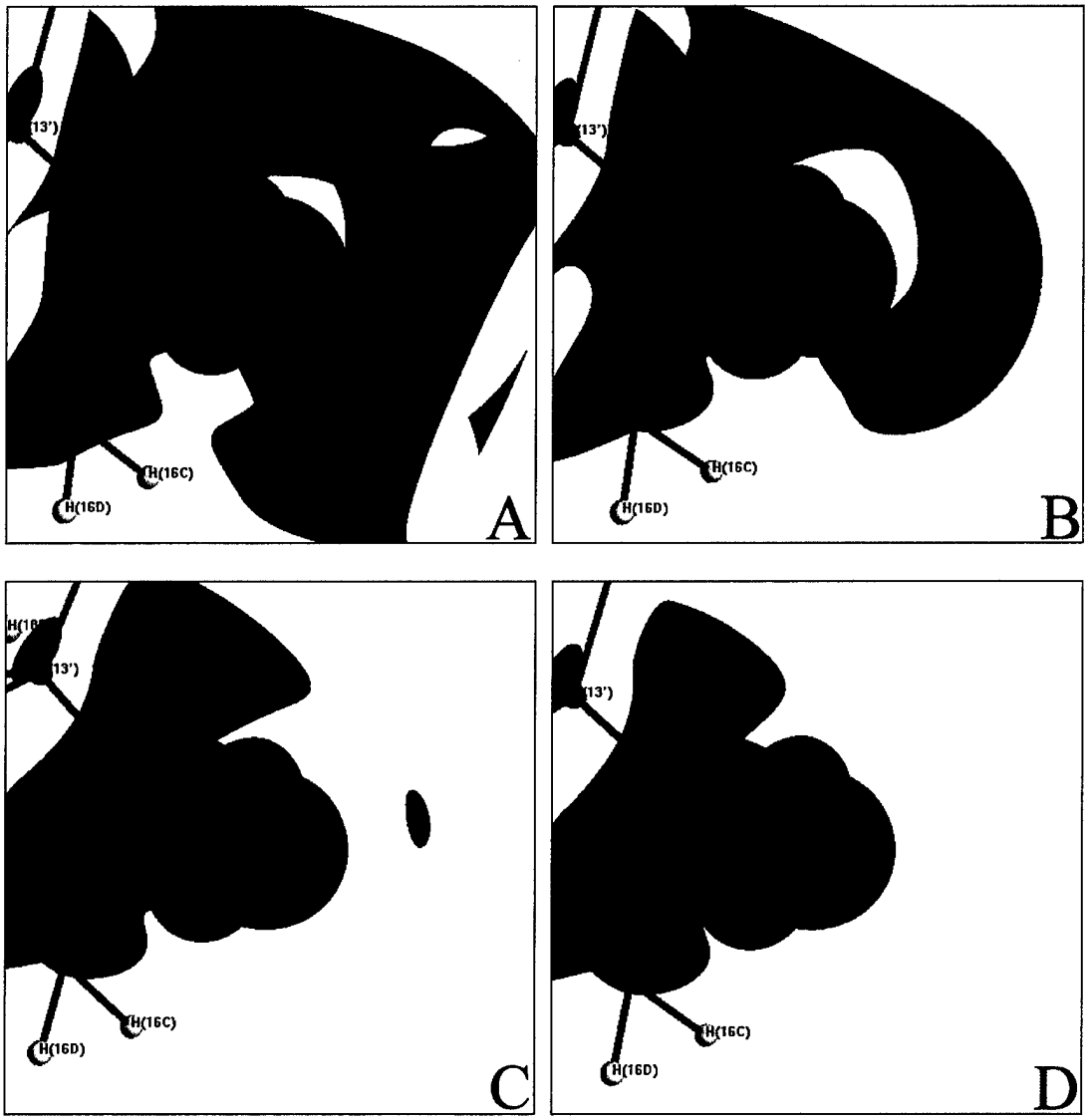

Figure 6. Electrostatic potential isosurfaces of the O2' hydroxy group of 17β-estradiol • methanol. The blue surface in each picture represents +1.0 eÅ^{-1}. The red surfaces represent the following potentials: A –0.05 eÅ^{-1}, B –0.10 eÅ^{-1}, C –0.15 eÅ^{-1}, D – 0.20 eÅ^{-1}.

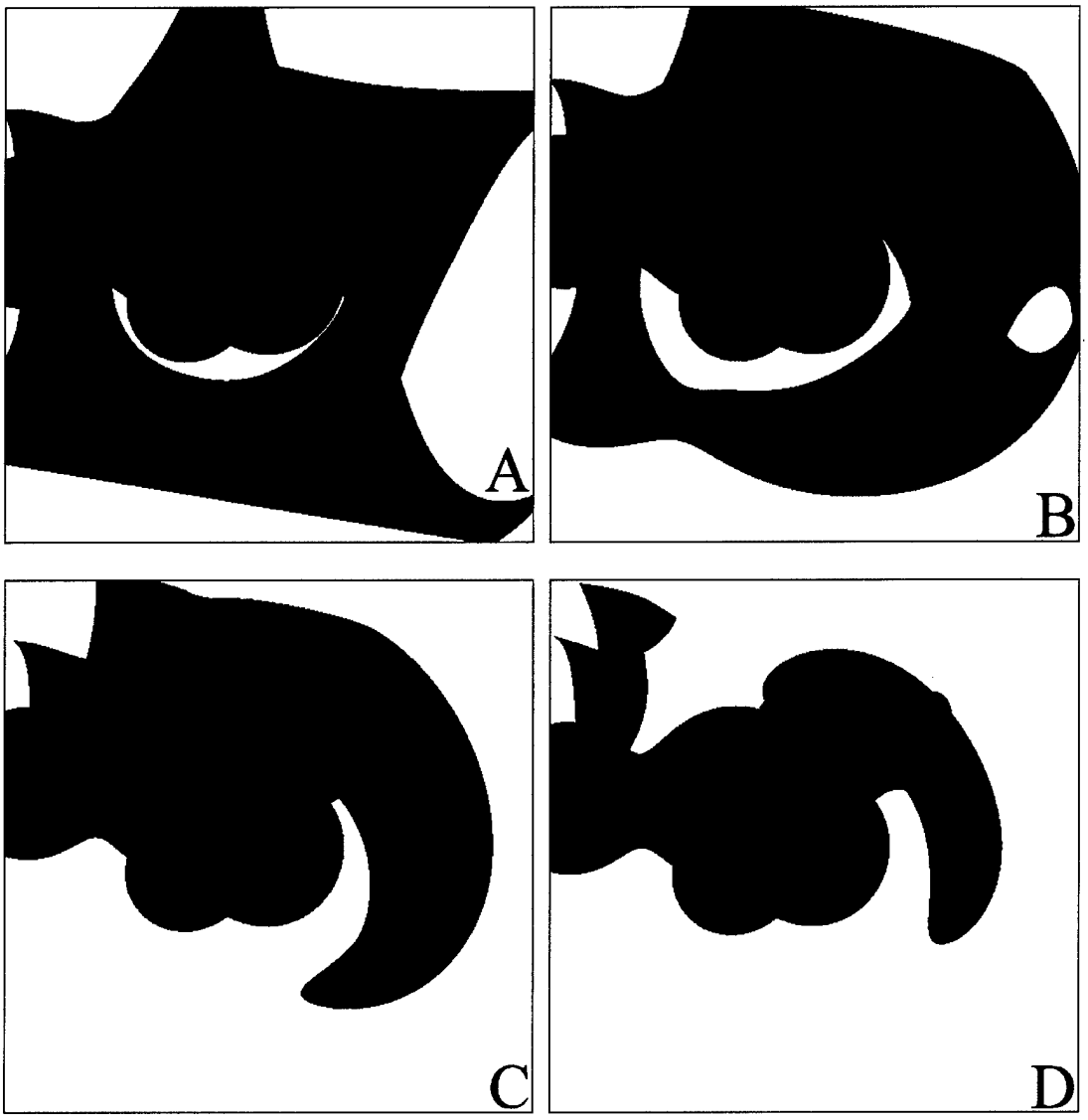

Figure 7. Electrostatic potential isosurfaces of the O1 hydroxy group of 17α-estradiol • ½ H_2O. The blue surface in each picture represents +1.0 eÅ^{-1}. The red surfaces represent the following potentials: A –0.05 eÅ^{-1}, B –0.10 eÅ^{-1}, C –0.15 eÅ^{-1}, D – 0.20 eÅ^{-1}.

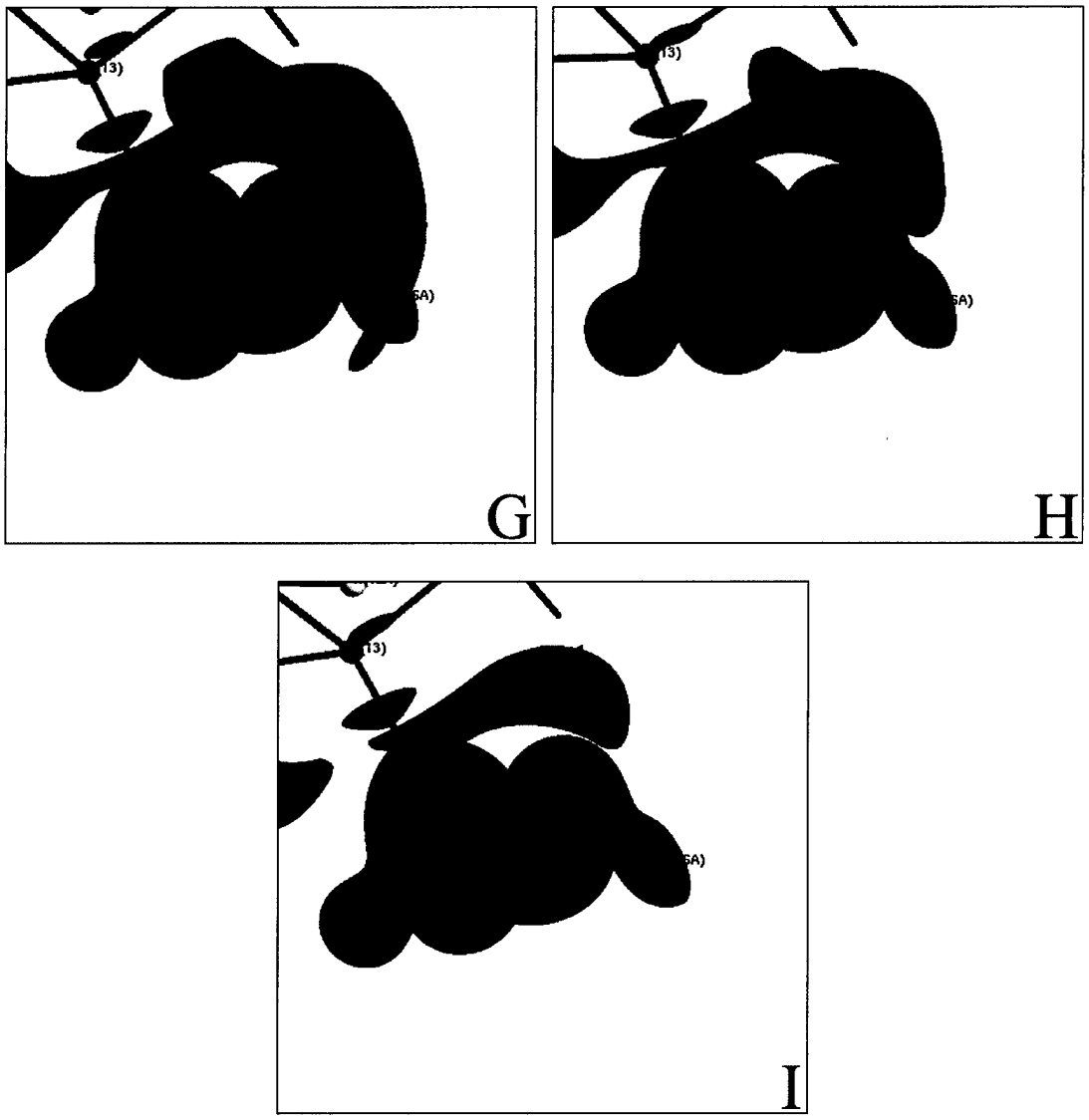

Figure 8. Electrostatic potential isosurfaces of the O2 hydroxy group of 17α-estradiol • ½ H_2O. The blue surface in each picture represents +1.0 eÅ^{-1}. The red surfaces represent the following potentials: A –0.05 eÅ^{-1}, B –0.10 eÅ^{-1}, C –0.15 eÅ^{-1}, D –0.20 eÅ^{-1}, E –0.25 eÅ^{-1}, F –0.30 eÅ^{-1}, G –0.35 eÅ^{-1}, H –0.40 eÅ^{-1}, I –0.45 eÅ^{-1}.